UILU-ENG-71-2006

CIVIL ENGINEERING STUDIES

STRUCTURAL RESEARCH SERIES NO. 372

STRENGTH AND DEFORMATION CHARACTERISTICS OF PLAIN CONCRETE SUBJECTED TO HIGH REPEATED AND SUSTAINED LOADS

by

Mohamed E. Awad

and

Hubert K. Hilsdorf

A Report on a Research Project
Sponsored By

THE NATIONAL SCIENCE FOUNDATION
Research Grant No. GK-1808

UNIVERSITY OF ILLINOIS
URBANA, ILLINOIS
FEBRUARY 1971

UILU-ENG-71-2006

Strength and Deformation Characteristics of Plain Concrete Subjected to High Repeated and Sustained Loads

by

Mohamed E. Awad

and

Hubert K. Hilsdorf

University of Illinois
Urbana, Illinois
February 1971

STRENGTH AND DEFORMATION CHARACTERISTICS OF PLAIN CONCRETE SUBJECTED TO HIGH REPEATED AND SUSTAINED LOADS

ABSTRACT

The investigation was concerned with the response of plain concrete when subjected to repeated or sustained high compressive loads. The objectives were: (1) to study the strength and deformation characteristics of concrete under such loading conditions, and (2) to propose an analytical procedure to predict concrete behavior under high repeated loads.

The first objective was realized through an experimental program. Plain concrete prisms (4 in. by 4 in. by 12 in.) were subjected to high repeated and sustained loads. Compressive loads were concentrically applied. Strains in the longitudinal and lateral directions were recorded throughout the life of a specimen. The test program was divided into three phases. Phase One dealt with the effect of maximum stress, stress range and concrete age at time of loading. Phase Two concerned with the effect of speed of testing on static and repeated load behavior. The relationship between the damage, caused by high repeated and sustained loads, less than those necessary to cause failure, and the remaining load carrying capacity of a specimen, was studied in Phase Three.

To achieve the second objective, two analytical models were formulated. These were based on the cycle and time-dependence of damage and of strains of concrete when subjected to high repeated or sustained stresses. For a given set of parameters, a damage model was proposed to predict the number

of cycles required to cause failure, while a failure strain model was developed to predict the total longitudinal strain accumulated at failure.

The experimental program showed that concrete response to high repeated loads is very much controlled by the time concrete has to resist stresses higher than its sustained load strength. For a maximum stress higher than the sustained load strength, a decrease in the stress range and/or the stress rate (test frequency) significantly increases the "sustained load" contribution to the overall behavior. The number of cycles to failure are smaller, and the exhibited strains throughout the loading history and at failure are larger, the greater the "sustained load" effect. Even if the effect of hydration during a test is excluded, concrete age at loading appears to have a significant effect on behavior of concrete subjected to high loads. In addition, it was shown by experiment, that plain concrete, subjected to high repeated and sustained loads, undergoes a "hardening" stage manifested by an increase in the static strength over the static strength prior to a sustained or repeated load test. This "hardening" is dominant during the earlier portion of the life of the specimen. The last portion is characterized by progressive crack propagation and a stress decrease until failure.

In the analytical study, a damage model was developed in which the cycle and time-dependent effects are expressed separately. The damage model was revised successively until excellent agreement, between calculated and observed failure cycles, was achieved. Also, an analytical model to determine the failure strain model was derived. The total strain was assumed to consist of an initial elastic strain, a cycle-dependent and a time-dependent strain. The agreement between calculated and observed failure strains ranged from poor to satisfactory, but the failure strains, calculated from the analytical model, gave the general tendencies which were observed in the experiments.

ACKNOWLEDGMENT

The study presented herein is part of the research program, "Progressive Fracture in Concrete Under Repeated High Compressive Loads," being conducted in the Department of Civil Engineering, University of Illinois at Urbana, Illinois. The investigation was supported by the National Science Foundation under Research Grant No. GK-1808.

Acknowledgment is due to S. I. Diaz, research assistant in Civil Engineering, for his cooperation and valuable suggestions. Thanks are extended to V. J. MacDonald and his staff for their help in the development of testing equipment and instrumentation as well as to Barbara Wilhelm who typed the final manuscript.

This report is a doctoral dissertation by Dr. Mohamed El-Mustafa Awad, submitted to the Graduate College of the University of Illinois in partial fulfillment of the requirements for the Ph.D. degree.

TABLE OF CONTENTS

CHAPTER Page

CHAPTER Page

CHAPTER Page

LIST OF TABLES

LIST OF FIGURES

Figure Page

Figure Page

Figure Page

Figure | Page

Figure | Page

Figure Page

DEFINITIONS AND NOTATION

DEFINITIONS:

Low Cycle Fatigue	Repeated load test in which the maximum stress level is above the sustained load strength.
Strain Envelope Curve	Locus of limiting stresses and longitudinal strains at failure. It describes failure of plain concrete subjected to a particular load history.
Cycle Ratio, $N = n/n_u$	Ratio of number of applied cycles to number of cycles which would cause failure.
Time Ratio, $T = t/t_u$	Ratio of the time a specimen is subjected to a given sustained stress to the time required to cause failure at the same stress.
Life Ratio, $L = \ell/\ell_u$	A general term used to refer to both cycle and time ratios.
Threshold Stress, f_{sh}	An arbitrary stress above which the time-dependent damage may develop or cracks propagate in plain concrete subjected to high repeated stresses.
Pure Fatigue	A hypothetical fatigue test in which the loads are applied at an infinitely high speed. Thus, the time a specimen has to resist stresses higher than its sustained strength is reduced to zero.
Reloading Strength, f_{cur}	Strength of a specimen loaded monotonically to failure, after it has been subjected to cyclic or sustained loads, at a life ratio less than unity.
Hardening	A term used to indicate the rise of the reloading strength above the initial static strength. The extent of hardening is expressed by the magnitude of this strength increase.
Damage	A term used to indicate the fall of the reloading strength below the initial static strength. The degree of damage is expressed by the magnitude of this strength reduction.

NOTATION*:

Capital Letters

A, B, C	Concrete batch designations as cast for the different phases.
D_n	Cycle-dependent damage.
D_t	Time-dependent damage.
F	Axial compressive load on test specimen.
F_{max}	Maximum load in fatigue test.
F_{min}	Minimum load in fatigue test.
F_u	Ultimate load capacity of test specimens.
K_1, K_2, K_3, K_4	Constants related to time-dependent damage.
L	Life ratio, $(\ell/\ell u)$
N	Cycle ratio, (n/n_u)
R	Stress range, $(\sigma_{max}-\sigma_{min})$
T	Time ratio, (t/t_u)

Small Letters

f	Stress, psi.
f_{cu}	Compressive strength of concrete as determined from 6 in. by 12 in. control cylinders, psi.
f_{cu28}	Compressive strength of concrete control cylinders at an age of 28-days.
f_{cup}	Compressive strength as determined from 4 in. by 4 in. by 12 in. concrete prisms.
f_{cur}	Reloading strength, psi.
f_{max}	Maximum stress in fatigue test, psi.

---

* The notations used in this report follow the proposed A.C.I. standard for preparation of notation as reported in the Journal of the A.C.I., August, 1970.

f_{min}	Minimum stress in fatigue test, psi.
f_{sus}	Sustained stress in sustained load test, psi.
$\dot{f}$	Stress rate, psi/min.
n	Number of applied cycles in fatigue test.
n_o	Cycles to failure under pure fatigue conditions.
n_u	Number of cycles to failure in a fatigue test.
$\bar{n}_u$	Logarithmic average of failure cycles of several specimens for a given parameter.
n_{uc}	Number of failure cycles as calculated by analytical damage models.
s	Standard deviation.
t	Duration of loading in sustained load test, minutes.
t_u	Time to failure in sustained load test, minutes.
$\bar{t}_u$	Logarithmic average of time to failure of several specimens for a given parameter.
t_{un}	Total testing time of a specimen subjected to repeated loads.

Greek Letters

α	Ratio of cyclic to time-dependent damage in low cycl fatigue, $\alpha = D_n/D_t$.
β	Stress rate expressed as ratio of static strength, $\beta = \dot{f}/f_{cup}$
ε	Strain, in/in x 10^{-3}
$\dot{\varepsilon}$	Strain rate, in/in/sec.

ε_h	Lateral strain.
ε_{hu}	Lateral strain at failure.
ε_ℓ	Longitudinal strain.
$\varepsilon_{\ell 1}$	Initial longitudinal strain to mark the maximum stress level.
$\varepsilon_{\ell\ell}$	Longitudinal strain accumulated at a certain life ration in addition to $\varepsilon_{\ell 1}$
$\varepsilon_{\ell n}$	Cycle-dependent longitudinal strain.
$\varepsilon_{\ell r}$	Strain ratio, $\varepsilon_{\ell r} = (\varepsilon_{\ell 1} + \varepsilon_{\ell\ell})/\varepsilon_{\ell u}$
$\varepsilon_{\ell t}$	Time-dependent longitudinal strain.
$\varepsilon_{\ell tu}$	Time-dependent failure strain under sustained load.
$\varepsilon_{\ell u}$	Longitudinal strain at failure.
$\varepsilon_{\ell uc}$	Longitudinal strain at failure as calculated from an analytical model.
ε_o	Longitudinal strain at failure for pure fatigue.
ε_v	Volumetric strain, $\varepsilon_v = \varepsilon_\ell - 2\varepsilon_h$
ε_{vu}	Volumetric strain at failure.
η	Life ratio below which the reloading strength is larger than the initial static strength.
ν	Poisson's ratio.
ν_u	Poisson's ratio at failure.
σ	Stress level, $\sigma = f/f_{cup}$
σ_{cur}	Reloading strength ratio, $\sigma_{cur} = f_{cur}/f_{cup}$

σ_{max}	Maximum stress level in fatigue test, $\sigma_{max} = \frac{f_{max}}{f_{cup}}$
σ_{min}	Minimum stress level in fatigue test, $\sigma_{min} = \frac{f_{min}}{f_{cup}}$
σ_s	Sustained load strength expressed as a ratio of static strength, $\sigma_s = f_s/f_{cup}$
σ_{sh}	Threshold stress level, $\sigma_{sh} = f_{sh}/f_{cup}$
σ_{sus}	Sustained stress level, $\sigma_{sus} = \frac{f_{sus}}{f_{cup}}$

Additional notations are defined in the text.

1. INTRODUCTION

1.1 The Problem

Under extreme conditions reinforced concrete structures may be exposed to a small number of high overloads approaching the ultimate load carrying capacity of a member. Such conditions may arise during earthquakes, high winds or blasts. They are also of significance for young concrete structures which may have to sustain heavy construction loads, and for the application of limit analysis to the design of reinforced concrete structures. However, little information on the behavior of concrete subjected to repetitions of high stresses, often referred to as low cycle fatigue, is available in the literature.

The problem in predicting and evaluating low cycle fatigue behavior of concrete lies in the fact that the repeatedly applied stresses may be larger than the sustained load strength (static fatigue strength) of the concrete. Thus, the period of time during which concrete has to resist stresses larger than the sustained load strength is significant. Then, concrete response may be both cycle and time dependent and the frequency at which the repeated loads are applied may become a major parameter.

1.2 Objective

The objective of this study was to investigate strength and deformation characteristics of plain concrete subjected to repeatedly applied high compressive stresses. The maximum stress, the difference between

maximum and minimum stress (stress range) and the rate of stress were the major parameters. Particular emphasis was placed upon studies of the role of time under load on the low cycle fatigue behavior of concrete. Analytical models and procedures were developed to predict concrete response under such loading conditions.

1.3 Scope

The experimental part of this investigation is subdivided into three phases which are described briefly in the following.

1.3.1 Phase One: Effect of Maximum Stress, Stress Range and Age at Loading on Behavior of Plain Concrete Subjected to High Loads

To investigate the behavior of plain concrete under various stresses, several series of prismatic specimens 4 in. by 4 in. by 12 in. were tested in axial, concentric compression. A total of 133 specimens were subjected to high sustained or repeated stresses. In the sustained load studies, the level of the sustained stress and the age of concrete at load application were the controlled parameters. The maximum stress level, the range of stress and the age at loading were the parameters for the repeated loading tests. All repeated loads were applied at a constant stress rate. The strength tests were complemented by careful measurements of concrete deformations in both the longitudinal and lateral directions.

1.3.2 Phase Two: Effect of Speed of Testing on Response of Plain Concrete to Static and High Repeated Loads

Specimens were tested to study the effect of rate of loading on the short-time strength and deformation characteristics of concrete. The

loads were applied at strain rates of 10^{-7}, 10^{-5}, and 10^{-3} in/in/sec, respectively. Specimens were used to investigate the effect of stress rate (frequency of testing) on concrete response to high repeated loads. The two stress rates chosen for this study were 600 and 60,000 psi/min, to supplement the stress rate of 6,000 psi/min which was used in Phase One.

1.3.3 Phase Three: Effect of High Repeated and Sustained Loads on Subsequent Static Strength

To study the relationship between the damage caused by high sustained and repeated overloads and the remaining load carrying capacity, a total of 66 specimens were loaded to a predetermined percentage of their lives under sustained and repeated loads. Then the compressive strength, hereafter referred to as reloading strength, was determined and compared with the strength of the specimens which had been loaded to failure monotonically without a previous load history. One level of sustained stress and two levels of repeatedly applied stresses were chosen. The age of concrete at testing was 28 days. Longitudinal and lateral strains were recorded.

In all phases of this investigation only one type of concrete and one type of specimen were used. For each parameter in Phase One and Phase Two from three to six specimens were tested to ascertain a statistically reliable answer. In Phase Three six to ten specimens were tested for each parameter.

In addition to longitudinal and lateral strains, also Poisson's Ratio, volumetric strain, and the difference in strain at maximum and minimum load, for a given cycle, were recorded in most cases.

2. REVIEW OF PERTINENT LITERATURE

In the following, the available research pertinent to this investigation will be summarized. Particular emphasis will be placed on the behavior of concrete subjected to various types of loading such as monotonically increasing loads, repeated and sustained loads and on the role of time on the response of concrete to such loads.

2.1 Effect of Rate of Loading on Concrete Response to Static Loads

It has been shown that the rate of applied stress or strain affects the short-time compressive strength of plain concrete significantly. A summary of the current specifications and data from various sources has been given by McHenry and Shidler [23]*. For stress rates between 10^{-1} and 10^{-4} psi/sec there is an approximately linear relationship between the strength and the logarithm of the speed of testing [16]. An increase of the stress rate by one order of magnitude results in a strength increase of about 3 to 5 percent. Further increase of the stress rate causes a more substantial gain of strength. For a stress rate of 10^{7} psi/sec the compressive strength of concrete is approximately 1.8 times the strength at a stress rate of 30 psi/sec [45]. The data reported by Evans [10] do not substantiate this trend and indicate no change in strength as the rate of loading is changed through a range of 1 to 10^{3} psi/sec. Similar effects were found for the effect of rate of straining. Abrams [1] determined the compressive strength of 6 in by 12 in cylinders using rates of 8.3×10^{-6}

---

* Numbers in [ ] refer to the corresponding entries in List of References.

to 2.1×10^{-4} in/in/sec. Watstein [45] compared the strength of concrete tested at very rapid strain rates with the strength obtained at an extremely slow rate of 1×10^{-6} in/in/sec. Abrams reported an increase of 8 percent in static strength when the strain rate was varied from 6.95×10^{-5} to 1.4×10^{-5} in/in/sec. Watstein reports a considerably smaller change in strength in the range of slower rates than was indicated by Abrams.

The rate of stress or strain also influences the shape of the stress-strain curve of concrete. Concrete deformations at a given stress increase with decreasing rate of stress or strain and the slope of the descending portion of the stress-strain relationship increases with decreasing strain rates.

2.2 Concrete Response to Repeated Loads (Fatigue)

A detailed review of previous investigations is given by Murdock [22] and Raithby, et al., [29]. In the following, only the most important findings are summarized.

It is generally agreed upon that plain concrete loaded in compression or flexure does not exhibit a fatigue limit up to 10 millions of load repetitions. A decrease in the range of stress, i.e., the difference between maximum and minimum stress, as well as of the applied maximum stress results in an increase of the fatigue life of plain concrete. The effect of mix proportions, static strength, stress distribution or direction of stress (tension or compression) can be taken into account by expressing the fatigue strength of a specimen as a fraction of the static strength of a similarly loaded companion specimen.

The influence of age at loading has been studied little in the past, but Kesler and Siess [19] stated that for fatigue testing the specimen should be at least three months old prior to loading, in order to eliminate the influence of continued hydration during the fatigue test. Kesler concluded that variations of the speed of testing between 70, 230 and 440 cycles per minute had no significant influence on fatigue performance of flexural specimens. Little has been done to investigate the effect of frequency on concrete when subjected to repeated compressive loads. Assimacopoulos, et al., [2] conducted tests on 2 in by 4 in cylinders at speeds of 500 and 9000 cycles per minute. No effect of rate of loading was observed but he stated that the number of tests were too small to arrive at final conclusions. Tests of specimens which did not fail before 4×10^6 cycles were terminated.

In most fatigue tests reported in the literature the loads alternated between a minimum and a maximum value which was held constant within a test. More realistic load histories were, however, investigated by Hilsdorf and Kesler [14] who studied the effect of periodic rests in between periods of cyclic loading. These tests showed that rest periods up to 5 minutes, which were introduced after every 4500 cycles of continuous cyclic loading, increased the fatigue strength of concrete subjected to flexure stresses; but that periods longer than 5 minutes had no additional beneficial effects. In addition, they also conducted fatigue tests in which the minimum and maximum stresses were varied within a test. They evaluated their data on the basis of various cumulative damage theories which are described in section 2.6 of this report and concluded that the Miner

hypothesis of linear cumulative damage can give either conservative or unconservative estimates of the fatigue strength of specimens subjected to varying stresses depending on the sequence of loading and the applied maximum stress level. From their experimental data they derived virtual stress-cycle relationships which can be used to predict the fatigue life of concrete under varying stresses using the linear Miner rule.

Hilsdorf and Kesler [14] in their work on cumulative damage in beam specimens concluded that fatigue behavior of concrete loaded in flexure could be explained in terms of cumulative strain, and that failure occurs as soon as the total strain reaches a limiting value. They also forwarded a failure concept to explain qualitatively the results of their experimental investigation. The true strength of concrete varies throughout a fatigue test. It may increase during the initial stages of the test and decrease as failure approaches.

2.3 Concrete Response to High Repeated Loads (Low Cycle Fatigue)

The investigations reviewed in section 2.2 mainly dealt with the fatigue behavior of concrete under comparatively low stresses causing failure after more than 1000 cycles. In the following, studies of concrete subjected to a small number of high overloads will be reviewed.

Sinha, Gerstle and Tulin [40] conducted one of the first investigations of strength and deformation characteristics of concrete subjected to high compressive stresses in the range of low cycle fatigue. They concluded that the behavior of concrete subjected to repeatedly applied high stresses can be predicted using the static stress-strain relationships as

a unique failure envelope. For a given maximum stress, the specimen will fail as soon as its strain reaches the value given by the descending portion of the static stress-strain curve at this stress. A load cycle will cause incremental strains only if a critical stress, corresponding to the intersection of the loading and unloading stress-strain curve of the fatigue test, is exceeded. This point is referred to as the shakedown limit. For stresses below this point the strains follow a closed loop without further development of permanent strains. It is shown also that the shakedown limit is a function of the stress amplitude; for a given maximum stress the shakedown stresses increases with a reduction of the stress range. Analytical relations were developed for the envelope curve, and for the unloading and reloading stress-strain curves during a fatigue test.

Karsan, [17], confirmed the existence of a unique envelope curve for plain concrete which coincides with the static stress-strain relationship. In contrast to Sinha's findings [40], Karsan states that the shakedown limit is primarily dependent on the maximum stress, but that it is independent of the minimum stress. In view of the wide scatter, the shakedown limit is defined as a range, with upper and lower limits. For higher maximum stresses the shakedown, i.e., the intersection between the loading and unloading stress-strain curve, approaches the upper limit. As long as the shakedown exceeds the lower shakedown limit, strains will accumulate until failure occurs. If the strains at maximum stress are below the lower shakedown limit, strains will accumulate only until the lower shakedown limit is reached. Then the strains will stabilize and will follow, in subsequent cycles, a closed hysteresis loop. Karsan developed analytical

expressions for the envelope curve, the upper and lower shakedown limits, and the loading and unloading curves which compare well with his experimental data.

It should be pointed out that neither Sinha, et al., [40], nor Karsan [17] included the effect of stress rate or time under load in their experimental studies. Since the static stress-strain relationship of concrete is not unique but a function of the stress or strain rate, it is unlikely that one particular envelope is valid to describe the behavior of concrete subjected to various stress histories in the range of low cycle fatigue.

Shah and Winter [39] reported that concrete subjected to five cycles of a maximum stress of 83 to 88 percent of the static ultimate strength, did not affect the subsequent static strength of the specimens. When the maximum stress was increased to 95 to 100 percent, seven of the eleven specimens tested failed before reaching the fifth cycle. Thus, it was concluded that the load capacity of the concrete decreased with every cycle. Specimens which did not fail after five cycles at a maximum load of 90 to 100 percent showed either a decrease or an increase in their static strength. It has been observed that the difference between the strain at the maximum and minimum load levels of one cycle gave an indication of the integrity of concrete.

2.4 Concrete Response to High Sustained Loads

Sustained stresses which are high enough to cause failure under a certain duration of loading can be considered a limiting case of low cycle fatigue in which the load range approaches zero.

Sell [36] studied the influence of sustained loading on the strength and deformation of concrete. His tests showed that the compressive stress concrete can sustain indefinitely may be up to 30 percent lower than the short-time strength. Particularly, young concrete continues to hydrate while under load; the resulting strength increase may partially offset or exceed the damaging effect of the sustained stress. The extent of hydration occurring while the specimen is under load depends on concrete age at the time of load application. Sell states that the effect of continued hydration and thus of concrete age at the time of load application can be taken into account if sustained stress is expressed as a fraction of the short time strength of a companion specimen at the time of failure of the sustained load specimen. He reported that under sustained loads, failure can occur only within a certain time period, the "critical period" which is shorter the younger the concrete at loading or the faster the strength gain, due to continued hydration, during the sustained load test. Depending on the age of concrete at loading,the failure strains can amount to two to four times the value of the short-time durations. Rüsch [35] showed that the sustained load strength of a concrete which is almost completely hydrated prior to loading, may be as low as 70 percent of its static strength at the time of application of the sustained load. Because of continued hydration under load,the sustained load strength, expressed as a fraction of the strength at the time of load application, is higher for young concrete than it is for old concrete. Rüsch assumed that the effect of concrete age at the time of load application is only due to continued hydration under load. Based upon this assumption he formulated

a relation to predict the sustained load strength of concrete for various ages of concrete at the time of load application. In this relationship the effect of continued hydration as well as the influence of load eccentricity are incorporated.

2.5 The Failure Mechanism of Concrete

2.5.1 Static Loads

In recent years considerable interest has centered on the mechanism of failure of concrete loaded in compression, which has been shown to be closely related to the development of small cracks, mainly in a direction parallel to the applied compressive stress, commencing well below the ultimate load. It is well established that cracks initiate at tensile stress concentrations arising from the heterogenous nature of the material, in which particles of aggregate are embedded in a matrix which is usually less stiff, and which contains flaws and voids.

Sturman, Shah and Winter [41] showed that tensile stresses are present at the mortar-aggregate interface prior to loading because of volume changes of the matrix caused by moisture loss. These stresses may result in bond cracks in concrete prior to loading. Under load, these cracks propagate or additional cracks are formed. Bond cracks between aggregate and the matrix begin to propagate noticeably at compressive stresses of approximately one-third of the ultimate load strength. At this level the stress-strain curve starts to deviate noticeably from a straight line. At about 70 to 90 percent of the ultimate strength, cracks start to

propagate through mortar and bridge between bond cracks to form a continuous crack pattern which eventually leads to failure of the specimen.

Also different approaches have been employed to study crack initiation and propagation and their effect upon the behavior of plain concrete under load. Simplified models have been used to show the local stress distribution in heterogeneous materials subjected to compressive stresses.

Shah and Winter [38] studied the properties of the mortar-aggregate interface and concluded that the interfacial surfaces are first to fail, and bond cracks form when the unconfined bond strength of the interface is exceeded. Thereafter, the interface carries its share of the load through friction. Using the Coulomb-Mohr theory they estimated the load at which bond cracking occurs and stated that it compares well with their experimental data. They further estimated the load at which cracks propagate in the mortar. In their paper, Shah and Winter [38], considered concrete to consist of small units composed of aggregate particles which are surrounded by mortar. Assuming a statistical strength distribution of these units they developed an expression for the stress-strain relation of concrete up to the maximum stress and through the descending portion. Glucklich [11] used fracture mechanics concepts to predict crack propagation in concrete subjected to compression. This approach will be discussed in more detail by Diaz [7].

Crack propagation in plain concrete was investigated employing various experimental techniques. Sturman, et al., [41], obtained slices from previously loaded concrete specimens and observed microcracks under a microscope after dying the cut sections. This technique has been used by

several other investigatiors [37,38]. An increase in volumetric strain of the concrete, increase of the attenuation, and reduction of the velocity of an ultrasonic pulse traveling through the concrete or measurements of acoustic emission also were accepted as indirect indications of microcracking in concrete subjected to static loads [33,34].

2.5.2 Repeated and Sustained Loads

Already in 1907 Van Ornum [42] noted that the stress-strain curve of concrete subjected to repeatedly applied axial compression is initially convex upwards, straightens after a few repetitions of load and finally becomes concave upwards and s-shaped as failure approaches. Many investigators confirmed these tendencies and concluded that the change in shape of the stress-strain diagram under repeated loads is an indication of the gradual disintegration of concrete.

Ruetz [33] and Rüsch [34] measured the intensity of noises emitted by concrete subjected to sustained compression and hypothesized that such noises are generated when cracks propagate. This technique is referred to as acoustic emission and is a generally accepted non-destructive testing technique. It was observed that after the initial load application the intensity of crack noises decreased but increased rapidly with approaching failure. Thus, a clear indication of the progressive nature of failure of concrete under sustained stresses was established.

Bennet and Raju [4] tested plain concrete prisms, to study the nature of fatigue damage under unidirectional compressive stresses. Crack initiation and propagation were examined microscopically and an analysis

of crack length distribution was conducted. Distinction was made between bond, matrix, and aggregate cracks. Bennet, et al., concluded that under fatigue loads a more extensive system of cracks develops than that which was observed in static tests, and that the progressive changes in the modulus of elasticity and the ultrasonic pulse velocity provided an indirect measure of the extent of damage caused by repeated compressive stresses. They attributed the marginal increase in the static strength, which was observed during a fatigue test, to the temperature rise due to the energy dissipation and the loss of gel moisture. They also stated that in fatigue at low stresses, the elastic strain, i.e., the strain which was recovered on removal of the load, increases continuously with increasing number of cycles.

Based upon this observation, Bennet, et.al., formulated a relationship between fatigue damage and the secant modulus to predict the remaining life of concrete at any stage.

Raju [30] used an ultrasonic pulse velocity technique to study microcracks in high strength concrete subjected to static and repeated compressive stresses. In the repeated load tests prismatic specimens were subjected to different maximum stress levels ranging from 53 to 85 percent of the static ultimate strength and a constant minimum stress level of 3 to 5 percent. The progressive nature of the failure of concrete under repeated loads was confirmed by the observations that in fatigue tests, leading to failure, the pulse velocity decreased continuously with increasing number of cycles. Raju gave an empirical relation to predict the fatigue life of a partially fatigued specimen from measurements of pulse

velocity. However, for this procedure, the initial pulse velocity prior to loading has to be known.

Shah and Chandra [37] studied the fracture of concrete under cyclic and sustained loading by microscopic observation of the concrete, and found progressive microcracking similar to the cracking process observed in static tests. They suggested two stages of crack propagation occurring under cyclic or sustained stresses. During the first stage lateral and volumetric strains increase at a constant rate. During the second stage both the lateral and volumetric strains increase at an increasing rate until failure occurs. If a specimen is loaded to failure before it reaches the second stage its strength may be up to 15 percent larger than that of an unloaded companion specimen. Therefore, Shah and Chandra hypothesized that during sustained loading, a consolidation of the paste occurs. Its strengthening may offset the damaging effect of the load.

This review of available experimental data clearly indicates that failure of concrete under sustained or repeated compressive stresses is caused by a gradual process of microcracking similar to the behavior under static load. However, the extent of cracking at failure may be larger than observed under static loading conditions. The effect of microcracking may be partially offset by some "hardening" which expresses itself in an increase of the static strength during the early stages of repeated or sustained load tests. The mechanism leading to this strength increase or the parameters controlling it are not clearly understood. Also, the mechanisms by which microcracks continue to propagate under cyclic or sustained stresses are still unknown, however, continued redistribution of stresses, creep, and stress corrosion have been suggested as possible reasons.

2.6 Cumulative Damage Analysis

Actual structural members may be subjected to a wide spectrum of repeated loads varying in magnitude, range and frequency. In contrast to this, most laboratory experiments on the fatigue behavior of materials are highly simplified and stresses varying between fixed limits are applied at a constant frequency until failure occurs. Thus, the problem arises to estimate the behavior of actual structures under realistic loading conditions from simplified laboratory experiments. For this, procedures have been developed by which fatigue damage caused by a certain number and type of repeated loads can be estimated. The damage caused by various portions of the entire load spectrum are added and failure will occur if the summation of all damage increments exceeds a limiting value. Therefore, such procedures are referred to as cumulative fatigue damage methods. The available information on cumulative fatigue damage procedures for concrete is scarce and has been reported already in section 2.2. However, extensive studies have been conducted to describe the behavior of metals under varying repeated loads. They will be summarized briefly as far as they are pertinent to the investigation reported herein.

One of the major difficulties in a cummulative damage analysis is the lack of an experimental method to measure damage or a suitable parameter to express damage. For metals, variations in static tensile strength may not be a good indication of fatigue damage, since the static tensile strength is controlled by the bulk properties of the material whereas fatigue failure is controlled by the propagation of a single crack which may not influence

the static tensile strength. However, this limitation does not necessarily apply to concrete where failure, both under static and repeated loads, occurs by a process of microcracking. In the earlier studies on cumulative damage, a certain function was assumed which expresses fatigue damage, and failure was arbitrarily defined to occur once damage was equal to unity. More recently, fracture mechanics concepts were introduced and subcritical crack growth was used as a measure of fatigue damage.

The classical approach in cumulative fatigue damage analysis is to assume that in a constant amplitude fatigue test damage accumulates linearly. This method is generally known as Miner's Rule [21]. It assumes that at any stage of the loading history of a material, the percentage of the life used is proportional to the cycle ratio at that loading condition. Failure occurs if the summation of all cycle ratios is equal to unity, i.e., $\Sigma \frac{n}{n_u} = 1.0$, where n is the number of cycles at a stress level σ, and n_u is the fatigue life of a specimen tested at that same stress level. The results of several investigations, however, have shown that this method is not always accurate and may give unconservative estimates [14,20,9]. With more data available for comparison [6,25], several new hypotheses have been proposed. These consist either of modifications of the linear hypothesis and the introduction of non-linear damage accumulation [14,25] or purely empirical relations [12]. Corten and Dolan [5] visualized the damage as a propagation of one or several cracks and therefore expressed damage in terms of the number of crack nuclei formed and the rate of crack propagation. Therefore, they formulated a cumulative fatigue damage hypothesis in which they accounted for a nucleation period which may be required to initiate permanent

fatigue damage. During this initial period the applied loads may harden rather than damage the material. Wei and Landes [46] considered the rate of fatigue crack growth in high strength steels in an aggressive environment to be composed of two components - a mechanical component, given as the rate of fatigue crack growth in an inert environment, and an environmental component, computed from the sustained load crack growth data obtained in an identical aggressive environment. Using this approach Wei and Landes were able to predict, at least qualitatively, the effect of corrosive environments on the fatigue behavior of high strength steels.

3. EXPERIMENTAL PROGRAM

3.1 Materials

3.1.1 Cement

Type 1 portland cement was used. Typical chemical and physical test data of the cement as supplied by the manufacturer are given in Table (3.1).

3.1.2 Aggregates

The fine aggregate was obtained from the Wabash River near Covington, Indiana. The coarse aggregate consisted of crushed limestone. The particle size distribution for sand and gravel was determined in accordance with the ASTM Specification C136-40. The gradation curves are shown in Fig. (3.1). The sand and the gravel had fineness moduli (ASTM C125-48) of 2.75 and 7.4, respectively. The bulk specific gravity and the absorption capacity for the fine aggregate were 2.60 and 1.6 percent; for the coarse aggregate they were 2.66 and 1.83 percent, respectively, (ASTM C127-42).

3.2 Mix Proportions

An attempt was made to keep concrete workability and compressive strength of all specimens as uniform as possible. The aggregates were predried and enough water was added to obtain a slump of 2 to 4 inches resulting in an average w/c of 0.78 and an average 28-day strength of about 4000 psi. The mix proportions of all series of specimens are shown

in Table (3.2). The ingredients were mixed for approximately 40 seconds dry, and 2 minutes wet in a horizontal cyclo-mixer with a capacity of half a cubic yard.

3.3 Test Specimens

The batches for Phase One were of sufficient size so that 15 control cylinders 6 in by 12 in and 12 prisms 4 in by 4 in by 12 in could be cast from each batch. For Phase Two and Phase Three only 12 control cylinders and 12 prisms were cast from each batch. The prisms were cast horizontally in steel forms constructed of steel channels. The forms were previously coated with a thin film of oil. The concrete was compacted with internal vibrators. The top surface of the cylinders was capped with cement paste, while that of the prisms was troweled within a few hours after casting. The prisms remained in the forms, covered with wet burlap for 24 hours. All specimens were then moist cured for a period of 6 days in a fog room at 75°F and then stored in the laboratory at 75°F and 50% R.H. until tested.

The cylinder strength of concrete from each batch of Phase One was determined after 3, 7, 14, 28, and 90 days from three control cylinders per age of testing. For all other phases the 90-days strength was not determined. Before testing, the ends of the prisms were ground smooth and flat on a flat steel plate using carborundum powder as an abrasive.

3.4 Instrumentation

For Phase One and Phase Three a conventional hydraulic testing machine with 300 kips capacity, fitted with a load and strain programmer was

used. Longitudinal and lateral strains were measured using a clip gauge as shown in Fig. (3.4). For the longitudinal gauge a flexible metal plate 1 in by 3/8 in by 1/16 in was attached to one end of a U-shaped aluminum frame such that the metal plate cantilevers from the aluminum frame at a right angle. The metal plate is the actual strain sensoring device and the moving part of the gauge. Two electric resistance gauges, with an active length of 1/8 in and a resistance of 120 ohms were mounted to it. Two fixed points of the gauge consisting of bolts with either a pin pointed or a flat end were screwed to the aluminum frame at a distance of 8 in from the flexible metal plate resulting in an active gauge length of 8 in. During strain measurements fixed points of the aluminum frame, as well as the free end of the cantilevering metal plate, rested on small aluminum gauge points which had been glued to the concrete surface as shown in Fig. (3.2). Deflections of the metal plate which were sensed by the attached SR-4 gauges are a measure of concrete deformations. The relationship between deflection and readings from the electric resistance gauges were determined by calibration on a mechanical supermicrometer. The clip gauge, used to measure the lateral strains, was similar to the gauge for longitudinal strains but with an active gauge length of 3 in. For easier mounting the aluminum frame holding the lateral strain gage was fitted into a rectangular cut-out of the frame for the longitudinal gauge, Fig. (3.3). During mounting, both gauges were connected by a pair of set screws which were removed during the test to allow independent movement of the gauges. The lateral gauge rested on aluminum gauge points as shown in Fig. (3.2).

Two sets of gauges were mounted on two opposite faces of the prism and held together by four springs, Fig. (3.4).

Leads from the longitudinal gauges were fed to a drum plotter which was part of the hydraulic testing machine. Thus, the average longitudinal compressive strains of two opposite sides of the specimen were recorded continuously as function of the applied loads. Leads from the two lateral gauges were connected to an X-Y plotter to give a continuous record of the average lateral tensile strains with load. The gauges were calibrated using a supermicrometer and their calibration was checked during and in between tests using an internal calibrator.

An overall view of the setup for Phase One and Phase Three is given in Fig. (3.5).

For Phase Two a closed loop hydraulic testing machine was used. The setup is shown in Fig. (3.7). The machine consisted of a loading frame with three hydraulic load activators, a hydraulic pump and three electronic programming and load control units. The three activators, with a capacity of 25 kips each, were arranged on the bottom head of the load frame such that they formed the corners of a triangle. The specimen was placed in the center of this triangle. Both top and bottom bearing platens rested on spherical balls and were connected to either the top head or the activators by flexible springs. In addition, spherical seats were mounted between the activators and the bottom bearing platen. Thus, the bottom platen was free to rotate and no horizontal forces could be transmitted into the specimen. The load in each activator could be controlled and programmed independently of each other. Three rather than one load activators were used in order to

be able to control the stress or strain distribution in the test specimen at any time. In a conventional testing machine it is difficult to load or strain a specimen concentrically even if the load axis coincides precisely with the axis of the specimen because of the inherent heterogenuity of concrete. With the closed loop system described above, concentric straining of the specimen during the initial load application could be insured by using strain gauges mounted on three sides of the specimen and automatically controlling the loads in three activators such that the strains on three sides are equal at all times and increasing at an equal predetermined rate. In addition to concentric straining, this test system allows the development of a variety of other plane stress or strain distributions in a specimen.

Three electric resistance gauges with an active gauge length of 6.25 in and a resistance of 300 ohms were glued to the centers of three faces of the prism. Each gauge was adjusted to a full range of 6×10^{-3} in/in.

The load and strain output from each activator was recorded continuously against time using an 8-channel plotter. At the same time, the load and strain outputs of the three activators were connected to an analog computer, which is programmed to record the average load-average compressive strain characteristics of an X-Y plotter during the whole test. Also, the average load and the average strain were recorded on the 8-channel plotter as a function of time [See Fig. B.7b, Appendix B]. In each case the load was recorded as a percentile of the ultimate capacity (25 kips foreach individual piston, and 75 kips for total capacity). Lateral tensile strains were not measured.

A specimen with gauges is shown in Fig. (3.6) and the entire setup used for Phase Two is shown in Fig. (3.7).

3.5. Load Pattern

Throughout the entire experimental program, loads were applied in a saw-tooth patter, Fig. (B.7b). Within each test the stress rate was maintained constant. In the conventional hydraulic testing machine used in Phase One and Phase Three, the rate controlling valves had to be adjusted at the beginning of the test and frequently checked thereafter. The stress rate was automatically set with high precision in the closed loop hydraulic machine used in Phase Two.

4. PHASE ONE: EFFECT OF MAXIMUM STRESS, STRESS RANGE AND AGE AT LOADING ON BEHAVIOR OF PLAIN CONCRETE SUBJECTED TO HIGH LOADS

4.1 Test Program and Procedures

This is a study of the response of plain concrete prisms subjected to high repeated and sustained loads. The sustained load tests which can be considered as a special limiting case of fatigue tests where the stress range is reduced to zero are reported separately for convenience.

Compressive loads were applied concentrically to all specimens. In the fatigue tests the main variables were the maximum stress, stress range, and the concrete age at time of load application. Four levels of maximum stress, $\sigma_{max} = f_{max}/f_{cup}$*, were investigated. They were 0.80, 0.85, 0.90, and 0.95 of the static ultimate strength, f_{cup}. The stress range, R, defined as the difference between the maximum and the minimum stress levels ranged from 0.05 to the level of σ_{max}. For the later case $\sigma_{min} \simeq 0$. For the tests with a nominal $\sigma_{min} = 0$, a minimum load less than 2 percent of the ultimate load had to be sustained to avoid impact; this minimum load is considered insignificant and will be neglected hereafter. The age of concrete at the time of loading was 7, 28, and 90 days. The investigation was limited to one type of concrete with a control cylinder strength, f_{cu28}, of 4000 psi after 28 days and to one type of specimen (4 in by 4 in by 12 in). The repeated loads were applied at a constant stress rate of $\pm$6000 psi/min throughout Phase One.

---

* Refer to List of Definitions and Notations.

Twenty-nine series, designated by the letter 'A', were tested within this phase. A total of 27 specimens were subjected to fatigue loads at an age of 7 days, 74 specimens at 28 days, and 32 specimens at 90 days. Tables(4.1), (4.2), and (4.3) show the number of specimens tested at each maximum stress level and stress range tested at 7, 28, and 90 days, respectively.

In the special case where R = 0, i.e., sustained load tests, three levels of the sustained stress, σ_{sus}, were studied: namely, 0.85, 0.90 and 0.95 of the static ultimate strength. The concrete age at time of loading was 7, 28, or 90 days. Table (4.4) gives the number of specimens tested at each level of σ_{sus} and at each age. Although the results from the sustained load tests will be presented separately, the tests were conducted simultaneously with the fatigue load experiments.

When a fatigue specimen is subjected to a certain maximum load, F_{max}, the ultimate load F_u of that particular specimen is not known, nor can the exact relation between F_{max} and F_u for that specimen be determined. Therefore F_u was estimated from the behavior of companion specimens. Each series tested in this phase consisted of 12 prisms (4 in by 4 in by 12 in). Three to four companion specimens were tested monotonically to failure at a strain rate of about 10^{-5} in/in/sec and the stress-strain characteristics both in longitudinal and lateral directions were determined. The maximum load, F_{max}, to which a series of fatigue specimens will be subjected can be determined by loading the specimens to a certain fraction of the average ultimate load, F_u, of the companion specimens. It proved to be more accurate, however, to determine F_{max} from the longitudinal strain measurements of companion specimens. If, for example, a fatigue specimen was

supposed to be subjected to $F_{max} = 0.90\ F_u$, then the average longitudinal strain, $\varepsilon_{\ell 1}$, of all companion specimens which was observed at a stress level of $0.90\ F_u$ was determined. To subject a fatigue specimen from the same series to $F_{max} = 0.90\ F_u$, the specimen was loaded, with the same strain rate of 10^{-5} in/in/sec, as used to test the companion specimens, until a longitudinal strain $\varepsilon_{\ell 1}$ was reached. The corresponding load was considered to be $F_{max} = 0.90\ F_u$. Knowing a certain desired range, R, the minimum load, F_{min}, could thus be calculated. Then values for F_{max} and F_{min} were set in the load programmer of the testing machine, and then the fatigue test was continued with the repeated load oscillating between these limits at a stress rate of 6000 psi/min. This procedure implies that variations in strength between specimens express themselves in corresponding variations of the stress-strain relationships. This trend was confirmed by the results from static tests. In addition to this procedure, F_{max} was also determined as a fraction of the average ultimate load of all companion specimens. Essentially the same general trends were obtained; however, the scatter of test data was considerably larger.

To correlate the results obtained from all batches, f_{max} and f_{min} were given as ratio of f_{cup}; hereafter referred to as the stress levels σ_{max} and σ_{min}.

Similar to the specimen subjected to fatigue loading, the level of sustained loads was defined by the longitudinal strain obtained from the static tests, $\varepsilon_{\ell 1}$, for a given stress level. The specimens were loaded with a strain rate of 10^{-5} in/in/sec until $\varepsilon_{\ell 1}$ was reached. The corresponding load was read from the load-strain curve while manually holding

the load constant. The load was then set in the load-programmer of the testing machine and held constant till failure.

The number of specimens and their batch designation subjected to fatigue loads at different maximum stress levels, σ_{max}, and stress ranges, R, are given in Tables (4.5), (4.6), and (4.7) for specimens tested at an age of 7, 28, and 90 days, respectively. Similar details for specimens subjected to sustained loads are given in Table (4.8).

In order to minimize the influence of continued hydration during the tests, especially of young concrete, the duration of a particular test had to be limited. Tests of the 7-day specimens were started on the evening of the sixth day and continued to the morning of the eighth day. All specimens which did not fail or which could not be tested within this period were loaded monotonically to failure to assess any changes in the stress-strain characteristics. Tests for the 28-day concrete were continued up to a concrete age of 30 days, and one week was allowed for the 90-day tests.

During fatigue testing, longitudinal and lateral strains were recorded continuously as a function of load. The following strain readings for each cycle are of particular interest: the maximum strain, ε_{max}, at σ_{max}, and the minimum strain, ε_{min}, at σ_{min}. The maximum strain observed at the last cycle, n_u, was designated by ε_u and will be referred to as the failure strain. Also, Poisson's ratio, ν, and the volumetric strain, ε_v, were determined from the strains at maximum stress levels. The corresponding values at failure were designated by ν_u and ε_{vu} respectively. Attention was also given to the value of $(\varepsilon_{max} - \varepsilon_{min})$, the differential strain of a cycle, and its variation throughout the specimen life.

During the sustained load tests, the longitudinal and lateral strains were also read as a function of time. Then the compressive, tensile, and volumetric strains, as well as Poisson's ratio, were calculated as functions of the time under sustained load. It is worth noting that the time and strains reported for the sustained load are those obtained during the sustained load interval, i.e., the initial strain $\varepsilon_{\ell 1}$ and the time taken to load to $\varepsilon_{\ell 1}$ were not included.

4.2 Test Results

4.2.1 Control Cylinders

The variation of the compressive strength with concrete age, as determined from control cylinders, is given in Fig. (4.1) for series A2 to A19 and in Fig. (4.2) for A20 to A30. Figs. (4.3) and (4.4) show the strength at different ages as a ratio of the 28-day strength, f_{cu28}.

4.2.2 Static Tests

For each batch, three to four specimens were tested monotonically to failure. Average stress-strain curves for concrete in the longitudinal direction tested after 7, 28, and 90 days are given in Fig. (4.5). Fig. (4.6) shows the stress-lateral strain characteristics for concrete tested at these ages. The same data are given in Figs. (4.7) and (4.8) with the stress, f , normalized with respect to the ultimate strength of the prism f_{cup}. According to Fig. (4.7) the stress ratio-strain relation for short time loading is not unique, but a function of the age at which concrete is tested. The descending portion of the stress ratio-longitudinal

strain curve is steeper for specimens tested at an age of 90 days compared to the behavior of specimens tested at 7 and 28 days.

4.2.3 High Repeated Loads: Effect of Maximum Stress, Stress Range and Age at Loading

In this section, the test results of specimens subjected to repeated loads are reported. Results of specimens subjected to sustained loads will be reported separately in section 4.2.4.

As mentioned earlier, the maximum stress level, σ_{max}, the stress range, $R = \sigma_{max} - \sigma_{min}$ and concrete age at time of loading are the parameters to be studied in this phase. Values for σ_{max} corresponding to 0.85, 0.90, and 0.95 were chosen for concrete tested at an age of 7, 28 or 90 days. The stress range was varied between R = 0.05 and $R = \sigma_{max}$, i.e., $\sigma_{min} = 0$. All fatigue tests were conducted at a constant stress rate of 6000 psi/min. Only a limited number of parameters were investigated for concrete ages of 7 and 90 days. The corresponding results are summarized in Tables (4.9) and (4.13). The test results obtained from specimens which were loaded at a concrete age of 28 days are given in Tables (4.10), (4.11), and (4.12) for maximum stress levels, σ_{max}, of 0.95, 0.90, and 0.85 and 0.80. In most cases four specimens were tested for each parameter. The logarithmic average of the cycles to failure, $\bar{n}_u$, for each parameter is calculated and tabulated in Table (4.14).

In addition, penetrants were used to investigate visually the crack pattern on the surfaces of some of the specimens during testing. A detailed report on the results of these studies will be given in [7].

4.2.3.1 Strength Data

Effect of maximum stress and stress range

Most fatigue data reported in the past were conducted at maximum stress levels well below the sustained load strength, thus causing failure after more than 1000 cycles. Under such conditions a decrease in the maximum stress and/or the stress range results in an increase of the number of cycles required to fail a specimen. The tabulated logarithmic averages of the cycles to failure in Table (4.14) also confirm the increase in cycles to failure with decreasing maximum stress level and/or stress range for the low cycle fatigue range. This trend is also apparent in Fig. (4.9) and Fig. (4.10). Fig. (4.9) gives the relationship between the cycles to failure and the maximum stress level, for constant stress ranges. However, decreasing R, at a constant σ_{max}, from its maximum value, i.e., $\sigma_{min} = 0$, to 0.50, results in a considerably higher increase in the cycles to failure when compared to a decrease from 0.50 to 0.05, particularly at high values of σ_{max}. In Fig. (4.10) the variations of the cycles to failure with the stress range for constant maximum stress levels are given. These relationships are almost vertical for higher maximum stress levels, particularly $\sigma_{max} = 0.95$, and stress ranges, R less than 0.50. On the other hand, for lower maximum stress levels, $\sigma_{max} = 0.85$, or stress ranges, R greater than 0.50, the number of cycles to failure is more sensitive to changes in either σ_{max} or R. The intersects of the average lines in Fig. (4.10) with the $\bar{n}_u$ axis, i.e., R = 0, represent an "equivalent time to failure" under sustained load. For maximum stresses below the sustained load strengths, one would expect the R versus $\bar{n}_u$ relationship to approach the $\bar{n}_u$ axis assymptotically, giving a value of $\bar{n}_u = \infty$ for R = 0.

Effect of concrete age at loading

The influence of concrete age at loading has been studied little in the past [35,36]. For fatigue tests at stresses below the sustained load strength it has been recommended to eliminate the influence of continued hydration and the subsequent gain in ultimate strength during testing [19]. In the range of low cycle fatigue, the short time needed to fail a specimen may justify disregarding effects of continuing hydration except for very young concrete.

Within this phase, concrete was subjected to repeated loading at an age of 7, 28, and 90 days. Since all tests had to be conducted in a single testing machine, a time limit had to be set for the testing of each batch as mentioned earlier. All the 7-day specimens were kept in the fog room till tested in the laboratory environment to minimize effects of the moisture content prior to testing. Specimens tested at 28 or 90 days were initially moist cured for seven days and left to dry in the laboratory environment until testing. Thus the moisture content of the concrete at the time of testing was different depending on the age of concrete. Static tests were often conducted at the end of the tests but no appreciable strength increase was noted.

The logarithmic average of the cycles to failure for one parameter is plotted in Fig. (4.11) as a function of concrete age. The curves show the effect of age on the fatigue life for maximum stress levels, σ_{max} = 0.95, 0.90, and 0.85 and stress ranges R = 0.50 and R = σ_{max}. Note that in each case the stress levels were determined as a fraction of f_{cup} at the time of loading. There is no clear indication of the dependence of

$\bar{n}_u$ on age at loading for R = σ_{max}. However, for σ_{max} = 0.90 and R = 0.50 $\bar{n}_u$ appears to increase with decreasing age and the 7-day specimens did not fail within the prescribed interval; consequently, no specimens were tested at σ_{max} = 0.85 and R = 0.50. This apparent increase in $\bar{n}_u$ for low ages was attributed to a significant gain in strength due to continuing hydration and becomes significant only in tests where failure did not occur after 30 hours of testing. These results confirm studies of the sustained load strength by Rüsch [35]. Rüsch reported that when young concrete is subjected to sustained loads, the combined weakening effect due to the load damage and the strengthening effect due to continuing hydration reach a net minimum after a certain time after loading. If the applied stresses are not high enough to cause failure, within that time, the specimen will not fail. Studies of the effect of concrete age on sustained load behavior will be reported in a subsequent section.

4.2.3.2 Strain Data

Effect of maximum stress and stress range

Concrete deformations during loading are frequently used as a qualitative measure of damage of concrete and may give an insight into the nature of failure. Often concrete failure has been associated with a limiting strain, and the strains at failure form the basis in structural concrete design. Therefore, the variation of longitudinal, lateral and volumetric strains, as well as Poisson's ratio and ($\varepsilon_{max} - \varepsilon_{min}$) with the number of applied cycles up to failure were investigated.

In Fig. (4.12) longitudinal and lateral strains are given as a function of applied number of cycles, n. The specimens were subjected to different maximum stress levels but the minimum stress was zero in all cases. Increasing the maximum stress level results in an increase in the initial strain, $\varepsilon_{\ell 1}$, to which the specimen was loaded before cycling. Nevertheless, the strains at failure increase with decreasing maximum stress level. For the same level of maximum stress, these failure strains are larger, the greater the number of cycles required to cause failure.

The effect of stress range on the development of concrete strains is shown in Fig. (4.13). Although initially all three specimens were subjected to the same initial strain, $\varepsilon_{\ell 1}$, i.e., the same σ_{max}, the failure strain, ε_u, increased with decreasing stress range or increasing number of cycles to failure. This is true for both longitudinal and lateral strains.

Also, the differential strain of a cycle, $(\varepsilon_{max} - \varepsilon_{min})$, was recorded. Van Ornum [42] had observed that the stress-strain curve of concrete subjected to repeatedly applied axial compression is initially convex upwards, straightens after a few repetitions of load and finally becomes concave upwards and S-shaped as failure approaches. The values of $(\varepsilon_{max} - \varepsilon_{min})$ as a function of the number of applied cycles, as given in Figs. (4.14) and (4.15) are in general agreement with Van Ornum's observations. The strain difference, $(\varepsilon_{max} - \varepsilon_{min})$, which is a measure of the elastic modulus, decreases rapidly for the first few cycles, then stabilizes and increases rapidly near failure. Actual stress-strain relationships recorded during fatigue tests also show these tendencies. Typical examples are given in Appendix B.

The variation of Poisson's ratio, ν, and the volumetric strain, ε_v, at the maximum stress level often have been considered a measure of the integrity of concrete subjected to compressive loads. Typical values for the variation of ν and ε_v with the number of cycles are shown in Figs. (4.16) and (4.17). Fig. (4.16) shows that for $\sigma_{max} = 0.95$ each additional cycle causes a continuous increase of ν and a decrease of ε_v. For $\sigma_{max} = 0.85$, ν is almost constant and ε_v increases slightly for intermediate cycles. At about 80 to 90 percent of the life, ν increases sharply and ε_v decreases to a negative value indicating a volume increase rather than a volume decrease. This phenomenon has been frequently observed and is associated with the opening of vertical cracks in a direction perpendicular to the direction of loading. Varying the stress range for a constant σ_{max} significantly influences the variation of ν and ε_v as shown in Fig. (4.17). An increase in the stress range, R, results in a higher initial value of ν. This value stays fairly constant until failure is imminent. At this stage ν starts to increase rapidly. However, the higher the stress range, the lower is ν at failure. A greater increase in ε_v is noted for higher stress ranges. But near failure, a volume increase is indicated by the sharp decrease of ε_v to a negative value in a similar fashion to the effect of varying σ_{max}.

Effect of concrete age at loading

Old concrete is less ductile than young concrete. This is demonstrated by the static stress-strain relationship shown in Fig. (4.7) for concrete tested at different ages. This variation in the stress-strain characteristic leads one to expect a similar effect of age on the

strain at failure, ε_u, in fatigue testing. Fig. (4.18) shows the variation of the longitudinal and lateral strains for three representative specimens tested at 7, 28, and 90 days, respectively. The maximum stress level and the range of stress are the same for all three specimens. All specimens show the usual slow increase of both the longitudinal and lateral strains with increasing number of applied cycles. At about 80 to 90 percent of the life the rate of strain increases continuously indicating failure. However, there is no indication that failure strains are influenced by concrete age at loading.

The differential strain of a cycle, $(\varepsilon_{max} - \varepsilon_{min})$, follows the general pattern observed earlier, as shown in Fig. (4.19): an initial decrease, then an almost constant value, followed by a rapid increase near failure. The compressibility of the specimen per cycle is more for the 28-day specimen than that of the 7- and 90-day specimens. The accumulated lateral strain, which may be a qualitative indication of the net width of vertical cracks, is larger for the 90-day specimens than for the 7- and 28-day specimens. Similarly, the increase in Poisson's ratio and the continuous decrease in the volumetric strain is more noticeable for the 90- and 7-day specimens compared to the 28-day specimens.

The observations reported on the effect of concrete age at loading apparently are not conclusive, and additional tests may be required. It is, however, likely that the effect of age of concrete on its deformation characteristics is minor if the stresses are expressed as ratio's of the short time strengths at the time of loading and if failure occurs within a short period of time.

4.2.4 High Sustained Loads: Effect of Sustained Stress and Age at Loading

Sustained loads, for which R = 0, can be considered a limiting case of fatigue loading. The tests were thus conducted to supplement the fatigue studies, but are reported separately for convenience. Table (4.15) gives the results for all specimens tested at an age of 7 days for the two levels of the sustained stress, 0.95 and 0.90. The results for the 28-day and the 90-day specimens are shown in Tables (4.16) and (4.17), respectively. The sustained stress levels were 0.95, 0.90 and 0.85. In these tables the strains and Poisson's ratio at failure are also given.

Three to four specimens were tested for each parameter. The corresponding average of the logarithm of time to failure for each parameter was calculated and is given in Table (3.18).

4.2.4.1 Strength Data

The sustained stress level and the concrete age at loading are the two major parameters which affect the response of plain concrete to sustained loads. It is well accepted that an increase of the sustained stress level, σ_{sus}, decreases the time to failure [35,36]. This phenomenon is quantitatively shown in Tables (4.15), (4.16) and (4.17) for concrete loaded at an age of 7, 28, and 90 days. Table (4.18) gives the logarithmic average of the time to failure as a function of both sustained stress level and concrete age at loading. The results are also plotted in Fig. (4.21), which gives the relationship between sustained stress level and time to failure. In this figure, also the time required to load the specimen to the initial sustained stress level is included in the time to failure, t_u. For

high sustained stresses, failure occurs within a certain time period which is shorter, the younger the concrete at the time of loading. However, for lower stress levels where the time to failure exceeds 1000 minutes, the time to failure of young concrete loaded at an age of 7 days is larger and shown by Rüsch [35] to be due to hydration occurring while the specimen is under load. Such hydration partially or completely offsets the damage caused by sustained loading. The potential of concrete for continued hydration will be the higher the smaller the extent of hydration prior to loading, i.e., the younger the concrete at the time of load application. "Post-hardening" or hydration under load is insignificant at high stresses when failure occurs already after a few minutes of loading. It becomes significant for low stress levels when the time to failure may be several days.

The strength-time relationships given in Figs. (4.1) and (4.2) show already that for the particular type of concrete tested in this investigation the difference in static strength between concrete tested after 28 and 90 days is negligible. Thus very little hydration, if any, will occur in concrete specimens subjected to sustained stresses at an age of 28 or 90 days, and the sustained load data for an age at loading of 28 or 90 days, as given in Fig. (4.21), are not affected by hydration after load application. Fig. (4.21) shows clearly that even if hydration effects are excluded, the time to failure for a given stress level depends on concrete age at time of load application.

4.2.4.2 Strain Data

It is generally accepted that an increase of the sustained stress level decreases the accumulated strain at failure [35,36]. However, similar to repeated loading, the strains at failure, ε_u, as well as the time to

failure, t_u, may vary considerably even for a given stress level. This is demonstrated in Fig. (4.22) where the variation of longitudinal and lateral strains with time under sustained stresses are given for four tests at a stress level $\sigma_{sus} = 0.90$. All specimens were from the same batch and were tested at an age of 28 days. There is a clear tendency for both longitudinal and lateral strains to increase with increasing time to failure.

The fact that a decrease of σ_{sus} leads to an increase of t_u and an increase in failure strain is demonstrated in Fig. (4.23). The three sets of data, representative for the logarithmic mean for each parameter, are shown. Unlike fatigue behavior, there is no initial abrupt increase in the compressive strains. At all three levels of sustained stress, the strains initially increase almost linearly with logarithm of time until failure is imminent. Then the strains increase rapidly until failure occurs. Lower levels of the sustained stress are characterized with high longitudinal strains and high lateral strains. Variations of Poisson's ratio, ν, and the volumetric strain, ε_v, with time are given in Fig. (4.24). The pattern is the same as observed in fatigue behavior. Near failure ν rapidly increases and ε_v decreases to a negative value, showing a volume increase rather than a volume decrease.

The effect of concrete age at loading is shown in Figs. (4.25) and (4.26). The longitudinal and lateral strains are consistently the smaller the younger the concrete. The absence of the initial abrupt increase in the strains of concrete under sustained loads can also be observed in Fig. (4.25). The variation of Poisson's ratio and the volumetric strain with time are given in Fig. (4.26). These data, for all ages and all stress levels, are similar to the data reported for fatigue tests.

Similar to ε_u, also the ultimate values ν_u and ε_{vu} tend to increase with increasing time to failure.

4.3 Evaluation of Test Results

4.3.1 Strength Data

In the range of low cycle fatigue, the maximum stress is above the sustained load strength. Therefore, the total time a specimen is subjected to a stress above its sustained load strength, or a certain minimum threshold stress above which microcracks may propagate under a sustained load, may become a significant parameter. Consequently, the behavior of the specimen may be subdivided into a "cyclic effect", which is a stress level and stress range dependent, and into a time dependent "sustained load or time effect". Experimental data reported later in this thesis (Chapter 6, Phase Three) will show that both cyclic and sustained loads can either have a strengthening effect, which may be due to compaction of the cement paste under load and/or relief of residual stresses, or a weakening effect due to accumulating damage or microcracking. These two effects are interchangeably referred to as "hardening" and "damaging" actions.

The interplay between sustained and fatigue loads is qualitatively apparent in Figs. (4.9) and (4.10). These figures show a comparatively insignificant increase in cycles to failure with a decrease in stress range for high maximum stress levels and low stress ranges. However, at lower levels of maximum stress, the number of cycles to failure increases continuously as the stress range, R, is reduced. At low values of R and high vaules of σ_{max}, the specimen is subjected to stresses above the sustained

load strength, during the major part of the total testing time. Then the life of the specimen is primarily influenced by the sustained load effect. The cyclic effect per cycle decreases with a decrease in R. However, because of the constant stress rate, the sustained load effect, per cycle, is independent of R for $\sigma_{min} < \sigma_s$ and decreases only slightly with a reduction of R for $\sigma_{min} > \sigma_s$. Thus decreasing R from e.g. 0.20 to 0.10 will reduce the net damage per cycle only insignificantly, and therefore, will have little influence on the number of cycles to failure.

For $\sigma_{max} = 0.85$ and R greater than 0.50, the cycles to failure are more sensitive to changes in either σ_{max} or R, because the specimen spends only a small fraction of the total testing time under high loads, therefore, the sustained load effect is reduced and the cyclic effect, which is a function of σ_{max} and R, is more dominant.

The relative contribution of the sustained and fatigue load to the specimen life can also be varied by varying the rate of load application during a fatigue test; a phenomenon which has been experimentally studied and will be reported in Chapter 5, Phase Two, of this work. Also, an analytical evaluation, given in Chapter 7, will demonstrate the dependence of low cycle fatigue behavior on cycle and time dependent parameters.

The effect of concrete age on its response to sustained loads was little stuied in the past. Sell [36] reported that the sustained load strength is independent of the age at loading if it is related to the short time strength at the time of failure. Rüsch [35] formulated a relationship to predict the sustained load strength of concrete in which he accounted for the strength increase due to continued hydration and the strength decrease as a result of the damage caused by the sustained loads. In his relation, Rüsch implicitly assumed a unique sustained stress level-time to failure relationship for

concrete under sustained stresses after hydration effects were eliminated. This relationship, which is independent of concrete age at time of loading, was obtained from concrete specimens concentrically loaded at an age of 56 days.

The results obtained herein consistantly show an increase in time to failure, the older the concrete, for all levels of sustained stress which were investigated, Fig. (4.21), except in cases where continued hydration during loading becomes significant, resulting in longer time to failure for young concrete. A similar behavior was observed for concrete subjected to repeated loading, as shown in Fig. (4.11).

Thus, in contrast to previous results [35] these data indicate that the sustained stress level-time to failure relationship is not independent of age even after elimination of hydration effects. This may be due to differences in moisture state which is affected by concrete age. The presence of water within the pores of concrete, might result in a shorter life as confirmed by Husak and Krokosky [15]. This might be due to stress corrosion of the cement paste [37], to the development of hydrostatic pressure in the water filled pores, or due to creep which is accelerated in the presence of moisture.

4.3.2 Strain Data

Concrete deformations developed during loading are significant because they are frequently used as a qualitative measure of damage of concrete and therefore may give an insight into the nature of concrete failure. Also, the existence of a unique envelope curve to describe the relationship between stress and strain at failure of concrete subjected to high compressive loads has been suggested by several investigators [17,40].

If such an envelope exists, a specimen will fail when certain combination of maximum stress and limiting longitudinal strain is reached, regardless of the amplitude of the applied loads [17]. The descending portion of the static stress-strain relationship in longitudinal compression has been suggested to be this unique envelope.

Therefore, in this investigation, concrete strains were recorded with three primary objectives:

a. To use the strain as an indicator or criterion of damage. The variation of longitudinal, lateral and volumetric strains, as well as Poisson's ratio with the duration of load were to be studied to check their validity as an indicator of the degree of damage, which might have been developed at a certain stage of the life of the specimen. This particular topic will be dealt with in more detail in Chapter Six of this thesis.

b. To study the validity of the stress-strain envelope criterion, and check the uniqueness of the descending portion of the static stress-longitudinal strain curve.

c. To investigate the variation of the failure strain, $\varepsilon_{\ell u}$, with the parameters studied, since $\varepsilon_{\ell u}$ is of importance in structural concrete design.

4.3.2.1 Strains Under High Repeated Loads

In this discussion, particular emphasis will be placed on longitudinal strains. Lateral and volumetric strains will be discussed further in Chapter Six.

Fig. (4.27), (4.28) and (4.29) give the variation of the compressive strains, at failure and half the life of the specimen, with the stress range for σ_{max} = 0.95, 0.90, and 0.85. The concrete specimens were 28 days old when loaded. The failure strain, $\varepsilon_{\ell u}$, shown for R = 1.00 is the value given by the descending portion of the static stress-strain curve and is shown only as a basis of comparison. The average curves representing the best fit to the experimental data are summarized in Fig. (4.30). The following conclusions were drawn from these relationships:

a. The compressive strain at failure and half the life is a function of both the maximum stress level and the stress range. The lower the maximum stress level, the larger the strain at failure and at half-life. A decrease in the stress range results in an increase of the failure strain.

b. The failure strain approaches the value given by the descending portion of the static stress-strain curve only for large stress ranges, where the minimum stress level is near zero. (This evidence will be used later in developing an analytical model to predict the failure strains, Chapter 7).

c. The effect of the stress range on failure strains is most significant for lower values of maximum stress. For σ_{max} = 0.95, a decrease of R increases the strain at failure and the half-life only slightly. For σ_{max} = 0.85, variation of R over the entire range significantly affects concrete strains.

These observations hold true throughout the life of the specimen, and not only at failure and half the life as demonstrated in Figs. (4.31) and (4.32). Fig. (4.31) shows the effect of the maximum stress level on the longitudinal strain as a function of the cycle ration, N, for $\sigma_{min} = 0$. The initial strain, $\varepsilon_{\ell 1}$, is highest for $\sigma_{max} = 0.95$, and lowest for $\sigma_{max} = 0.80$. Nevertheless, even before 10 percent of the failure cycles are applied, the specimens loaded to $\sigma_{max} = 0.80$ exhibit larger strains than those loaded to $\sigma_{max} = 0.95$. The failure strains, $\varepsilon_{\ell u}$, increases as σ_{max} is reduced.

The effect of stress range on the development of longitudinal strains is given in Fig. (4.32). All specimens were loaded to $\sigma_{max} = 0.85$, therefore, the initial strain, $\varepsilon_{\ell 1}$, is the same in all cases. For comparison also the strain, as given by the descending portion of the static stress-strain curve, was marked on the line N = 1.0. This strain was already accumulated after 10 percent of the life for R = 0.05, and after 90 percent for R = 0.85. The strains at failure, $\varepsilon_{\ell u}$, increase noticeably with a decrease of the stress range.

In Fig. (4.33), longitudinal strains at failure, which were observed in all individual fatigue tests for various maximum stress levels and stress ranges, are plotted versus cycles to failure; all specimens were tested at an age of 28 days. The strains at half life are given in Fig. (4.34). Although there is an appreciable scatter, there is a clear tendency for the failure strain to increase with an increase in the number of cycles to failure. The average lines of the longitudinal strains at failure and those at half life obtained from Figs. (4.33) and (4.34) are plotted

in Fig. (4.35). The corresponding average lines for each maximum stress level are also shown for comparison. These data indicate that the dominant parameter influencing the failure strain is the number of cycles to failure, n_u. Maximum stress level and stress range affect the failure strain only to the same extent as they influence the failure cycles.

As mentioned earlier, it is likely that the longitudinal strains are also affected by the age of concrete at loading. Fig. (4.36) shows the effect of maximum stress on the longitudinal strains of concrete specimens loaded at 7 days. Similar to the tests of concrete at an age of 28 days, the strains increase as the maximum stress level is reduced. For concrete loaded at an age of 90 days, Fig. (4.37), the difference in the initial strain of specimens loaded at different stress levels dominates and the failure strains is little affected by variation of σ_{max}.

To study the effect of concrete age on the longitudinal strains - cycle ratio relationship, representative test data from each age group are given in Figs. (4.38), (4.39), and (4.40) for $\sigma_{max} = 0.95$, $\sigma_{max} = 0.90$ and $\sigma_{max} = 0.85$, respectively. The initial strain, $\varepsilon_{\ell 1}$, is lowest for the 7-day concrete, however, it is not significantly different for the 28-day and the 90-day specimens. In addition, the following observations were made:

a. The compressive strains were lower for the younger concrete throughout the life of the specimen when compared with the older concrete subjected to similar load conditions.

b. The 28-day specimens showed the highest strains throughout their fatigue life for all levels of maximum stress.

c. The scatter in strains of the 90-day concrete were appreciably larger than those observed for the 7-day and the 28-day specimens.

Thus, on the basis of these results, it seems reasonable to suggest that the age of concrete has some effect on the deformation characteristics of concrete subjected to repeated loading. However, more conclusive answers could only be sought through a more extensive experimental study.

4.3.2.2 Strains Under High Sustained Loads

It was already shown in Fig. (4.22) that for a given concrete age and a given sustained stress level, the longitudinal failure strain, $\varepsilon_{\ell u}$, increases with increasing time to failure. A similar tendency also exists for the lateral strains. In addition, it was observed, Fig. (4.23), that the failure strain increases as the level of sustained load is reduced. This suggested a plot of longitudinal strains at failure, $\varepsilon_{\ell u}$, versus the logarithm of time to failure, t_u, for all levels of the sustained stress, σ_{sus}, as given in Fig. (4.41). Independent of the sustained stress level, the strain at half life as well as at failure increases with the time to failure, t_u, similar to the relation between $\varepsilon_{\ell u}$ and n_u, as given in Fig. (4.35). These relationships can be represented reasonably well by two straight lines. Fig. (4.42) further illustrates that the interrelationship between longitudinal strain and time under constant level of sustained stress holds true throughout the life of the specimen.

The effect of age at loading becomes apparent in the strain-time ratio curves given in Fig. (4.43). The strains are the smallest for the

7-day concrete. The 28-day concrete showed the largest longitudinal strains, while the 90-day concrete showed the largest lateral strains. Although the range of the failure time required to rupture concrete at 90 dyas is noticeably higher than that needed for 28-day concrete, Fig. (4.21), the longitudinal strains for the former is always smaller. It was also found that a linear relationship between $\varepsilon_{\ell u}$ and the logarithm of t_u also holds for concrete subjected to high sustained stresses at an age of 90 days, Fig. (4.4).

The observations made on concrete behavior when subjected to high sustained stresses can be summarized as follows:

a. For the same level of sustained stress, specimens loaded at the same age may fail after different durations of loading. The longer the time to failure, the larger the accumulated longitudinal and lateral strains at failure.

b. The variations of the volumetric strain and Poisson's ratio follows the same pattern whether concrete is subjected to high repeated or sustained loads.

c. The longitudinal strains at failure under sustained stresses are significantly larger than those predicted by the descending portion of the static stress-strain curve. These failure strains also depend on the age of concrete, Fig. (4.45), similar to the short time stress-strain characteristics.

d. The strains at failure, $\varepsilon_{\ell u}$, can be related to the duration of time to failure of a specimen, t_u, subjected to a constant high sustained stress level by a relation of the form $\varepsilon_{\ell u} = A + B \text{ Log } t_u$, where A and B are constants incorporating the effect of age at loading and the type of concrete used. Such a relation takes into account the scatter of data for a given parameter, as well as variations in $\varepsilon_{\ell u}$ and t_u for the same sustained stress level.

4.3.2.3 Failure Envelope

One of the objectives in evaluating the longitudinal strains of plain concrete subjected to high repeated and sustained stresses, was to test the uniqueness of the descending portion of the static stress-strain curve as a limiting strain failure criterion. The existence of such a unique failure envelope becomes already questionable if one takes into account that even the static stress-strain curve is not unique but a function of the stress or strain rate and the age at which the concrete is tested. In addition, the data reported previously show that even for a constant stress level, the longitudinal strain at failure is dependent on the specimen life, both for fatigue and sustained loads. The longer the time to failure, the larger the strain at failure. From the limited experimental study it was also observed that the failure strain is a function of the age of concrete at loading.

The average longitudinal strains for different stress ranges, R, are given in Fig. (4.46) as a function of the maximum stress level, ε_{max}. The same figure also shows the longitudinal strains as given by the static stress-strain curve determined at a strain rate of 10^{-5} in/in/sec. Fig. (4.46) again shows that the static stress ratio - longitudinal strain curves for plain concrete is not a unique failure envelope. In addition, it can be seen that concrete strain at failure lies between two extreme values: a minimum value given by the descending portion of the static stress-strain diagram, and a maximum value as obtained in sustained load tests. The failure strain under fluctuating loads is the higher the smaller the stress range.

4.4 Summary and Conclusions

In Phase One, the response of plain concrete subjected to high repeated and sustained compressive loads was investigated. The maximum stress, the stress range, and the concrete age at load application were the main variables in the fatigue tests. Under sustained loads, the sustained stress level and the concrete age at loading were studied. The effect of these parameters on concrete strength and strains was evaluated. Longitudinal, lateral, and volumetric strains, as well as Poisson's ratio and the differential strain of a cycle were recorded throughout the specimen life and at failure.

The findings of this phase can be summarized as follows:

a. The static stress ratio - longitudinal strain relationship is dependent on the concrete age at testing. The younger

the concrete at testing, the larger the strains at a given stress level. The descending portion of the curve is steeper, the older the concrete at loading.

b. When concrete is subjected to high repeated stresses, a decrease of maximum stress level and/or stress range results in an increase of the cycles to failure. This increase in failure cycles is insignificant for high maximum stress levels and low stress ranges. This is attributed to the domineering influence of the time dependent "sustained load effect". The "cyclic effect", which depends on stress range and maximum stress level is more important for lower stress levels and larger stress ranges.

c. The age of concrete at which it is subjected to repeated loads seems to have little effect on the number of cycles to failure for stress levels larger than 0.90. Under sustained stresses of 0.95 and 0.90 of the static ultimate strength, the time to failure decreases with decreasing age of concrete. For lower sustained or repeated stresses, the load dependent damage can be offset partially by a gain in strength due to the continued hydration during loading. This leads to an increase in cycles or time to failure of young concrete compared to the fatigue life of older concrete.

d. The variation of longitudinal and lateral strains of concrete subjected to high repeated or sustained stresses is

characterized by an increase during the initial stages of loading. This is followed by a period of stabilization, and a rapid increase of strain near failure indicating rapid crack propagation. The volumetric strains increase initially, then they stabilize and decrease near failure to a negative value indicating a volume increase rather than a volume decrease. Corresponding tendencies were observed for the variation of Poisson's ratio.

e. The failure strains under repeated loads are higher, the lower the level of the maximum stress and/or the stress range. The failure strains under sustained loads are higher, the lower the sustained stress level.

f. For the same stress level, the failure strains are higher, the longer the time to failure for a particular specimen.

g. Longitudinal strains at failure under high sustained stresses are the higher, the older the concrete at the time of loading.

h. There is a linear relationship between the longitudinal strain at failure and the logarithm of the cycles to failure which is little affected by stress range and maximum stress level. A similar relation exists between longitudinal failure strain and logarithm of time to failure for concrete under sustained loads.

i. For concrete subjected to high repeated or sustained stresses there is no unique criterion describing the longitudinal strain at failure. In all cases, the failure strain is

larger than the strains given by the descending portion of the static stress-strain curve. For each maximum stress level, the failure strain is larger, the smaller the stress range; the largest failure strains were observed for sustained stresses where the stress range is zero.

5. PHASE TWO: EFFECT OF SPEED OF TESTING ON RESPONSE OF CONCRETE TO STATIC AND HIGH REPEATED LOADS

5.1 Introduction

It was shown in Phase One that in the range of low cycle fatigue, where the maximum stress level is higher than the sustained load strength, both 'sustained-load' and 'cyclic' effects contribute to the response of plain concrete when subjected to high repeated loads. The sustained load effect is a function of the time the concrete has to resist high stresses. Thus, it is likely that the frequency of testing would affect both strength and strain of concrete subjected to such high repeated loads. Throughout Phase One a stress rate of 6000 psi/min was kept constant, even in the test series where the range of stress was the major parameter, resulting in a variable frequency of testing for different stress ranges.

To the author's knowledge no previous attempt has been made to study the effect of rate of load application or frequency, on concrete response to high levels of compressive loads. In fatigue tests on concrete beams subjected to comparatively low repeated flexural loads, the frequency of testing was varied between a maximum of 440 and a minimum of 70 cycles/min [18]. It was concluded that there is no significant effect of test frequency on the cycles to failure and it was suggested that considerable time can be saved in future investigations by conducting flexural fatigue tests at the high speed. In axial compression, reported test data [2] are limited and show no consistent frequency effect on concrete fatigue strength.

The purpose of this phase was to study the effect of speed of testing on the response of concrete to both static and high repeated loads. In the repeated load tests only one maximum stress level of 0.90 of the static ultimate strength, as determined at a strain rate of 10^{-5} in/in/sec, was investigated.

5.2 Test Program and Procedures

Details of mix proportions, specimen size, curing, instrumentations, etc., for this phase, have already been given in Chapter Three. All specimens were tested at an age of 28 days, and only longitudinal strains were measured.

Sixty control cylinders were tested to show the variation of concrete strength with age; batches designated by the letter C were cast and a total of 45 prisms (4 in by 4 in by 12 in) were tested to study the effect of speed of testing on concrete subjected to static and repeated loads.

For the static tests, two groups, each consisting of three prisms from batch C1, were tested to failure at strain rates of 10^{-3} and 10^{-7} in/in/sec. Three prisms from batch C1 were also tested statically at the basic strain rate of 10^{-5} in/in/sec to further check the reliability of the strain measurements of Phase One as compared with this phase, and to be used as a basis for defining the maximum stress level and the stress range in fatigue tests.

Specimens from series C2 to C5 and those remaining from C1 were subjected to repeated loads. The repeated loads were applied following a saw-tooth pattern at constant stress rates, of 600 or 60,000 psi/min, to

supplement the tests from Phase One which were conducted at a stress rate of 6,000 psi/min. The maximum stress level, σ_{max}, was 0.90, and the stress range, $R = \sigma_{max} - \sigma_{min}$, was 0.10, 0.50, and 0.90. The static strength of the prism, f_{cup}, is the average of specimens tested at a strain rate of 10^{-5} in/in/sec. The maximum stress level, σ_{max}, was defined by the average longitudinal strain, $\varepsilon_{\ell 1}$, obtained from companion specimens as already described in Phase One.

The number of specimens tested for each parameter is given in Table (5.1). Batch designations and test programs are summarized in Table (5.2).

5.3 Test Results

5.3.1 Control Cylinders

Twelve control cylinders were cast with each batch to show the variation of concrete strength with age. A group of three cylinders were tested at an age of 3, 7, 14, and 28 days. The results are given in Fig. (5.1). Fig. (5.2) gives the variation of average strength, normalized by the 28-days strength, with concrete age.

5.3.2 Static Tests

The static tests conducted at the basic strain rate of 10^{-5} in/in/sec were used to define the maximum stress level in the fatigue tests. An average static stress-strain curve is given in Fig. (5.3). Fig. (5.4) gives the same relationship with the stress normalized by the ultimate strength of the prism, f_{cup}.

5.3.3 Effect of Strain Rate on Behavior Under Static Loads

Table (5.3) summarizes the results of the static tests at the various strain rates. Considering the strain rate of 10^{-5} in/in/sec as the base, an increase of the strain rate by two orders of magnitude, to 10^{-3} in/in/sec, increased the static strength by 15 percent but reduced the ultimate static strain by 5 percent. Reducing the strain rate to 10^{-7} in/in/sec, resulted in an 8.5 percent decrease of the static strength, and increased the ultimate static strain by as much as 44 percent. It has been observed by Watstein [45] and confirmed herein, that at strain rates higher than 10^{-5} in/in/sec the strength increase, with increasing strain rate, is more pronounced than at lower strain rates.

The average stress-strain curves for the tests conducted at various strain rates are given in Fig. (5.5). These were plotted also in Fig. (5.6) with the stress normalized by the corresponding prism strength. The effect of the strain rate on concrete strain is evident already at stresses less than 50 percent of the static strength, but it becomes more pronounced at higher stresses, and for the descending portion of the stress-strain curves.

5.3.4 Effect of Stress Rate on Behavior Under High Repeated Loads

Test results from specimens subjected to high repeated loads with a stress rate of 60,000 psi/min are tabulated in Table (5.4). For each specimen the cycles to failure, n_u, the strains at maximum and minimum stress level of the last cycle, and the corresponding ultimate strain obtained from the basic static tests, are given. Similar data for specimens

loaded at a rate of 600 psi/min are given in Table (5.5). Other parameters being constant, a decrease in stress rate resulted in a decrease in the number of cycles to failure, while the strain at failure increased significantly.

The effect of stress rate on the fatigue strength of concrete is more apparent in Fig. (5.7). There, the variation of cycles to failure with the stress range is given. The maximum stress level, σ_{max}, was kept constant at 0.90. For a constant stress range, varying the stress rate from 600 psi/min to 60,000 psi/min increased the average cycles to failure by more than one order of magnitude. The average lines of Fig. (5.7) are presented in Fig. (5.8) together with the average relationship for a stress rate of 6,000 psi/min obtained in Phase One. For each of the three stress rates, a decrease in the stress range increases the number of cycles to failure.

The variation of longitudinal strains with number of applied cycles for stress rates of 600 and 600,000 psi/min is shown in Fig. (5.9). The data are representative of the mean values of each parameter. Specimens loaded at the lower stress rate generally showed larger strain for a given number of cycles than the specimen loaded at the higher stress rate. For the same stress range, also, the failure strains were the higher the lower the stress rate. In Fig. (5.10) the longitudinal strain is given as a function of the cycle ratio, $N = n/n_u$, for the two stress rates and two stress ranges. The following observations were made:

a. For a constant stress range, the strains at the lower stress rate are larger throughout the life of the specimen and at failure.

b. In tests at the lower stress rate, a large fraction of the failure strain is accumulated during the initial 10 percent of the fatigue life of the specimen. For intermediate life ratios, from 0.10 to 0.90, the strains increase linearly. Near failure, the strains accumulate and quickly increase to failure for both stress rates. These observations are in agreement with those of Phase One.

c. For a constant stress rate, decreasing the stress range significantly increases concrete strains throughout the life history, as well as at failure, as shown in Fig. (5.11).

5.4 Evaluation of Test Results

5.4.1 Effect of Strain Rate on Behavior Under Static Loads

The test data are in agreement with those obtained in previous investigations and therefore will not be discussed any further.

5.4.2 Effect of Stress Rate on Behavior Under High Repeated Loads.

The experimental results of Phase One and Phase Two have confirmed that the strength and deformations of concrete subjected to high repeated loads are dependent on the rate of load application. In Fig. (5.12), the cycles to failure are given as function of the stress rate for σ_{max} = 0.90 and R = 0.10, 0.5 and 0.90. These data clearly show that the cycles to failure increase with increasing stress rate and/or decreasing stress range. A change in the stress rate and/or the stress range will influence the time span during which a specimen has to resist stresses

higher than a certain threshold stress, i.e., the "sustained load effect". For the same stress rate, increasing the stress range reduces the failure cycles, and therefore reduces this time, and thus, the "sustained load" contribution to ultimate failure. For a given stress range, the lower the strain rate, the larger the "sustained load effect" and the less the "cyclic effect". The role of sustained load and cyclic effects will be discussed further in Chapter 7 of this report.

In addition to the effect of stress rate during a fatigue test, also the strain rate used in static tests of companion specimens, deserves attention: In Phase One the static tests were conducted at a strain rate of 10^{-5} in/in/sec and the fatigue tests were run at a stress rate of 6000 psi/min. If the stress level for the fatigue test at a stress rate of 60,000 psi/min would be determined from static tests at a strain rate faster than 10^{-5} in/in/sec, then, the maximum stress used in the fatigue tests would be higher, and consequently, the number of cycles to failure lower than the values reported in this section. Under such conditions the effect of stress rate on the fatigue behavior of concrete may be considerably less than that shown in Fig. (5.12).

To further substantiate the effect of stress rate on the fatigue life of concrete subjected to high compressive stresses, a statistical analysis was performed to check the statistical significance of the difference between sets of data obtained for different stress rates. The analysis was based on the logarithm of the failure cycles. This analysis is described in more detail in Appendix A. The results for stress ranges

of 0.90, 0.50, and 0.10, respectively, are given in Tables (5.7), (5.8), and (5.9). The probability that a set of experiments falls within the range given by the data of this investigation was at least 76 percent. Comparing results from tests at various stress rates and constant range of stress, consistently yielded a probability of 99.9 percent that the cycles to failure were higher the higher the stress rate.

The variation of concrete strains at half-life and at failure with the range of stress are given in Fig. (5.13). For comparison, the failure strain at $\sigma_{max} = 1.0$, obtained in static tests which were conducted at 10^{-5} in/in/sec, is indicated at R = 1.00. It is evident that for a constant stress rate, the strains are higher the lower the stress range. For a constant stress range, the strains increase with decreasing stress rates.

Fig. (5.14) and (5.15) show the relationship between the failure strain and the number of cycles to failure for all specimens tested in this phase at stress rates of 600 and 60,000 psi/min, respectively. Fig. (5.16) gives a similar relationship for specimens tested in Phase One at a stress rate of 6,000 psi/min. Also included in these three diagrams are the average values of failure strains and cycles to failure for the various stress ranges and stress rates. Similar to the data already reported in Phase One, Fig. (4.35), there is a unique relationship between failure strain, $\varepsilon_{\ell u}$, and cycles to failure, n_u, for a given stress rate, which is independent of the stress range. Because of the increase in cycles to failure with a reduction of stress range, also the average failure strain increases as the stress range is reduced. This effect is most pronounced for low stress rates and less visible for high stress rates. Fig. (5.17)

summarizes the relationship between the average failure strain for a given set of parameters, i.e., cycles to failure, stress range, and stress rate. Generally, it may be concluded that the strain at failure is larger, the longer the time a specimen spends at a stress level larger than a threshold stress.

5.5 Summary and Conclusions

The effect of speed of testing on static and fatigue strength of concrete at high stresses was studied. The static loads were applied at three different strain rates: namely, 10^{-3}, 10^{-5}, and 10^{-7} in/in/sec. The static stress-strain relationship obtained with a strain rate of 10^{-5} in/in/sec was used to define the stress levels in repeated load tests. The same strain rate was used in applying the first cycle of a fatigue test. The fluctuating loads were applied at two stress rates, 600 and 60,000 psi/min, to supplement the stress rate of 6,000 psi/min at which all fatigue tests of Phase One were conducted. The results obtained were evaluated to show the effect of speed of testing on concrete strength and strains. The findings of this phase can be summarized as follows:

a. The static stress-strain relationship is dependent on the strain rate. High strain rates cause a more significant increase in concrete strength, while low strain rates significantly increase the longitudinal strains.

b. The rate at which companion specimens are loaded statically to failure and which is maintained during the first cycle of a fatigue test may influence the maximum stress and, thus, the number of cycles to failure of a fatigue test.

c. The number of cycles to failure is smaller and the failure strain is larger, the lower the stress rate maintained during repeated loads.

d. In the range of low cycle fatigue, lower stress rates increase the "sustained load effect", while high stress rates increase the "cyclic effect".

e. The effect of strain and stress rates further invalidate the uniqueness of the static stress-strain curve as a limiting strain failure criterion.

6. PHASE THREE: EFFECT OF HIGH REPEATED AND SUSTAINED LOADS ON SUBSEQUENT STATIC STRENGTH

6.1 Introduction

It has been stated previously that the significant effect of test frequency on the fatigue strength of concrete at high stress levels may be attributed to a combination of two parameters, namely, the number of applied cycles and the length of time during which a specimen has to sustain stresses larger or equal to a certain threshold stress. In order to evaluate the experimental data accordingly, it is necessary to determine the damage which occurs in concrete during either a sustained load or a fatigue test. It is assumed, for the time being, that the strength of a specimen (from here on referred to as the reloading strength) after a certain number of cycles, less than those causing failure, is a valid indication of the amount of damage caused by cyclic loading. Likewise, the reloading strength of a specimen subjected to sustained loads for a time less than that to cause failure is an indication of sustained load damage. At first glance, one is inclined to assume that during the course of a sustained or repeated load test the initial static strength decreases progressively with time or number of applied cycles. The literature contains reports on a limited number of tests conducted to determine the variation of the static strength of concrete at different stages of its load history [4,14,39,43]. As reported earlier, data from these investigations suggest that the strength of concrete, after a limited number of load cycles have been applied, may either be unaffected or may even be larger than the strength of a specimen without previous load history.

The objective of this phase was to supplement these results by investigating the static strength of concrete prisms after they had been subjected to high repeated and sustained stresses. To avoid ambiguity, certain terms used in this section are defined here:

a. Static strength, f_{cup}: average strength obtained by testing companion specimens, without previous load history, statically to failure at a strain rate of 10^{-5} in/in/sec.

b. Cycle ratio, N: ratio of number of applied cycles to number of cycles to cause failure.

c. Time ratio, T: ratio of time a specimen is subjected to sustained stress to the time required to cause failure.

d. Life ratio, L: refers to both N and T, i.e., partial loading under fatigue or sustained loads.

e. Reloading strength, f_{cur}: strength of specimen loaded monotonically to failure after it has been subjected to a known life ratio. The reloading strength ratio, $\sigma_{cur} = f_{cur}/f_{cup}$, gives the reloading strength as a fraction of the static strength. σ_{cur} is equal to unity for L = 0. For L = 1.0, i.e., at failure, $\sigma_{cur} = \sigma_{max}$ (or σ_{sus}).

6.2 Test Program and Procedures

Details of mix proportions, curing, casting and preparation of specimens were already given in Chapter Three. All specimens were tested at an age of 28 days. Longitudinal and lateral strains were measured.

This phase of the study comprises three subphases:

Phase 3-A deals with the variation of the reloading strength of plain concrete prisms subjected to sustained loads at a constant stress level, $\sigma_{sus} = 0.90$. Specimens were subjected to time ratios of 0.30, 0.60 and 0.90. The objective of Phase 3-B was to study the variation of reloading strength of concrete when subjected to cyclic loading between a maximum stress level of 0.90 and a zero minimum stress level. Cycle ratios of 0.30, 0.60 and 0.90 were investigated.

Phase 3-C was similar to Phase 3-B, but the level of the maximum stress was 0.95. Specimens were subjected to cycle ratios of 0.20 and 0.40.

The stress required to reach a certain stress level was determined by initially loading the specimen to a certain longitudinal strain, $\varepsilon_{\ell 1}$, as described in Phase One.

As pointed out previously, the scatter of experimental data in sustained load and fatigue testing is considerable even if specimens from the same batch are subjected to the same type and magnitude of load and even if all other controllable factors are kept constant. However, it has also been noticed in Phase One, Fig. (4.22), that a specimen with a longer life exhibits larger longitudinal strains. This tendency was utilized to determine the life ratio taken up prior to loading a specimen monotonically to failure.

To determine the duration of loading for specimens of Phase 3-A, after which a certain life ratio was reached, two sets of curves were prepared from the data of Phase One for all specimens subjected to σ_{sus} = 0.90 at an age of 28 days. The first set shows the variation of the longitudinal strains with duration of loading and is shown in Fig. (4.22), while the second set gives the relation between longitudinal strains and the time ratio, Fig. (4.42). For each new batch of concrete tested within subphase 3-A one or two additional specimens were tested to failure under sustained loads and these results were added to the data from Phase One. Figs. (4.22) and (4.42) clearly show that for a given stress ratio the longer the time to failure the larger is the longitudinal strain observed after a given time ratio. For the reloading strength experiments of phase 3-A, a record of longitudinal strain versus time was kept during each test and the values plotted in diagrams which contained the data shown in Fig. (4.22). The time to failure, t_u, and thus, the longitudinal strain, corresponding to a predetermined time ratio, was estimated assuming that t_u of the specimen being tested is equal to t_u of a specimen whose longitudinal strain-time relationship coincided with that of the partially loaded specimen. In several cases, extrapolation between two curves, from those closest to the strain-time relationship of the specimen for which t_u had to be determined, was required. However, in general, it was fairly easy to determine the strain corresponding to the required time ratio. An example of the use of this procedure is shown in Fig. (6.7). In this way the specimens were subjected to time ratios of 0.30, 0.60 and 0.90. Once the desired time ratio was reached, the specimen was loaded to failure

to determine the reloading strength at that instant of its life history. For this, the same strain rate of 10^{-5} in/in/sec, used in the static tests and in initially loading the specimen to the level of the sustained stress, was used.

In Phase 3-B, specimens were subjected to cycle ratios of 0.30, 0.60 and 0.90, at a maximum stress level of 0.90, before loading the specimens statically to failure. To estimate the cycles to failure, n_u, sets of curves similar to those of phase 3-A, and showing the variation of the longitudinal strains with the number of cycles and cycle ratio, were prepared from the data of Phase One, for specimens subjected to $\sigma_{max} = 0.90$ and $\sigma_{min} = 0$ and failing after various values of n_u. The number of cycles to failure, n_u, and the longitudinal strain at which a certain cycle ratio, N, had been reached, were determined employing a procedure similar to that outlined for phase 3-A.

Similarly, in phase 3-C, specimens were subjected to cycle ratios of 0.20 and 0.40, at a maximum stress level of 0.90, to determine their reloading strength.

A total of 66 specimens was tested within this phase. Batches tested are designated by the letter B. Twenty-five specimens from B1 and B4 were tested within Phase 3-A, 29 specimens from batches B5 to B10 were tested for Phase 3-B and 12 specimens from B11 and B12 were tested for Phase 3-C. For each set of parameters (stress level and life ratio) additional specimens were tested until the difference in test results, for the variables to be studied, became statistically significant. Details of testing and batch designations are given in Table 6.1.

6.3 Test Results

6.3.1 Control Cylinders

Concrete compressive strength was determined from 6 x 12 in. cylinders tested at an age of 3, 7, 14 and 28 days, respectively. The variation of strength with age is given in Fig. (6.1). Figure (6.2) shows the strength as a ratio of the 28-day strength.

6.3.2 Static Tests

For each of the 12 batches tested within this phase, three to four specimens were tested statically to failure at a strain rate of 10^{-5} in/in/sec. Longitudinal and lateral strains were averaged, and are shown in Figs. (6.3) and (6.4). The same data are given in Figs. (6.5) and (6.6) where the stress is expressed as a ratio of the prism strength, f_{cup}. The longitudinal strain, $\varepsilon_{\ell 1}$, which marked the sustained and maximum stress levels in sustained and repeated load tests for each batch, was determined as described previously.

6.3.3 Effect of Sustained Loads on Subsequent Static Strength

(Phase 2-A: $\sigma_{sus} = 0.90$)

The results from tests, in which specimens were loaded to failure after a time ratio of 0.30, 0.60 and 0.90 had been applied, are given in Table (6.2). The initial longitudinal strain, $\varepsilon_{\ell 1}$, varied from 1.21 to 1.39 x 10^{-3} in/in corresponding to an average of 1.22 x 10^{-3} in/in from the static stress-strain curves. The additional longitudinal strain accumulated during sustained loads, $\varepsilon_{\ell\ell}$, and the time required to reach

that strain, prior to reloading, varied over a wide range for each of the time ratios. This was to be expected from the results reported in Phase One of this work and shown here in Fig. (6.7). Also given in Table (6.2) is the reloading strength ratio at the corresponding time ratio. There is a noticeable increase in the reloading strength ratio for specimens loaded at a time ratio of 0.30, while the reloading strength ratio of specimens loaded at a time ratio of 0.90, is less than unity. To further substantiate this tendency a statistical analysis of the obtained data was conducted. A more complete account of this analysis is given in Appendix A. According to Table (6.3), the mean of the reloading strength at a time ratio of 0.30 is 4.6 percent higher than the static strength, and 0.9 percent higher when the time ratio was increased to 0.60. For a time ratio of 0.90, the mean reloading strength was, however, 2.5 percent lower than the static strength. When these means were compared to the static strength, the mean values of the reloading strength at a life ratio of 0.30 and 0.60 gave a 0.99 and 0.67 probability to be higher than the static strength. At a time ratio of 0.90 the reloading strength was lower than the static strength with a 0.996 probability. A probability higher than 0.83 was obtained for the range of test data at each of the three investigated time ratios. In comparing the mean reloading strength ratio at each time ratio, a probability of 0.95 was obtained for the reloading strength ratio to be higher at T = 0.30 than at T = 0.60, and a probability of 0.97 that the reloading strength at a time ratio of 0.6 is higher than that at a time ratio of 0.90. According to this analysis considerable confidence can be placed on the validity of the experimental data.

6.3.4 Effect of Cyclic Loads on Subsequent Static Strength

(A) Phase 3-B: $\sigma_{max} = 0.90$

Table (6.4) shows the results from tests conducted within this subphase. As expected, longitudinal strains and number of applied cycles, at a given cycle ratio, varied over a wide range. A cycle ratio of 0.30 resulted in an increase in the reloading strength ratio while a strength decrease was observed for the 0.90 cycle ratio. Details of the statistical analysis are given in Appendix A, and Table (6.5) summarizes the results of this analysis.

The mean reloading strength of the 10 specimens loaded to failure at a cycle ratio of 0.30 showed an increase of 5 percent over the initial static strength. The mean of the 9 specimens subjected to N = 0.60, and the 10 specimens subjected to N = 0.90, exhibited a decrease in reloading strength of 0.90 percent and 5.0 percent, respectively. When these means were compared with the static strength, the mean values of the reloading strength at a cycle ratio of 0.30 gave a probability of 0.999 to be higher than the static strength. At cycle ratios of 0.60 and 0.90 the mean reloading strength was lower than the static strength with 0.79 and 0.999 probabilities, respectively. A probability higher than 0.82 was obtained for the range of test data at each of the three cycle ratios investigated. In comparing the mean reloading strength ratio at each time, a probability of 0.999 was obtained for the reloading strength ratio to be higher at N = 0.30 than at N = 0.60, and a probability of 0.997 to be higher at a life ratio of 0.60 than at 0.90. With such degree of confidence it is reasonable to accept the validity of the experimental data.

(B) Phase 3-C: $\sigma_{max} = 0.95$

Results of the 12 specimens loaded to failure, after they had been subjected to cycle ratios of 0.20 or 0.40, are given in Table (6.6). The reloading strength showed only a marginal increase for specimens loaded to failure at N = 0.20 and a marginal decrease for those subjected to N = 0.40. Nevertheless, the statistical analysis gave more than 0.90 probability in the range of test data as shown in Table (6.7). The probability of the mean reloading strength at N = 0.20 to be higher than at N = 0.40 is 0.99. A probability greater than 0.99 was obtained that the mean of the reloading strength at N = 0.20 is higher and that at N = 0.40 it is lower than the static strength.

The mean values of the reloading strength ratio are given as a function of the life ratio in Fig. (6.8), for all of the three subphases. By definition, the reloading strength ratio, σ_{cur}, is equal to unity for a zero life ratio. For a life ratio of unity the reloading strength ratio is equal to the initially applied stress level.

6.4 Evaluation of Test Results

It is hypothesized that concrete may undergo various stages in its response to concentric compressive load of high magnitude. During the initial stages the cement paste may be compacted, i.e., the spacing between the gel particles may be reduced, thus increasing the extent of Van der Waal's bonding; or residual stresses, caused by the drying shrinkage of the paste, may be relieved. Therefore, concrete strength may increase during this stage. Under load the weak bond between aggregate

and paste may start to fail resulting in microcracking and a gradual strength reduction. Near failure these interfacial cracks propagate through the mortar and are finally linked together to form a continuous failure plane. Tests reported in the literature were conducted in an attempt to explain qualitatively or quantitatively the effect of these strength increasing and strength decreasing mechanisms. These strengthening and weakening mechanisms are investigated within this phase by observing the variation of both reloading strength and deformation characteristics with life ratio throughout the loading history.

6.4.1 Strength Data

Figure (6.8) shows the variation of the mean reloading strength ratio with life ratio for all parameters studied in this phase. Although at first sight the strength increase above the static strength might seem small or even insignificant, the following considerations may prove the opposite: For a maximum sustained stress level of 0.90 the applied loads have to cause a damage equivalent to a reduction of 10 percent of the static strength. Since during an intermittent stage the reloading strength was increased by about 5 percent of the static strength, the damage has to be 50 percent more before the reloading strength ratio reaches the applied stress level at failure. The same reasoning applies to both fatigue test series. The effect of such an apparently small strength increase becomes even more apparent if we determine the increase in specimen life as a result of 5 percent reduction in the stress level. According to Phase One, Fig. (4.9), a reduction of the maximum stress level from 0.95 to 0.90 would increase the failure cycles from 13 to 133 cycles. A similar decrease in

the level of the sustained stress would increase the time to failure from 7 to 33 minutes.

The results given in Fig. (6.8) suggest that the variation of reloading strength ratio with life ratio is only a function of the magnitude of the maximum stress level, but that it is little affected by the stress range. This follows from a comparison of the data obtained for sustained and repeated loads, which are almost identical for a stress level of 0.90. It is possible that for lower stress levels the maximum reloading strength ratio would be even higher than 1.05 as shown in Fig. (6.8). This assumption is supported by an observed increase of up to 15 percent when concrete specimens were loaded to one million cycles at a maximum stress level ranging from 0.30 to 0.53 [4].

The higher increase in the reloading strength for lower applied stress levels, hypothesized above for the range of low cycle fatigue can be more clearly visualized with the aid of the diagrammetic sketch given in Fig. (6.9). There, a possible variation of the maximum gain in the reloading strength ratio is given as a function of the applied maximum stress level. The data of phase three define but only a small portion of the curve. The boundary conditions for the reloading strength ratio are:

a. $\sigma_{cur} = 1.0$ for $\sigma_{max} = 0.0$

b. $\sigma_{cur} = 1.0$ for $\sigma_{max} = 1.0$

As shown in Fig. (6.9) the reloading strength ratio has to attain a maximum value at a stress level lower than 0.90 but higher than zero. Unfortunately, data obtained from previous investigations cannot be used to better define the sought relationship, because there is no way to assess

the life ratio corresponding to the varying degrees of increase in static strength, reported in the literature.

Figure (6.8) also shows that the reloading strength was larger than the static strength for an average life ratio of 0.60 at a stress level of 0.90. Only during the final 40 percent of the life did the damage cause a reduction of the reloading strength below the static strength. For a stress level of 0.95, the reloading strength remained higher than the static strength for life ratios up to 0.30.

6.4.2 Strain Data

In this section, concrete strains will be analyzed to see whether they reflect the extent of damage caused by the applied loads throughout concrete life.

In the following, it will be tested whether the extent of damage, expressed by a certain reloading strength ratio, can be estimated from the concrete strain, $\varepsilon_{\ell 1} + \varepsilon_{\ell\ell}$, where $\varepsilon_{\ell 1}$ corresponds to the strain immediately after load application, and $\varepsilon_{\ell\ell}$ is the additional strain accumulated during sustained or repeated loading. From a practical viewpoint, it would be of particular interest to find whether a certain concrete strain, below which concrete damage is insignificant, can be defined.

Fig. (6.10) shows the relationship between the reloading strength ratio and the strain ratio for specimens subjected to a sustained stress level of 0.90. The strain ratio is defined as the ratio between the total strain prior to reloading to failure, $\varepsilon_{\ell 1} + \varepsilon_{\ell\ell}$, and the estimated failure strain, $\varepsilon_{\ell u}$, which would have been obtained had the

specimen been subjected to the sustained stress until failure. The procedure for estimating the failure strain, $\varepsilon_{\ell u}$, and the failure time, t_u, has already been given in section 6.2. Also shown in Fig. (6.10) are the mean values of the reloading strength ratio at time ratios of 0.30, 0.60, and 0.90. The average line drawn through the mean values also represents the individual data points satisfactorily. A similar plot is given in Fig. (6.11) for the repeated load tests, where the maximum stress level is 0.90. For convenience, the data from all subphases are summarized in Fig. (6.12). In Fig. (6.12), for a stress level of 0.90, the strain ratio at the time of load application, i.e., $\varepsilon_{\ell\ell}/\varepsilon_{\ell u}$, for the sustained load data, is lower than that for the repeated loads, because the failure strain for sustained loading is higher than for repeated loads (Phase One, Fig. (4.46)). Increasing the maximum stress level to 0.95 increased the initial strain and decreased the failure strain, so that the initial strain ratio was even higher than for the 0.90 stress level fatigue test. The following conclusions were drawn from these diagrams.

a. For both repeated and sustained loading and at a maximum stress level of 0.90, the reloading strength continued to be higher than the initial static strength from the time the loads were applied until the concrete strains reached approximately 70 percent of their value at failure. This unique strain ratio was attained at a life ratio of about 0.60.

b. Although at a stress level of 0.95 the rise of the reloading strength above the static strength was only half of that

at 0.90, the reloading strength continued to be higher until the concrete strains were approximately 70 percent of their failure value. However, this strain ratio was reached at a life ratio of about 0.30.

c. From the limited data available it may therefore be concluded tentatively that under both sustained or repeated loading at different stress levels, the reloading strength is equal to or larger than the initial static strength, as long as the total strain is less than 70 percent of the failure strain for a given load condition.

Finally, it was tested whether the rate of change of longitudinal strains and the variations of volumetric strain during a fatigue or sustained load test can serve as an indication of the reloading strength, and thus the damage accumulated during the test.

In Fig. (6.13), the variation of rate of change of longitudinal strain with life ratio, $d(\varepsilon_{\ell 1} + \varepsilon_{\ell\ell})/dL$, is given for both sustained and fatigue tests at a stress level of 0.90. These data are an average of four tests. Also included in Fig. (6.13) is an average plot of the reloading strength ratio-life ratio relationship for the sustained and fatigue tests. Initially, the rate of change of strain decreases sharply. At a time ratio of 0.50 for the sustained load tests, and a cycle ratio of 0.40 for the fatigue tests, the rate of change of strain reaches a minimum. For a life ratio greater than 0.60, the rate of change of strain increases rapidly for both tests up to a maximum value at failure. Comparing the variations of the rate of change of strain and the reloading strength with the life ratio shows that the initial rapid reduction of the rate of

change of strain conforms with the increase in reloading strength ratio. The rate of change of strain assumes a stable value when the reloading strength ratio reaches its maximum value and starts to decrease. At a life ratio of about 0.60, the rapid increase in the rate of change of strain corresponds to a stage where the reloading strength decreased to a value equal to the static strength. Thus, if one defines the strengthening mechanism interval as the life ratio during which the reloading strength ratio increases from unity to its maximum value, then it can be concluded that the strengthening effect prevails during the initial rapid decrease of the rate of change of strain. On the other hand, the weakening mechanism is indicated by the stabilization of the rate of change of strain and its rapid increase to failure; the transition point being an indication of a unity reloading strength ratio of 1.0.

The strengthening and weakening mechanisms can also be qualitatively defined by comparing the volumetric strain-life ratio relationship with the reloading strength ratio-life ratio relationship. Fig. (6.14) shows the variation of the volumetric strain and reloading strength ratio with life ratio for sustained and fatigue load tests at a stress level of 0.90. In each case, the volumetric strain is an average of four tests. The volumetric strain exhibits an initial increase to reach its maximum value at a life ratio of about 0.30 for the sustained load, and at a life ratio of about 0.20 for the fatigue load tests. For both tests, and at an approximate life ratio of 0.50, the volumetric strain starts decreasing rapidly to reach a negative value before failure, indicating a volume increase rather than a volume decrease. Comparing the variation of the volumetric strain with that of the reloading strength ratio shows that

the initial increase of the volumetric strain corresponds to the initial increase of the reloading strength. The reloading strength ratio decreases to a value of unity when the volumetric strain decreases rapidly to its initial value. Thus, it can be concluded that the strengthening mechanism interval is indicated by the initial increase in volumetric strain. The short stabilization period in volumetric strain with life ratio and its rapid decrease to a negative value before failure indicate that the weakening mechanism dominates. The transition point is an indication of a reloading strength ratio of 1.0.

It is worth noting that the variation of lateral strains and the differential strain of a cycle, $\varepsilon_{max} - \varepsilon_{min}$, as well as Poisson's ratio, with the number of applied cycles, exhibited similar stages. Thus, it can be stated that generally, the variation of concrete strains, Poisson's ratio and modulus of elasticity (proportional to $\varepsilon_{max} - \varepsilon_{min}$) with life ratio, shows the competing process of strengthening by compaction and weakening by microcracking. Initially, the strengthening effect is dominant. For intermediate life ratios, the strengthening and weakening mechanism balance each other. The final stage is characterized by the dominance of the weakening effect which leads to reduction of strength to the level of the applied loads at failure.

6.5 Summary and Conclusions

Concrete specimens were subjected to predetermined life ratios at a sustained stress level of 0.90 and fatigue stress level of 0.90 and 0.95, and then were tested statically to failure to determine their reloading strength. Longitudinal and lateral strains were measured. The statistical

analysis performed on the experimental data resulted in a high degree of confidence and thus justified the following conclusions:

a. The variation of the reloading strength ratio with the life ratio is dependent on the magnitude of the maximum stress level, but is independent of the stress range.

b. For a stress level of 0.90, the reloading strength is higher than the static strength as long as the life ratio is less than 0.60. A maximum gain in strength of 5 percent was obtained when the maximum stress level was 0.90. This increase dropped to 2.5 percent when the maximum stress level was increased to 0.95. Results from other investigations indicate that this strength increase would be larger for lower maximum stress levels.

c. The reloading strength is higher than the static strength, as long as the concrete strains are less than about 70 percent of their failure value. This strain ratio was obtained at a life ratio of 0.60 for a maximum stress level of 0.90, and a life ratio of 0.30 for a maximum stress level of 0.95.

d. The variation of concrete longitudinal, lateral, and volumetric strains, as well as Poisson's ratio and elastic modulus with life ratio, gave a good qualitative indication of strength variation. The initial rapid increase of concrete strains is a reasonable manifestation of the strengthening mechanism resulting from compaction of the matrix and/or relief of residual stresses. The stabilization

of strains for intermediate life ratios, and their rapid increase near failure are indicative of the weakening mechanism due to progressive failure, and thus reduction of strength to reach the applied stresses at failure. The same behavior was observed for the variation of the rate of change of longitudinal strain and the volumetric strain with life ratio.

7. CUMULATIVE DAMAGE OF CONCRETE SUBJECTED TO HIGH REPEATED LOADS

7.1 Objective

It has been hypothesized in previous chapters that plain concrete response to high repeated loads is both cycle- and time-dependent. It was hypothesized, furthermore, that the cycle-dependent effect is a function of maximum stress and stress range, while the time-dependent effect is only a function of the maximum stress and the time concrete has to resist stresses higher than a particular threshold stress, above which crack propagation or "damage" may occur under sustained stress.

In this chapter an analytical model will be formulated to express the cycle- and time-dependent effects separately, so that the response of plain concrete to high repeated loads can be predicted. Both number of cycles to failure, and total longitudinal strain at failure, will be dealt with. The analytical model will reflect the effect of maximum stress level, stress range, and stress rate. However, hydration effects will not be considered.

Two analytical models will be developed: the first model is used to predict cycles to failure. It is based on the extent of "damage" caused by repeated loads. The second model is used to predict the longitudinal strains at failure, and is based on cycle- and time-dependent strains.

7.2 Justification of Analysis

The hypothesis, that concrete response to high repeated loads, is cycle- and time-dependent, has been derived from the experimental data

reported in the previous chapters. Within Phase One, it has been noted that for maximum stress levels, σ_{max} = 0.90 or 0.95, a reduction in range of stress, below a certain value, increases the cycles to failure only little. However, for lower stress levels the cycles to failure increase rapidly with decreasing stress range.

At high stress levels concrete has to sustain stresses well above its sustained load strength, so that failure may eventually occur even if the stress were kept constant. Under such conditions, the time to failure may be more significant than the actual number of cycles. Since a reduction of the stress range, for a given stress rate, does not decrease the time per cycle during which the specimen has to sustain a stress larger than the sustained load strength, the time the specimen has to sustain high stresses is constant for a given number of cycles and may be the controlling factor. The data obtained in Phase Two showed that concrete response to high repeated stress is less dependent on stress range, but highly influenced by the stress-rate, and the cycles to failure increase significantly as the stress rate increases. This is particularly true for small stress ranges, Fig. (5.8), and again the total time to failure, rather than the number of load repetitions, may be governing.

The deformation characteristics of concrete subjected to high repeated loads are also time-dependent, Fig. (5.10), both during the test and at failure. Failure strains are higher, the slower the stress rate, i.e., the longer the time spent at high stresses.

From the foregoing, it seems justified and feasible, at least in theory, to be able to formulate analytical models which express concrete failure cycles and failure strains as cycle- and time-dependent portions, thereby predicting plain concrete behavior in the range of low cycle fatigue.

7.3 Analytical Models

7.3.1 Damage

The term "damage" is used here to define a state of a material in which the applied loads have caused the strength of the material to fall below its initial static strength. In the case of concrete, such damage may correspond to a particular state of crack intensity or crack propagation. By definition, damage is equal to unity at failure.

7.3.1 The Approach

Many problems arise in formulating an analytical model to predict low cycle fatigue damage of plain concrete. Consequently, several simplifying assumptions had to be made initially. Some of these assumptions have to be revised, later on, to achieve better agreement between results, as predicted by the model, and the observed data already reported in earlier chapters. Three phenomena observed in the experiments deserve particular attention when formulating such an analytical model:

a. Repeated and sustained loads affect concrete differently at different stages of the load history. Although concrete continues to deform at varying rates during a fatigue test, its reloading strength stays above its initial static strength for a considerable portion of the total life as shown in Fig. (6.8) of Phase Three. Thus, the applied loads are said to cause "hardening". The hardening period is followed by a stage during which "damage" or progressive microcracking dominates, so that the reloading

strength is less than the initial static strength. However, in the following analysis, the hardening effect is not taken into account and it was assumed that concrete, after being subjected to a certain life ratio, during which no damage or hardening occurs, undergoes a progressively increasing damage until failure.

b. To describe the behavior of concrete under sustained loads, a definite maximum stress can be given below which concrete will not fail or is not progressively damaged. This threshold stress is referred to as the sustained load strength. In fatigue loading, however, especially for large stress ranges, the choice of a threshold stress, below which time effects do not have to be taken into account, is rather arbitrary because damage or microcracking, initiated at a high stress, may continue to propagate also at stresses less than the sustained load strength. For small stress ranges, where the minimum stress level is larger than the sustained strength, the minimum stress may be a proper choice for the threshold stress.

c. Even if cycle-and time-dependent damage, occurring in low cycle fatigue, can be successfully expressed independent of each other, the superposition of the two damage components, to predict total behavior, is a subtle matter which may introduce unpredictable errors.

In the following, three different models, to describe low cycle fatigue behavior of concrete, will be analyzed, and the various problems described above will be taken into account to varying degrees.

7.3.1.2 First Model

The following assumptions are made:

1. Hardening action exhibited at the earlier part of the life of the specimen is neglected, and damage is assumed to propagate from the time loads are applied until failure.
2. Cycle-dependent damage accumulates linearly with the applied number of cycles to failure.
3. Time-dependent damage is caused only by stresses higher than a certain threshold stress, and the damage accumulates linearly with time until load.
4. The threshold stress, σ_{sh}, is assumed to be equal to the sustained load strength of concrete as long as the minimum stress, in the fatigue test, is below the sustained load strength. If the minimum stress is larger than the sustained load strength, the threshold stress is assumed to be equal to the minimum stress.
5. Total damage, in a fatigue test, is determined by simple addition of the cycle- and time-dependent damage portions.

(a) Cycle-Dependent Damage

Let n_u be the actual number of cycles causing failure of a specimen subjected to high repeated loads at a particular stress rate. If time dependent damage can be eliminated, i.e., if the stress rate ratio, β, were infinite, then the specimen would resist n_o cycles until failure, where $n_o > n_u$. In the following, n_o is referred to as the number of cycles to failure under pure fatigue conditions. Assuming linear damage accumulation the cycle-dependent damage in an actual fatigue test after n cycles, therefore, is:

$$D_n = \frac{n}{n_o} \tag{7.1}$$

(b) Time-Dependent Damage

In the fatigue tests the loads were increased or decreased at a constant stress rate ratio, β. In order to calculate the time-dependent damage occurring during a particular cycle, the stress-time history, of a repeated load test, above the threshold stress level, σ_{sh}, is approximated by a step function, in which a constant sustained stress level, σ, acts for a finite time Δt. If the time to failure under a constant stress, σ, is t_u then the damage caused by this stress level during the time increment Δt is:

$$\Delta D_{tl} = \frac{\Delta t}{t_u}$$

For half a cycle, this stress level, σ, varies from a lower limit equal to the threshold stress level, σ_{sh}, to an upper limit equal to the maximum stress level, σ_{max}.

Now, as $\Delta t \rightarrow dt$, the total time dependent damage for a complete cycle is:

$$D_{t1} = 2\int_{\sigma_{sh}}^{\sigma_{max}} \frac{dt}{t_u}$$

since linear accumulations of damage with time was assumed, each cycle causes the same amount of time-dependent damage and after n cycles one obtains:

$$D_t = 2n\int_{\sigma_{sh}}^{\sigma_{max}} \frac{dt}{t_u} \tag{7.2}$$

Since the loads are applied at a constant stress rate,

$$\frac{d\sigma}{dt} = \beta$$

or

$$dt = \frac{1}{\beta}\, d\sigma \tag{7.3}$$

To express t_u in terms of the sustained stress level, experimental data obtained within this study, Chapter 4, Phase One, and elsewhere [7,35] are given in Fig. (7.1). The data are approximated reasonably well by:

$$t_u = 240\ \left(\frac{1 - \sigma}{\sigma/\sigma_s - 1}\right)^2 \tag{7.4}$$

with $\sigma_s = 0.70$ and t_u in minutes.

Substituting Eq. (7.3) and Eq. (7.4) in Eq. (7.2) yields

$$D_t = \frac{2n}{240\beta}\int_{\sigma_{sh}}^{\sigma_{max}} \left(\frac{\sigma/\sigma_s - 1}{1 - \sigma}\right)^2 d\sigma \tag{7.5}$$

It should be noted here that such a simple integration was possible only because of the assumption of linear damage accumulation. If a non-linear damage accumulation is assumed a complex integral would have been obtained which could not be readily solved and a step-by-step integration process of the loading and unloading parts of each applied cycle, would be necessary.

Integrating , Eq. (7.5) one obtains, for the time-dependent damage:

$$D_t = \frac{n}{\beta}\left\{\frac{1}{120\,\sigma_{sus}^2}\left(\frac{(\sigma_{max} - \sigma_s)^2}{1 - \sigma_{max}} - \frac{(\sigma_{sh} - \sigma_s)^2}{1 - \sigma_{sh}} + 2(\sigma_{max} - \sigma_{sh}) + 2\,(1 - \sigma_s)\,\log_e \frac{1 - \sigma_{max}}{1 - \sigma_{sh}}\right)\right\}$$

or

$$D_t = K_1 \frac{n}{\beta} \tag{7.6}$$

where k_1 is equal to the expression between the brackets $\{\{\}\}$.

According to assumption 4, the threshold stress, σ_{sh}, is

$$\sigma_{sh} = \sigma_{min} \quad \text{if} \quad \sigma_{min} > \sigma_s$$

and

$$\sigma_{sh} = \sigma_s \quad \text{if} \quad \sigma_{min} < \sigma_s$$

(c) Combined Damage

In accordance with assumption 5, the total damage caused by cycles of repeated loads, applied at a constant stress rate, β, is:

$$D_{tn} = D_n + D_t$$

Substituting Eq. (7.1) and Eq. (7.6) for D_n and D_t, results in:

$$D_{tn} = \frac{n}{n_o} + K_1 \frac{n}{\beta} \tag{7.7}$$

At failure,

$$n = n_{uc}$$

and

$$D_{tn} = 1.0$$

With these conditions, Eq. (7.7) can be rearranged to read:

$$n_{uc} = \frac{n_o}{1 + k_1 \frac{n_o}{\beta}} \tag{7.8}$$

The above equation yields a theoretical number of cycles to failure, n_{uc}, which can be calculated if the failure cycles for pure fatigue, n_o, are known. The calculated failure cycles, n_{uc}, are equal to the pure fatigue failure cycles, n_o, if the loads are applied with an infinite speed, i.e., $\beta = \infty$, since the time-dependent damage is zero. A reasonable method to estimate n_o will be to rearrange Eq. (7.8) to express n_o as a function of n_{uc}. By substituting the observed failure cycles, n_u, for n_{uc}, for each studied parameter, a value of n_o can be calculated. Then Eq. (7.7) reads:

$$n_o = \frac{n_u}{1 - k_1 \frac{n_u}{\beta}} \tag{7.9}$$

Experiments were carried out at a maximum stress level, σ_{max} = 0.90, stress ranges, R = 0.10, 0.50, and 0.90, and at stress rates, β = 0.15, 1.5 and 15 $\frac{psi}{psi}$ min (note that $\beta = \dot{f}/f_{cup}$ where f_{cup} = 4000 psi), Fig. (5.8).

For low values of β, the time-dependent damage is dominant so that n_u is very insensitive to variations in n_o. Therefore, for each stress range, and $\sigma_{max} = 0.90$, n_o was calculated only from the data obtained for the fastest stress rate, i.e., $\beta = 15$. The results are given in Table (7.1). Then, Eq. (7.8) was used to calculate n_{uc} for the different stress ranges and stress rates as shown in Table (7.2). For a stress range of $R = 0.10$, n_{uc} could not be determined because, under the assumptions made in deriving the model, the time-dependent damage alone would be larger than unity.

Agreement between calculated and observed experimental data is poor. However, both experimental and calculated failure cycles show the same trend. The discrepencies between analysis and tests may be attributed to the assumption that the cycle- and time-dependent damages propagate progressively from the beginning of the test until failure (Assumption 1). This assumption contradicts the experimental findings of Phase Three, Chapter 4, which show that the material initially hardens resulting in a strength higher than its initial strength. In fact, for a maximum stress level of .90, hardening dominates up to a life ratio of 0.60. Consequently, the first model was revised accordingly.

7.3.1.3 Second Model

In this model, it will be assumed that the applied loads have no effect from the time the loads are applied until a certain life ratio has been reached. Thereafter, the two damage components propagate

linearly until failure. Assumptions 2, 3, 4, and 5, of the first model, are retained.

With zero damage up to a life ratio of η, damage can be expressed as follows:

a. The cycle damage caused by a cycle ratio $(1 - \eta)$ is

$$D_n = \frac{(1 - \eta)n_{uc}}{(1 - \eta)n_o} = \frac{n_{uc}}{n_o} \tag{7.10a}$$

where $\frac{1}{(1 - \eta)n_o}$ is the damage per cycle caused by pure fatigue loading.

b. The time-dependent damage also propagates through a life ratio of $(1 - \eta)$, thus:

$$D_t = (1 - \eta)K_1 \frac{n_{uc}}{\beta}$$

where K_1 is given by Eq. (7.6).

With $$K_2 = (1 - \eta)K_1 \tag{7.10b}$$

one obtains

$$D_t = K_2 \frac{n_{uc}}{\beta} \tag{7.10c}$$

c. The combined damage at failure is thus given by:

$$1.0 = \frac{n_{uc}}{n_o} + K_2 \frac{n_{uc}}{\beta}$$

or

$$n_{uc} = \frac{n_o}{1 + K_2 \frac{n_o}{\beta}} \tag{7.11}$$

and

$$n_o = \frac{n_u}{1 - K_2 \frac{n_u}{\beta}} \tag{7.12}$$

Eq. (7.11) and Eq. (7.12) correspond to Eq. (7.8) and Eq. (7.9) of the First Model.

To calculate the pure fatigue failure cycles, n_o, K_2 has to be determined from Eq. (7.10b). The following values were obtained.

For R = 0.10 . . . . . $K_2 = 0.912 \times 10^{-3}$ (7.13a)

for R = 0.50 and 0.90 . . . $K_2 = 0.816 \times 10^{-3}$ (7.13b)

As described earlier, Eq. (7.12) was used to calculate the pure fatigue failure cycles, n_o, for the various stress ranges, using the results from the fatigue tests at the highest stress rate. The calculated values for n_o are given in Table (7.1). The largest difference between n_o and n_u was observed for the smallest stress range, an expected result, because the smaller the range the greater the time-dependent damage, and thus, the fewer the observed fatigue cycles.

Using Eq. (7.11) the theoretical failure cycles, n_{uc}, were calculated for each parameter and are compared with the experimental data in Table (7.2). They are also shown in Fig. (7.2). For R = 0.10, the agreement is acceptable. However, the difference between calculated and observed values increases with increasing stress range.

In determining the K_2 values of Eq. (7.11), the threshold stress level, σ_{sh}, was justifiably assumed to be equal to σ_{min} when R = 0.10. For the stress range of R = 0.50 and 0.90, σ_{sh} was assumed to be equal to the sustained load strength, $\sigma_s = 0.70$. Thus, any time-dependent crack propagation or damage occurring at stresses lower than the sustained strength was neglected. Therefore, the time-dependent damage may have been underestimated, so that, the calculated failure cycles are significantly higher than the experimental data. For the highest stress rate,

this discrepency fades away as time effects contribute only little to the total damage. Maintaining the general approach to distinguish between cycle- and time-dependent damage, better agreement between experiments and analysis may be obtained if we assume the threshold stress to be stress range dependent for a constant maximum stress level. Such an assumption has been made and is described in the following section.

7.3.1.4 Third Model

In addition to the assumptions made in deriving Eq. (7.11) for the Second Model, it is now assumed that for a constant maximum stress level the threshold stress decreases with increasing range. Since the choice of particular values for σ_{sh} is arbitrary, the validity of a certain value for σ_{sh} could only be checked by comparing calculated and experimental failure cycles.

The following values were assumed for the threshold stress:

$$\sigma_{sh} = \sigma_{min} \qquad \text{for} \qquad \sigma_{min} > \sigma_s$$

$$\sigma_{sh} = 0.74 - 0.20R \quad \text{for} \quad \sigma_{min} < \sigma_s$$

The two conditions yield the following values of σ_{sh} for the different stress ranges:

$$R = 0.10 \ . \ . \ . \ . \ . \ \sigma_{sh} = 0.80$$

$$R = 0.50 \ . \ . \ . \ . \ . \ \sigma_{sh} = 0.65$$

$$R = 0.90 \ . \ . \ . \ . \ . \ \sigma_{sh} = 0.55$$

The resulting K values, now designated as K_3, were calculated and used in the evaluation of Eq. (7.11) and Eq. (7.12) in place of K_2. The results are summarized in Table (7.2) and Fig. (7.3). It can be seen that the calculated failure cycles, as predicted by the Third Model, agree very well with the observed values for the stress ranges and stress rates investigated.

7.3.1.5 General Considerations

The First Model for damage of concrete subjected to high repeated stresses resulted in calculated failure cycles which were, except for R = 0.90, much smaller than the observed values, because the time-dependent damage was overestimated. By introducing the "damage life", $(1 - \eta)$, in the Second Model, excellent agreement was achieved for R = 0.10. An equally good agreement was obtained for R = 0.50 and 0.90 after the threshold stress was defined, arbitrarily, to be stress range dependent.

In reality, these refinements of the initial assumptions, leading to the various models, are adjustments of the time-dependent damage such that the resulting calculated failure cycles compare well with the experimental data. Although good reasons for these adjustments were given, it could also be concluded that the cycle- and time-dependent damage can not be simply superimposed, or added arithmetically, to predict failure cycles of concrete subjected to repeated high loads.

Instead of using the arguments which lead to the Second and the Third Model, agreement between experiment and analysis can also be

obtained by arbitrarily adjusting the time-dependent damage, with a stress range-dependent factor, K_4. If damage at failure is expressed by:

$$1.0 = \frac{n_{uc}}{n_o} + K_4 \frac{n_u}{\beta} \tag{7.14}$$

then the following values for K_4 result in excellent agreement between analysis and test data:

$$\text{For } R = 0.10;\ K_4 = 0.752 \times 10^{-3} \tag{7.15a}$$

$$\text{For } R = 0.50;\ K_4 = 1.632 \times 10^{-3} \tag{7.15b}$$

$$\text{For } R = 0.90;\ K_4 = 6.12 \times 10^{-3} \tag{7.15c}$$

7.3.1.6 Relative Magnitude of Cycle- and Time-Dependent Damage

In the following, the interplay between cycle- and time-dependent damage will be discussed. The ratio between cycle-dependent and time-dependent damage is defined as:

$$\alpha = \frac{D_n}{D_t} \tag{7.16}$$

where D_n is the cycle-dependent damage and D_t is the time-dependent damage, hence:

$$\alpha = \frac{n_{uc}}{n_o} \frac{\beta}{K_3 n_o} = \frac{\beta}{K_3 n_o} \tag{7.17}$$

The α-values were calculated according to the Third Model. Fig. (7.4) shows the relationship between α and the stress range for $\sigma_{max} = 0.90$. With decreasing stress range and decreasing rate the cycle-dependent damage is reduced rapidly and is only a small fraction of the

time-dependent damage; e.g., for a stress rate of 600 psi/min and a stress range of 0.90, only 6 percent of the total damage at failure is caused by the cyclic component. In general, it can be concluded that behavior of plain concrete subjected to high repeated stress is significantly controlled by the sustained load action

7.3.1.7 General Interpretation of Strength Data

Using the Third Analytical Model, the experimental data, obtained in Phase One, were explained. Fig. (7.5) gives the relationship between calculated and observed cycles to failure for $\sigma_{max} = 0.90$. Also included are the failure cycles for pure fatigue, n_o, as a function of the stress range. The following observations were made:

a. The pure fatigue failure cycles represent the expected tendency satisfactorily, approaching an infinite value for a zero stress range.

b. The higher the stress range, the larger the cycle-dependent damage. Therefore, at high stress rates the observed failure cycles are close to the estimated values for pure fatigue.

c. For small stress ranges and low stress rates, both observed and calculated values show the domineering influence of the sustained load action. This is evidenced by the small increase in failure cycles with a reduction of the range, since the average lines assume an orientation almost parallel to the stress range axis. This phenomenon fades

away with increasing stress range and/or stress rate. For the relation between cycles to failure and stress range, the limit is given by the pure fatigue condition.

d. The cycles to failure under pure fatigue should also be dependent on the maximum stress level. However, no dependable values for n_o at $\sigma = 0.95$ and 0.85 can be given, because for these stress levels only one stress rate ($\beta = 1.5$) was investigated. Nevertheless, the observation given in (c) can explain, qualitatively, the behavior of the specimens tested in Phase One for $\sigma_{max} = 0.95$, 0.90, and 0.85 as shown in Figs. (4.9 and 4.10). For $\sigma_{max} = 0.95$, the cyclic effect governs failure only at large stress ranges; while the sustained load action dominates at smaller stress ranges; therefore, below $R = 0.50$, the relation between R and n_u is almost vertical. Reducing the stress level to $\sigma_{max} = 0.85$ reduces the time-dependent damage even at low stress ranges. Thus, the observed failure cycles continue to increase with decreasing R.

7.3.2 Failure Strain

In the following, an analytical model, to predict the longitudinal failure strain of plain concrete subjected to high repeated stresses, is described. The model will be formulated for a maximum stress

level of 0.90 to allow comparison of the predicted failure strains with experimental data obtained within Phase One and Phase Two.

7.3.2.1 The Approach

It is assumed that the failure strain of concrete, under high repeated loads, consists of the following components:

(a) An initial "elastic" strain, $\varepsilon_{\ell 1}$, which depends on the maximum stress level. It is the strain which is observed at the maximum stress level of the first load cycle, or at the beginning of a sustained load test. Naturally, this value is not a pure "elastic" strain but includes an irreversible component.

(b) A cycle-dependent strain, $\varepsilon_{\ell n}$.

(c) A time-dependent strain, $\varepsilon_{\ell t}$, caused by stresses above the sustained load strength, f_s.

(d) A creep strain, $\varepsilon_{\ell c}$, which is caused by stresses below the sustained load strength.

Thus, a calculated failure strain can be expressed as:

$$\varepsilon_{\ell uc} = \varepsilon_{\ell 1} + \varepsilon_{\ell n} + \varepsilon_{\ell t} + \varepsilon_{\ell c} \qquad (7.18)$$

This approach is justified by previous experimental evidence, which shows that, for a constant maximum stress level, concrete deformation characteristics are stress range as well as stress rate dependent.

7.3.2.2 The Model

The strain components given by Eq. (7.18) will now be evaluated, independently, and thereafter superimposed to determine a theoretical failure strain, $\varepsilon_{\ell uc}$. Their values will be compared with the experimental values, $\varepsilon_{\ell u}$, from Phase Three.

(a) Initial Elastic Strain, $\varepsilon_{\ell 1}$

This is the strain given by the stress ratio-strain relationship which is obtained at a strain rate of 10^{-5} in/in/sec, for a stress level $\sigma = 0.90$. This strain rate was used for the initial load application in all fatigue and sustained load tests. From Fig. (4.46) an average value of

$$\varepsilon_{\ell 1} = 1.40 \text{ X } 10^{-3} \text{ in/in} \tag{7.19}$$

was obtained.

(b) Cycle-Dependent Strains, $\varepsilon_{\ell n}$

To define this strain component, the failure strain of concrete, under pure fatigue conditions, $\varepsilon_{\ell no}$, has to be determined. Based on the observed failure strains shown in Fig. (4.46), the strain given by the descending portion of the stress-strain curve minus the initial elastic strain seems to be a reasonable choice. If a linear accumulation of the strain, $\varepsilon_{\ell n}$, with pure fatigue cycles, n_o, is assumed*, then the cycle

* The assumption of a linear strain accumulation is of course not in close agreement with experimental data. However, analysis of failure strains, using more realistic strain-cycle or strain-time relationships, is extremely difficult and does not promise to yield significantly different results.

dependent strain is readily given as:

$$\varepsilon_{\ell n} = \frac{n_{uc}}{n_o} \varepsilon_{\ell no} \tag{7.20}$$

(c) Time-Dependent Strain, $\varepsilon_{\ell t}$

This portion of the failure strain can be evaluated by an approach similar to that already used to evaluate the time-dependent damage. By assuming that a sustained stress level, σ, acts over a finite time interval, Δt, during each half cycle, and again assuming a linear strain-time relationship*, the time-dependent strain accumulated in one cycle can be expressed by:

$$\varepsilon_{\ell t1} = 2 \int \frac{dt}{t_u} \varepsilon_{\ell tu} \tag{7.21}$$

then the total time dependent strain after n_{uc} cycles can be expressed as follows:

$$\varepsilon_{\ell t} = 2\, n_{uc} \int \frac{dt}{t_u} \varepsilon_{\ell tu} \tag{7.22}$$

where, $\varepsilon_{\ell tu}$ is the time-dependent failure strain under the sustained stress, σ.

The integration of Eq. (7.22) has to be performed for a stress interval varying from a threshold stress, σ_{sh}, to the maximum stress level, σ_{max}. The terms dt and t_u are already given by Eq. (7.3) and (7.4), respectively. To formulate a relationship between $\varepsilon_{\ell tu}$ and σ, the failure strain envelope for sustained stress, as given in Fig. (4.46), was used. For each sustained stress level, the time-dependent failure strain, $\varepsilon_{\ell tu}$, is the total strain at failure less the initial elastic strain, $\varepsilon_{\ell 1}$. Fig. (7.6)

shows the variation of $\varepsilon_{\ell tu}$ with the sustained stress level, σ. The experimental data can be approximated by:

$$\varepsilon_{\ell tu} = 18\ (1 - \sigma) \tag{7.23}$$

The substitution of Eq. (7.3, 7.4, and 7.23) in Eq. (7.22) yields:

$$\varepsilon_{\ell t} = \frac{n_{uc}}{\beta} \cdot K \tag{7.24a}$$

with

$$K = \frac{3}{20} \int_{\sigma_{sh}}^{\sigma_{max}} \frac{(\frac{\sigma}{\sigma_s} - 1)^2}{(1 - \sigma)}\ d\sigma \tag{7.24b}$$

The level of the threshold stress level, σ_{sh}, was defined as follows:

$$\sigma_{sh} = \sigma_{min} \qquad \text{if} \qquad \sigma_{min} > \sigma_s$$

$$\sigma_{sh} \quad \sigma_s \qquad \text{if} \qquad \sigma_{min} < \sigma_s$$

The K-values for the different stress ranges were calculated accordingly to determine the time-dependent strain given by Eq. (7.24a).

(d) Creep Strain, $\varepsilon_{\ell c}$

Although this is a time-dependent strain, similar to $\varepsilon_{\ell t}$, it is treated separately for convenience. The term $\varepsilon_{\ell c}$ is the time dependent strain accumulated during the time the specimen has to resist stresses lower than its sustained load strength. This strain was estimated using

the rate of creep method [32]. Let us assume that creep is proportional to stress and can be expressed by:

$$c = \omega(t) \tag{7.25}$$

where c = creep under a constant stress of 1 psi.

For a stress f acting during a time interval dt,

$$d\varepsilon_c = f \frac{dc}{dt} dt \tag{7.26a}$$

where ε_c = creep strain caused by a stress f.

Thus the total creep strain at time t is:

$$\varepsilon_c = \int_0^t f \cdot \frac{dc}{dt} \cdot dt \tag{7.26b}$$

where f may be a function of time.

For half a cycle of a constant stress rate fatigue test, the stress, f, is a function of time, and is given by:

$$f = f(t) = \dot{f}t + f_{min} \tag{7.27a}$$

The upper limit of the integral in Eq. (7.26b) will correspond to the time required to load from the minimum stress to the sustained strength, f_s, i.e.,

$$t = (f_s - f_{min}) \frac{1}{\dot{f}} \tag{7.27b}$$

To calculate the creep strain per cycle, a linear creep-time relationship was assumed. Then Eq. (7.25) reads:

$$c = A.t \tag{7.27c}$$

or

$$\frac{dc}{dt} = A \tag{7.27d}$$

With Eq. (7.26b), (7.27a), (7.27b) and (7.27d), the total creep accumulated during n_{uc} cycles is:

$$\varepsilon_{\ell c} = 2An_{uc} \int_{o}^{(f_s - f_{min}) \frac{1}{\dot{f}}} (\dot{f}t + f_{min})dt$$

Performing the integration, the equation can be reduced to:

$$\varepsilon_{\ell c} = A \frac{n_{uc}}{\dot{f}} (f_s^2 - f_{min}^2) \tag{7.28}$$

After non-dimensionalizing the right hand side of Eq. (7.28) by the static strength, f_{cup}, the creep strain can be expressed in terms of stress levels,

$$\varepsilon_{\ell c} = A \frac{n_{uc}}{\beta} (\sigma_s^2 - \sigma_{min}^2) f_{cup}$$

The assumption of a linear creep-time relationship as given by Eq. (7.27c) is rather crude. However, if a more realistic, i.e., a non-linear function were used, the creep strain would be different for each cycle and the integration of the total creep strain, over n_{uc} cycles, would be very difficult. In order to approximate the true creep-time relationship more closely, different values for the coefficient, A, in Eq. (7.27c), will be chosen depending on the time to failure of the particular specimen for which the creep strain, $\varepsilon_{\ell c}$, has to be estimated. The coefficient, A, will be chosen such that the assumed linear relationship coincides with the true creep-time relationship at t = 0 and at t = 1/2 t_{un}, where t_{un} is the total testing time until failure of a specimen subjected to repeated loads. This method is illustrated in Fig. (7.7) which also includes a

realistic relationship for the development of creep under a sustained stress with time [46].

In the following, a relationship for the coefficient, A, will be developed. For this, the creep strain, ε_c, will be expressed as a fraction of the elastic strain, $\varepsilon_{e\ell}$:

$$\varepsilon_c = \varepsilon_{e\ell} \cdot \Phi$$

where Φ is the time-dependent ratio of creep strain to elastic strain. It is assumed that it approaches a finite value of ϕ_∞ for $t = \infty$.

For $f = 1$ psi and $\varepsilon_{e\ell} = f/E$, the unit creep, c, is given by:

$$c = \frac{\Phi}{E} \tag{7.30a}$$

If it is assumed, furthermore, that the linear creep function reaches a value of $\Phi = \Phi_\infty$ after a time m, as shown in Fig. (7.7), then the linear variation of Φ with time can be expressed by:

$$\Phi = \frac{t}{m} \quad \Phi_\infty$$

Then Eq. (7.30a) can be transformed to:

$$c = \frac{\Phi_\infty}{mE} \cdot t \tag{7.30b}$$

which gives a value of the coefficient A:

$$A = \frac{\Phi_\infty}{mE} \tag{7.31}$$

The parameter m has to satisfy the condition stated earlier, that the straight line approximations, for the creep-time relationship, coincide with the experimental curve, given in Fig. (7.7), at half the total test time, 1/2 t_{un}, of a particular specimen subjected to repeated loads.

Then, according to Fig. (7.7), m is

$$m = \frac{t_{un}}{2(\Phi/\Phi_\infty)} \tag{7.32}$$

where Φ/Φ_∞ is the fraction of the creep ratio developed after a time $t = 1/2\ t_{un}$. The duration of a fatigue test, t_{un}, can be determined from the stress range, R, the stress rate ratio, β, and the number of cycles to failure, n_{uc}, calculated from Eq. (7.11). It is:

$$t_{un} = \frac{2R}{\beta}\ n_{uc} \tag{7.33}$$

Substituting Eq. (7.33) in Eq. (7.32) gives:

$$m = \frac{R\ n_{uc}}{\beta(\Phi/\Phi_\infty)} \tag{7.34}$$

After substituting Eq. (7.34) in Eq. (7.31) the coefficient, A, is:

$$A = \frac{\Phi_\infty}{E} \cdot \frac{\beta(\Phi/\Phi_\infty)}{R \cdot n_{uc}}$$

The time t_{un} was calculated for each data point using Eq. (7.33), and then the creep ratio ϕ/ϕ_∞ was determined from Fig. (7.7). To calculate A, also a realistic choice of Φ_∞ has to be made. For stress levels less than 0.4, the assumed proportionality of stress and creep is valid, and Φ_∞ ranges from about 1.0 to 4.0 [32]. For larger stress levels, Φ_∞ may be as large as 10 as given in [35], since, under a sustained stress slightly below the sustained load strength, creep deformations up to 10 times the elastic strains may develop. Since in the fatigue tests to be evaluated the entire stress range, from the minimum stress level up to the sustained strength, have to be taken into account, a value of $\Phi_\infty = 8$ was chosen. The modulus of elasticity needed to calculate the coefficient A was taken as the secant modulus between $\sigma = 0$ and $\sigma = \sigma_s = 0.70$ from Fig. (4.46).

7.3.2.3 General Expression and Application

Now the total failure strain predicted by the analytical model can be expressed by:

$$\varepsilon_{\ell uc} = \varepsilon_{\ell 1} + \varepsilon_{\ell no} \frac{n_{uc}}{n_o} + K \frac{n_{uc}}{\beta} + \frac{(\Phi/\Phi_\infty)}{R} \cdot \frac{\Phi_\infty}{E/f_{cup}} \cdot (\sigma_s^2 - \sigma_{min}^2) \qquad (7.35)$$

Eq. (7.35) can be applied generally to all low cycle fatigue tests. However, the pure fatigue failure cycles, n_o, have to be known. Since n_o has to be determined from fatigue tests conducted at high stress rates, where time effects become small, Eq. (7.35) can be evaluated only for the tests conducted at a stress level of 0.90 for which fatigue data, at high stress rates, are available.

In Table (7.3) the failure strain components, and the total failure strain, as predicted by the analytical model, Eq. (7.35), have been tabulated. Also shown are the observed failure strains as given in Fig. (5.13). The following conclusions can be made:

a. The failure strains can reasonably be subdivided into initial strains, cycle-dependent strains and time-dependent strains.

b. The failure strains predicted by the analytical model show the expected tendencies as confirmed by the experiments in Phase One and Phase Two, i.e., the failure strain is larger, the smaller the range of stress and the slower the rate of load application. This tendency is not as clear for large stress ranges and varying stress rates.

c. Comparing the numerical values of the calculated strains with those observed, it is evident that the calculated values are too large for small stress ranges and too small for large stress ranges. The failure strains are in good agreement for intermediate stress range values. The same discrepancies have been noted previously for the cycles to failure predicted from the First Model. The difference between calculated and observed failure strains, for small stress ranges, may be due to an overestimate of the time-dependent strains. The difference, at large stress ranges, may be due to an underestimate of the time-dependent strains. In either case, it is reasonable to suggest that the linear addition of the strain components is the source of discrepancy. Also, cracks, initiated at high stresses, propagate at lower stresses, a phenomenon which is not taken into account in the analysis, and which may be responsible for the differences between the analysis and experiments for large stress ranges.

d. It has been shown by the experiments of Phase One, Fig. (4.46), that for a given stress level the maximum strains were observed when the applied stress was kept constant until failure. This criterion is similar in nature to cycles to failure under pure fatigue conditions, n_o, used in the damage model. However, such a criterion could not be incorporated in the strain analysis.

e. Similar to the damage analysis, arbitrary coefficients can be introduced to adjust the time-dependent strains, so that agreement between analysis and experiments is enforced. The coefficients, K_4, as given in Eq. (7.15) for the damage analysis, are smaller than unity for R = 0.10 and R = 0.50 and larger than unity for R = 0.90. The coefficients necessary to adjust the time-dependent part of the calculated strains, Table (7.3), would satisfy these conditions. However, they are not equal to the K_4 values of the damage analysis.

f. Similar to the damage analysis, the cycle-dependent strains, given in Table (7.3), are very small for small stress ranges because the failure strain, in a small range fatigue test, is dominated by the length of time during which a specimen has to sustain stresses above the sustained strength. The longer the total time necessary to cause failure, the larger the failure strain. This tendency is demonstrated by the calculated failure strains as well as the experimental data given in Fig. (5.13).

8. SUMMARY AND CONCLUSIONS

8.1 Summary

The objectives of this investigation were to study the strength and deformation characteristics of plain concrete when subjected to repeatedly applied high compressive loads, and to propose an analytical approach to predict plain concrete behavior under such loading conditions.

8.1.1 Experimental Program

Tests were conducted on 4 in by 4 in by 12 in plain concrete prisms. The program consisted of three phases.

In Phase One the effect of maximum stress, stress range, and age at loading, on concrete response to high repeated and sustained stresses, was studied. The maximum stress was 0.95, 0.90, 0.85, and 0.80 of the initial static strength. The stress range varied from the maximum stress level to zero. Age of concrete at loading was primarily 28 days. However, some tests were conducted at 7 and 90 days. In all cases, longitudinal and lateral strains were recorded throughout the loading history. A detailed study of their variation, as well as the volumetric strain and Poisson's ratio, is given in Chapter 4.

In Phase Two the effect of speed of testing, on static and repeated load behavior was studied. Concrete specimens were loaded to failure, statically, at three different strain rates of 10^{-7}, 10^{-5}, and 10^{-3} in/in/sec. In the repeated load tests, the loads were applied at rates of 600 and 60,000 psi/min to supplement those of Phase One, which

were conducted at a stress rate of 6,000 psi/min. Within Phase Two a maximum stress level of 0.90 was maintained; the stress range was 0.10, 0.50, or 0.90 of the static ultimate strength. The age of concrete at the time of testing was 28 days. Longitudinal strains were measured using SR-4 bond gauges. The results from this phase are given in Chapter 5.

Phase Three concerned itself with the variation of the static strength of concrete during repeated or sustained load tests. At an age of 28 days the test specimens were subjected to high repeated or sustained loads until 30, 60, or 90 percent of their life had been consumed. Then the specimens were loaded to failure. In the repeated load tests, maximum stress levels of 0.95 and 0.90 were studied, while the minimum stress was zero. The repeated loads were applied at a stress rate of 6,000 psi/min. During loading to failure, the basic strain rate of 10^{-5} in/in/sec was maintained. In the sustained load tests, the stress was 0.90 of the static ultimate strength. In all tests the longitudinal and lateral strains were recorded continuously. Test data and evaluation are reported in Chapter 6.

8.1.2 Analytical Investigation

The experimental program showed that the behavior of plain concrete, when subjected to high repeated loads, is very much time-dependent. It was thus hypothesized that concrete response to such high repeated loads can be subdivided into cycle-dependent and time-dependent fractions. The cycle-dependent effects depend only on the number of load repetitions,

while the time dependent effects are controlled by the total time-concrete has to resist stresses higher than a certain threshold stress. On this basis, two analytical models were formulated. One was based on the extent of cracking or "damage" to predict the number of cycles required to cause failure under a given set of variables, and the other was based on cycle- and time-dependent strains to theoretically predict the longitudinal strains at failure when concrete is subjected to high repeated stresses.

Excellent agreement between experimental data and calculated values was obtained for the number of cycles to failure. The agreement was less satisfactory for predictions of the failure strains. It was suggested that a simple summation of the cycle- and time-dependent effects, to predict plain concrete response to high repeated loads, may be the main cause of discrepancy between calculated and observed values.

8.2 Conclusions

Based on the test results and the analytical studies presented herein, the following conclusions, regarding the behavior of plain concrete, when subjected to high repeated and sustained loads, can be drawn:

a. The static stress-strain relationship of plain concrete is highly dependent on the strain rate, as well as the age of concrete at loading. High strain rates cause a significant increase in concrete strength, while low strain rates significantly increase the strains at a given stress. The younger the concrete at testing, the

higher the strains at a given stress for both the increasing, and the descending portion of the stress-strain relationship.

b. When concrete is subjected to high repeated stresses, a decrease in either the maximum stress level, the stress range, or the stress rate, results in an increase of the cycles to failure. The increase in failure cycles, with decreasing stress range, becomes insignificant at high maximum stress levels, small stress ranges and low stress rates, because under these conditions the "sustained load", or time-dependent effect, is dominant, i.e., the total time of testing, rather than the number of cycles to failure, is the controlling parameter.

c. During the course of repeated or sustained tests, the static strength of concrete does not decrease continuously with the number of applied cycles or time under load. During the initial stages of the test, concrete undergoes a "hardening" stage resulting in an increase of the static strength. The length of this "hardening" stage, and the magnitude of the strength increase, is a function of the maximum stress applied during the test.

d. The variation of longitudinal and lateral strains of concrete with the number of applied cycles in fatigue tests, or the time under load in sustained load tests, is characterized by an initial abrupt increase of strains. This is followed by

a period of stabilization during which strains increase almost linearly with time of cycles and a final stage of rapid strain increase near failure. The volumetric strains and Poisson's ratio show a similar variation during the life history of a specimen.

e. The failure strain under repeated loads are the higher, the lower the level of the maximum stress, the smaller the stress range, or the slower the stress rate. The failure strains under sustained loads increase with decreasing sustained stress level. The failure strain is, in all cases, larger than the strain given by the descending portion of the static stress-strain curve. For the same stress level, the failure strains are higher the longer it takes to fail a concrete specimen. For fatigue tests, at a given stress rate, a linear relationship exists between failure strain and logarithm of failure cycles. A similar relation exists between failure strains and logarithm of time to failure under sustained loads.

f. An analytical model, which is based on the extent of cracking or damage caused by high repeated loads, and in which the cycle- and time-dependent damage are expressed independently, predicts the number of cycles to failure very satisfactorily.

g. The model to predict failure strains is based on the assumption that the failure strain of concrete, subjected to high repeated loads, consists of an initial elastic strain, a cycle-dependent and a time-dependent strain. The agreement

between calculated and observed failure strains ranged from poor to satisfactory, but the failure strains, calculated from the analytical model, gave the general tendencies, which were observed in the experiments.

LIST OF REFERENCES

[1] Abrams, D. A., "Effect of Rate of Application of Load on Compressive Strength of Concrete," Proc. ASTM, Volume 17, Part II, p. 364 (1917).

[2] Assimacopoulos, M., Warner, R. F. and Ekberg, C. E., Jr., "High Speed Fatigue Tests on Small Specimens of Plain Concrete," Journal, Prestressed Concrete, September 1959, Volume 4, No. 2.

[3] Baker, A. L. L., "A Criterion of Concrete Failure," The Institution of Civil Engineers, Proc., Volume 45, February 1970.

[4] Bennet, E. W. and Raju, N. K., "Cumulative Fatigue Damage of Plain Concrete in Compression," Dept. of Civil Engineering, University of Leeds.

[5] Corten, H. T. and Dolan, T. J., "Cumulative Fatigue Damage," The International Conference on Fatigue of Metals, Institute of Mechanical Engineering (London), and ASME (New York), September 10-14, 1956.

[6] Corten, H. T., Sinclair, G. M. and Dolan, T. J., "An Experimental Study of the Influence of Fluctuating Stress Amplitude on Fatigue Life of 75S-T6 Aluminum," 1954, Proc. ASTM, Volume 54, p. 737.

[7] Diaz, S. I., "Fracture Mechanisms in Concrete Under Static, Sustained and Repeated Loads," Ph.D. Thesis, University of Illinois, Urbana, To be Published June 1971.

[8] Dixon, W. J. and Massey, F. J., Jr., "Introduction to Statistical Analysis," Third Edition, McGraw-Hill.

[9] Dolan, T. J., Richart, F. E. and Work, C. E., "The Influence of Fluctuations in Stress Amplitude on the Fatigue of Metals," 1949, Proc. ASTM, Volume 49, p. 646.

[10] Evans, R. H., "Effect of Rate of Loading on the Mechanical Properties of Some Materials," Journal, Institute of Civil Engineers, Volume 18, p. 296 (1942).

[11] Glucklick, J., "On the Compression Failure of Plain Concrete," T. & A. M. Report No. 215, University of Illinois, Urbana, March 1962.

[12] Henry, D. L., "A Theory of Fatigue Damage Accumulation in Steel," Preprint Paper No. 54-A-77, 1954, ASME.

[13] Hilsdorf, H. K. and Kesler, C. E., "The Behavior of Concrete in Flexure Under Varying Repeated Loads," T. & A. M. Report No. 172, August 1960.

[14] Hilsdorf, H. K. and Kesler, C. E., "Fatigue Strength of Concrete Under Varying Flexural Stresses," Journal of the A. C. I., Proc. Volume 63, No. 10, October 1966.

[15] Husak, A. D. and Krokosky, E. M., "Static Fatigue of Hydrated Cement Concrete," Private Communication, Submitted to A. C. I., November 4, 1969.

[16] Jones, P. G. and Richart, F. E., "The Effect of Testing Speed on Strength and Elastic Properties of Concrete," Proc. A. S. T. M., Volume 36, 1936, p. 380.

[17] Karsan, D. I., "Behavior of Plain Concrete Under Variable Load Histories," Ph.D. Thesis, Rice University, Civil Engineering Department, 1968.

[18] Kesler, C. E., "Effect of Speed of Testing on Flexural Fatigue Strength of Plain Concrete," Highway Research Board, Proc. 32, 1953, pp. 251-258.

[19] Kesler, C. E. and Siess, C. P., "Static and Fatigue Strength of Concrete," ASTM Preprint No. 96a, Philadelphia, 1955.

[20] Liu, H. W. and Corten, H. T., "Fatigue Damage During Complex Stress Histories," NASA N D-256, Washington, November 1959.

[21] Miner, M. A., "Cumulative Damage in Fatigue," Transactions, American Society of Mechanical Engineering, Volume 67, 1945, pp. A159-A164.

[22] Murdock, John W., "A Critical Review of Research on Fatigue of Plain Concrete," U. of I. Engineering Exp. Station, Bulletin No. 475.

[23] McHenry, D. and Shideler, J. J., "Review of Data on Effect of Speed in Mechanical Testing of Concrete," ASTM Spec. Tech. Publ. No. 185, 1956, pp. 72-82.

[24] Newmark, N. M., "A Review of Cumulative Damage in Fatigue," A Technical Report, Civil Engineering Department, University of Illinois, Urbana, July 1950.

[25] Newmark, N. M., "A Review of Cumulative Damage," in "Fatigue and Fracture of Metals," Edited by W. M. Murrey (John Wiley and Sons, Inc., New York), 1952.

[26] Opele, E. W. and Muir, S. E., "Some Fatigue Tests of High-Strength Concrete in Axial Compression," Journal, ACI Proc., Vol. 63, January 1966.

[27] Ople, F. S. and Hulsbos, C. L., "Probable Fatigue Life of Plain Concrete with Stress Gradient," Journal, ACI, Proc., Vol. 63, 1966, pp. 59-81.

[28] Popovic, S., "A Review of Stress-Strain Relationships for Concrete," Journal, A.C.I., March 1970, pp. 243-248.

[29] Raithby, K. D. and Whiffin, A. C., "Failure of Plain Concrete Under Fatigue Loading -- A Review of Current Knowledge," Road Research Laboratory, Growthorne, England, 1968.

[30] Raju, N. K., "Small Concrete Specimens Under Repeated Compressive Loads by Pulse Velocity Technique," Journal of Materials, JMLSA, Vol. 5, No. 2, June 1970, pp. 262-272.

[31] Robinson, G. S., "Methods of Detecting the Formation and Propagation of Microcracks in Concrete," International Conference on the Structure of Concrete, London.

[32] Ross, A. D., "Creep of Concrete Under Variable Stress," Journal, ACI, March 1958, No. 9, Volume 29, pp. 739-758.

[33] Ruetz, W., "The Two Different Physical Mechanisms of Creep of Concrete," International Conference in the Structure of Concrete, Paper C2, September 1965.

[34] Rüsch, H., "Physical Problems Arising in the Testing of Concrete," Zement-Kalk-Gips, Volume 12, 1959, pp. 1-9.

[35] Rüsch, H., "Research Towards a General Flexural Theory for Structural Concrete," Journal, ACI, Proc. No. 57, No. 1, July 1960, pp. 1-28.

[36] Sell, R., "Investigation into the Strength of Concrete Under Sustained Load," RILEM Bulletin No. 5, December 1959, Paris, pp. 1-13.

[37] Shah, S. P. and Chandra, S., "Fracture of Concrete Subjected to Cyclic and Sustained Loading," Private Communication.

[38] Shah, S. P. and Winter, G., "Inelastic Behavior and Fracture of Concrete," Ph.D. Thesis, Cornell University, Ithaca, September 1965, 153 pp.

[39] Shah, S. P. and Winter, G., "Response of Concrete to Repeated Loading," Paper Submitted to the RILEM International Symposium on the Effects of Repeated Loading on Materials and Structural Elements, September 1966, Mexico, D.F.

[40] Sinha, B. P., Gerstle, K. H. and Tulin, L. G., "Stress-Strain Relations for Concrete Under Cyclic Loading," Journal , ACI, Proc., Vol. 61, No. 2, February 1964, pp. 195-212.

[41] Sturman, G. M., Shah, S. P. and Winter, G., "Microcracking and Inelastic Behavior of Concrete," Proc. of the International Symposium on Flexural Mechanics of Reinforced Concrete, Miami, Florida, November 1964, pp. 473-493.

[42] Van Ornum, J. L., "Fatigue of Concrete," Trans., ASCE, Volume 58, 1907, pp. 294-320.

[43] Verna, J. R. and Stelson, T. E., "Repeated Loading Effect on Ultimate Static Strength of Concrete Beams," Journal of ACI, Proc. 60, 1963, pp. 743.

[44] Washa, G. W. and Fluck, P. G., "Effect of Sustained Loading on Compressive Strength and Modulus of Elasticity of Concrete," Journal of ACI, Proc. 46, 1950, pp. 693-700.

[45] Watstein, D., "Effect of Straining Rate on the Compressive Strength and Elastic Properties of Concrete," Proc., ACI, Volume 49, 1953, p. 729.

[46] Wei, R. P. and Landes, J. D., "Correlation between Sustained Load and Fatigue Crack Growth in High-Strength Steels," Materials Research and Standards, MTRSA, Volume 9, No. 7, pp. 25-28.

[47] _____, "Recommendations for an International Code of Practice for Reinforced Concrete," American Concrete Institute (Detroit) and the Cement and Concrete Association (London), Lund, Humphries, and Co., Ltd., London, 1965, pp. 38-45.

TABLE 3.1

CHEMICAL AND PHYSICAL PROPERTIES OF THE CEMENT USED TOGETHER WITH PERTINENT SPECIFICATION REQUIREMENTS -- MANUFACTURER'S DATA

	Test	(Typical) SPEED, type 1	ASTM C 150-68
(1)	Fineness, Blaine, sq cm/gm	3560	2800 avg. min.
(2)	Soundness, autoclave expansion, %	0.02	0.08 max.
(3)	Time of Set, Gillmore:		
	Initial, minutes	200	60 min.
	Final, hours	6	10 max.
(4)	Air Content of Mortar, %	8.6	12.0 max.
(5)	Compressive Strength, psi:		
	3-day	3100	1200
	7-day	4150	2100
	27-day	5750	3500
(6)	C_3S	57	--
	C_2S	18	--
	C_3A	10.0	--
	C_4AF	7	--
	SO_3	2.47	3.0
	Alkalies, as Na_2O	0.45	--
	MgO	2.25	5.0 max.
(7)	Loss on Ignition, %	1.4	3.0
(8)	Insoluble Residue, %	0.18	0.75

TABLE 3.2

CONCRETE MIX PROPORTIONS

Series Designation	Phase Number	Weight in lbs.				Slump (in.)
		Cement	Sand	Gravel	Water	
A2 - A19	One	90	351	408	77.5	2 to 3
A20 - A30	One	85	340	440	83.0	2-1/2 to 3
C1 - C5	Two	63	255	330	60	2-1/2 to 4
B1 - B12	Three	63	255	330	60	2-1/2 to 4

TABLE 4.1

PHASE ONE

NUMBER OF SPECIMENS PER VARIABLE SUBJECTED TO REPEATED LOADS AT AN AGE OF 7 DAYS

Stress Range R	Maximum Stress Level, σ_{max}		
	0.95	0.90	0.85
0.00	4	3	1
0.50	4	3	1
0.85	-	-	3
0.90	-	4	-
0.95	4	-	-
Subtotal	12	10	5

Total number of specimens tested is 27.

Series tested are: A21; A23; A24; A25; A26; A30.

TABLE 4.2

PHASE ONE

NUMBER OF SPECIMENS PER VARIABLE SUBJECTED TO REPEATED LOAD AT AN AGE OF 28 DAYS

Stress Range	Maximum Stress Level, σ_{max}			
R	0.95	0.90	0.85	0.80
0.00	4	4	4	-
0.05	4	4	3	-
0.10	4	3	-	-
0.20	4	4	-	-
0.30	4	4	2	-
0.50	4	4	4	-
0.80	-	-	-	3
0.85	-	-	3	-
0.90	-	4	-	-
0.95	4	-	-	-
Subtotal	28	27	16	3

Total number of specimens tested is 74.

Series tested are: A2; A3; A4; A5; A7; A8; A10; A12; A14; A18; A19; A20; A27; A28; A29.

TABLE 4.3

PHASE ONE

NUMBER OF SPECIMENS PER VARIABLE
SUBJECTED TO REPEATED LOADS AT AN AGE OF 90 DAYS

Stress Range	Maximum Stress Level, σ_{max}		
R	0.95	0.90	0.85
0.00	4	3	2
0.50	5	4	3
0.85	-	-	3
0.90	-	4	-
0.95	4	-	-
Subtotal	13	11	8

Total number of specimens tested is 32.

Series tested are: A6; A9; A11; A13; A15; A16; A17; A22.

TABLE 4.4

PHASE ONE

NUMBER OF SPECIMENS PER VARIABLE
SUBJECTED TO SUSTAINED LOADS

Sustained Stress Level, σ_{sus}	Concrete Age at Loading (Days)	Number of Specimens Tested
0.95	7	4
0.95	28	4
0.95	90	4
0.90	7	3
0.90	28	4
0.90	90	3
0.85	7	1
0.85	28	4
0.85	90	3

Total number of specimens tested is 30.

Series tested are: A4; A11; A13; A16; A17; A18; A22; A24; A25; A26; A27.

TABLE 4.5

PHASE ONE

DETAILS OF REPEATED LOAD TESTS
AT 7 DAYS

Series Designation	Number of Static Tests	Maximum Stress Level, σ_{max}	Minimum Stress Level, σ_{min}	Number of Specimens Tested
A21	3	.95	.95	2
		.95	.45	2
		.95	.00	4
A23	4	.90	.00	2
A24	3+3	.95	.95	2
		.95	.45	2
A25	2+3	.90	.90	1
		.90	.40	2
		.90	.00	1
		.85	.00	1
A26	4	.90	.90	2
		.90	.40	1
		.90	.00	1
		.85	.00	2
A30	3	.85	.85	1
		.85	.35	1

Total number of specimens tested is 27.

TABLE 4.6

PHASE ONE

DETAILS OF REPEATED LOAD TESTS AT 28 DAYS

Series Designation	Number of Static Tests	Maximum Stress Level, σ_{max}	Minimum Stress Level, σ_{min}	Number of Specimens Tested
A2	4	.95	.90	2
		.95	.85	1
		.95	.65	1
		.95	.45	1
		.95	.00	1
A3	3	.90	.85	1
		.90	.80	1
		.90	.60	1
		.90	.40	1
		.90	.00	1
A4	3	.85	.85	3
A5	4	.85	.80	1
		.85	.35	1
		.85	.00	1
A7	4	.95	.85	1
		.95	.65	1
		.95	.45	1
		.95	.00	1
A8	4	.90	.85	
		.90	.80	1
		.90	.60	1
		.90	.40	1
		.90	.00	1
A10	4	.95	.90	1
		.95	.85	1
		.95	.65	1
		.95	.45	1
A12	4	.90	.85	1
		.90	.80	1
		.90	.60	1
		.90	.00	1
A14	3	.85	.80	1
		.85	.00	1
A18	4	.85	.85	1
		.85	.80	1
		.85	.35	2
		.85	.00	1
A19	4	.95	.75	4
		.85	.35	1
A20	3	.95	.95	1
		.95	.90	1
		.95	.85	1
		.95	.65	1
		.95	.45	1
		.95	.00	2
A27	3	.95	.95	3
		.90	.90	4
		.90	.85	1
A28	3	.90	.70	4
		.90	.60	1
		.90	.40	2
		.90	.00	1
A29	4	.85	.55	2
		.80	.00	3

Total number of specimens tested is 74.

TABLE 4.7

PHASE ONE

DETAILS OF REPEATED LOAD TESTS AT 90 DAYS

Series Designation	Number of Static Tests	Maximum Stress Level, σ_{max}	Minimum Stress Level, σ_{min}	Number of Specimens Tested
A6	4	.95	.45	1
		.95	.00	4
A9	4	.90	.00	2
A11	4	.95	.95	2
		.95	.45	4
A13	3	.95	.95	2
A15	3	.90	.40	2
		.90	.00	2
A16	3	.90	.90	1
		.90	.40	2
		.85	.35	2
		.85	.00	1
A17	3	.90	.90	2
		.85	.85	2
		.85	.00	2
A22	3	.85	.35	1

Total number of specimens tested is 32.

TABLE 4.8

PHASE ONE

DETAILS OF SUSTAINED LOAD TESTS

Series Designation	Sustained Stress Level, σ_{sus}	Concrete Age at Loading (Days)	Number of Specimens Tested
A4	0.85	28	3
A11	0.95	90	2
A13	0.95	90	2
A16	0.90	90	1
A17	0.90	90	2
A17	0.85	90	2
A18	0.85	28	1
A20	0.95	28	1
A21	0.95	7	2
A22	0.85	90	1
A24	0.95	7	2
A25	0.90	7	1
A26	0.90	7	2
A27	0.95	28	3
A27	0.90	28	4
A30	0.85	7	1

Total number of specimens tested is 30.

TABLE 4.9

PHASE ONE

TEST RESULTS OF SPECIMENS SUBJECTED TO REPEATED LOADS

σ_{max} = 0.95, 0.90 and 0.85 Age: 7 Days

Series	Static Tests			Repeated Load Tests*								
							Longitudinal		Lateral			
	f_{cup} (psi)	$\varepsilon_{\ell u}$	ε_{hu}	σ_{max}	σ_{min}	n_u (cycles)	ε_{max}	ε_{min}	ε_{max}	ε_{min}	ν_u	ε_{vu}
A21	2360	1.394	0.310	.95	.45	73	2.063	1.719	--	--	--	--
A21	2360	1.394	0.310	.95	.45	70	2.123	1.794	--	--	--	--
A24	2220	1.288	0.273	.95	.45	274	2.437	2.093	1.298	1.096	0.532	-0.160
A24	2220	1.288	0.273	.95	.45	259	2.468	2.125	0.789	0.632	0.320	-0.890
A21	2360	1.394	0.310	.95	.00	10	1.688	0.713	0.566	0.160	0.335	0.555
A21	2360	1.394	0.310	.95	.00	16	1.625	0.719	0.566	0.230	0.348	0.493
A21	2360	1.394	0.310	.95	.00	27	2.156	1.025	1.565	0.859	0.726	-0.974
A21	2360	1.394	0.310	.95	.00	61	2.438	1.438	0.942	0.583	0.508	-0.04
A25	2500	1.307	0.328	.90	.40	>13500	>1.688	>1.500	>0.393	>0.365	--	--
A25	2500	1.307	0.328	.90	.40	>4000	>1.394	>1.200	>0.383	>0.340	--	--
A26	2420	1.456	0.333	.90	.40	>6043	>2.006	>1.775	>0.1252	>1.182	--	--
A23	2420	1.250	0.147	.90	.00	124	2.313	1.400	0.989	0.902	0.428	0.334
A23	2420	1.250	0.147	.90	.00	141	2.188	1.275	1.355	0.966	0.620	-0.523
A25	2500	1.307	0.328	.90	.00	92	2.125	1.262	2.498	1.564	1.175	-2.87
A26	2420	1.456	0.333	.90	.00	43	2.238	1.219	1.499	0.919	0.670	-0.760
A25	2500	1.307	0.328	.85	.00	378	2.713	1.788	3.164	2.251	1.166	-3.615
A26	2420	1.456	0.333	.85	.00	173	2.300	1.456	4.123	3.090	1.792	-5.945
A26	2420	1.456	0.333	.85	.00	190	2.181	1.500	2.500	1.465	1.147	-2.820
A30	2420	1.456	0.333	.85	.35	>4286	--	--	--	--	--	--

* Given are failure strains in in/in x 10^{-3}

TABLE 4.10

PHASE ONE

TEST RESULTS OF SPECIMENS SUBJECTED TO REPEATED LOADS

σ_{max} = 0.95 Age: 28 Days

Static Tests				Repeated Load Tests*							
						Longitudinal		Lateral			
Series	f_{cup} (psi)	$\varepsilon_{\ell u}$	ε_{hu}	R	n_u (cycles)	ε_{max}	ε_{min}	ε_{max}	ε_{min}	ν_u	ε_{vu}
A2	4730	2.206	0.443	0.95	10	2.500	1.044	1.665	0.733	0.666	-0.830
A7	4660	1.969	0.583	0.95	16	3.540	2.269	1.998	1.499	0.565	-0.459
A20	3520	1.812	0.363	0.95	8	1.944	1.030	0.573	0.450	0.295	0.798
A20	3520	1.812	0.363	0.95	9	1.967	0.913	0.799	0.413	0.406	0.370
A2	4730	2.206	0.443	0.50	179	3.600	2.931	2.731	2.398	0.759	-1.860
A7	4660	1.969	0.583	0.50	157	3.031	2.375	1.868	1.562	0.616	-0.705
A10	3860	1.987	0.462	0.50	73	2.438	1.963	1.199	1.122	0.491	0.040
A20	3520	1.812	0.363	0.50	353	3.206	2.775	2.664	2.258	0.831	-2.122
A2	4730	2.206	0.443	0.30	63	2.769	2.469	0.999	0.916	0.361	0.771
A7	4660	1.969	0.583	0.30	147	2.988	2.638	2.424	2.125	0.811	-1.861
A10	3860	1.987	0.462	0.30	296	2.938	2.675	1.292	1.242	0.440	0.353
A20	3520	1.812	0.363	0.30	362	2.956	2.743	1.548	1.425	0.524	-0.141
A19	5180	2.081	0.266	0.20	59	2.688	2.438	1.382	1.206	0.867	-1.975
A19	5180	2.081	0.266	0.20	110	2.813	2.706	2.165	1.998	0.770	-1.516
A19	5180	2.081	0.266	0.20	139	2.844	2.694	0.982	0.889	0.345	0.879
A19	5180	2.081	0.266	0.20	155	3.125	2.875	2.664	2.364	0.852	-2.203
A2	4730	2.206	0.443	0.10	369	3.406	3.338	2.940	2.761	0.863	-2.475
A7	4660	1.969	0.583	0.10	125	2.844	2.756	1.568	1.441	0.552	-0.293
A10	3860	1.987	0.462	0.10	548	2.963	2.931	1.995	1.945	0.673	-1.027
A20	3520	1.812	0.363	0.10	272	2.875	2.800	1.832	1.632	0.637	-0.788
A2	4730	2.206	0.443	0.05	97	2.825	2.750	1.505	1.465	0.553	-0.185
A2	4730	2.206	0.443	0.05	163	2.688	2.669	1.166	1.066	0.434	0.357
A10	3860	1.987	0.462	0.05	369	2.644	2.631	1.149	1.002	0.435	0.346
A20	3520	1.812	0.363	0.05	306	2.719	2.656	0.606	0.543	0.223	1.507

* Given are failure strains in in/in x 10^{-3}

TABLE 4.11

PHASE ONE

TEST RESULTS OF SPECIMENS SUBJECTED TO REPEATED LOADS

σ_{max} = 0.90 Age: 28 Days

Stress	Static Tests			Repeated Load Tests*							
						Longitudinal		Lateral			
	f_{cup} (psi)	$\varepsilon_{\ell u}$	ε_{hu}	R	n_u (cycles)	ε_{max}	ε_{min}	ε_{max}	ε_{min}	ν_u	ε_{vu}
A3	4930	2.060	--	0.90	192	2.540	1.250	--	--	--	--
A8	4350	1.831	0.443	0.90	101	2.631	1.438	1.615	0.992	0.614	-0.599
A12	4200	1.844	0.949	0.90	123	2.444	1.250	--	--	--	--
A28	3400	1.706	0.423	0.90	130	2.950	1.875	2.920	2.094	0.990	-2.891
A3	4930	2.060	--	0.50	1027	3.230	2.680	--	--	--	--
A8	4350	1.831	0.443	0.50	1815	4.244	3.731	3.330	3.050	0.785	-2.416
A28	3400	1.706	0.423	0.50	241	2.875	2.425	1.832	1.469	0.637	-0.788
A28	3400	1.706	0.423	0.50	628	3.163	2.775	3.080	2.617	0.974	-2.998
A3	4930	2.060	--	0.30	1067	3.300	3.000	--	--	--	--
A8	4350	1.831	0.443	0.30	1124	3.063	2.688	1.931	1.765	0.631	-0.800
A12	4200	1.844	0.949	0.30	577	2.969	2.756	5.261	4.735	1.772	-7.554
A28	3400	1.706	0.423	0.30	112	2.188	1.950	1.832	1.415	0.837	-1.476
A28	3400	1.706	0.423	0.20	306	2.344	2.176	1.832	1.665	0.781	-1.319
A28	3400	1.706	0.423	0.20	332	3.031	2.838	1.632	1.505	0.538	-0.232
A28	3400	1.706	0.423	0.20	1157	3.219	3.088	2.158	1.908	0.670	-1.097
A28	3400	1.706	0.423	0.20	2893	3.806	3.706	3.730	3.510	0.980	-3.653
A3	4930	2.060	--	0.10	3948	3.550	3.450	--	--	--	--
A8	4350	1.831	0.443	0.10	3657	3.444	3.319	1.200	1.200	0.348	1.044
A12	4200	1.844	0.949	0.10	3546	3.819	3.756	1.165	1.156	0.306	1.488
A3	4930	2.060	--	0.05	869	2.920	2.870	--	--	--	--
A8	4350	1.831	0.443	0.05	574	2.731	2.688	1.832	1.782	0.671	-0.932
A12	4200	1.844	0.949	0.05	1113	2.606	2.606	1.565	1.548	0.600	-0.524
A27	3620	1.687	0.266	0.05	3597	3.613	3.575	2.181	2.091	0.604	-0.750

* Given are failure strains in in/in x 10^{-3}

TABLE 4.12

PHASE ONE

TEST RESULTS OF SPECIMENS SUBJECTED TO REPEATED LOADS

σ_{max} = 0.85 and 0.80 Age: 28 Days

Series	Static Tests			Repeated Load Tests*								
							Longitudinal		Lateral			
	f_{cup} (psi)	$\varepsilon_{\ell u}$	ε_{hu}	σ_{max}	σ_{min}	n_u (cycles)	ε_{max}	ε_{min}	ε_{max}	ε_{min}	ν_u	ε_{vu}
A5	4720	1.906	0.483	0.85	0.00	412	2.625	1.325	--	--	--	--
A14	4380	1.800	0.366	0.85	0.00	494	3.563	2.219	4.662	3.330	1.309	-5.762
A18	5440	1.875	0.533	0.85	0.00	525	3.063	1.794	2.098	1.305	0.685	-1.133
A5	4720	1.906	0.483	0.85	0.35	2241	3.125	2.638	1.688	1.515	0.540	-0.252
A18	5440	1.875	0.533	0.85	0.35	1235	3.038	2.506	2.821	2.438	0.929	-2.604
A18	5440	1.875	0.533	0.85	0.35	3517	3.688	3.125	3.437	3.034	0.932	-3.186
A19	5180	2.081	0.493	0.85	0.35	4839	3.981	3.375	1.732	1.449	0.435	0.518
A29	3620	1.625	0.376	0.85	0.55	8363	3.794	3.588	3.746	3.563	0.987	-3.700
A29	3620	1.625	0.376	0.85	0.55	12982	4.188	3.938	3.230	3.014	0.771	-2.273
A5	4720	1.906	0.483	0.85	0.80	17193	9.250	9.194	4.063	3.913	0.439	1.125
A14	4380	1.800	0.366	0.85	0.80	63511	4.250	4.238	2.331	2.298	0.548	-0.412
A18	5440	1.875	0.533	0.85	0.80	13408	3.500	3.500	2.997	2.964	0.856	-2.494
A29	3620	1.625	0.376	0.80	0.00	2159	3.500	2.425	5.028	3.816	1.437	-6.557
A29	3620	1.625	0.376	0.80	0.00	2358	3.400	2.438	1.782	1.515	0.524	-0.163
A29	3620	1.625	0.376	0.80	0.00	2724	4.550	3.344	5.611	4.602	1.233	-6.672

* Given are failure strains in in/in x 10^{-3}

TABLE 4.13

PHASE ONE

TEST RESULTS OF SPECIMENS SUBJECTED TO REPEATED LOADS

σ_{max} = 0.95, 0.90 and 0.85 Age: 90 Days

Series	Static Tests			Repeated Load Tests*								
							Longitudinal		Lateral			
	f'_{cup} (psi)	$\varepsilon_{\ell u}$	ε_{hu}	σ_{max}	σ_{min}	n_u (cycles)	ε_{max}	ε_{min}	ε_{max}	ε_{min}	ν_u	ε_{vu}
A6	4600	1.612	0.609	0.95	0.45	216	2.344	1.863	1.665	1.272	0.710	-0.986
A11	4170	1.644	0.683	0.95	0.45	40	1.788	1.381	2.281	2.025	1.276	-2.775
A11	4170	1.644	0.683	0.95	0.45	94	2.188	1.719	1.582	1.365	0.723	-0.976
A11	4170	1.644	0.683	0.95	0.45	1167	3.094	2.600	3.190	2.817	1.031	-3.287
A11	4170	1.644	0.683	0.95	0.45	2203	2.687	2.219	1.365	1.215	0.508	-0.043
A6	4600	1.612	0.609	0.95	0.00	62	2.469	1.112	3.829	2.331	1.551	-5.190
A6	4600	1.612	0.609	0.95	0.00	67	2.438	1.063	1.965	1.086	0.806	-1.492
A6	4600	1.612	0.609	0.95	0.00	93	2.175	0.900	0.932	0.510	0.429	0.310
A6	4600	1.612	0.609	0.95	0.00	117	2.125	0.937	1.665	0.733	0.784	-1.205
A15	3720	1.456	0.500	0.90	0.40	93	1.613	1.219	1.565	1.272	0.971	-1.518
A15	3720	1.456	0.500	0.90	0.40	>4336	>1.844	>1.563	>0.311	>0.698	--	--
A16	5650	1.819	0.626	0.90	0.40	285	2.469	1.900	2.797	2.231	1.133	-3.126
A16	5650	1.819	0.626	0.90	0.40	347	2.563	1.938	2.498	2.005	0.975	-2.433
A9	3840	1.650	0.866	0.90	0.00	44	2.188	1.088	0.966	0.599	0.441	0.256
A9	3840	1.650	0.866	0.90	0.00	181	2.113	0.938	1.815	1.099	0.859	-1.517
A15	3720	1.456	0.500	0.90	0.00	81	2.188	1.044	2.165	1.259	0.989	-2.142
A15	3720	1.456	0.500	0.90	0.00	205	2.181	1.063	2.191	1.365	1.005	-2.201
A16	5650	1.819	0.626	0.85	0.35	2193	2.375	2.356	1.965	1.748	0.827	-1.554
A16	5650	1.819	0.626	0.85	0.35	5466	2.756	2.263	1.182	0.932	0.429	0.392
A22	3890	1.725	0.676	0.85	0.35	11818	3.275	2.831	3.323	2.997	1.015	-3.372
A16	5650	1.819	0.626	0.85	0.00	136	2.313	0.938	1.498	0.633	0.648	-0.685
A17	4750	1.862	0.866	0.85	0.00	359	2.531	1.225	3.330	1.881	1.316	-4.129
A17	4750	1.862	0.866	0.85	0.00	596	2.469	1.188	4.872	2.791	1.973	-7.275

* Given are failure strains in in/in x 10^{-3}

TABLE 4.14

PHASE ONE

LOGARITHMIC AVERAGE OF CYCLES TO FAILURE

Maximum Stress Level, σ_{max}	Minimum Stress Level, σ_{min}	Stress Range R	Age in Days		
			7	28	90
			Failure Cycles, $\bar{n}_u$		
0.95	0.90	0.05	-	204	-
0.95	0.85	0.10	-	286	-
0.95	0.75	0.20	-	108	-
0.95	0.65	0.30	-	176	-
0.95	0.45	0.50	138	163	290
0.95	0.00	0.95	22	13	81
0.90	0.85	0.05		1189	
0.90	0.80	0.10		3715	
0.90	0.70	0.20		764	
0.90	0.60	0.30		527	
0.90	0.40	0.50	> 6832	730	447
0.90	0.00	0.90	92	133	107
0.85	0.80	0.05	-	24500	-
0.85	0.55	0.30	-	10420	-
0.85	0.35	0.50	-	2650	6397
0.85	0.00	0.85	232	473	143
0.80	0.00	0.80	-	2400	-

TABLE 4.15

PHASE ONE

TEST RESULTS OF SPECIMENS SUBJECTED TO SUSTAINED LOADS

σ_{sus} = 0.95, 0.90 and 0.85 Age: 7 Days

Series	Static Load Tests			Sustained Load Tests*							
	f_{cup} (psi)	$\varepsilon_{\ell u}$	ε_{hu}	σ_{sus}	Failure Time, t_u hrs.	mins.	secs.	$\varepsilon_{\ell u}$	ε_{hu}	ν_u	ε_{vu}
A21	2360	1.394	0.310	0.95	0	3	06	0.800	0.306	0.3825	0.188
A21	2360	1.394	0.310	0.95	0	6	46	1.125	2.125	1.8888	-3.125
A24	2220	1.288	0.273	0.95	0	4	16	0.960	0.340	0.3541	0.280
A24	2220	1.288	0.273	0.95	0	1	19	0.512	0.100	0.1953	0.312
A25	2500	1.307	0.328	0.90	0	25	51	1.519	1.367	0.8999	-1.215
A26	2420	1.456	0.333	0.90	0	7	28	1.200	0.660	0.5500	-0.120
A26	2420	1.456	0.333	0.90	0	9	17	0.975	1.184	1.2143	-1.393
A30	2165	1.456	0.333	0.85	21	30	0	----did not fail----------			

* Given are failure strains in in/in x 10^{-3}

TABLE 4.16

PHASE ONE

TEST RESULTS OF SPECIMENS SUBJECTED TO SUSTAINED LOADS

σ_{sus} = 0.95, 0.90 and 0.85 Age: 28 Days

Series	Static Tests			Sustained Load Tests*							
	f_{cup} (psi)	$\varepsilon_{\ell u}$	ε_{hu}	σ_{sus}	Failure Time, t_u hrs.	mins.	secs.	$\varepsilon_{\ell u}$	ε_{hu}	ν_u	ε_{vu}
A20	3520	1.812	0.363	0.95	0	49	22	2.037	1.713	0.8409	-1.389
A27	3620	1.687	0.266	0.95	0	3	54	1.400	1.700	1.2142	-2.000
A27	3620	1.687	0.266	0.95	0	2	57	1.350	1.200	0.8889	-1.050
A27	3620	1.687	0.266	0.95	0	5	04	1.250	0.924	0.7392	-0.598
A27	3620	1.687	0.266	0.90	0	13	48	1.287	1.367	1.0621	-1.447
A27	3620	1.687	0.266	0.90	0	18	11	1.787	1.250	0.6994	-0.713
A27	3620	1.687	0.266	0.90	0	25	46	1.700	2.233	0.6496	-1.029
A27	3620	1.687	0.266	0.90	3	2	03	3.437	3.233	0.9406	-3.029
A18	5440	1.875	0.533	0.85	23	51	00	3.181	1.617	0.5083	-0.053
A4	3340	1.750	0.500	0.85	1	41	16	2.337	2.984	1.2768	-3.631
A4	3340	1.750	0.500	0.85	3	09	45	2.337	2.014	0.8617	-1.691
A4	3340	1.750	0.500	0.85	7	17	15	3.200	2.857	0.8928	-2.714

* Given are failure strains in in/in x 10^{-3}

TABLE 4.17

PHASE ONE

TEST RESULTS OF SPECIMENS SUBJECTED TO SUSTAINED LOADS

σ_{sus} = 0.95, 0.90 and 0.85 Age: 90 Days

Series	Static Tests			Sustained Load Tests*							
	f_{cup} (psi)	$\varepsilon_{\ell u}$	ε_{hu}	σ_{sus}	Failure Time, t_u hrs.	mins.	secs.	$\varepsilon_{\ell u}$	ε_{hu}	ν_u	ε_{vu}
A11	4170	1.644	0.683	0.95	0	19	15	0.825	0.914	1.1078	-1.003
A11	4170	1.644	0.683	0.95	1	28	47	1.125	1.467	1.1304	-1.809
A13	4170	1.644	0.683	0.95	0	19	39	0.900	1.406	1.5622	-1.912
A13	4170	1.644	0.683	0.95	0	21	32	0.850	1.904	2.2400	-2.958
A16	5650	1.819	0.626	0.90	2	52	02	1.431	1.750	1.2229	-2.069
A17	4750	1.862	0.866	0.90	3	32	48	1.800	2.050	1.1388	-2.300
A17	4750	1.862	0.866	0.90	6	55	43	1.350	1.300	0.9629	-1.250
A17	4750	1.862	0.866	0.85	69	56	40	2.537	1.934	0.7623	-1.331
A17	4750	1.862	0.866	0.85	68	27	00	2.681	1.750	0.6527	-0.819
A22	3890	1.725	0.676	0.85	101	39	33	2.968	1.900	0.6401	-0.832

* Given are failure strains in in/in x 10^{-3}

TABLE 4.18

PHASE ONE

LOGARITHMIC AVERAGE OF TIME TO FAILURE

σ_{sus}	Age in Days		
	7	28	90
	(Minutes)		
0.95	3.29	7.32	29.16
0.90	12.38	32.94	247.70
0.85	1290.00	331.10	4719.00

TABLE 5.1

PHASE TWO

NUMBER OF SPECIMENS PER VARIABLE

σ_{max} = 0.90 Age: 28 Days

Stress Range	Stress Rate, psi/min	
R	600	60,000
0.10	6	4
0.50	4	4
0.90	4	4
Subtotal	14	12

Total number of specimens tested is 26.

Series tested are: C1; C2; C3; C4; C5.

TABLE 5.2

PHASE TWO

DETAILS OF TESTING

σ_{max} = 0.90 Age: 28 Days

Series Designation	Number of Static Tests	Stress Range R	Stress Rate, $\dot{f}$ psi/min	Number of Specimens Tested
C1	3	0.10	600	2
C2	2	0.90	60,000	4
		0.50	60,000	2
		0.10	60,000	1
C3	2	0.10	60,000	1
		0.90	600	1
		0.50	600	2
		0.10	600	1
C4	3	0.50	60,000	1
		0.90	600	2
		0.10	600	1
C5	2	0.50	60,000	1
		0.10	60,000	2
		0.90	600	1
		0.50	600	2
		0.10	600	2

Total number of specimens tested is 26.

TABLE 5.3

PHASE TWO

TEST RESULTS OF STATIC TESTS

Strain Rate, $\dot{\varepsilon}$ in/in/sec	Specimen Number	Ultimate Static Strength f_{cup} (psi)	Ultimate Strain, $\varepsilon_{\ell u}$ (in/in x 10^{-3})
10^{-3}	1	5006	1.86
	2	5100	1.98
	3	5100	1.92
	Average	5070	1.92
10^{-5}	1	4388	2.04
	2	4730	2.10
	3	4102	1.92
	Average	4407	2.02
10^{-7}	1	4083	2.70
	2	3984	3.06
	3	4036	2.97
	Average	4034	2.91

TABLE 5.4

PHASE TWO

TEST RESULTS OF REPEATED LOAD TESTS

$\sigma_{max} = 0.90 \quad \dot{f} = 60{,}000$ psi/min

Series	Static Tests		Repeated Load Tests†			
	f_{cup} (psi)	$\varepsilon_{\ell u}$	R	n_u	Longitudinal ε_{max}	Longitudinal ε_{min}
C2	3800	1.770	0.90	395	3.110	1.600
C2	3800	1.770	0.90	508	2.780	1.460
C2	3800	1.770	0.90	528	3.140	1.660
C2	3800	1.770	0.90	224	3.060	1.530
C2	3800	1.770	0.50	1922	2.430	1.840
C2	3800	1.770	0.50	21300	3.200	2.940
C2	3800	1.770	0.10	10020	3.420	3.350
C3	4190	1.950	0.10	39000*	--	--
C4	3860	1.700	0.50	3063	2.630	2.180
C5	4055	2.070	0.50	5930	3.140	2.620
C5	4055	2.070	0.10	5467	2.870	2.790
C5	4.55	2.070	0.10	15438	3.400	3.290

† Given are failure strains in in./in. x 10^{-3}.

* Did not fail.

TABLE 5.5

PHASE TWO

TEST RESULTS OF REPEATED LOAD TESTS

$\sigma_{max} = 0.90$ $\quad \dot{f} = 600$ psi/min

Series	Static Tests		Repeated Load Tests*			
	f_{cup} (psi)	$\varepsilon_{\ell u}$	R	n_u	Longitudinal ε_{max}	Longitudinal ε_{min}
C1	4407	2.020	0.10	78	3.480	3.210
C1	4407	2.020	0.10	72	3.920	3.732
C3	4190	1.950	0.90	18	3.370	1.920
C3	4190	1.950	0.50	64	3.130	2.540
C3	4190	1.950	0.50	287	4.380	3.840
C3	4190	1.950	0.10	331	4.810	4.640
C4	3860	1.700	0.90	13	--	--
C4	3860	1.700	0.90	98	3.640	2.290
C4	3860	1.700	0.10	3150	4.970	4.880
C5	4055	2.070	0.90	25	2.990	1.750
C5	4055	2.070	0.50	250	3.600	3.070
C5	4055	2.070	0.50	56	3.200	2.670
C5	4055	2.070	0.10	1086	4.590	4.480
C5	4055	2.070	0.10	26	2.970	2.850

* Given are failure strains in in/in x 10^{-3}

TABLE 5.6

PHASE TWO

LOGARITHMIC AVERAGE OF CYCLES TO FAILURE

Stress Range	Stress Rate, $\mathring{f}$ (psi/min)		
	600	6,000	60,000
R	Failure Cycles, $\bar{n}_u$		
0.90	28	133	392
0.50	127	730	5222
0.10	234	3715	13480

TABLE 5.7

PHASE TWO

RESULTS OF STATISTICAL ANALYSIS

$\sigma_{max} = 0.90$ R = 0.90

Data Set	Stress Rate, psi/min	No. of Tests	Maximum Log, n_u	Minimum Log, n_u	Mean $\bar{x}$*	Variance S^2	Std. dev. S	Probability of Range of Data max. to min. (%)	90% Probability Interval max.	90% Probability Interval min.	Probability that	Probability is (%)
1	60,000	4	2.723	2.350	2.594	.022	.149	76.00	2.839	2.349	$\bar{x}_1 > \bar{x}_2$	>99.9
2	6,000	4	2.283	2.004	2.123	.010	.101	83.00	2.289	1.957	$\bar{x}_2 > \bar{x}_3$	>99.99
3	600	4	1.991	1.114	1.440	.111	.334	79.00	1.989	0.891	--	--

N.B.: Statistical analysis is based on the logarithm of the number of cycles to failure.

* $\bar{x} = \bar{n}_u$, the logarithmic average of the number of cycles to failure.

TABLE 5.8

PHASE TWO

RESULTS OF STATISTICAL ANALYSIS

$\sigma_{max} = 0.90$ R = 0.50

Data Set	Stress Rate, psi/min	No. of Tests	Maximum Log, n_u	Minimum Log, n_u	Mean $\bar{x}$*	Variance S^2	Std. Dev. S	Probability of Range of Data max to min (%)	90% Probability Interval max	90% Probability Interval min	Probability that	Probability is (%)
1	60,000	4	4.328	3.284	3.718	0.154	0.393	80.30	4.363	3.072	$\bar{x}_1 > \bar{x}_2$	99.95
2	6,000	4	3.259	2.382	2.863	0.104	0.322	82.70	3.393	2.333	$\bar{x}_2 > \bar{x}_3$	99.95
3	600	4	2.458	1.748	2.103	0.107	0.327	72.90	2.641	1.565	--	--

N.B.: Statistical analysis is based on the logarithm of the number of cycles to failure.

* $\bar{x} = \bar{n}_u$, the logarithmic average of the number of cycles to failure.

TABLE 5.9

PHASE TWO

RESULTS OF STATISTICAL ANALYSIS

σ_{max} = 0.90 R = 0.10

Data Set	Stress Rate psi/min	No. of Tests	Maximum Log, n_u	Minimum Log, n_u	Mean, $\bar{x}$*	Variance S^2	Std. Dev. S	Probability of Range of Data max to min (%)	90% Probability Interval max	90% Probability Interval min	Probability that	Probability is (%)
1	60,000	4	4.591	3.738	4.130	0.097	0.311	82.70	4.534	3.726	$\bar{x}_1 > \bar{x}_2$	99.98
2	6,000	3	3.596	3.550	3.570	0.000	0.019	76.5	3.595	3.545	$\bar{x}_2 > \bar{x}_3$	99.99
3	600	6	3.498	1.415	2.370	0.524	0.724	84.1	3.311	1.429	--	--

N.B.: Statistical analysis is based on the logarithm of the number of cycles to failure.

* $\bar{x} = \bar{n}_u$, the logarithmic average of the number of cycles to failure.

TABLE 6.1

PHASE THREE

DETAILS OF TESTING

Phase	Series Designation	Maximum Stress Level, σ_{max}	Stress Range, R	Life Ratio, L Applied Prior to Reloading	Number of Specimens Tested
3-A	B1	.90	0.00	0.30	2
	B1	.90	0.00	0.60	1
	B1	.90	0.00	0.90	1
	B2	.90	0.00	0.30	2
	B2	.90	0.00	0.60	2
	B2	.90	0.00	0.90	2
	B3	.90	0.00	0.30	2
	B3	.90	0.00	0.60	3
	B3	.90	0.00	0.90	3
	B4	.90	0.00	0.30	4
	B4	.90	0.00	0.90	3
3-B	B5	.90	0.90	0.90	1
	B6	.90	0.90	0.30	2
	B6	.90	0.90	0.60	3
	B6	.90	0.90	0.90	1
	B7	.90	0.90	0.30	2
	B7	.90	0.90	0.60	1
	B7	.90	0.90	0.90	2
	B8	.90	0.90	0.60	1
	B8	.90	0.90	0.90	2
	B9	.90	0.90	0.30	3
	B9	.90	0.90	0.60	2
	B9	.90	0.90	0.90	3
	B10	.90	0.90	0.30	3
	B10	.90	0.90	0.60	2
	B10	.90	0.90	0.90	1
3-C	B11	.95	0.95	0.20	2
	B11	.95	0.95	0.40	1
	B12	.95	0.95	0.20	4
	B12	.95	0.95	0.40	5

Total number of specimens tested is 66.

TABLE 6.2

PHASE 3-A

RESULTS OF SUSTAINED LOAD TESTS

$\sigma_{sus} = 0.90$

Test Number	Series	f_{cup} (psi)	Time Ratio, T Applied Prior to Reloading	Initial Strain $\varepsilon_{\ell 1}$ (in/in x 10^{-3})	Strain Caused by Applied Loads $\varepsilon_{\ell\ell}$ (in/in x 10^{-3})	Time Prior to Reloading (hrs)	Reloading Strength Ratio, σ_{cur}
1	B1	3960	0.30	1.21	0.68	0.583	1.015
2	B1	3960	0.30	1.22	0.69	0.738	1.108
3	B2	4200	0.30	1.38	0.72	0.354	1.010
4	B2	4200	0.30	1.38	0.72	0.290	1.012
5	B3	4360	0.30	1.33	1.06	0.938	1.030
6	B3	4360	0.30	1.31	1.07	0.875	1.031
7	B4	4400	0.30	1.38	1.07	1.050	1.041
8	B4	4400	0.30	1.38	0.94	0.663	1.041
9	B4	4400	0.30	1.39	1.11	1.496	1.071
10	B4	4400	0.30	1.38	1.13	1.805	1.101
1	B4	3960	0.60	1.23	1.01	1.900	0.957
2	B2	4200	0.60	1.38	0.95	1.443	1.080
3	B2	4200	0.60	1.38	0.95	0.338	0.950
4	B3	4360	0.60	1.32	1.43	2.542	1.040
5	B3	4360	0.60	1.31	1.44	2.082	1.032
6	B3	4360	0.60	1.31	1.25	1.135	0.992
1	B1	3960	0.90	1.22	1.43	1.850	1.032
2	B2	4200	0.90	1.38	1.14	0.437	0.970
3	B2	4200	0.90	1.38	1.14	0.373	1.002
4	B3	4360	0.90	1.31	1.44	1.269	0.970
5	B3	4360	0.90	1.31	1.18	0.551	0.938
6	B3	4360	0.90	1.31	1.38	1.280	0.971
7	B4	4400	0.90	1.38	1.25	0.883	0.990
8	B4	4400	0.90	1.38	1.38	0.841	0.966
9	B4	4400	0.90	1.38	1.33	0.702	0.935

TABLE 6.3

PHASE 3-A

RESULTS OF STATISTICAL ANALYSIS OF SUSTAINED LOAD TESTS

$\sigma_{sus} = 0.90$

Data Set	Time Ratio T	No. of Tests	Mean $\bar{x}$*	Max. Value of σ_{cur} (%)	Min. Value of σ_{cur} (%)	Variance S^2	Std. Dev. S	Probability of Range of Data max to min	90% Probability Interval max	90% Probability Interval min	Probability that	Probability is (%)	Probability that	Probability is (%)
1	0.30	10	1.046	110.8	101.9	11.438	3.38	82.64	110.16	99.04	$\bar{x}_1 > \bar{x}_2$	95.34	$\bar{x}_1 > 100$	99.94
2	0.60	6	1.009	108.0	95.0	21.675	4.65	83.50	108.55	93.25	$\bar{x}_2 > \bar{x}_3$	96.78	$\bar{x}_2 > 100$	67.36
													$\bar{x}_2 < 100$	32.64
3	0.90	9	0.9749	103.2	93.5	8.132	2.86	89.59	102.19	92.79	---	--	$\bar{x}_3 < 100$	99.6

* $\bar{x}$: Reloading strength ratio, σ_{cur}.

TABLE 6.4

PHASE 3-B

RESULTS OF REPEATED LOAD TESTS

$\sigma_{max} = 0.90$ R = 0.90

Test No.	Series	f_{cup} (psi)	Cycle Ratio Applied Prior to Reloading N	Initial Strain, $\varepsilon_{\ell 1}$ (in/in x 10^{-3})	Strain Caused by Applied Loads, $\varepsilon_{\ell\ell}$ (in/in x 10^{-3})	Cycles Prior to Reloading	Reloading Strength Ratio, σ_{cur}
1	B6	4560	0.30	1.13	.09	14	1.015
2	B6	4560	0.30	1.09	.14	23	1.030
3	B7	4170	0.30	1.31	.08	6	1.021
4	B7	4170	0.30	1.31	.09	6	1.046
5	B9	3820	0.30	1.06	.25	21	1.078
6	B9	3820	0.30	1.06	.28	35	1.112
7	B9	3820	0.30	1.06	.27	25	1.084
8	B10	4120	0.30	1.13	.15	6	1.021
9	B10	4120	0.30	1.13	.14	11	1.032
10	B10	4120	0.30	1.13	.21	17	1.060
1	B6	4560	0.60	1.16	.55	90	1.032
2	B6	4560	0.60	1.09	.17	30	1.028
3	B6	4560	0.60	1.09	.26	22	0.960
4	B7	4170	0.60	1.31	.19	7	0.976
5	B8	4030	0.60	1.13	.34	11	0.965
6	B9	3820	0.60	1.06	.38	20	0.995
7	B9	3820	0.60	1.06	.46	50	1.047
8	B10	4120	0.60	1.13	.31	12	0.966
9	B10	4120	0.60	1.13	.34	11	0.950
1	B5	3950	0.90	1.25	.69	35	0.925
2	B6	4560	0.90	1.16	.48	46	0.998
3	B7	4170	0.90	1.31	.49	16	0.9225
4	B7	4170	0.90	1.31	.27	9	0.9188
5	B8	4030	0.90	1.13	.13	3	0.915
6	B8	4030	0.90	1.13	.59	18	0.935
7	B9	3820	0.90	1.06	.64	47	0.960
8	B9	3820	0.90	1.06	.81	54	0.988
9	B9	3820	0.90	1.06	.82	56	1.000
10	B10	4120	0.90	1.16	.65	19	0.935

TABLE 6.5

PHASE 3-B

RESULTS OF STATISTICAL ANALYSIS OF REPEATED LOAD TESTS

σ_{max} = 0.90 R = 0.90

Data Set	Cycle Ratio N	No. of Tests	Mean $\bar{x}^*$ (%)	Max Value of σ_{cur} (%)	Min Value of σ_{cur} (%)	Variance S^2	Std. Dev. S	Probability of Range of Data max to min	90% Probability Interval max	90% Probability Interval min	Probability that	Probability is (%)	Probability that	Probability is (%)
1	0.30	10	105	111.2	101.5	9.53	3.09	84.85	110.8	99.2	$\bar{x}_1 > \bar{x}_2$	99.99	$\bar{x}_1 > 100$	99.999
2	0.60	9	99.1	104.70	95.0	11.52	3.395	83.65	104.7	93.5	$\bar{x}_2 > \bar{x}_3$	99.7	$\bar{x}_2 > 100$	21.19
													$\bar{x}_2 < 100$	78.81
3	0.90	10	95.0	100	91.5	9.52	3.09	81.84	100.08	89.92	--	--	$\bar{x}_3 < 100$	99.999

* $\bar{x}$: Reloading strength ratio, σ_{cur}

TABLE 6.6

PHASE 3-C

RESULTS OF REPEATED LOAD TESTS

σ_{max} = 0.95 R = 0.95

Test No.	Series	f_{cup} (psi)	Cycle Ratio,N Applied Prior to Reloading	Initial Strain, $\varepsilon_{\ell 1}$ (in/inx10^{-3})	Strain Caused by Applied Loads, $\varepsilon_{\ell\ell}$ (in/inx10^{-3})	Cycles Prior to Reloading	Reloading Strength Ratio σ_{cur}
1	B11	4020	0.20	1.31	.11	3	1.013
2	B11	4020	0.20	1.31	.06	3	1.030
3	B12	3940	0.20	1.25	.08	4	1.041
4	B12	3940	0.20	1.25	.09	3	0.995
5	B12	3940	0.20	1.25	.10	3	1.035
6	B12	3940	0.20	1.25	.09	3	1.001
1	B11	4020	0.40	1.31	.21	6	0.980
2	B12	3940	0.40	1.25	.24	8	0.975
3	B12	3940	0.40	1.25	.13	3	0.990
4	B12	3940	0.40	1.25	.13	3	0.975
5	B12	3940	0.40	1.25	.23	5	0.965
6	B12	3940	0.40	1.25	.13	3	0.953

TABLE 6.7

PHASE 3-C

RESULTS OF STATISTICAL ANALYSIS OF REPEATED LOAD TESTS

$\sigma_{max} = 0.95$ R = 0.95

Data Set	Cycle Ratio, N	Number of Tests	Mean, $\bar{x}^*$(%)	Max. Value of σ_{cur}(%)	Min. Value of σ_{cur}(%)	Variance S^2	Std. dev. S	Probability of Range of data max. to min.	Probability that	Probability is (%)	Probability that	Probability is (%)
1	0.40	6	101.9	104.1	99.5	3.0	1.73	90.7	$\bar{x}_1 > \bar{x}_2$	99.99	$\bar{x}_1 > 100$	99.65
2	0.40	6	97.3	99.0	95.3	1.35	1.16	94.1	-	-	$\bar{x}_2 > 100$	99.99

* $\bar{x}$: Reloading strength ratio, σ_{cur}

TABLE 7.1

PURE FATIGUE FAILURE CYCLES

$\sigma_{max} = 0.90$

Designation	Stress Rate Ratio, β	Stress Range, R	Observed Failure Cycles,* n_u	Constant, K ($\times 10^{-3}$)	$K\frac{n_u}{\beta}$	Pure Fatigue Failure Cycles, n_o
First Model	15	0.10	16,000	2.280	>1.0	-
	15	0.50	4,900	2.040	0.666	14,671
$n_o = \frac{n_u}{1-K_1\frac{n_u}{\beta}}$	15	0.90	390	2.040	0.053	412
Second Model	15	0.10	16,000	0.912	0.973	593,000
	15	0.50	4,900	0.816	0.267	6,685
$n_o = \frac{n_u}{1-K_2\frac{n_u}{\beta}}$	15	0.90	390	0.816	0.021	398
Third Model	15	0.10	16,000	0.912	0.973	593,000
	15	0.50	4,900	1.960	0.641	13,600
$n_o = \frac{n_u}{1-K_3\frac{n_u}{\beta}}$	15	0.90	390	6.272	0.163	466

* Read from average lines of Fig. (5.8).

TABLE 7.2 .

CALCULATED FAILURE CYCLES

$\sigma_{max} = 0.90$

			First Model			Second Model			Third Model		
R	β	n_u	n_o	$K_1 \frac{n_o}{\beta}$	n_{uc}	n_o	$K_2 \frac{n_o}{\beta}$	n_{uc}	n_o	$K_3 \frac{n_o}{\beta}$	n_{uc}
0.10	0.15	210	--	--	--	593,000	360.2	165	593,000	3602	165
0.10	1.50	1900	--	--	--	593,000	360.2	1642	593,000	360.2	1642
0.10	15.00	16000	--	--	--	593,000	360.2	16000	593,000	36.02	16000
0.50	0.15	125	14,671	199.5	73	6,685	36.37	179	13,600	177.89	76
0.50	1.50	720	14,671	19.95	700	6,685	3.64	1441	13,600	17.89	724
0.50	15.00	4900	14,671	1.995	4900	6,685	0.36	4900	13,600	1.78	4900
0.90	0.15	28	412	5.61	62	398	2.17	126	446	19.48	23
0.90	1.50	133	412	0.56	264	398	0.22	326	446	1.95	158
0.90	15.00	390	412	0.056	390	398	0.02	390	446	0.2	390

TABLE 7.3

CALCULATED FAILURE STRAINS
$\sigma_{max} = 0.90$

R	β	n_{uc}	n_o	$\varepsilon_{\ell 1}$ [1]	$\varepsilon_{\ell n}$ [2]	K	$\varepsilon_{\ell t}$ [3]	$\frac{1}{2}t_{un}$ (mins)	$\frac{\phi}{\phi_\infty}$	$\varepsilon_{\ell c}$ [4]	$\varepsilon_{\ell uc}$ [5]	$\varepsilon_{\ell u}$ [6]
.10	0.15	165	593000	1.4	0	0.0053	5.86	--	--	--	5.86	4.18
.10	1.50	1642	593000	1.4	0	0.0053	5.84	--	--	--	5.84	3.26
.10	15.00	16000	593000	1.4	0.03	0.0053	5.69	--	--	--	5.69	3.26
.50	0.15	76	13600	1.4	0.01	0.0058	2.95	254	.099	0.63	3.58	3.26
.50	1.50	724	13600	1.4	0.06	0.0058	2.81	242	.097	0.62	3.49	3.00
.50	15.00	490	13600	1.4	0.43	0.0058	1.90	164	.080	0.51	2.84	2.98
.90	0.15	23	446	1.4	0.06	0.0058	0.89	138	.079	0.41	1.36	3.12
.90	1.50	158	446	1.4	0.42	0.0058	0.62	95	.063	0.34	1.37	2.60
.90	15.00	390	446	1.4	1.05	0.0058	0.15	24	.028	0.15	1.35	2.61

1 Initial elastic strain

2 Cycle dependent strain, $\varepsilon_{\ell n} = \varepsilon_{\ell \eta o} \cdot \frac{n_{uc}}{n_o}$ ----($\varepsilon_{\ell no} = 1.20$)

3 Time dependent strain, $\varepsilon_{\ell t} = K \cdot n_{uc}/\beta$

4 Creep strain, $\varepsilon_{\ell c} = \frac{n_{uc}}{\beta} \cdot \frac{F_a}{a} \cdot \frac{f_{cup}}{E} \cdot \phi_\infty \, (\sigma^2_{sus} - \sigma^2_{min})$ ---- ($\phi_\infty = 8$)

5 Calculated failure strain, $\varepsilon_{\ell uc} = \varepsilon_{\ell 1} + \varepsilon_{\ell \eta} + \varepsilon_{\ell t} + \varepsilon_{\ell c}$

6 Experimental failure strain

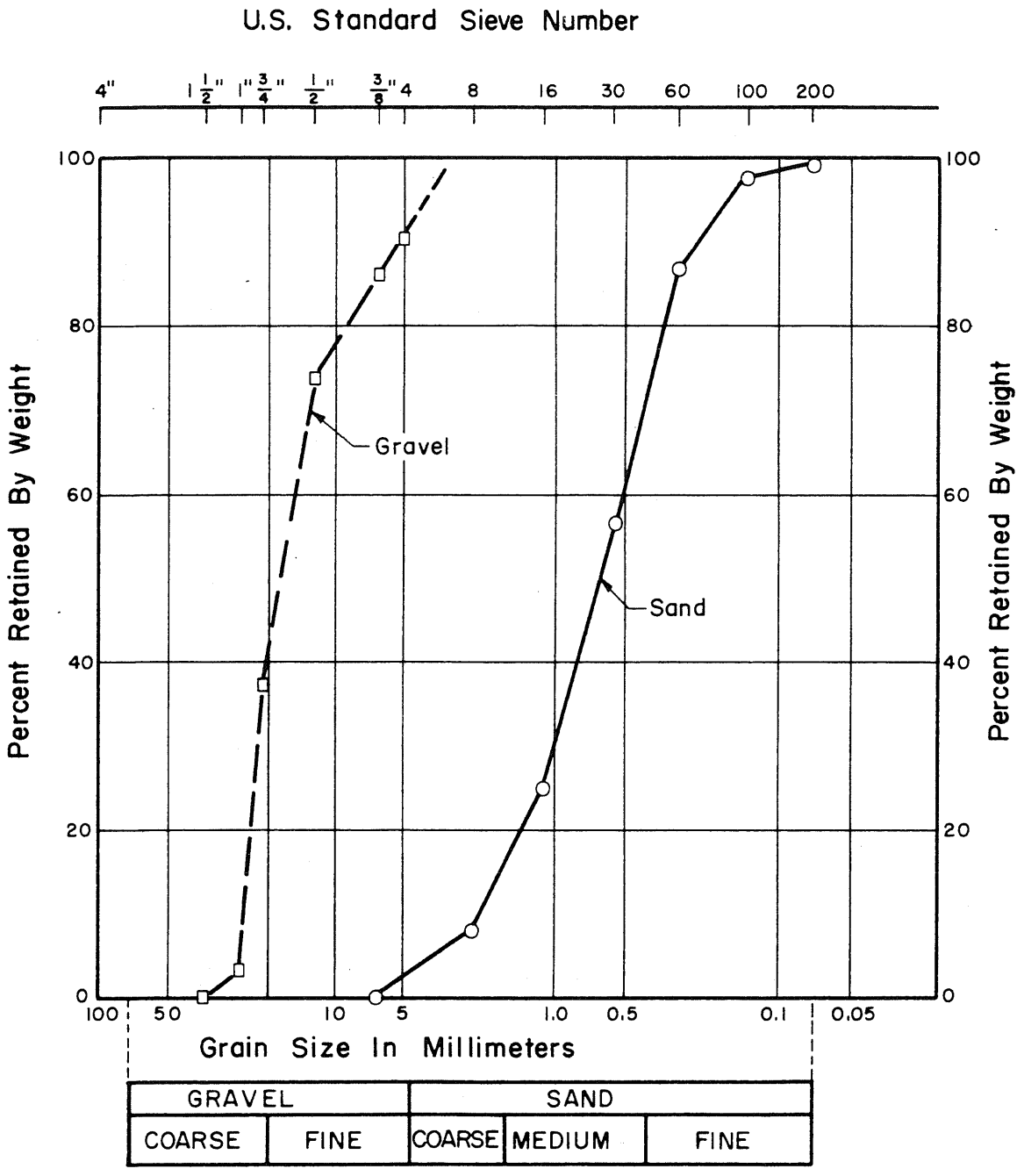

FIG. 3.1 GRADATION CURVES FOR FINE AND COARSE AGGREGATES

FIG. 3.2 VIEW OF CONCRETE PRISM WITH ALUMINUM GAGE POINTS

FIG. 3.3 VIEW OF CLIP GAUGES USED TO MEASURE THE LONGITUDINAL AND LATERAL STRAINS OF SPECIMENS TESTED IN PHASES ONE AND THREE

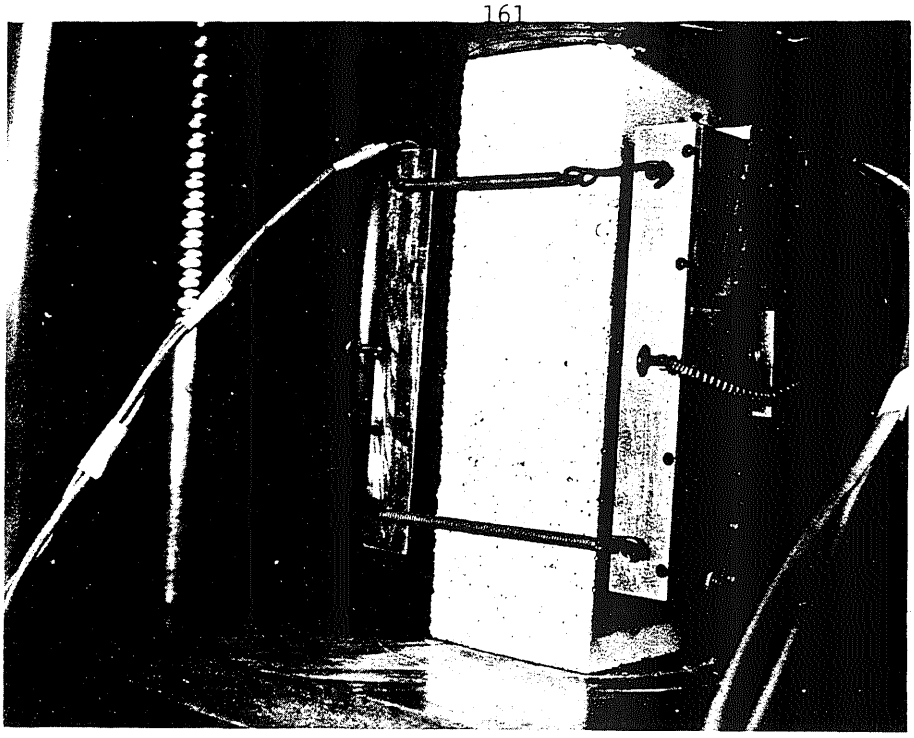

FIG. 3.4 VIEW OF CLIP GAUGES MOUNTED ON A CONCRETE PRISM AND PLACED IN HYDRAULIC TESTING MACHINE

FIG. 3.5 VIEW OF TEST SET-UP FOR PHASE ONE AND PHASE THREE

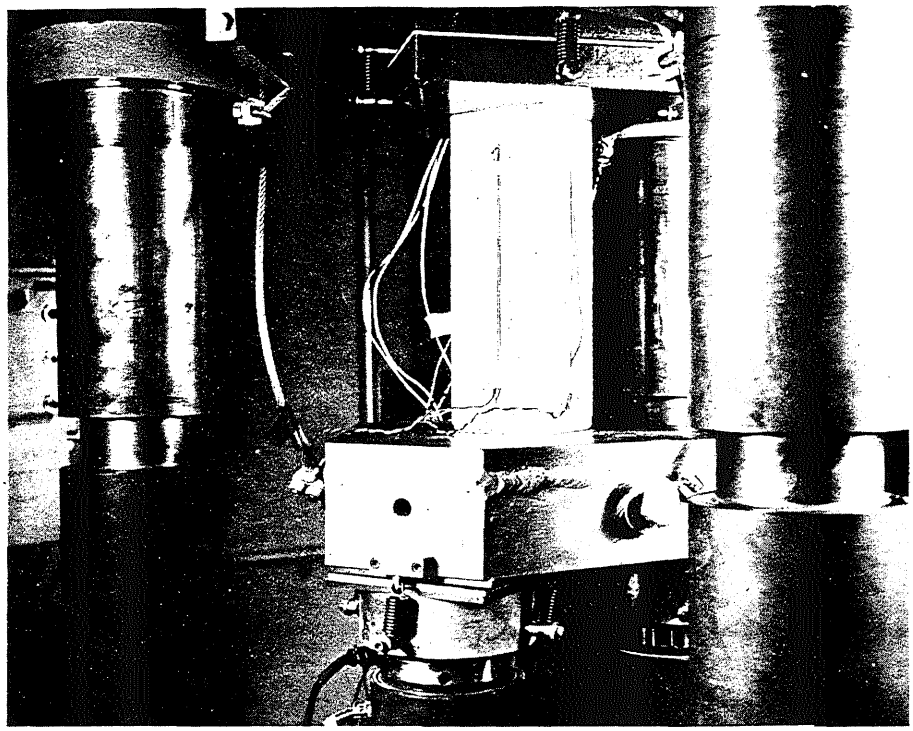

FIG. 3.6 VIEW OF CONCRETE PRISM WITH BONDED SR-4 GAUGES - PHASE TWO

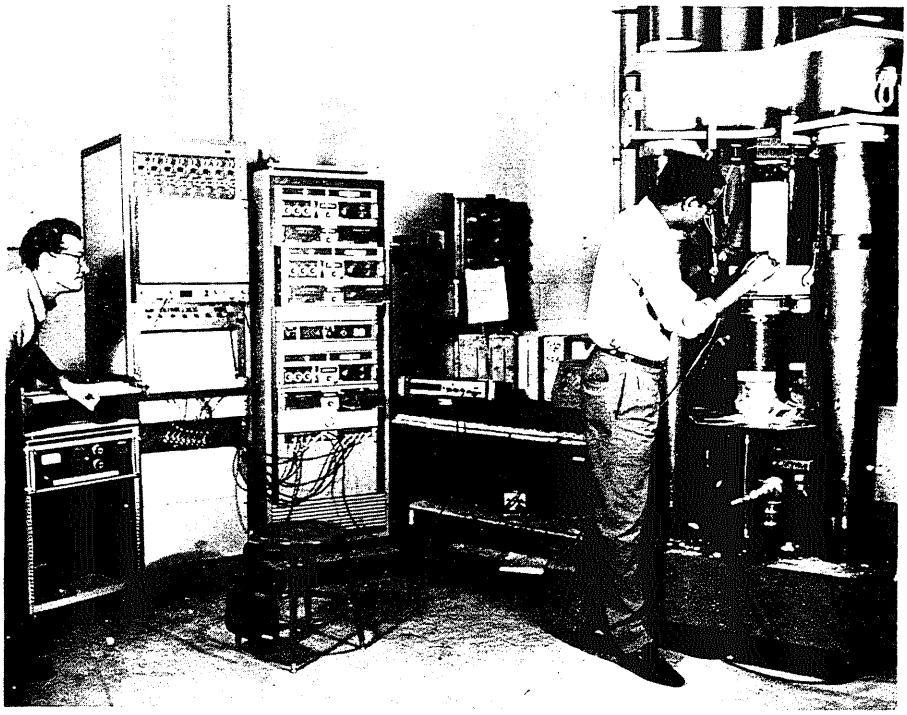

FIG. 3.7 VIEW OF TEST SET-UP FOR PHASE TWO

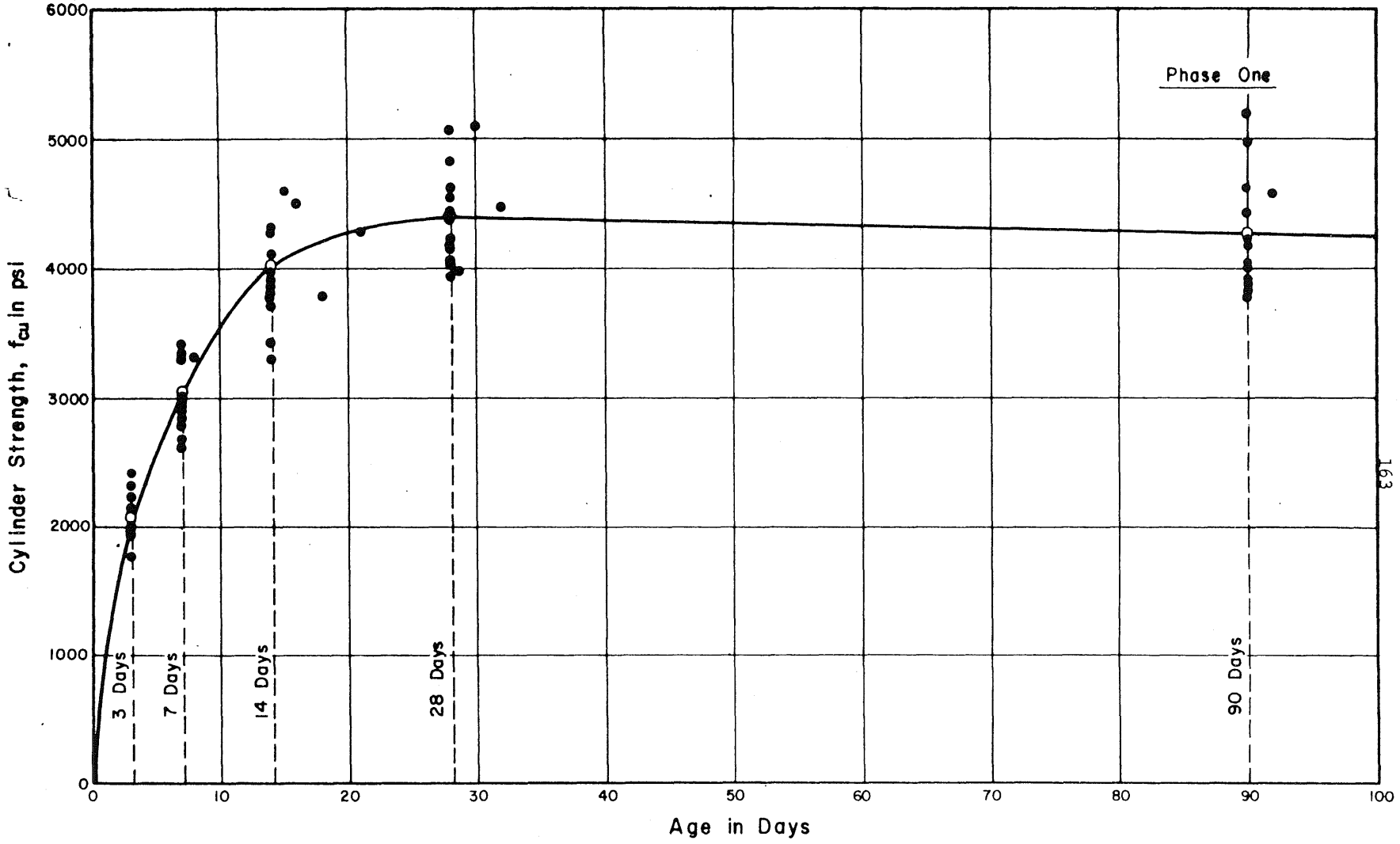

FIG. 4.1 DEVELOPMENT OF CONCRETE CYLINDER STRENGTH WITH AGE : BATCHES A2 TO A19

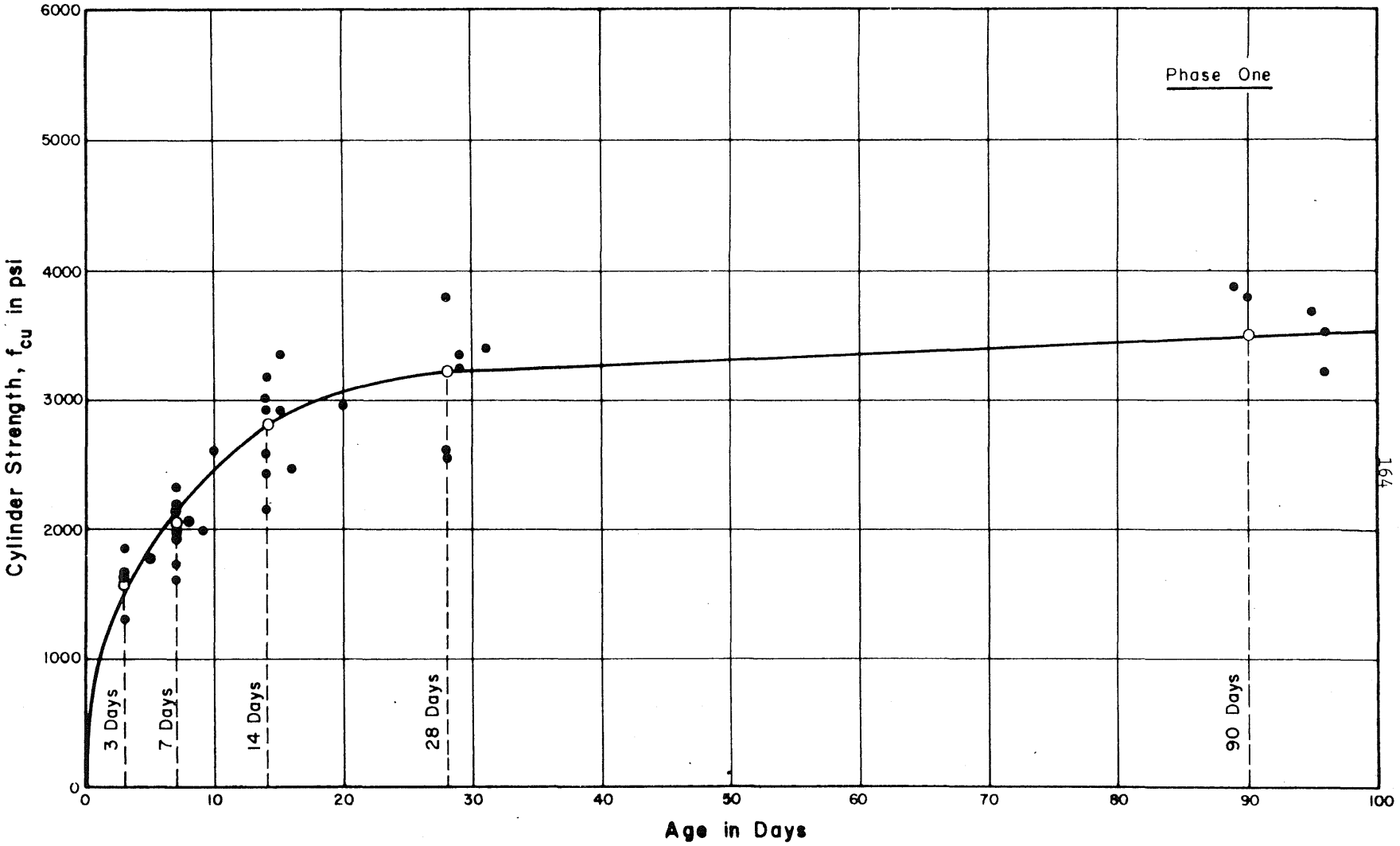

FIG. 4.2 DEVELOPMENT OF CONCRETE CYLINDER STRENGTH WITH AGE : BATCHES A20 TO A30

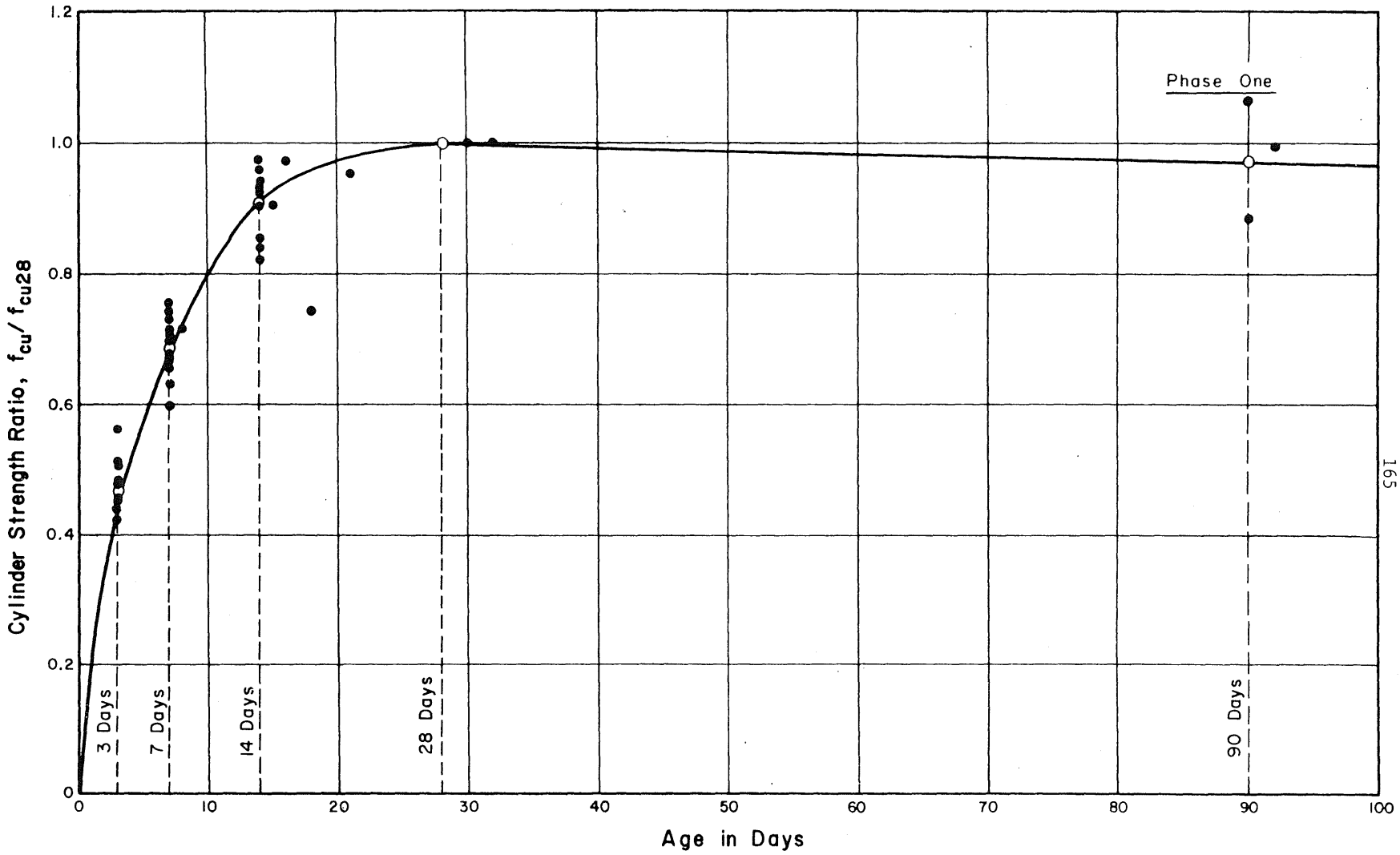

FIG. 4.3 VARIATION OF CYLINDER STRENGTH RATIO WITH CONCRETE AGE : BATCHES A2 TO A19

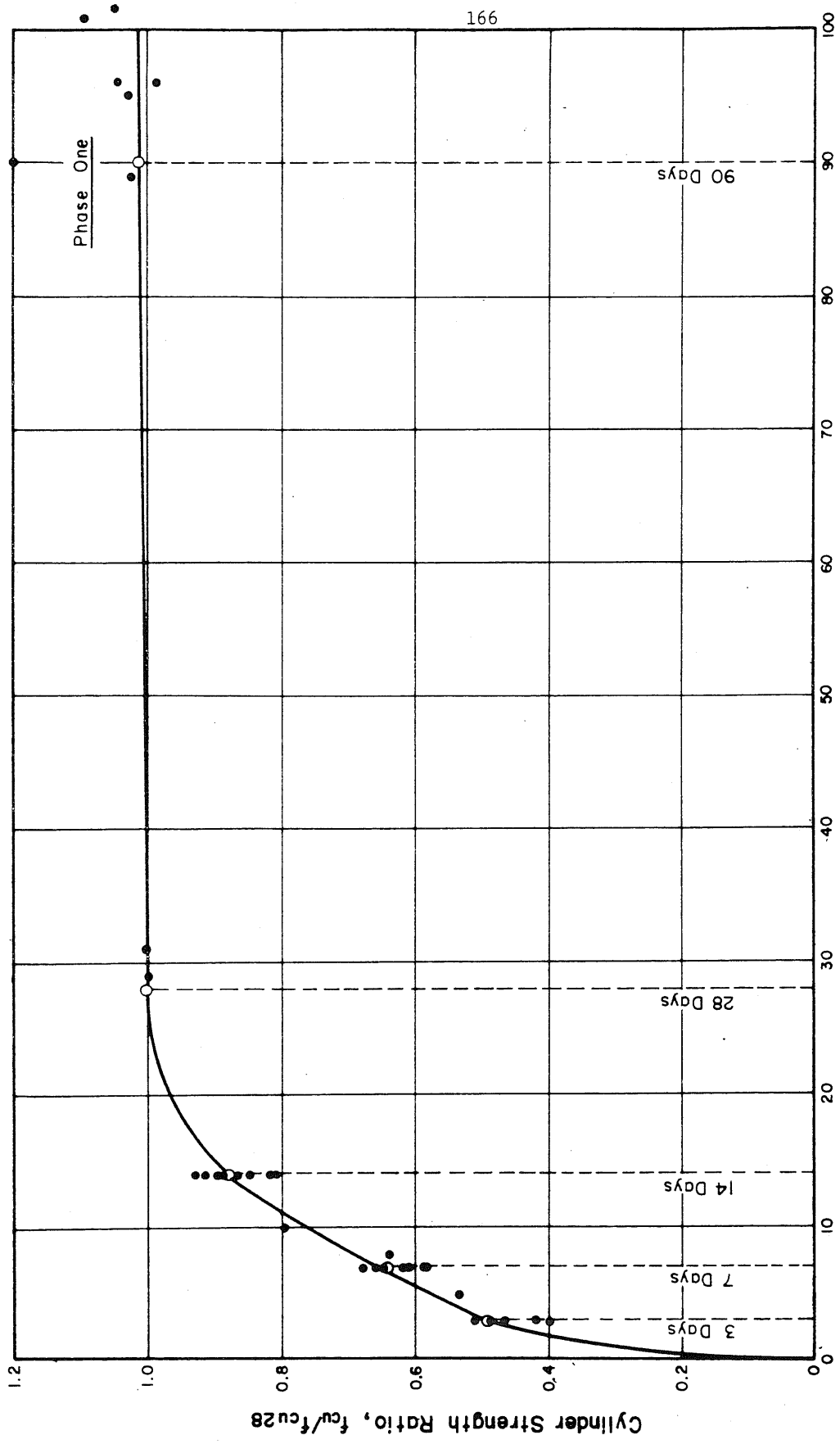

FIG. 4.4 VARIATION OF CYLINDER STRENGTH RATIO WITH CONCRETE AGE : BATCHES A20 TO A30

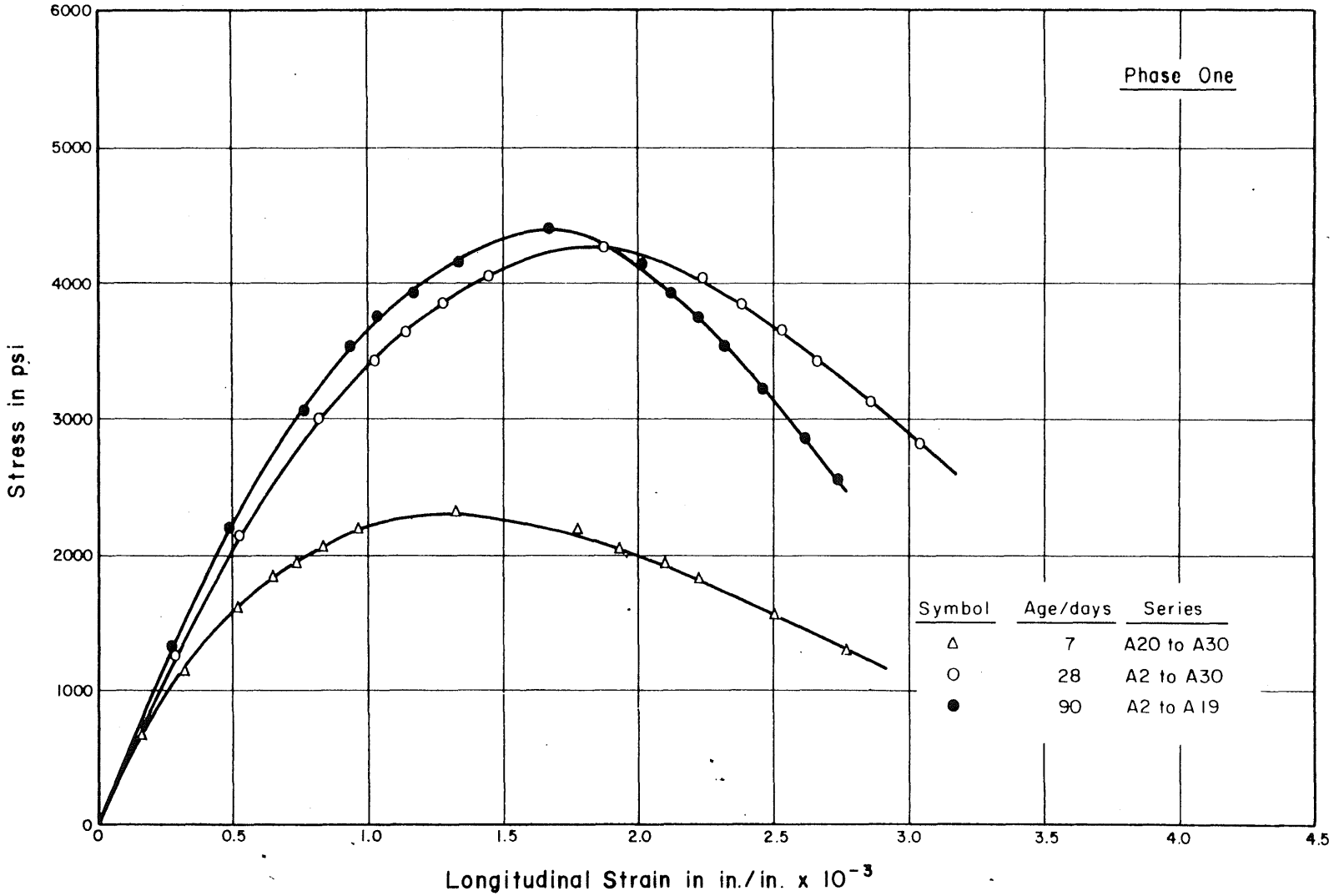

FIG. 4.5 STATIC STRESS–LONGITUDINAL STRAIN CHARACTERISTICS OF CONCRETE PRISMS TESTED AT 7, 28 AND 90 DAYS

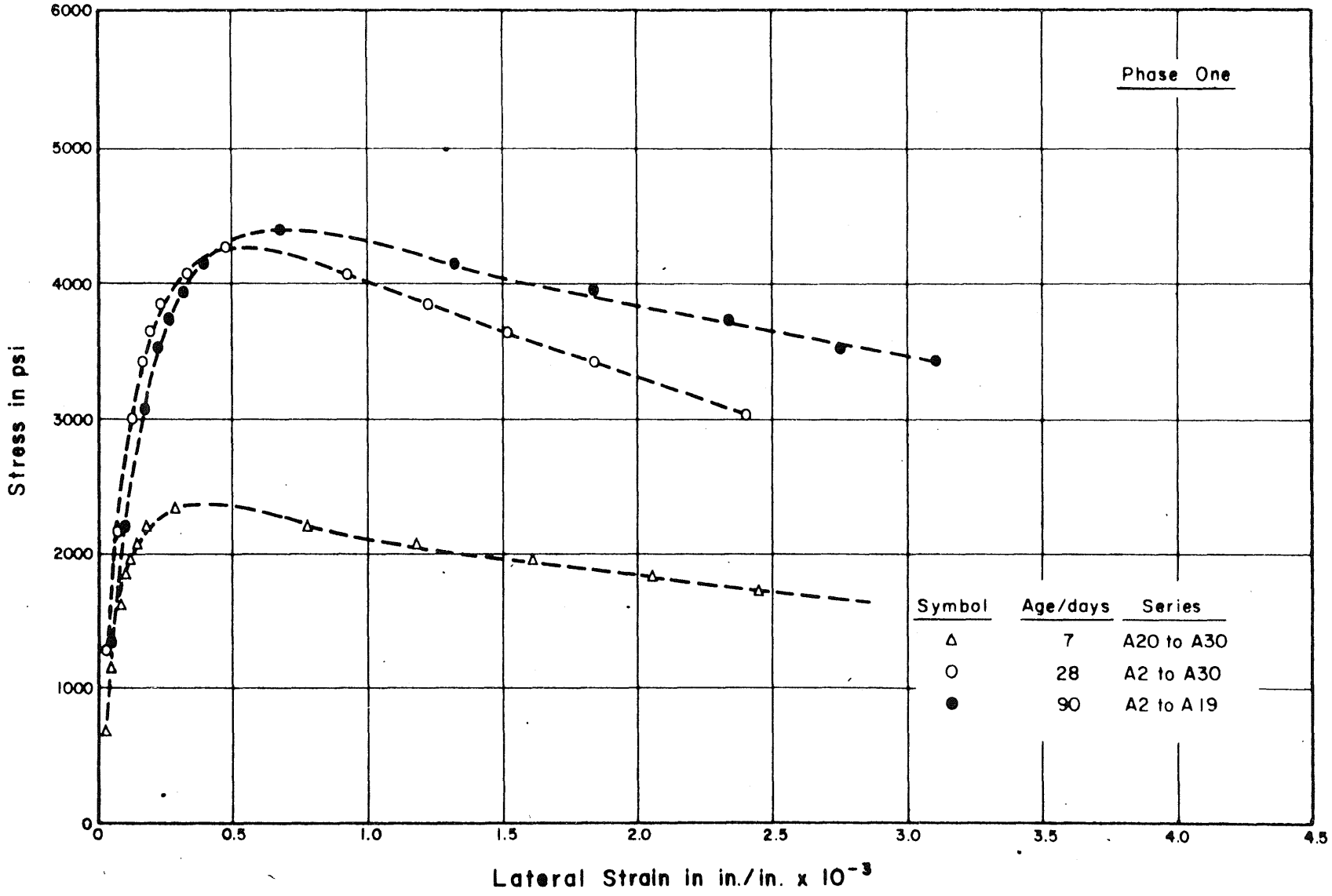

FIG. 4.6 STATIC STRESS–LATERAL STRAIN CHARACTERISTICS OF CONCRETE PRISMS TESTED AT 7, 28 AND 90 DAYS

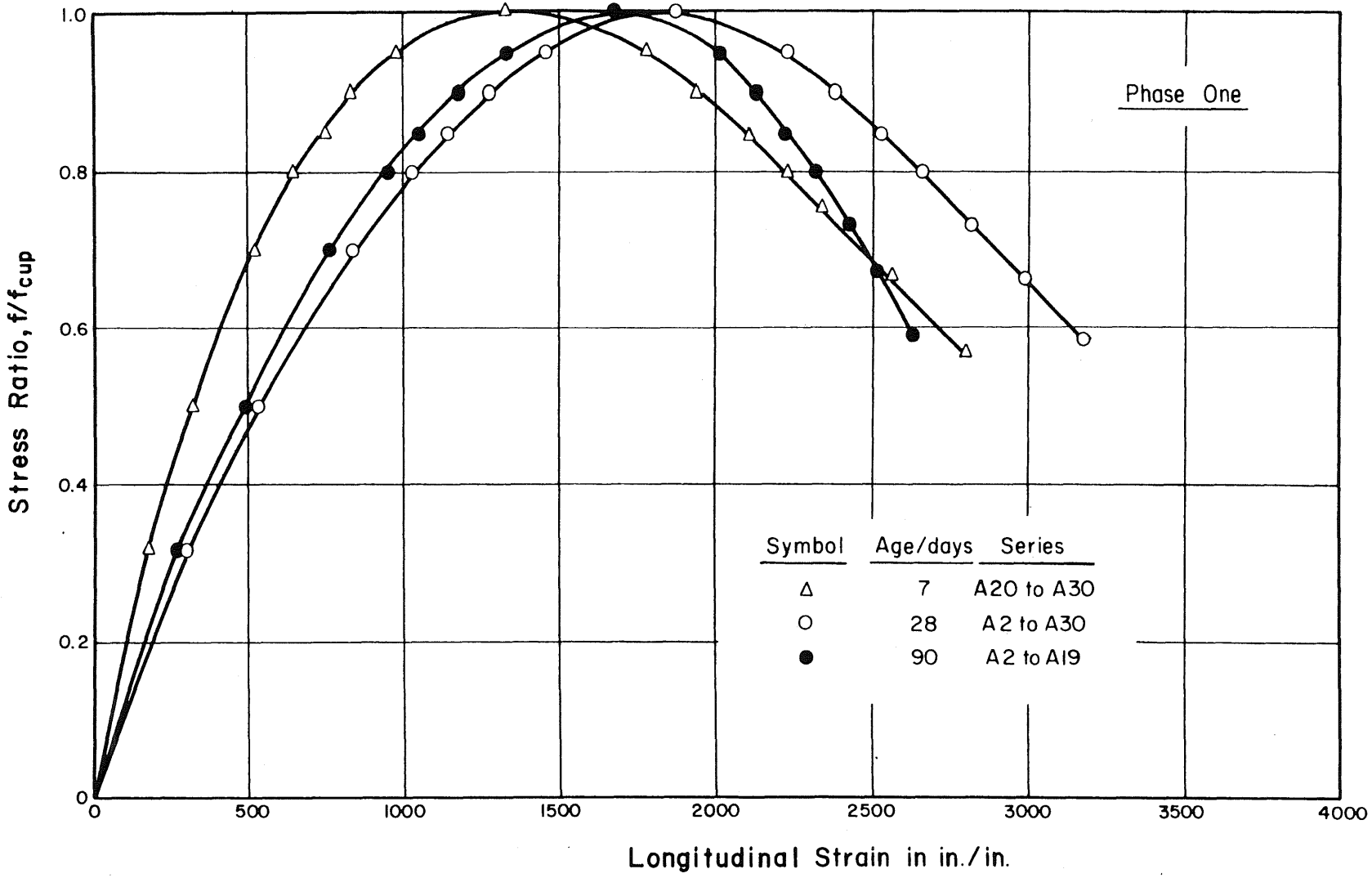

FIG. 4.7 STATIC STRESS RATIO—LONGITUDINAL STRAIN CHARACTERISTICS OF CONCRETE PRISMS TESTED AT 7, 28 AND 90 DAYS

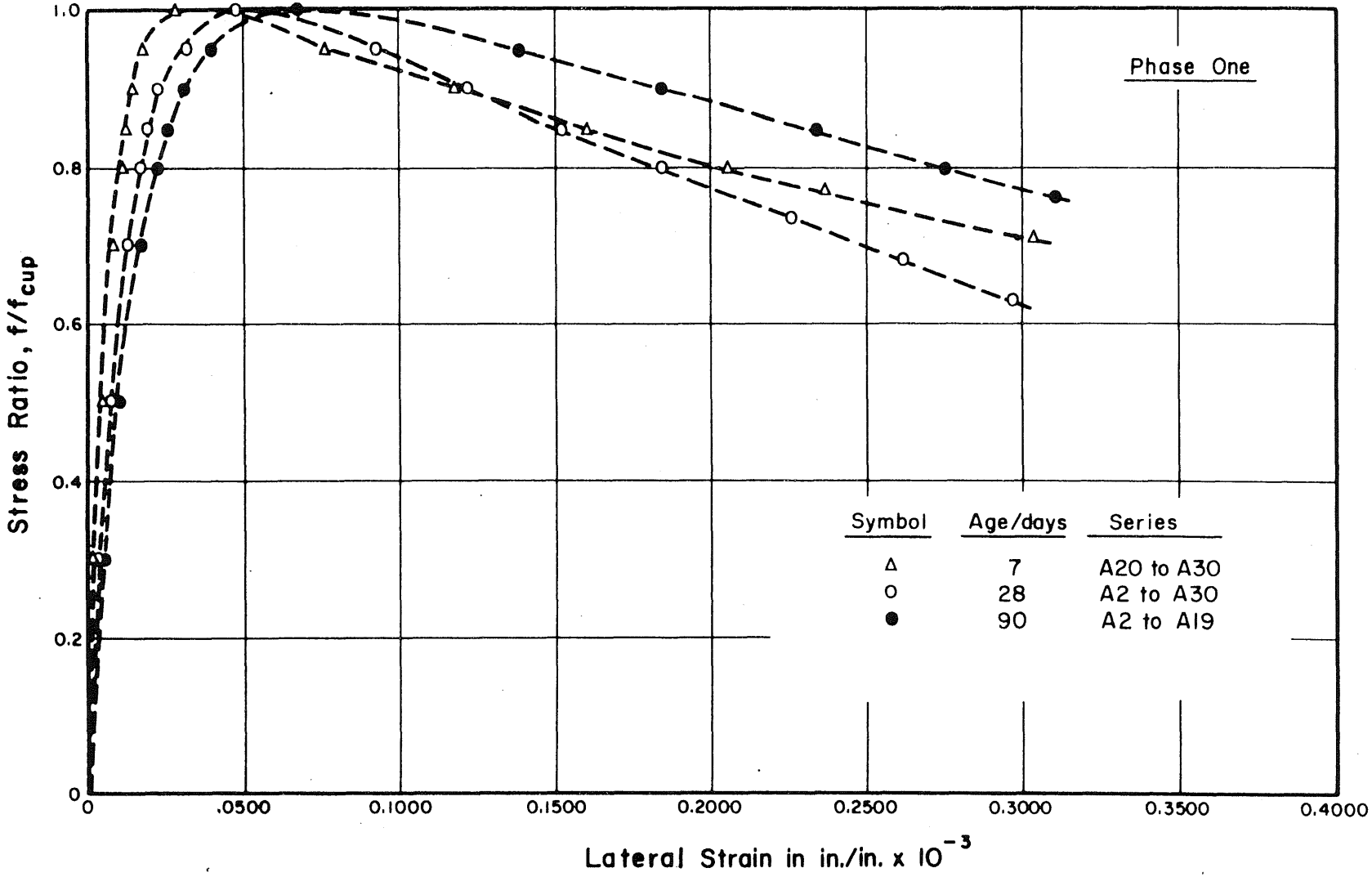

FIG. 4.8 STATIC STRESS RATIO–LATERAL STRAIN CHARACTERISTICS OF CONCRETE PRISMS TESTED AT 7, 28 AND 90 DAYS

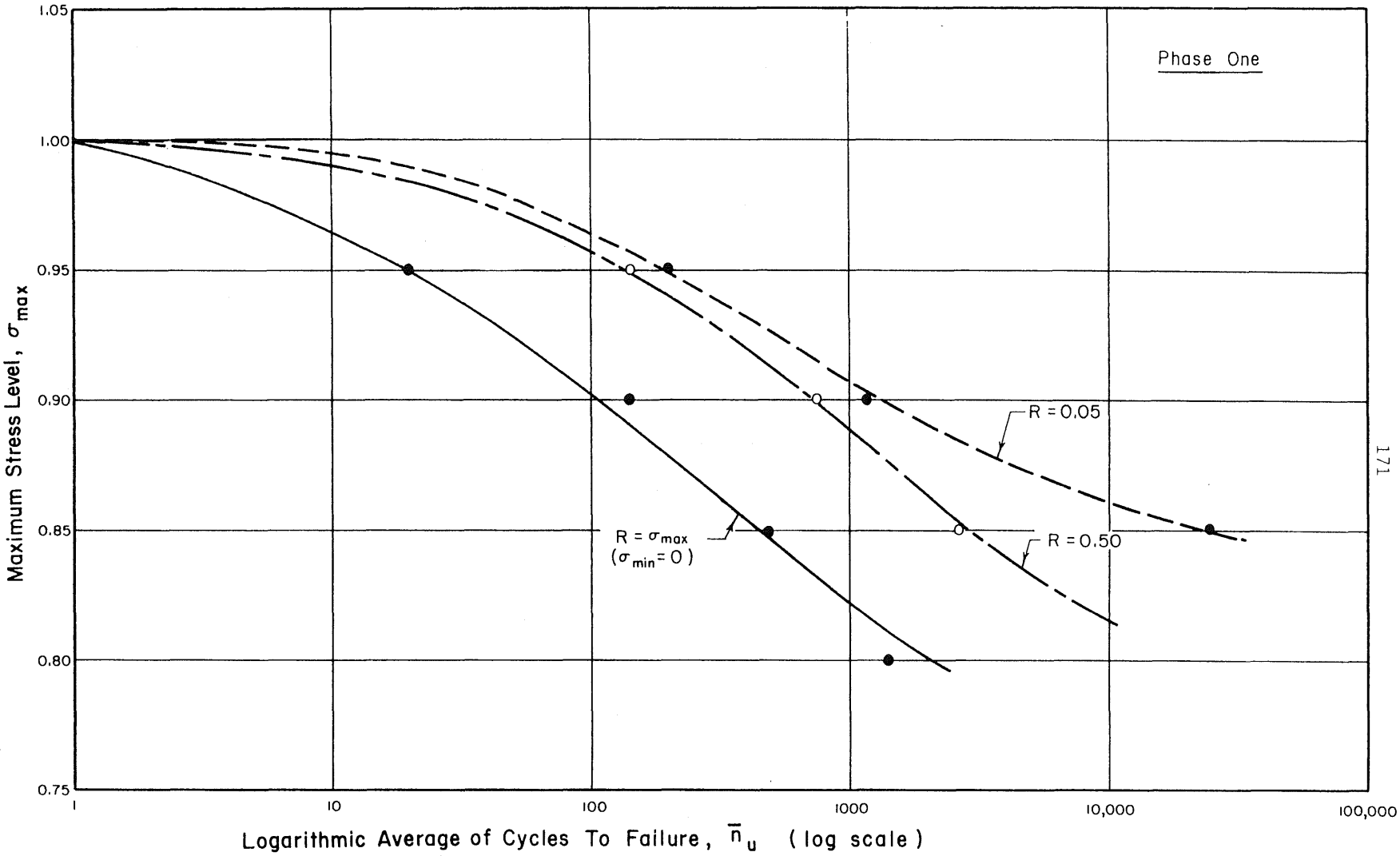

FIG. 4.9 MAXIMUM STRESS LEVEL-CYCLES TO FAILURE RELATIONSHIP FOR DIFFERENT STRESS RANGES: AGE AT LOADING: 28 DAYS

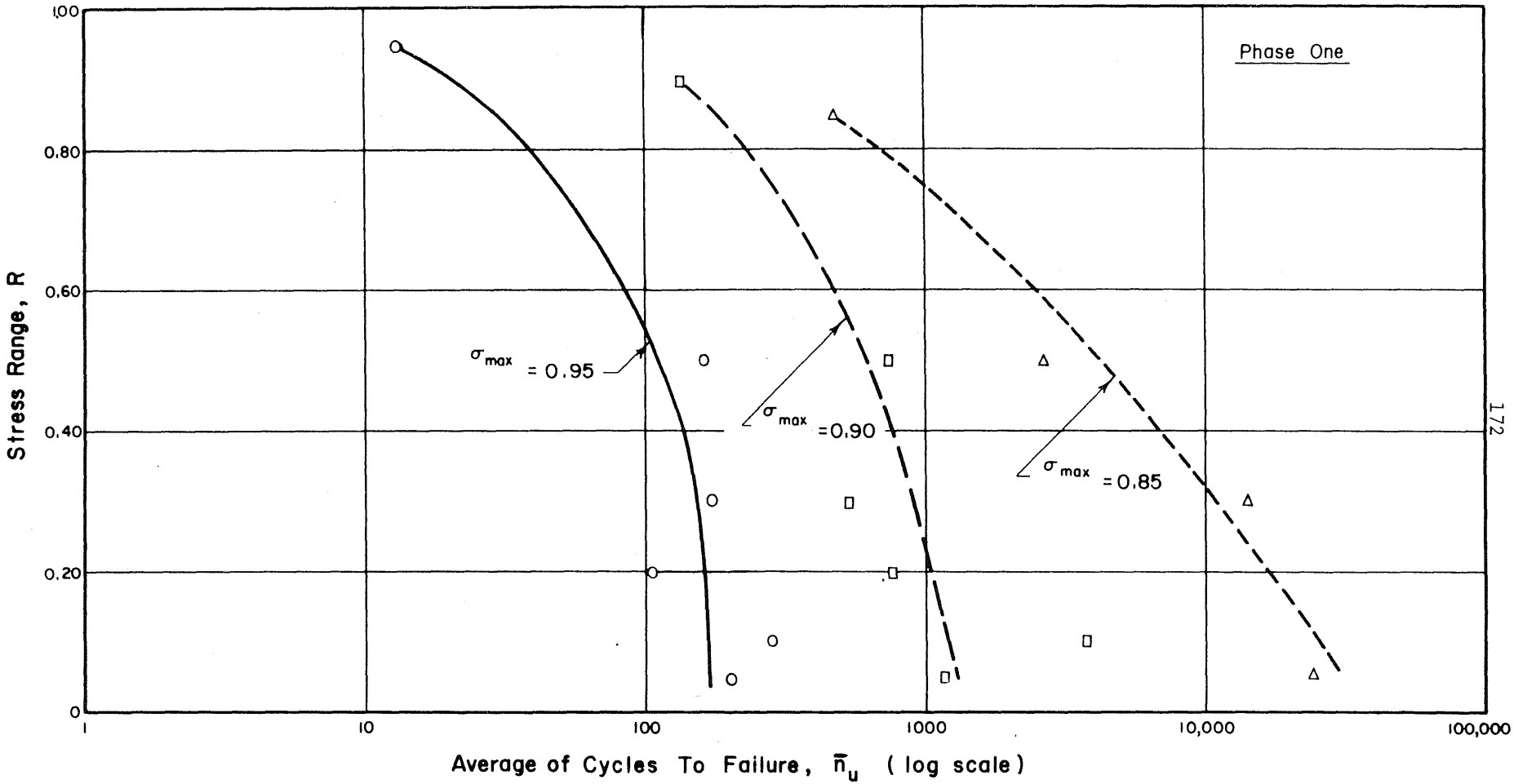

FIG. 4.10 STRESS RANGE–CYCLES TO FAILURE RELATIONSHIP FOR DIFFERENT LEVELS OF MAXIMUM STRESS : AGE AT LOADING: 28 DAYS

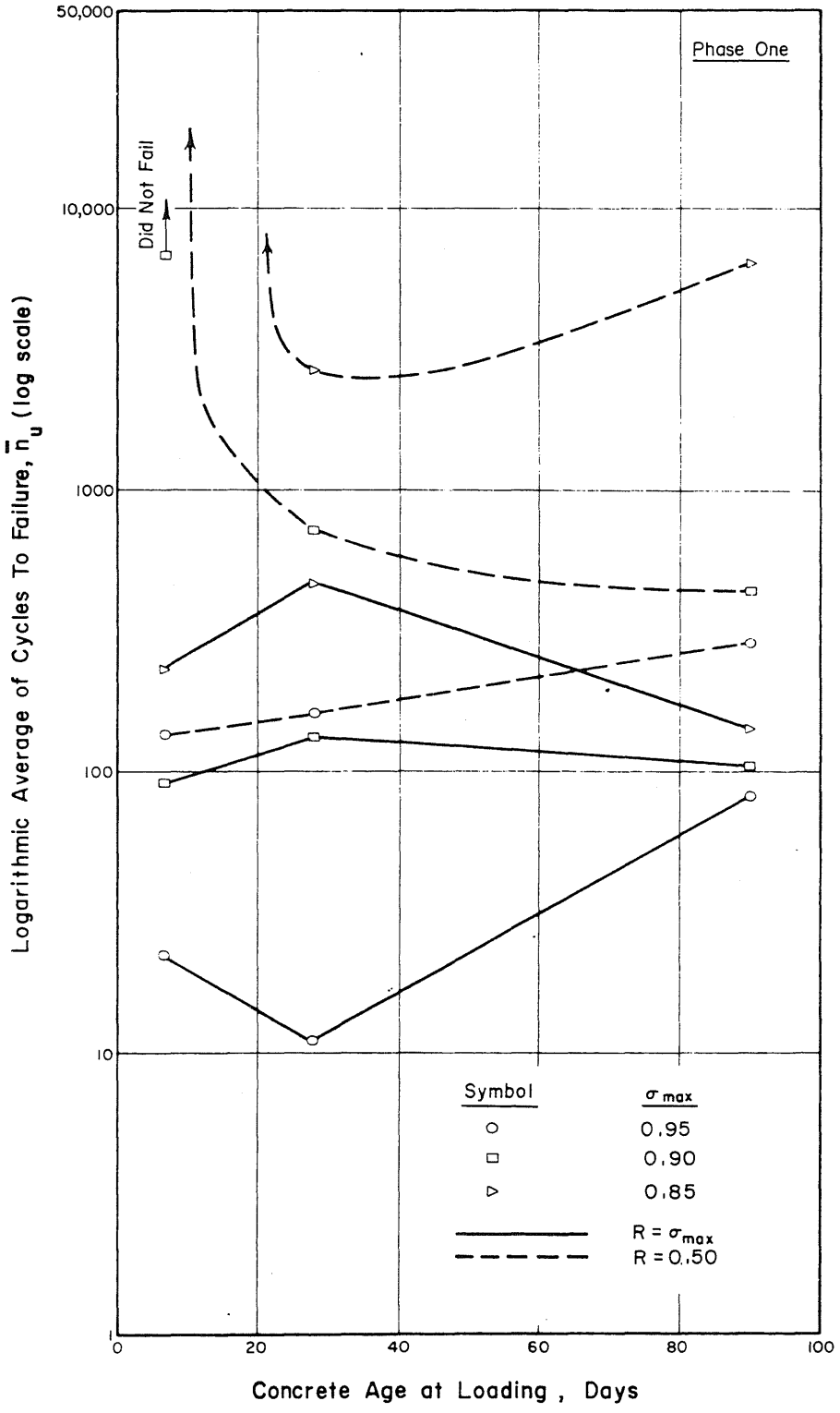

FIG. 4.11 EFFECT OF CONCRETE AGE AT TIME OF LOADING ON ITS FATIGUE LIFE FOR DIFFERENT MAXIMUM STRESS LEVELS AND DIFFERENT STRESS RANGES

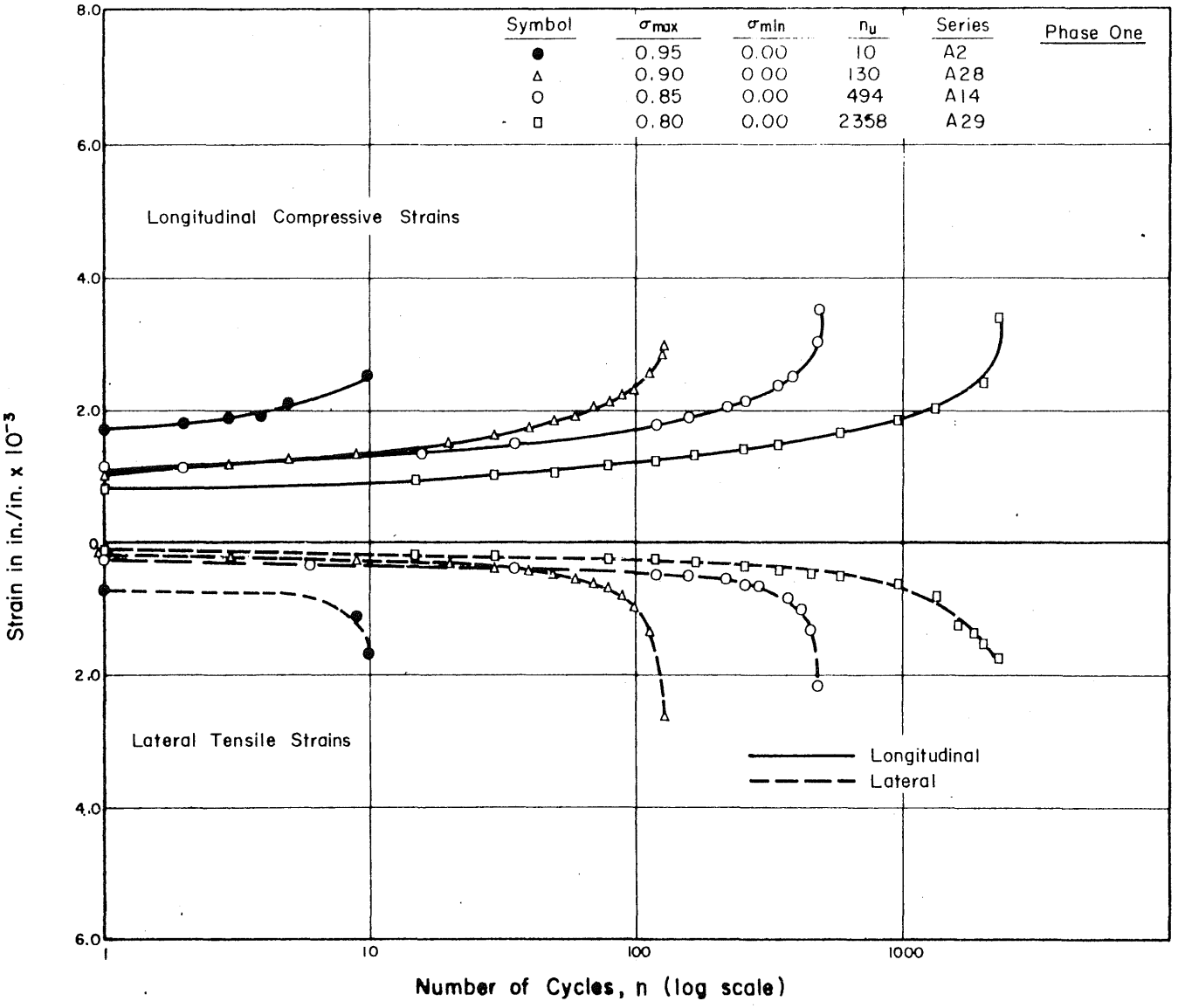

FIG. 4.12 LONGITUDINAL AND LATERAL STRAINS AT MAXIMUM STRESS AS FUNCTION OF NUMBER OF APPLIED CYCLES FOR DIFFERENT MAXIMUM STRESS LEVELS: AGE AT LOADING: 28 DAYS

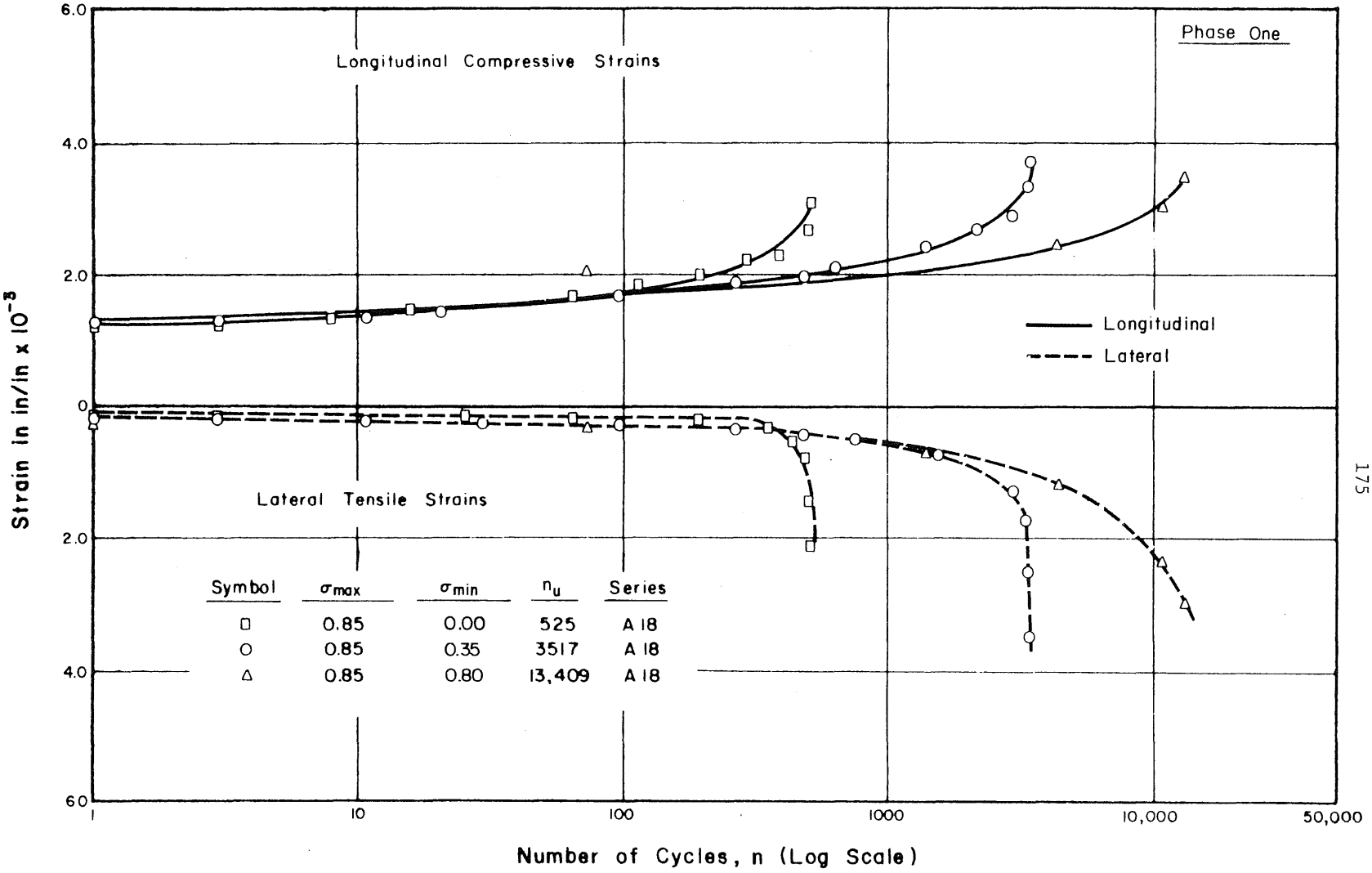

FIG. 4.13 LONGITUDINAL AND LATERAL STRAINS AT MAXIMUM STRESS AS FUNCTION OF NUMBER OF APPLIED CYCLES FOR DIFFERENT STRESS RANGES : AGE AT LOADING : 28 DAYS

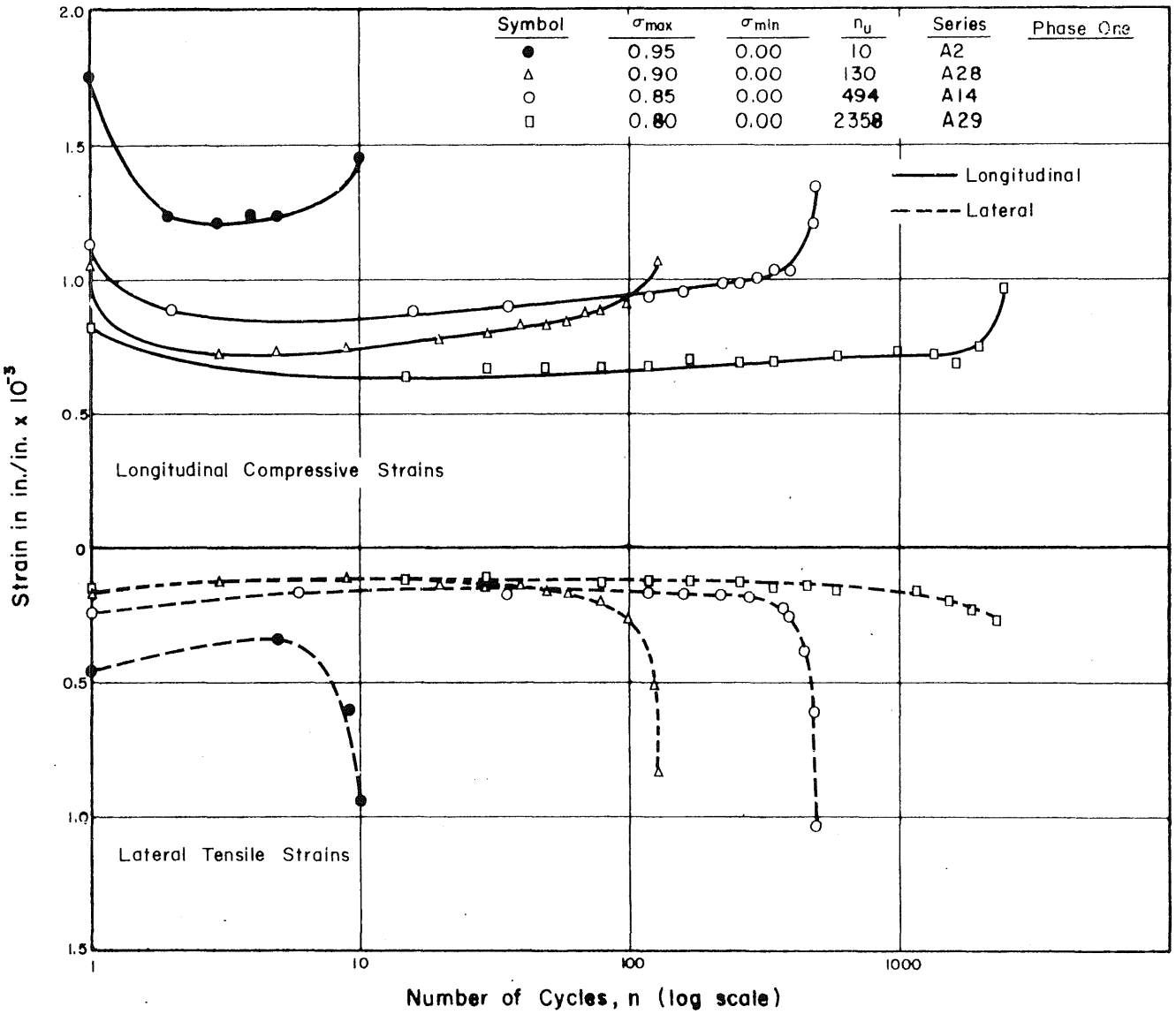

FIG. 4.14 ($\epsilon_{max} - \epsilon_{min}$) AS FUNCTION OF NUMBER OF APPLIED CYCLES FOR DIFFERENT MAXIMUM STRESS LEVELS : AGE AT LOADING : 28 DAYS

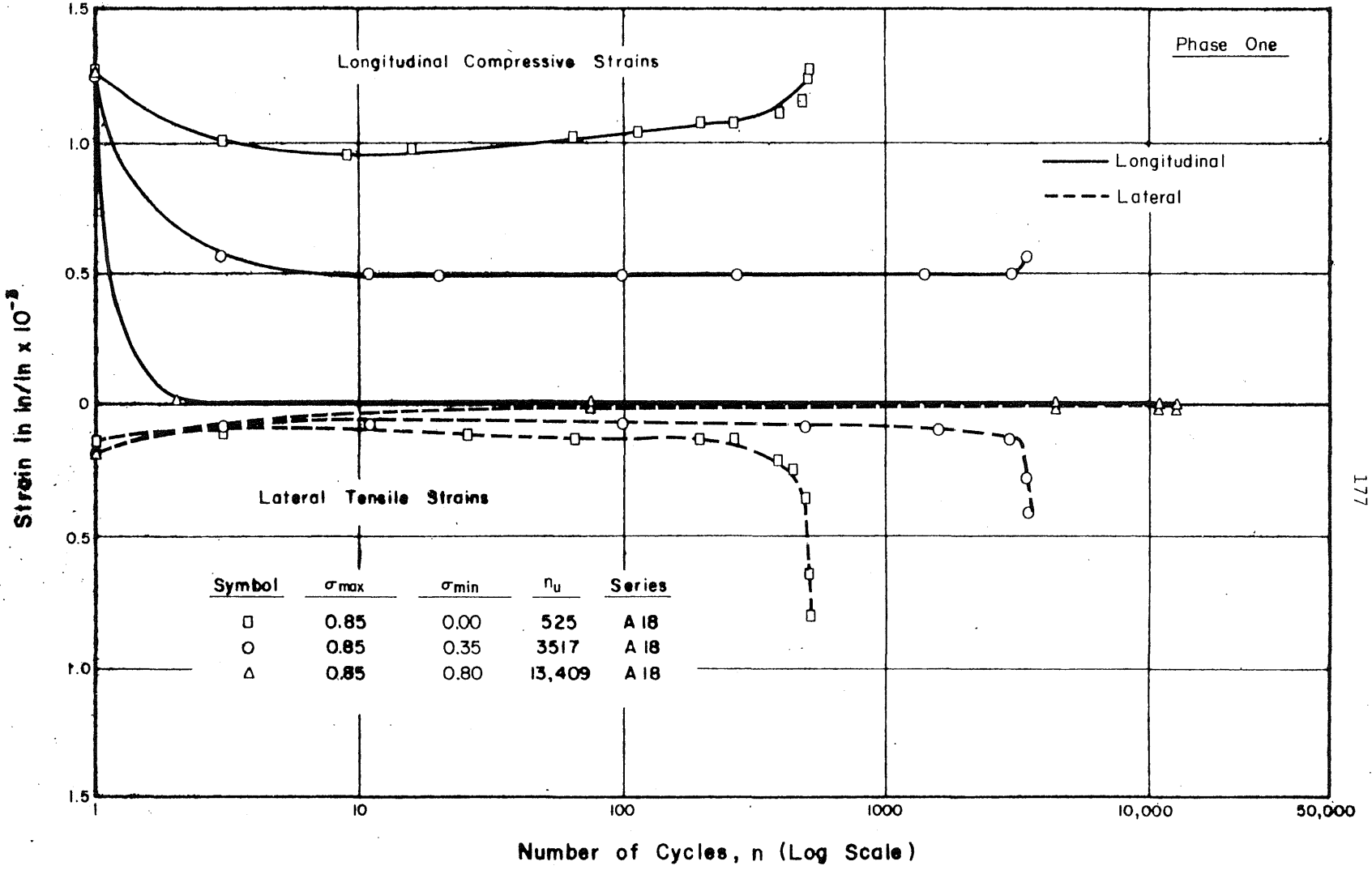

FIG. 4.15 ($\epsilon_{max} - \epsilon_{min}$) AS FUNCTION OF NUMBER OF APPLIED CYCLES FOR DIFFERENT RANGES OF STRESS : AGE AT LOADING : 28 DAYS

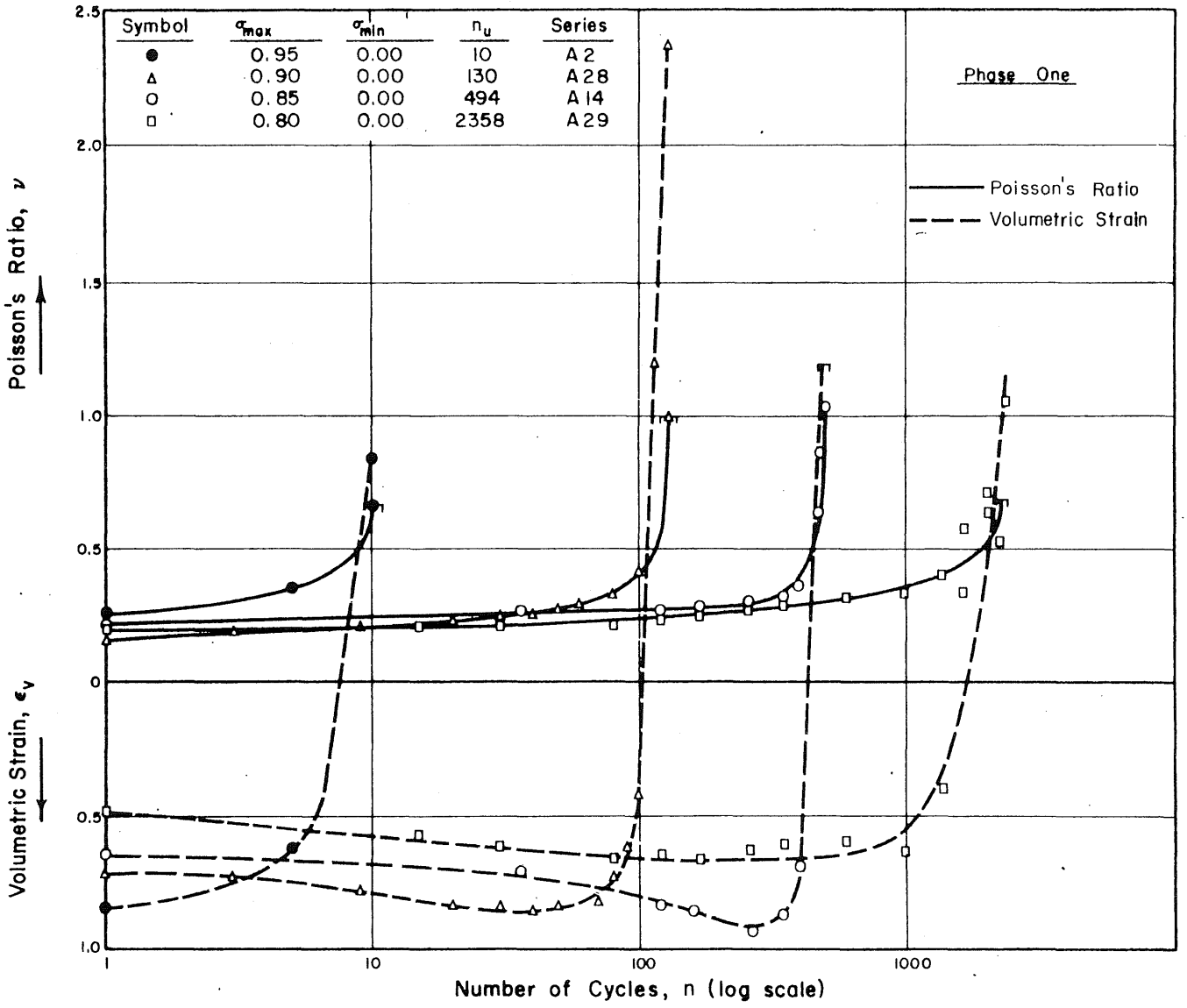

FIG. 4.16 POISSON'S RATIO AND VOLUMETRIC STRAIN AT MAXIMUM STRESS AS FUNCTION OF NUMBER OF APPLIED CYCLES FOR DIFFERENT MAXIMUM STRESS LEVELS : AGE AT LOADING: 28 DAYS

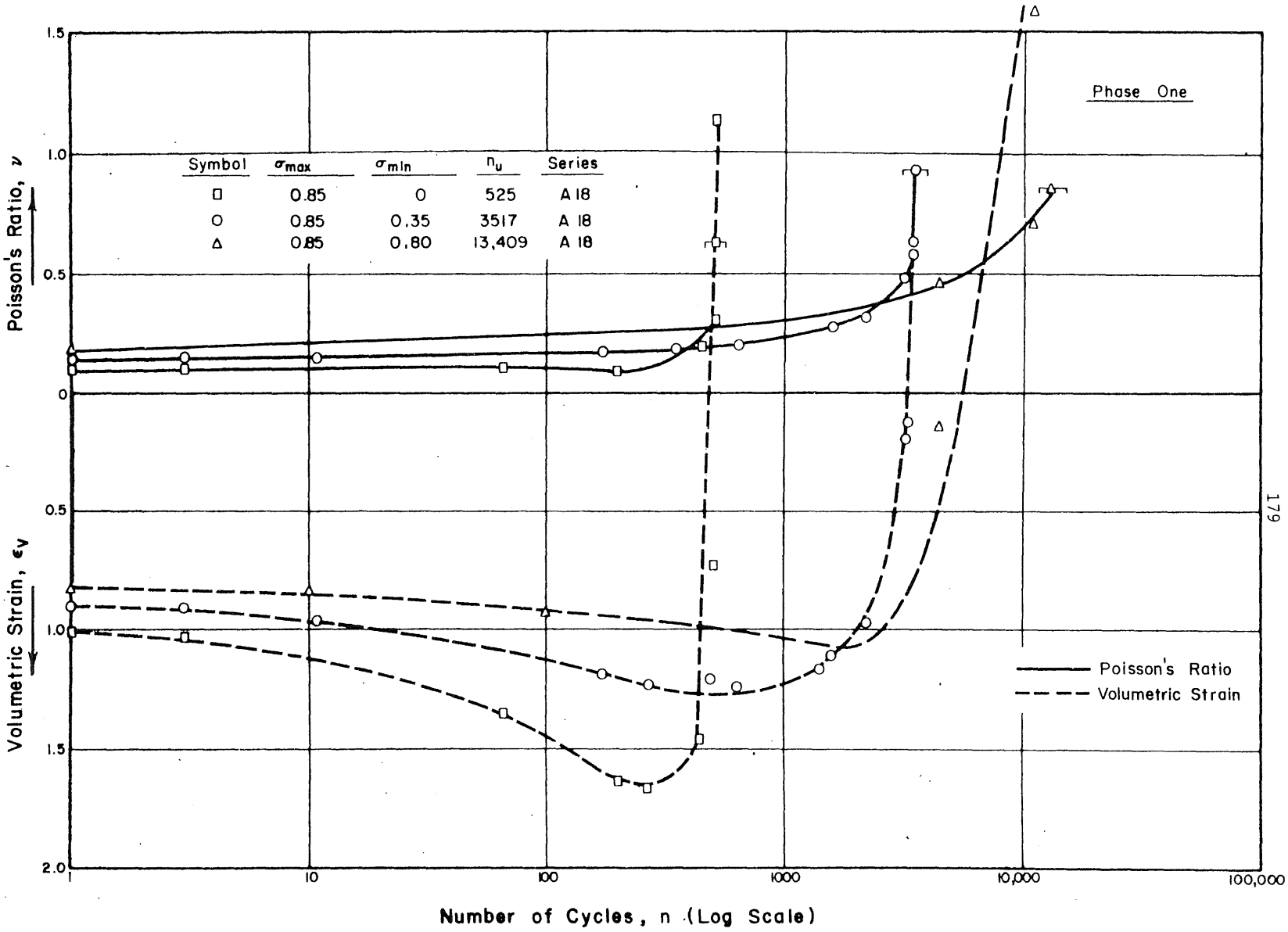

FIG. 4.17 POISSON'S RATIO AND VOLUMETRIC STRAIN AT MAXIMUM STRESS AS FUNCTION OF NUMBER OF APPLIED CYCLES FOR DIFFERENT STRESS RANGES: AGE AT LOADING: 28 DAYS

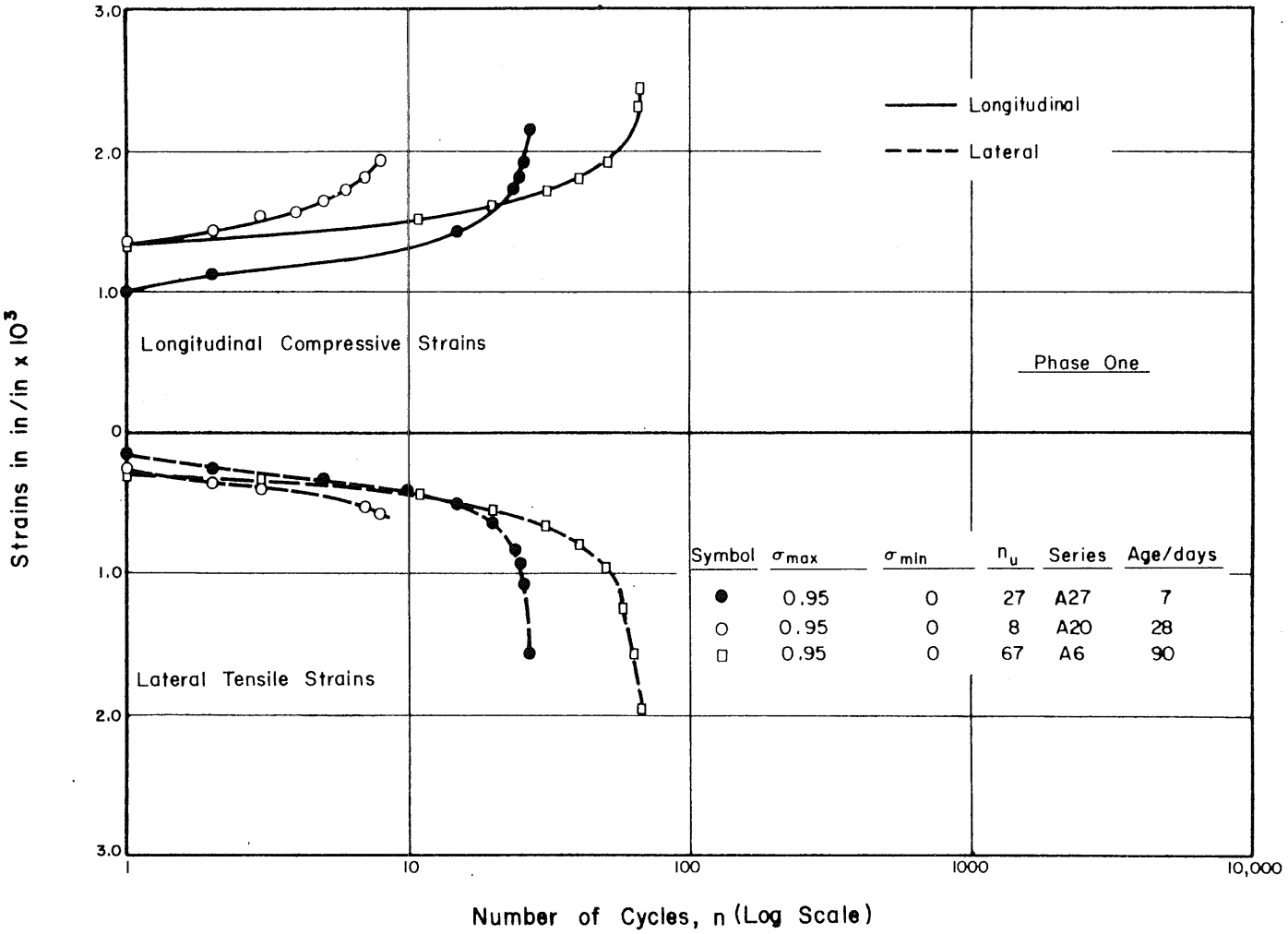

FIG. 4.18 LONGITUDINAL AND LATERAL STRAINS AT MAXIMUM STRESS AS FUNCTION OF NUMBER OF APPLIED CYCLES FOR CONCRETE TESTED AT 7, 28 AND 90 DAYS

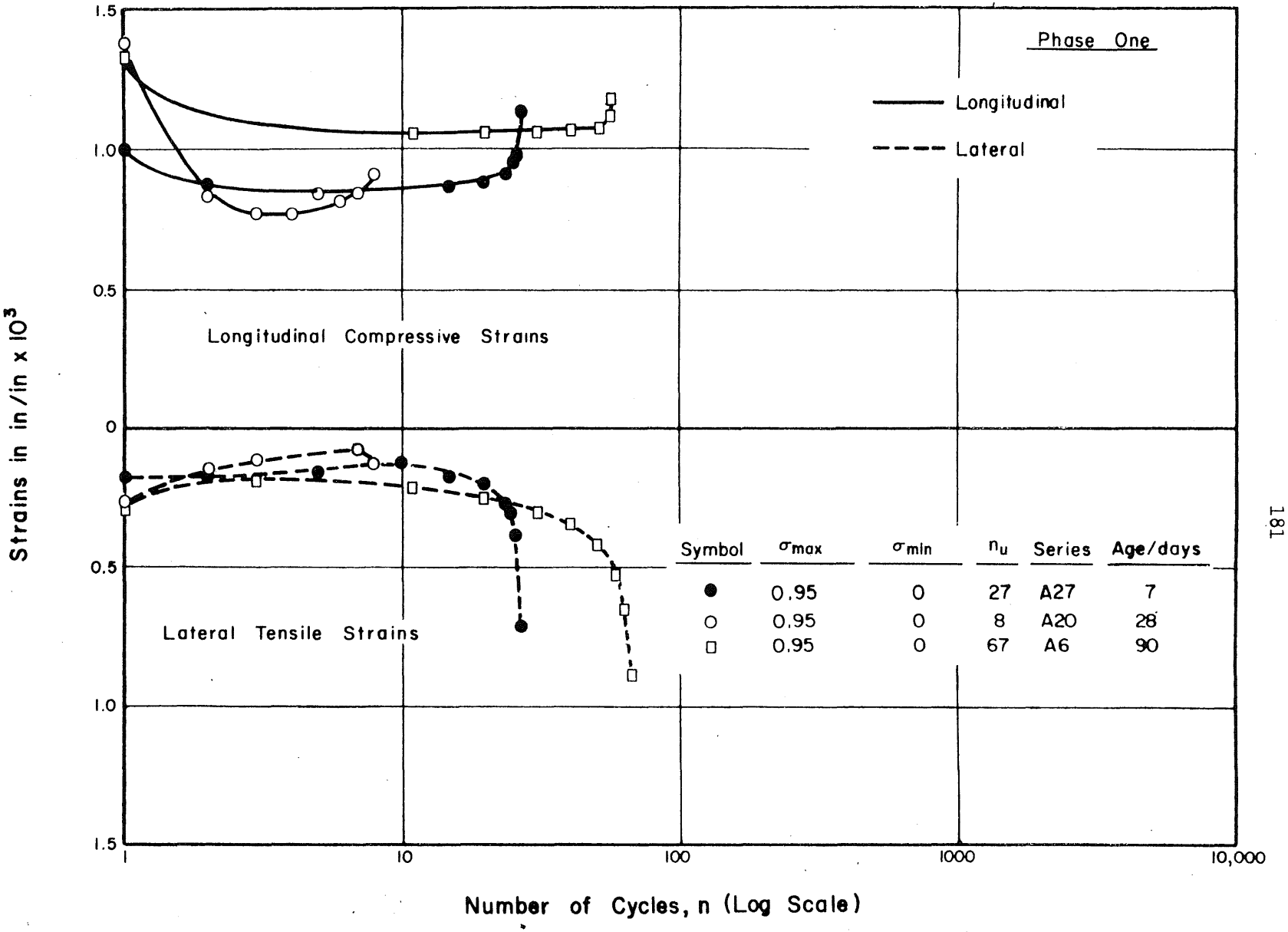

FIG. 4.19 ($\epsilon_{max} - \epsilon_{min}$) AS FUNCTION OF NUMBER OF APPLIED CYCLES FOR CONCRETE TESTED AT 7, 28 AND 90 DAYS

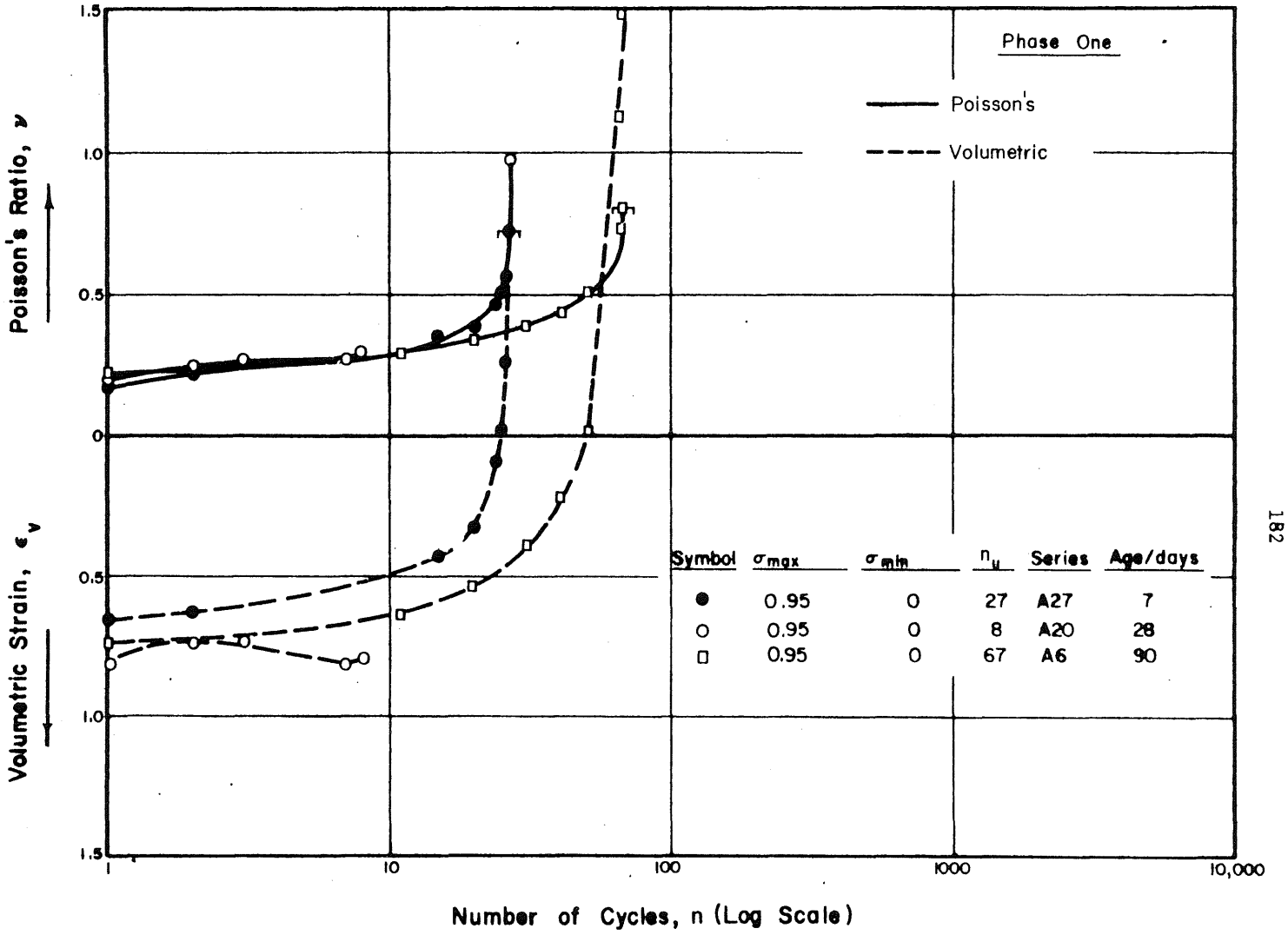

FIG. 4.20 POISSON'S RATIO AND VOLUMETRIC STRAIN AT MAXIMUM STRESS AS FUNCTION OF NUMBER OF APPLIED CYCLES FOR CONCRETE TESTED AT 7, 28 AND 90 DAYS

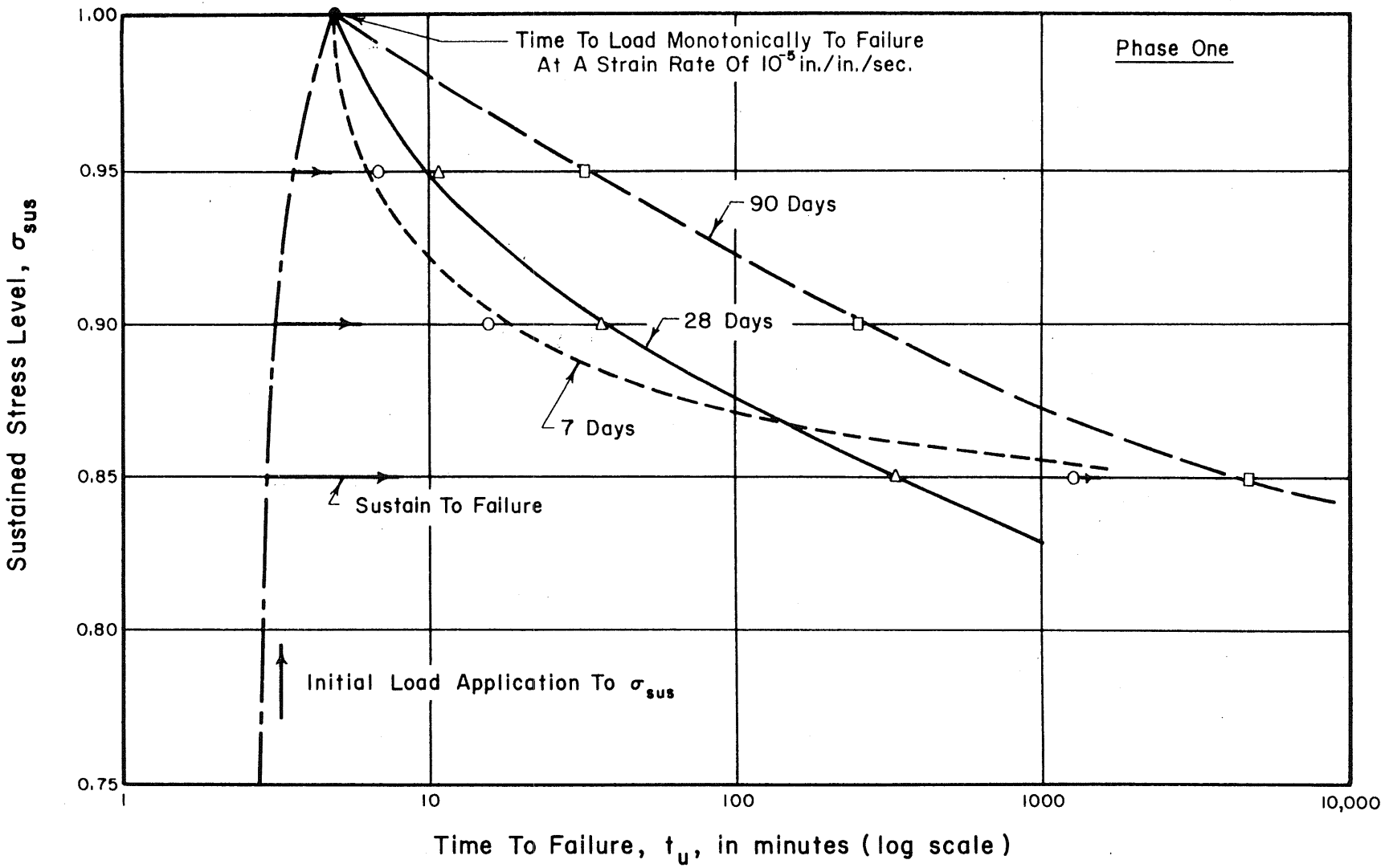

FIG. 4.21 EFFECT OF AGE AT LOADING ON TIME TO FAILURE OF CONCRETE SUBJECTED TO DIFFERENT LEVELS OF SUSTAINED STRESS

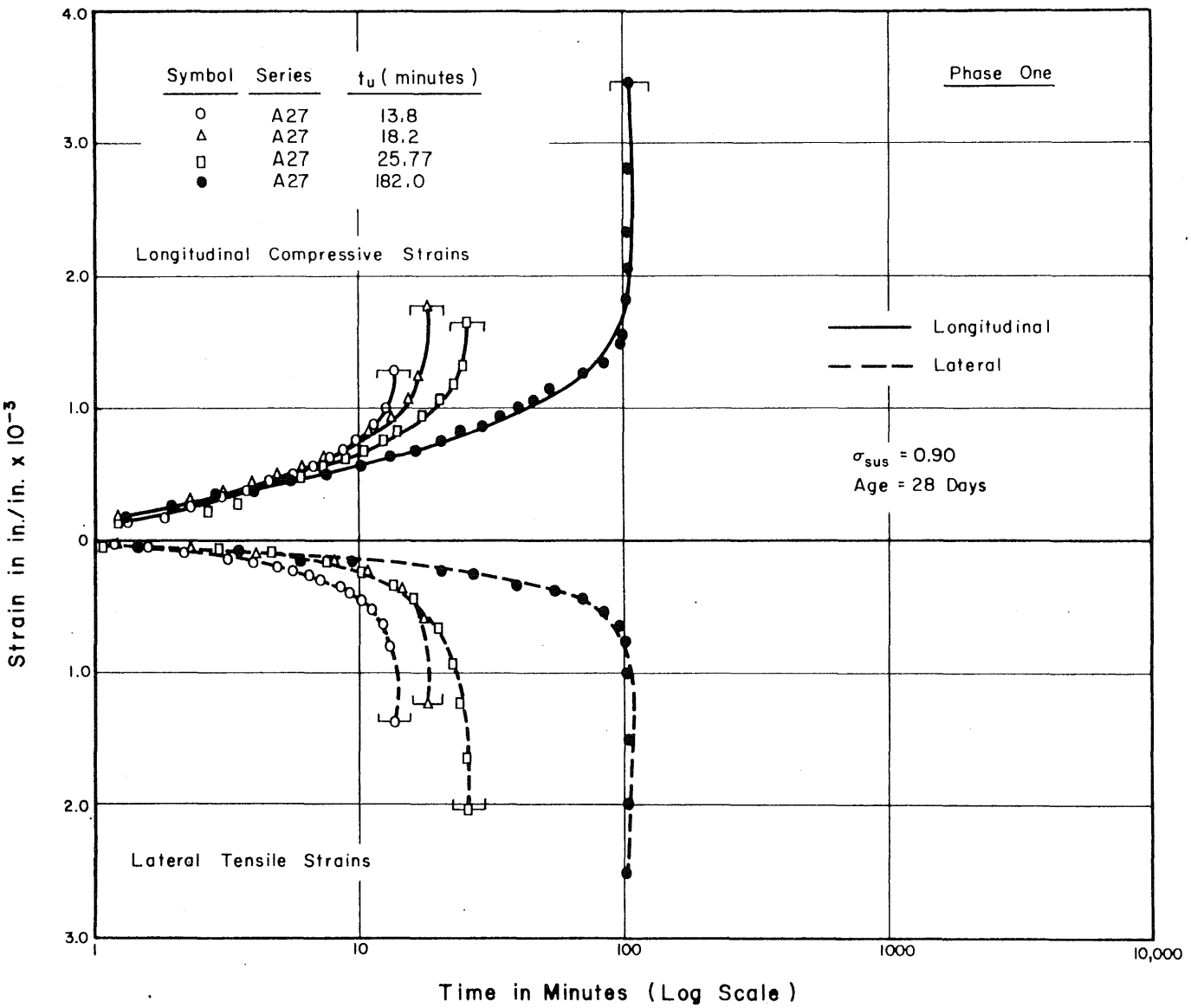

FIG. 4.22 LONGITUDINAL AND LATERAL STRAINS AS FUNCTION OF DURATION OF LOADING FOR CONCRETE SUBJECTED TO A SUSTAINED STRESS LEVEL OF 0.90 AT AN AGE OF 28 DAYS

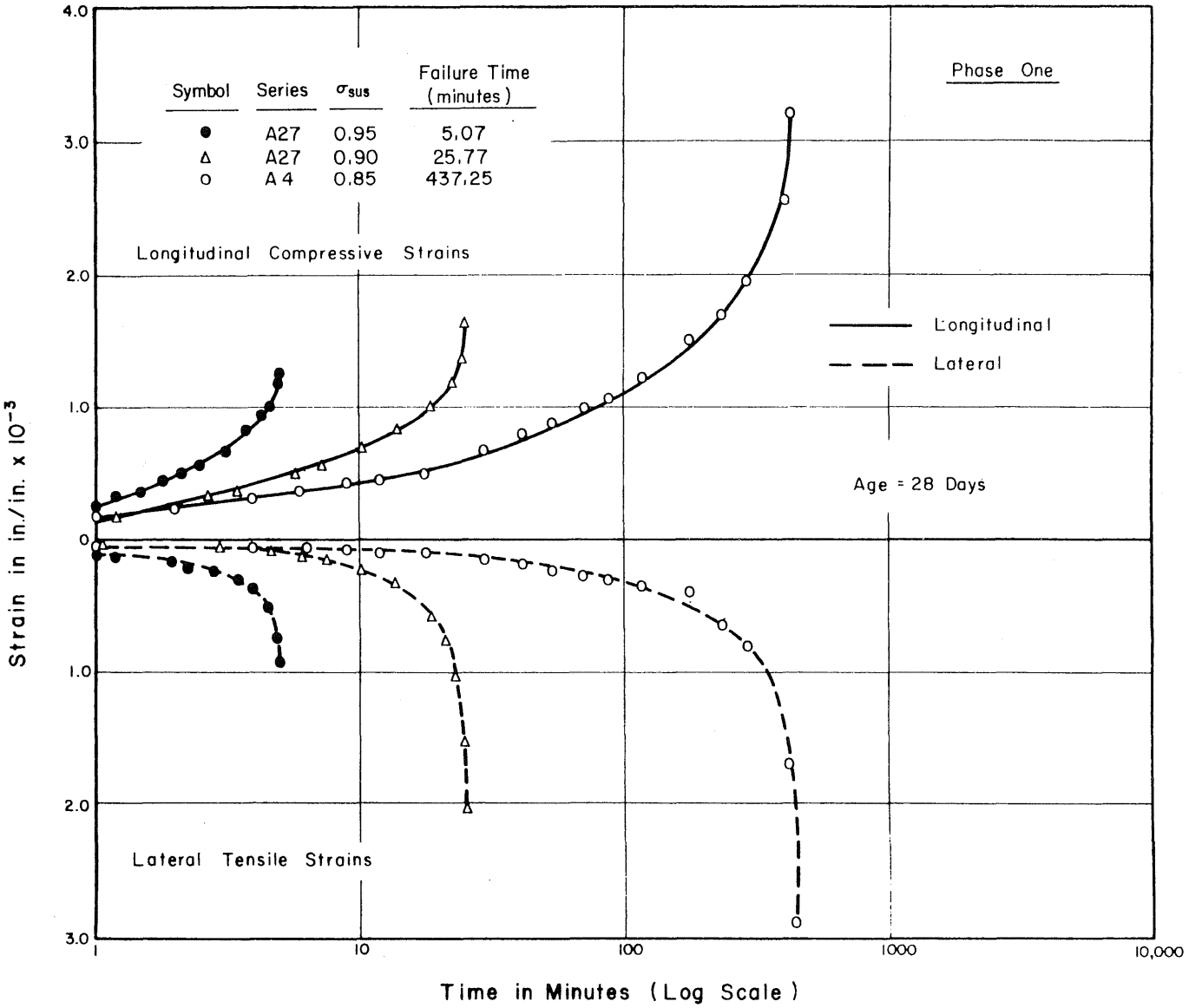

FIG. 4.23 LONGITUDINAL AND LATERAL STRAINS AS FUNCTION OF DURATION OF LOADING WITH TIME FOR CONCRETE SUBJECTED TO DIFFERENT SUSTAINED STRESS LEVELS AT AN AGE OF 28 DAYS

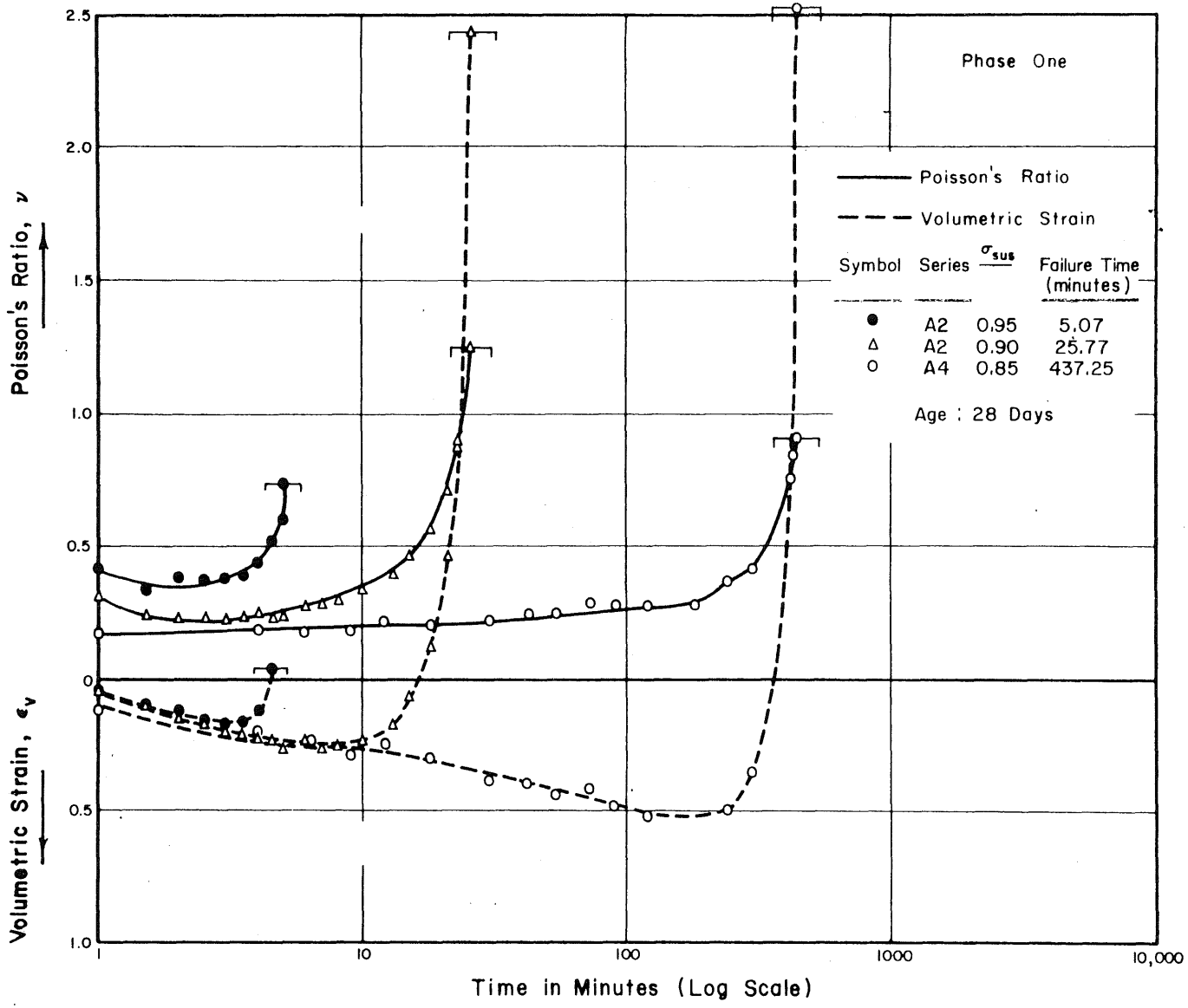

FIG. 4.24 POISSON'S RATIO AND VOLUMETRIC STRAIN AS FUNCTION OF DURATION OF LOADING FOR CONCRETE SUBJECTED TO DIFFERENT SUSTAINED STRESS LEVELS AT AN AGE OF 28 DAYS

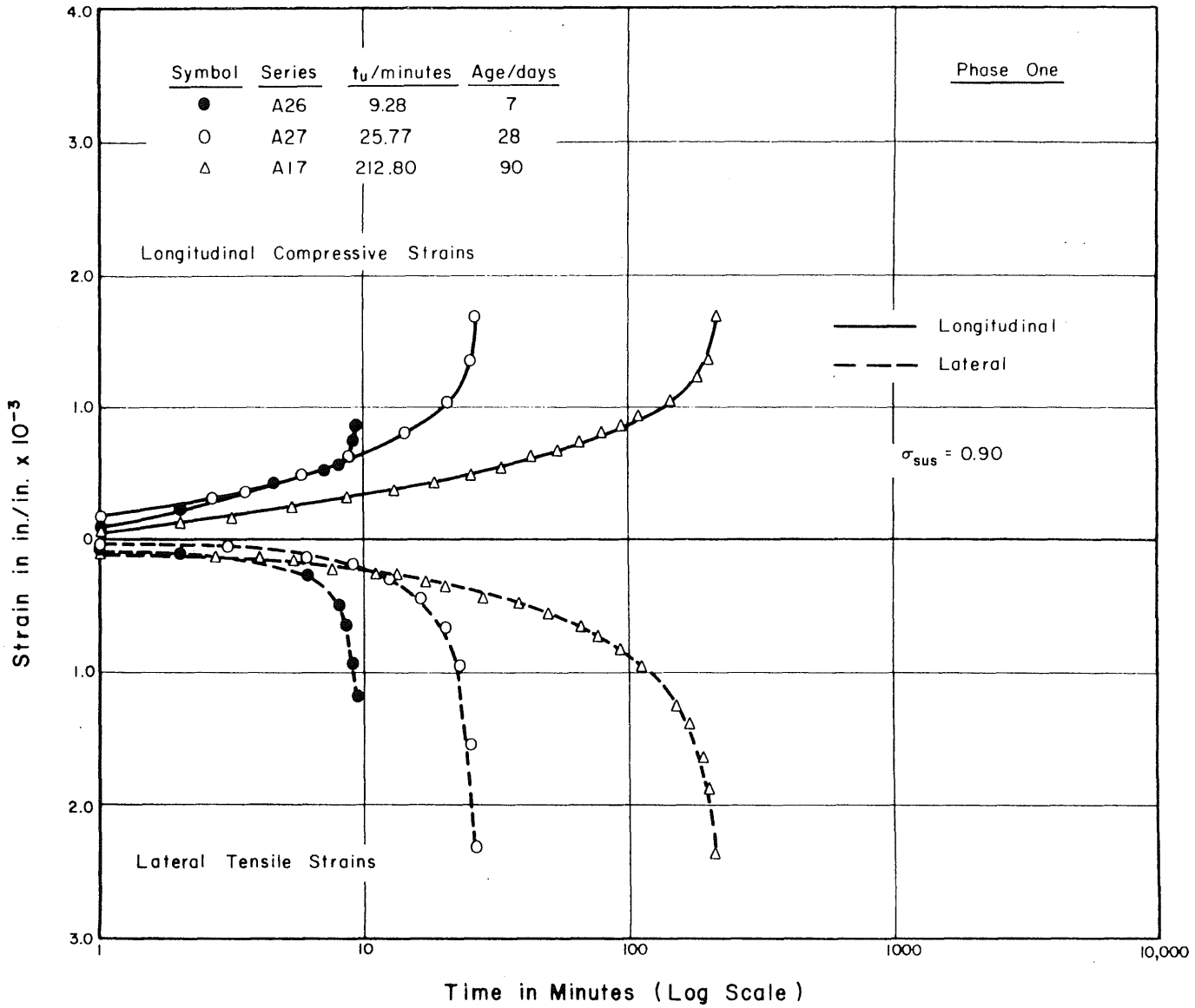

FIG. 4.25 LONGITUDINAL AND LATERAL STRAINS AS FUNCTION OF DURATION OF LOADING FOR CONCRETE SUBJECTED TO A SUSTAINED STRESS LEVEL OF 0.90 AT AN AGE OF 7, 28 AND 90 DAYS

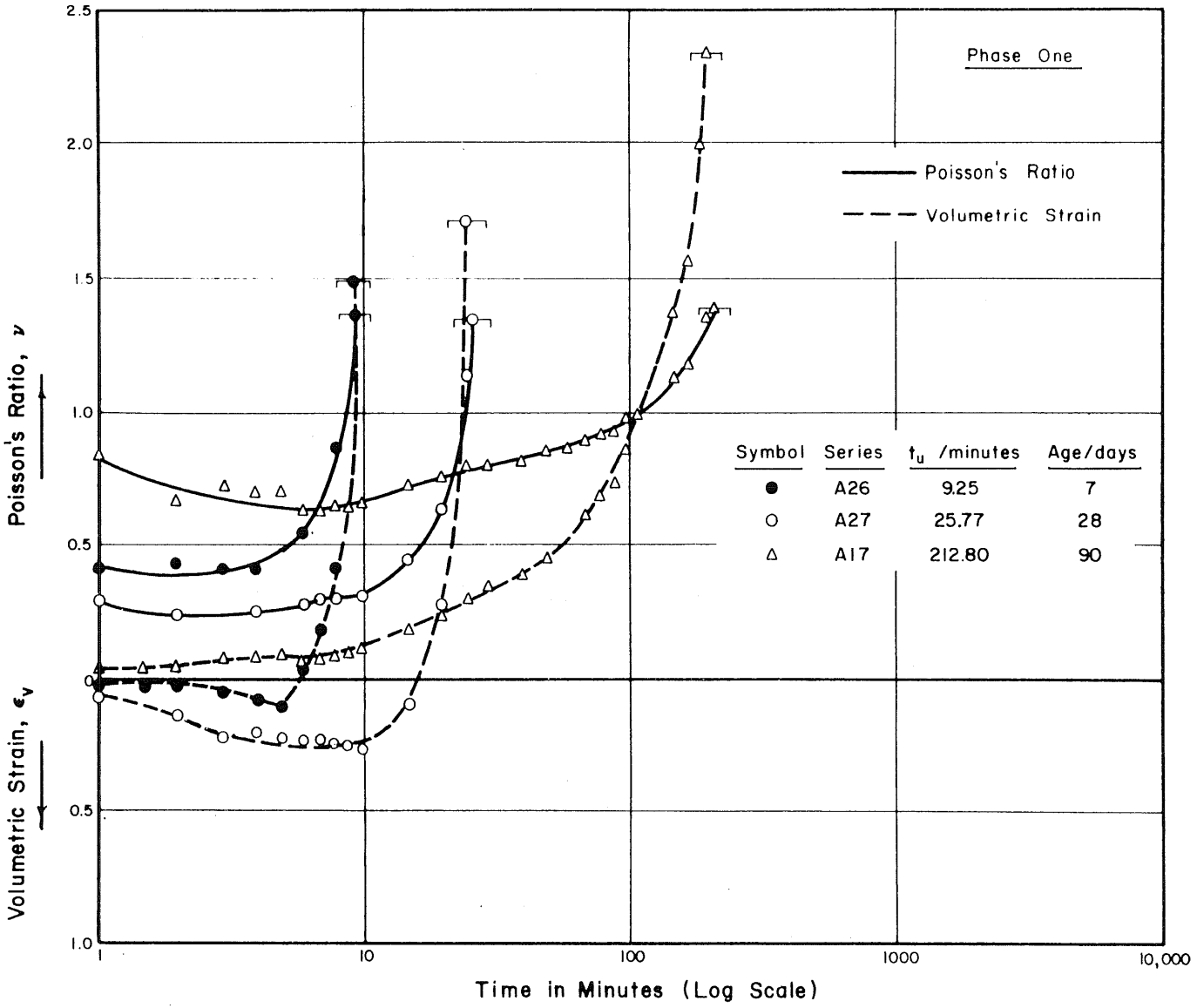

FIG. 4.26 POISSON'S RATIO AND VOLUMETRIC STRAIN AS FUNCTION OF DURATION OF LOADING FOR CONCRETE SUBJECTED TO A SUSTAINED STRESS LEVEL OF 0.90 AT AN AGE OF 7, 28 AND 90 DAYS

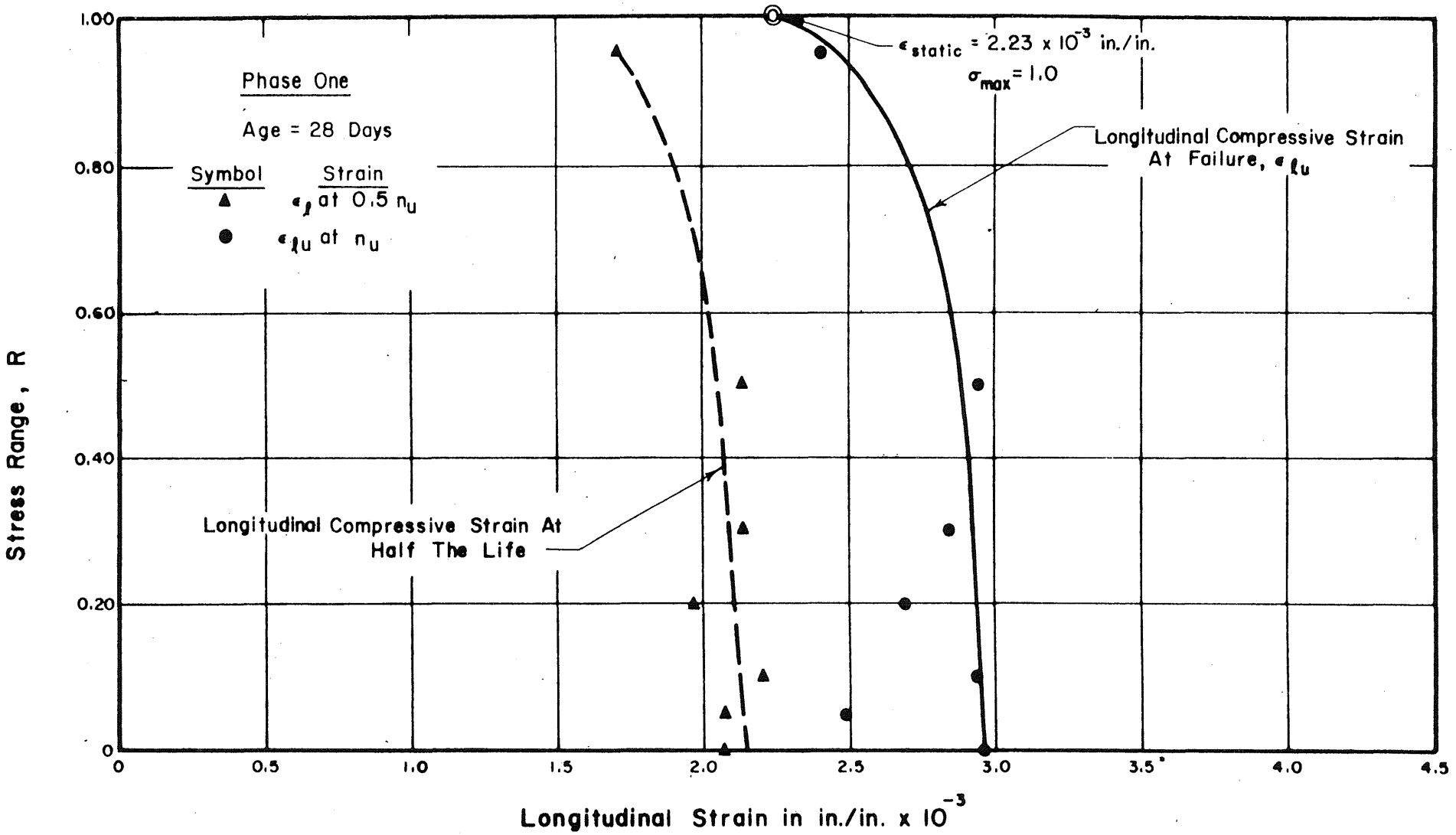

FIG. 4.27 LONGITUDINAL STRAIN AS FUNCTION OF STRESS RANGE AT HALF LIFE AND AT FAILURE FOR A MAXIMUM STRESS LEVEL OF 0.95 ; AGE AT LOADING ; 28 DAYS

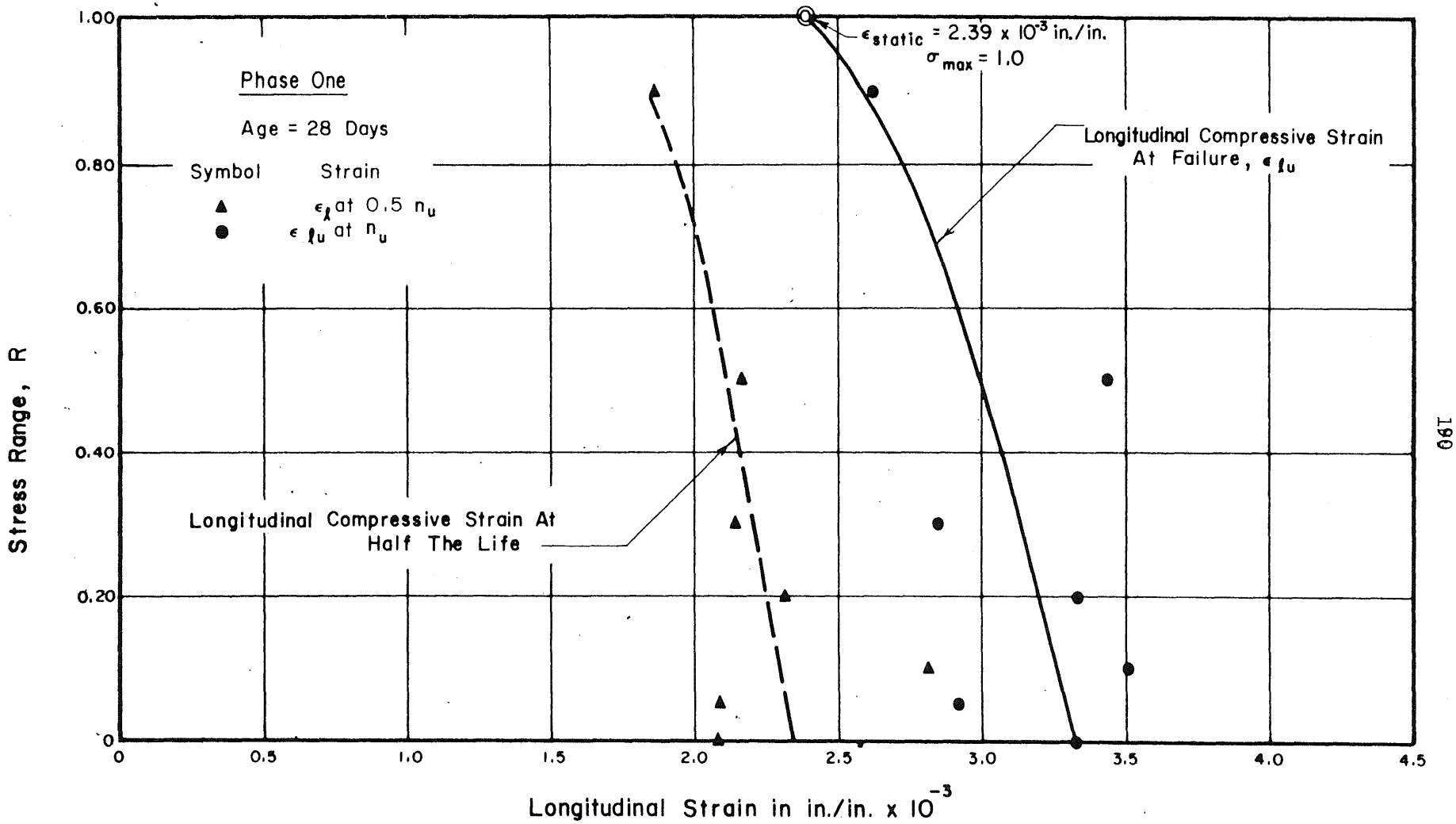

FIG. 4.28 LONGITUDINAL STRAIN AS FUNCTION OF STRESS RANGE AT HALF LIFE AND AT FAILURE FOR A MAXIMUM STRESS LEVEL OF 0.90 ; AGE AT LOADING ; 28 DAYS

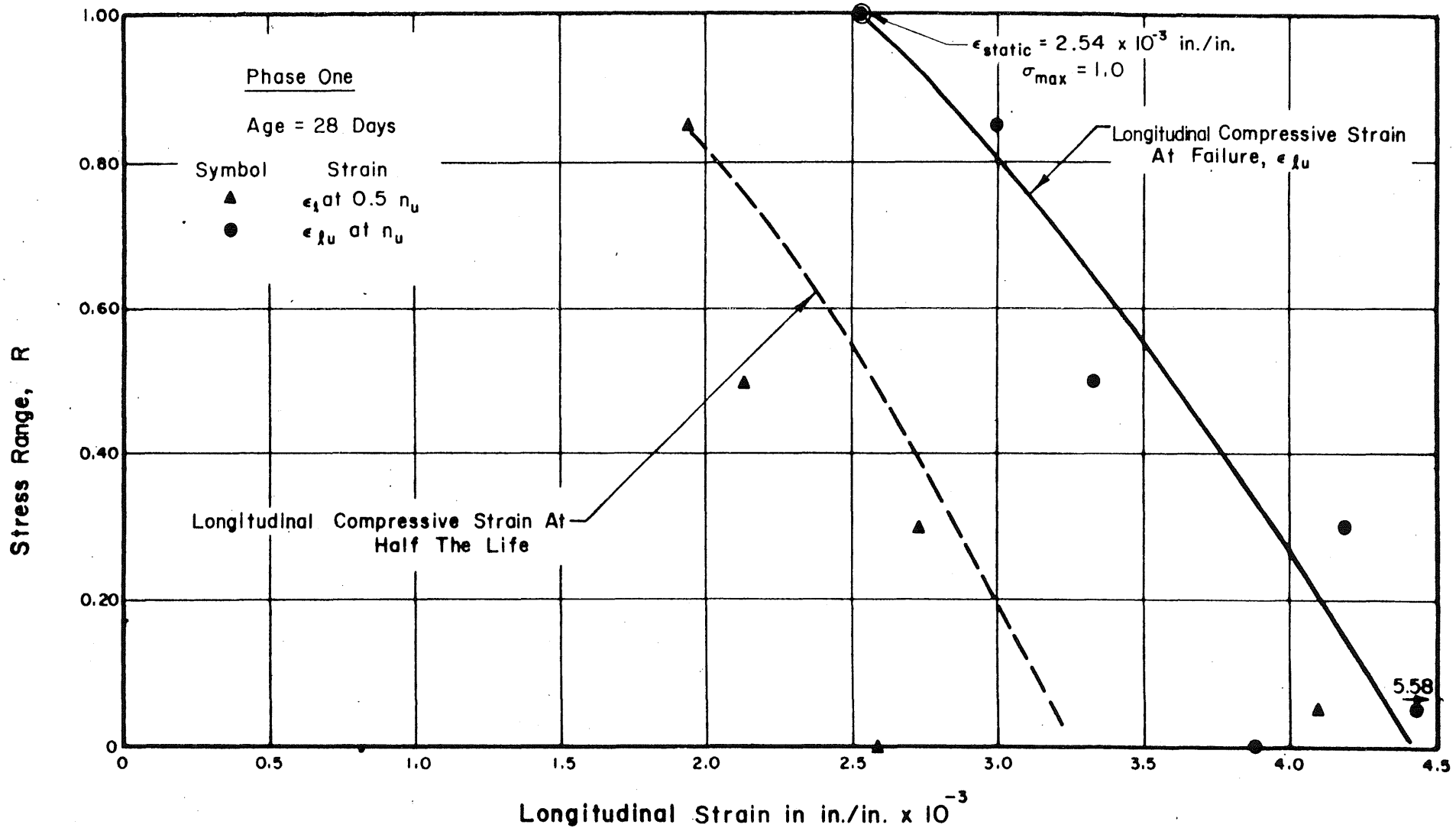

FIG. 4.29 LONGITUDINAL STRAIN AS FUNCTION OF STRESS RANGE AT HALF LIFE AND AT FAILURE FOR A MAXIMUM STRESS LEVEL OF 0.85 ; AGE AT LOADING ; 28 DAYS

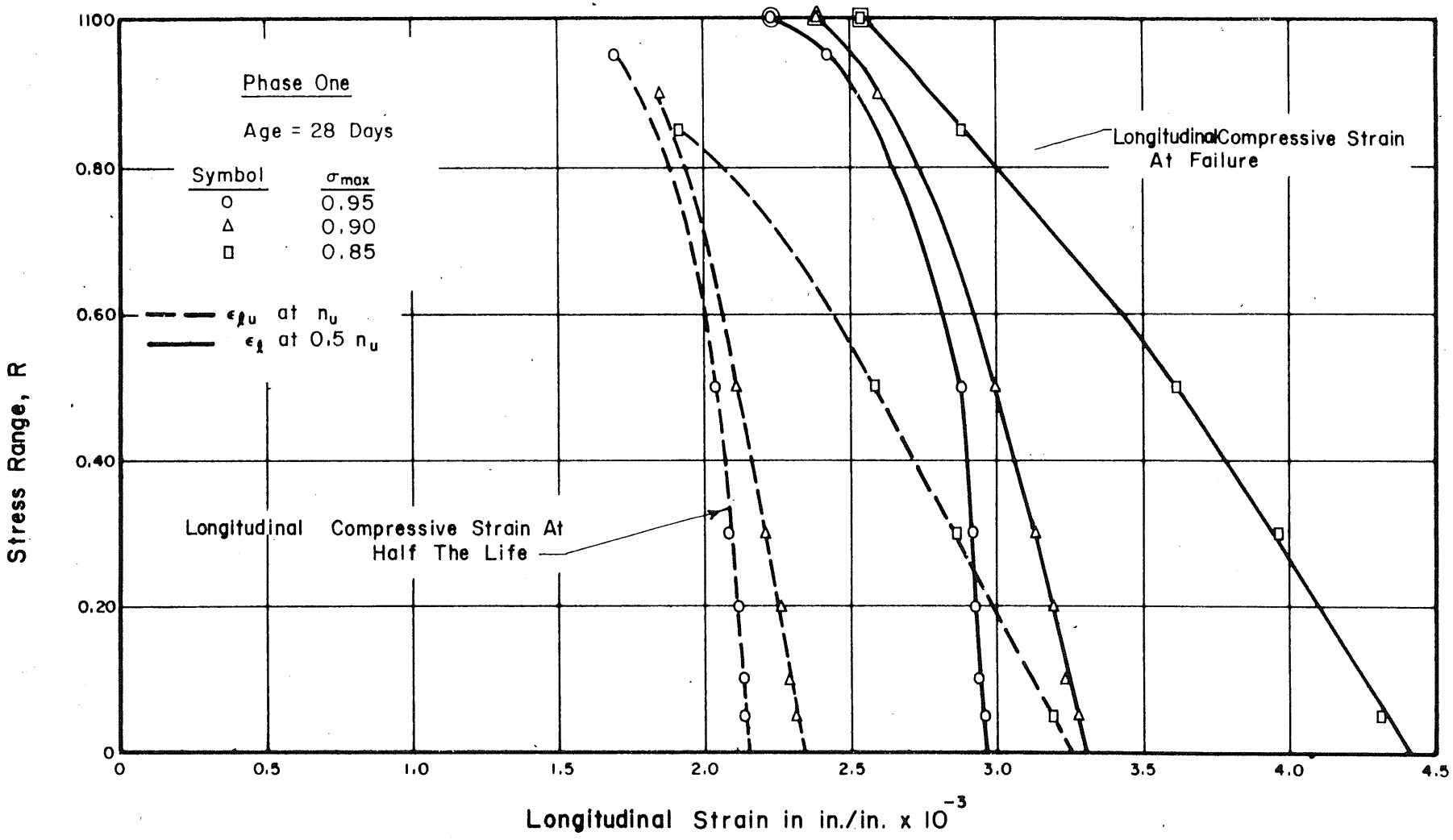

FIG. 4.30 LONGITUDINAL STRAIN AS FUNCTION OF STRESS RANGE AT HALF LIFE AND AT FAILURE FOR DIFFERENT LEVELS OF MAXIMUM STRESS ; AGE AT LOADING ; 28 DAYS

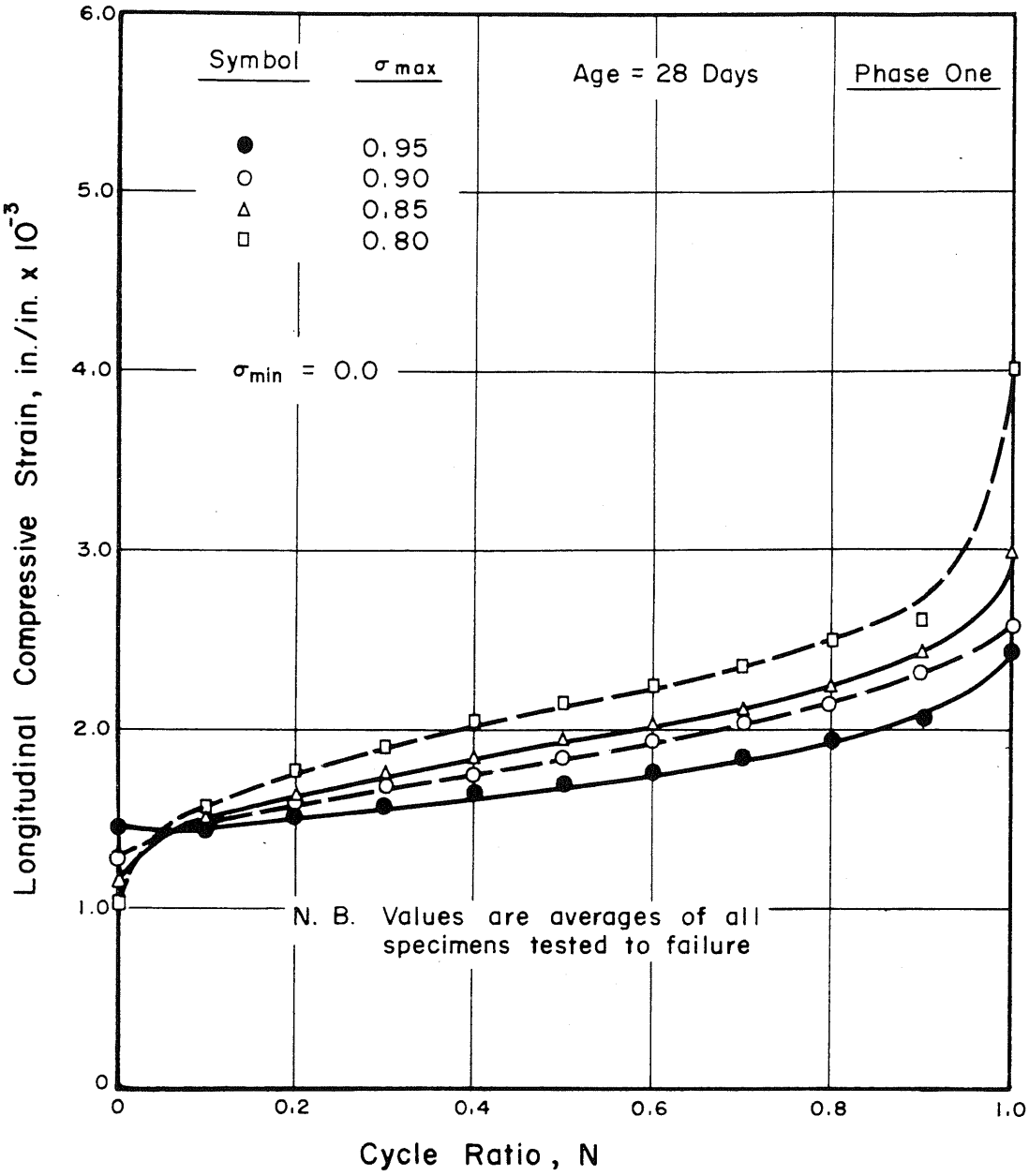

FIG. 4.31 LONGITUDINAL STRAIN AS FUNCTION OF CYCLE RATIO FOR CONCRETE SUBJECTED TO DIFFERENT MAXIMUM STRESS LEVELS AT AN AGE OF 28 DAYS

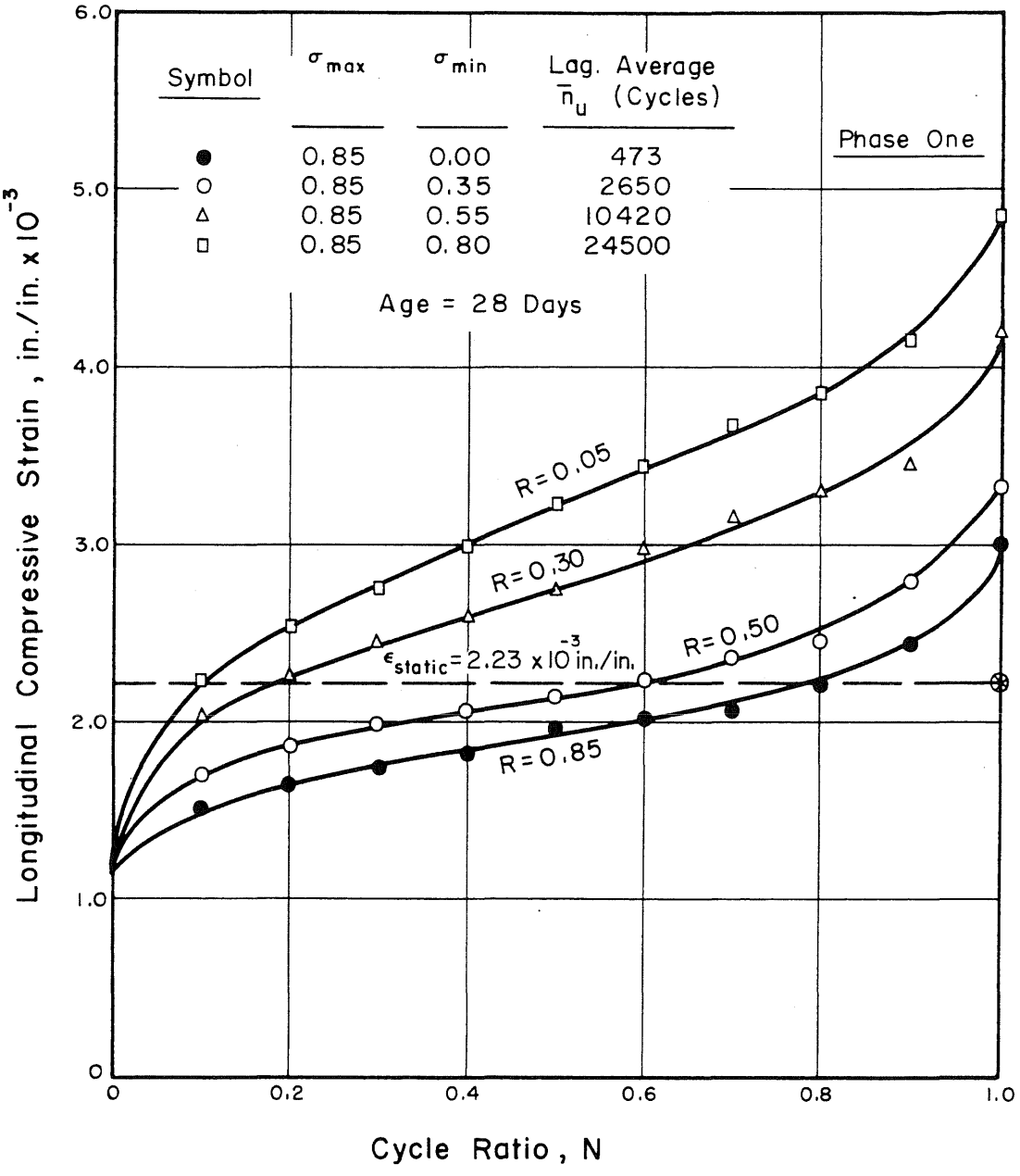

FIG. 4.32 LONGITUDINAL STRAIN AS FUNCTION OF CYCLE RATIO FOR CONCRETE SUBJECTED TO A MAXIMUM STRESS LEVEL OF 0.85 AND DIFFERENT STRESS RANGES ; AGE AT LOADING ; 28 DAYS

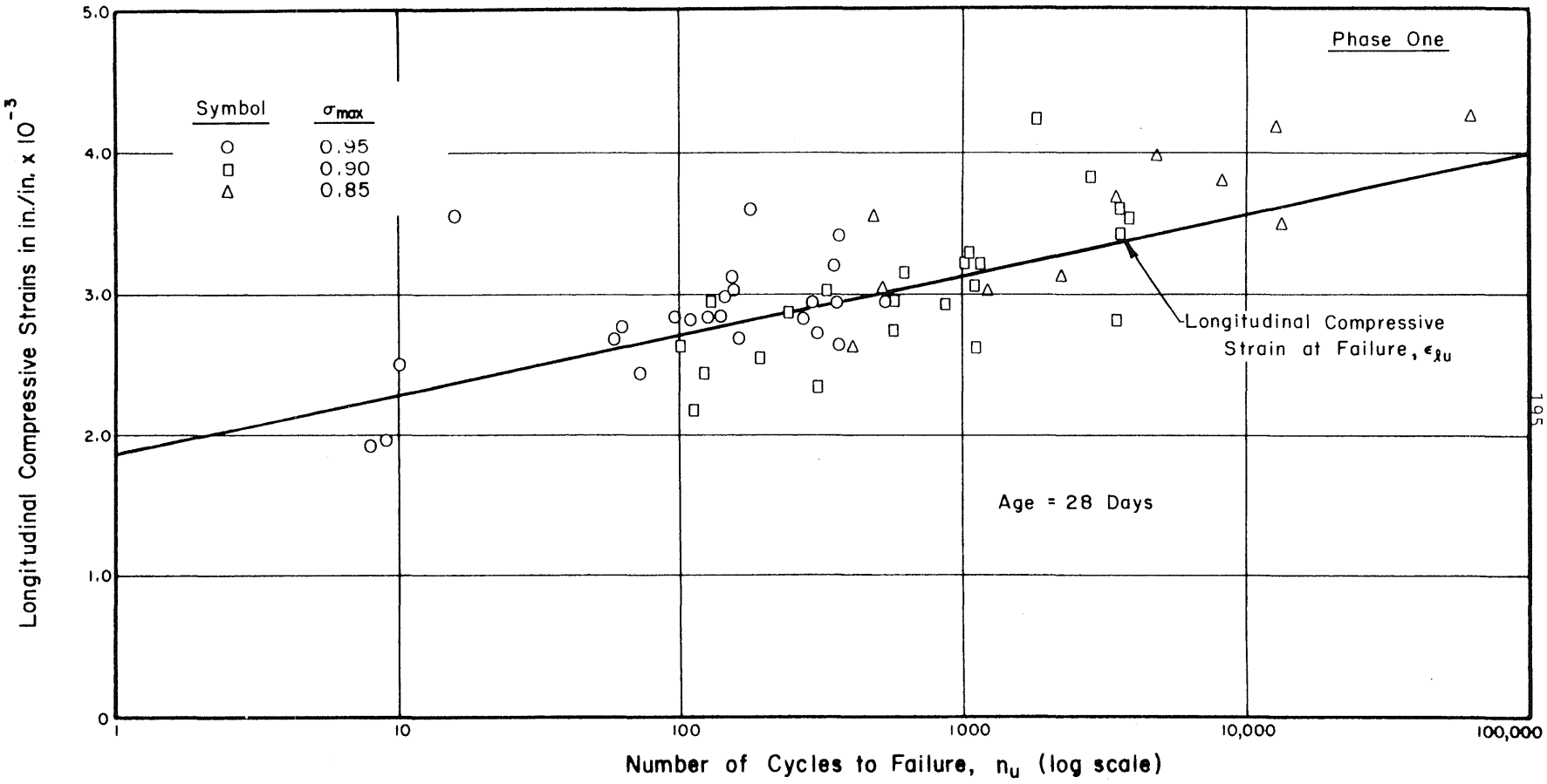

FIG. 4.33 LONGITUDINAL STRAIN AT FAILURE AS FUNCTION OF CYCLES TO FAILURE FOR CONCRETE SUBJECTED TO DIFFERENT STRESS LEVELS AT AN AGE OF 28 DAYS

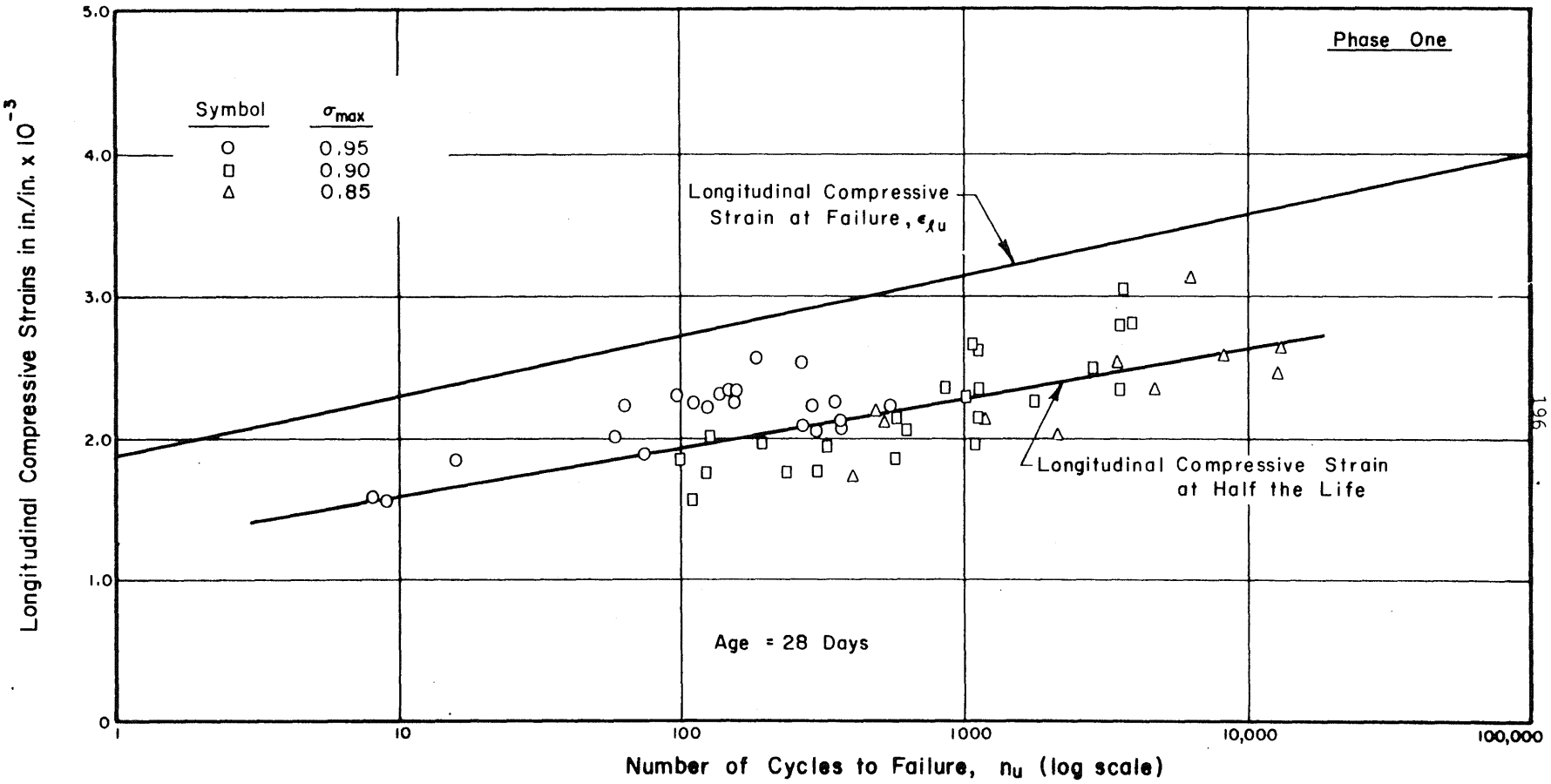

FIG. 4.34 LONGITUDINAL STRAIN AT HALF LIFE AS FUNCTION OF CYCLES TO FAILURE FOR CONCRETE SUBJECTED TO DIFFERENT STRESS LEVELS AT AN AGE OF 28 DAYS

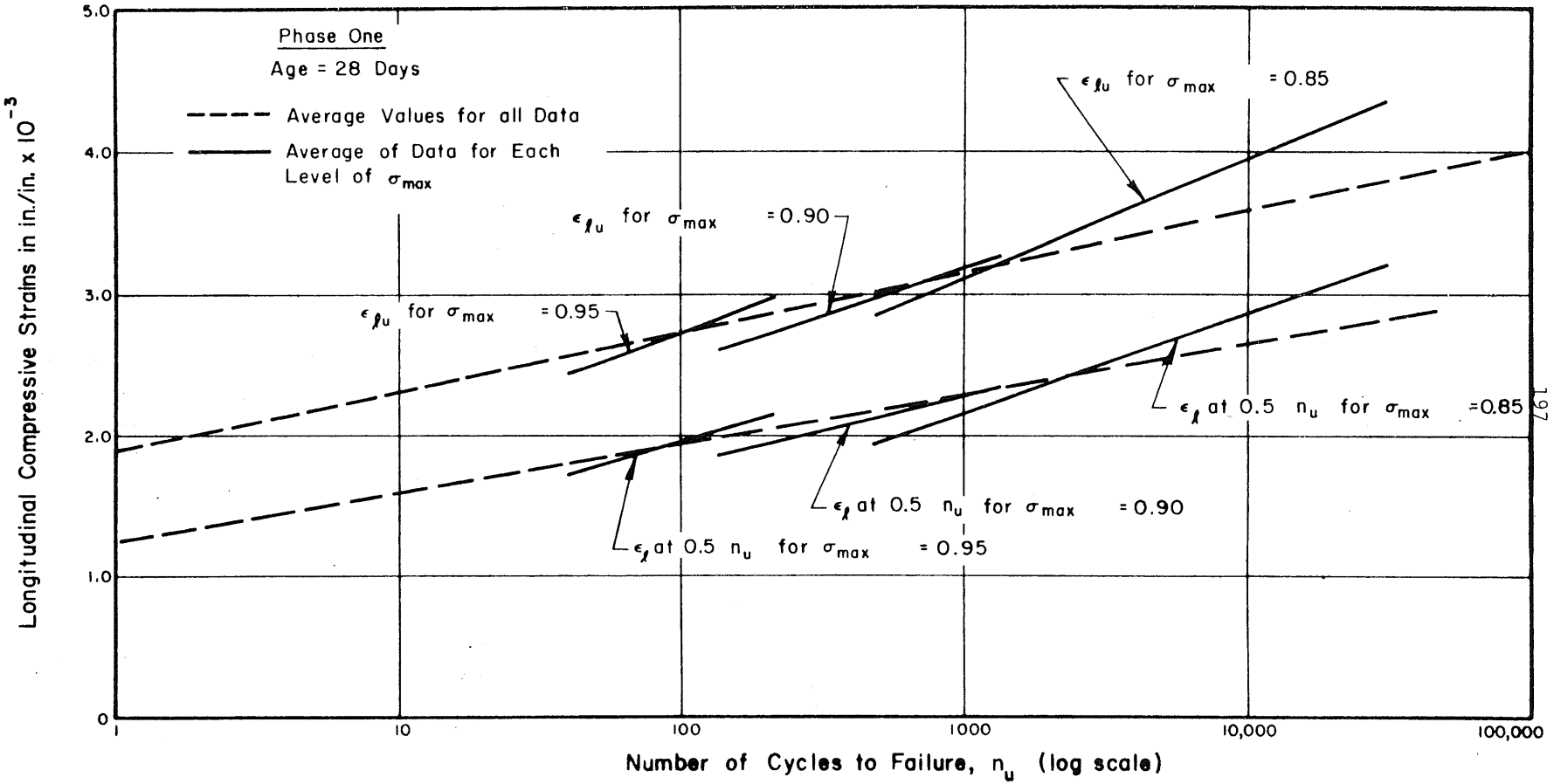

FIG. 4.35 COMPARISON OF AVERAGE LONGITUDINAL STRAIN-CYCLE RELATIONSHIPS FOR CONCRETE SUBJECTED TO DIFFERENT MAXIMUM STRESS LEVELS AT AN AGE OF 28 DAYS

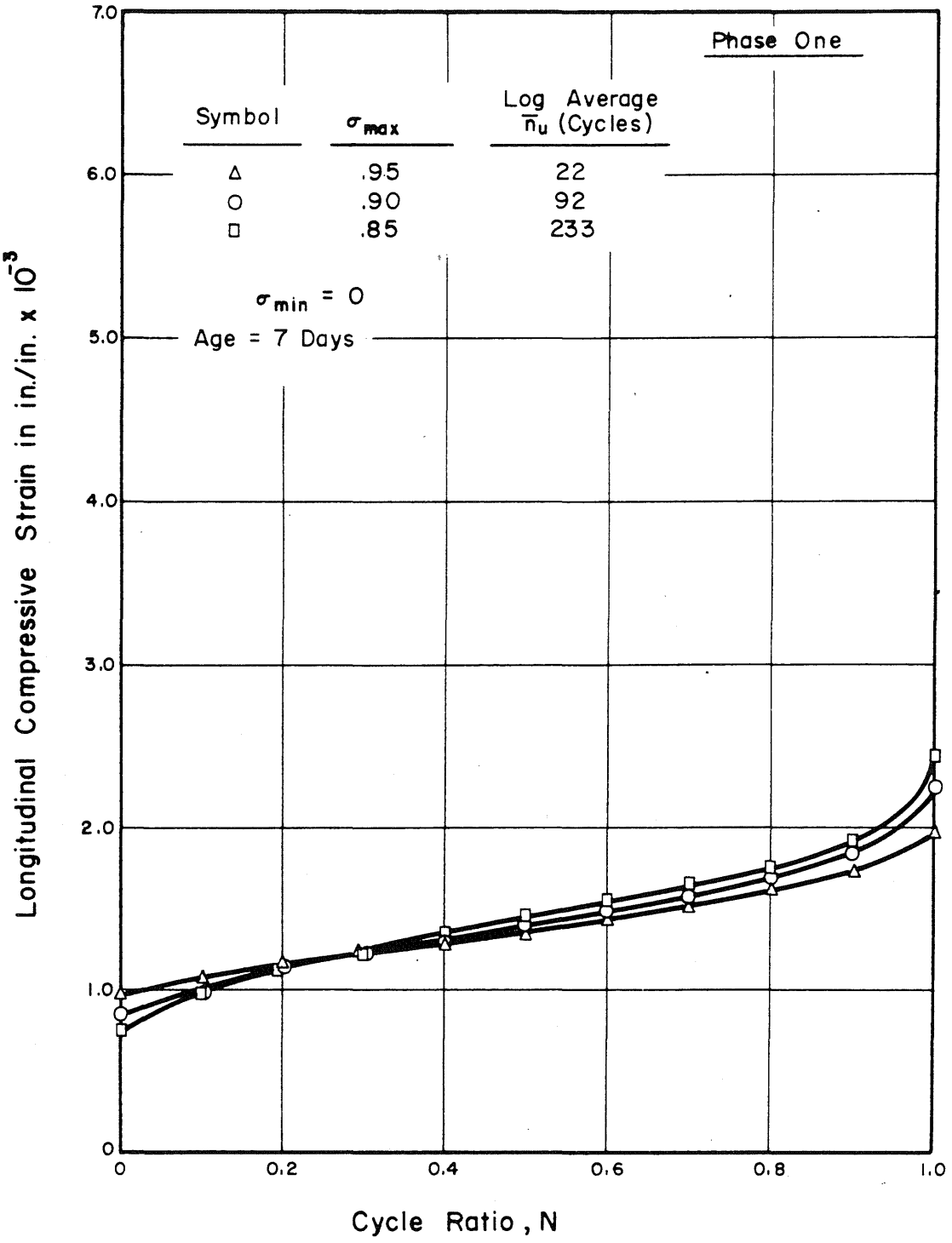

FIG. 4.36 LONGITUDINAL STRAIN AS FUNCTION OF CYCLE RATIO FOR CONCRETE SUBJECTED TO DIFFERENT MAXIMUM STRESS LEVELS AT AN AGE OF 7 DAYS

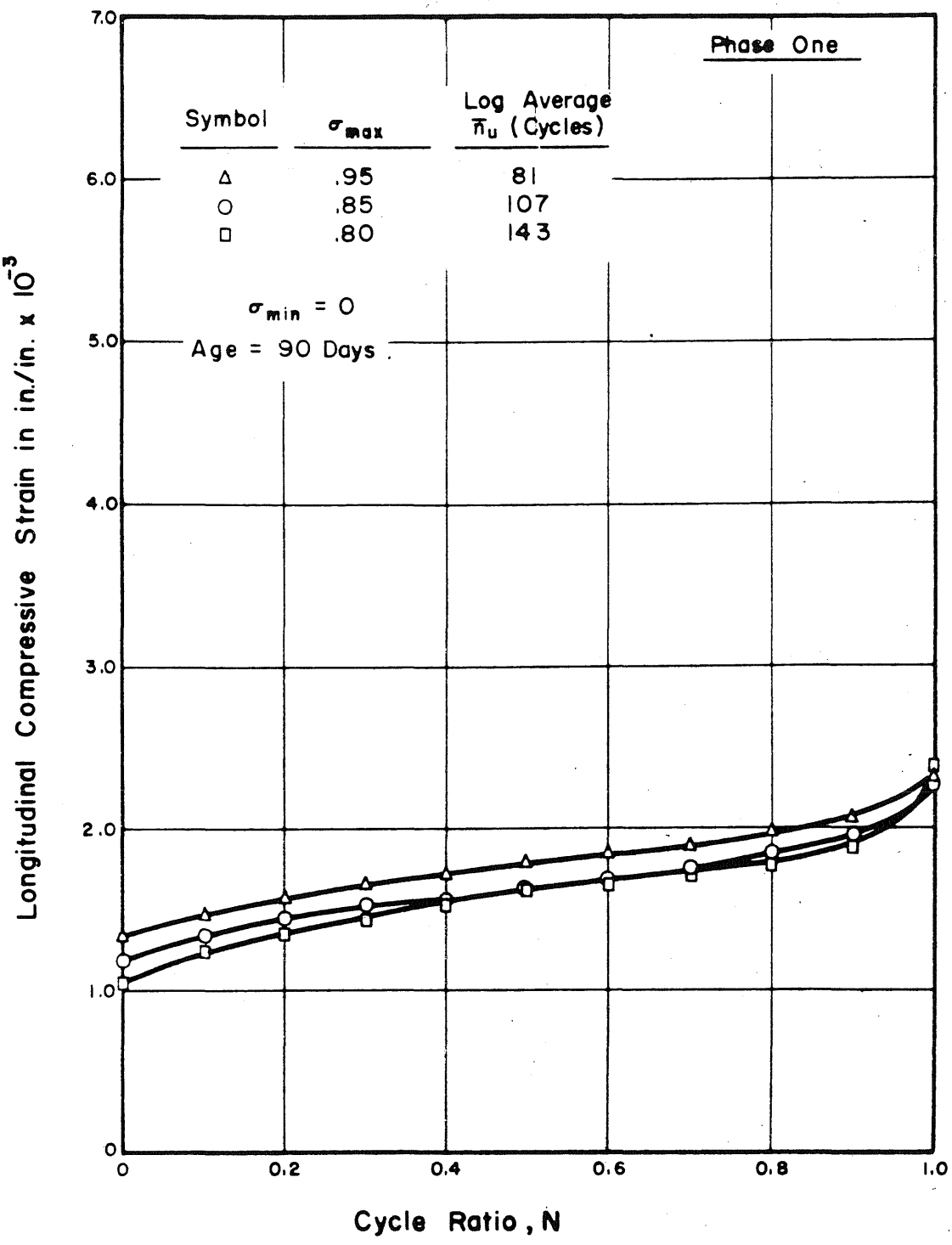

FIG. 4.37 LONGITUDINAL STRAIN AS FUNCTION OF CYCLE RATIO FOR CONCRETE SUBJECTED TO DIFFERENT MAXIMUM STRESS LEVELS AT AN AGE OF 90 DAYS

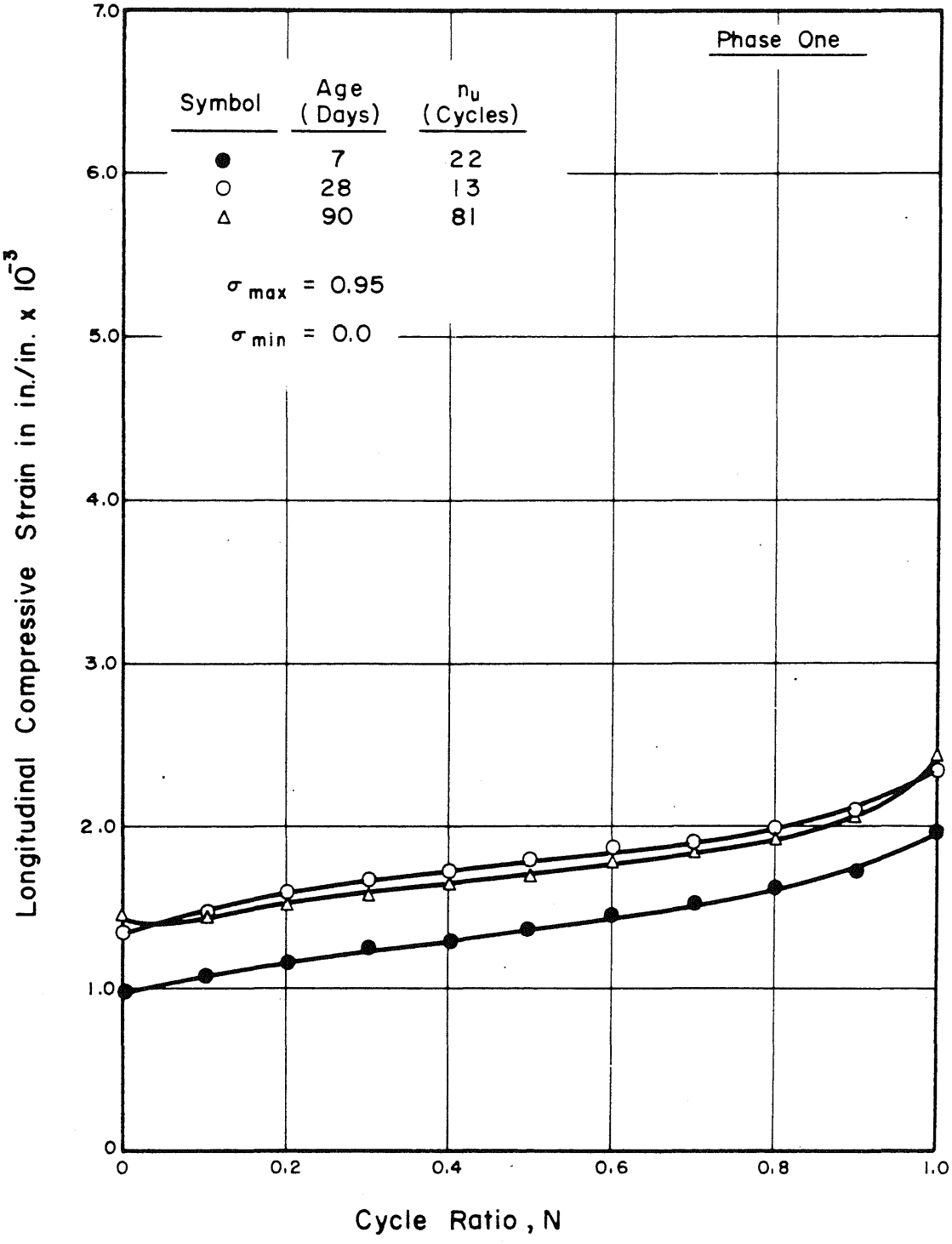

FIG. 4.38 EFFECT OF AGE AT LOADING ON LONGITUDINAL STRAIN–CYCLE RATIO RELATIONSHIP FOR CONCRETE SUBJECTED TO A MAXIMUM STRESS LEVEL OF 0.95 AND A STRESS RANGE OF 0.95

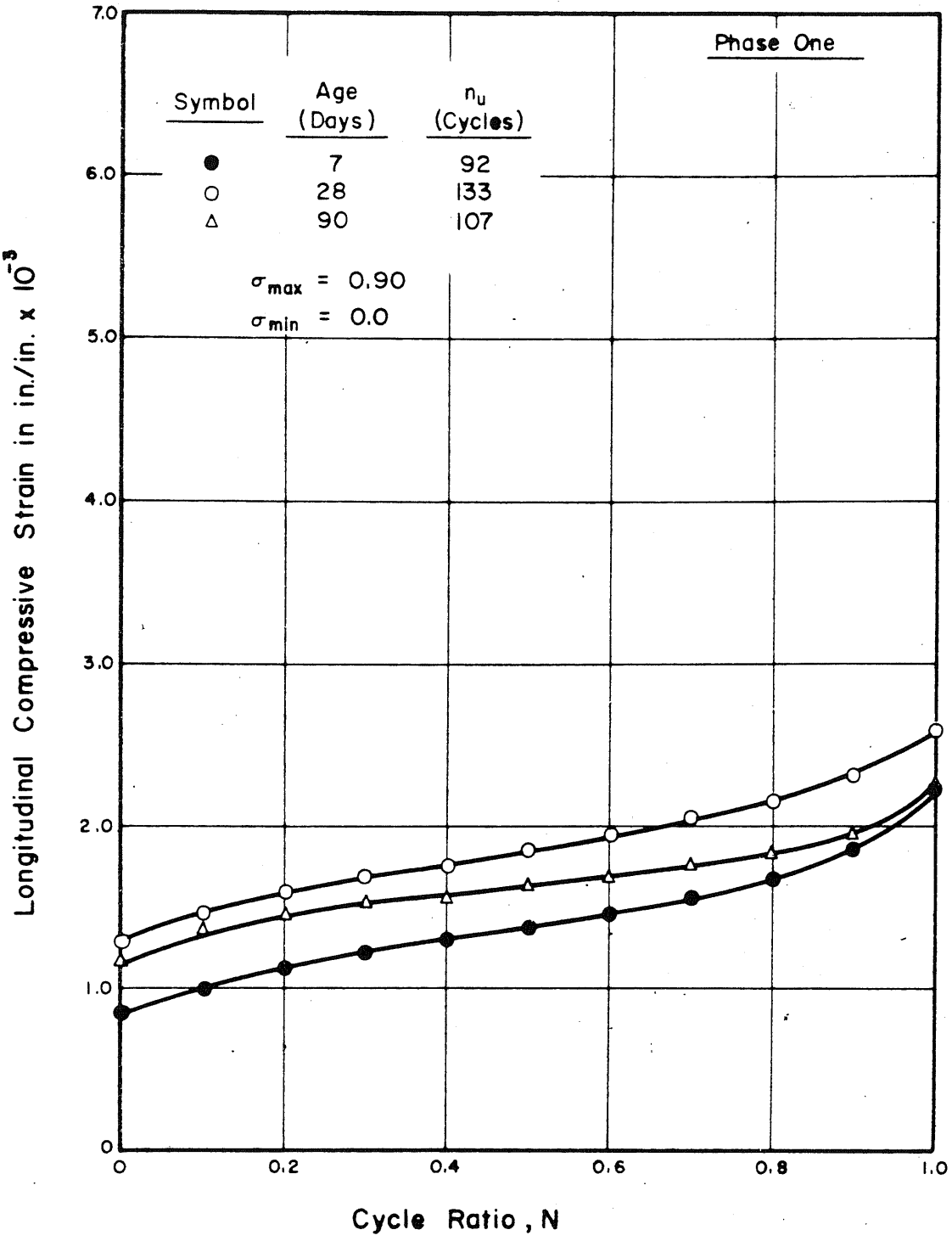

FIG. 4.39 EFFECT OF AGE AT LOADING ON LONGITUDINAL STRAIN-CYCLE RATIO RELATIONSHIP FOR CONCRETE SUBJECTED TO A MAXIMUM STRESS LEVEL OF 0.90 AND A STRESS RANGE OF 0.90

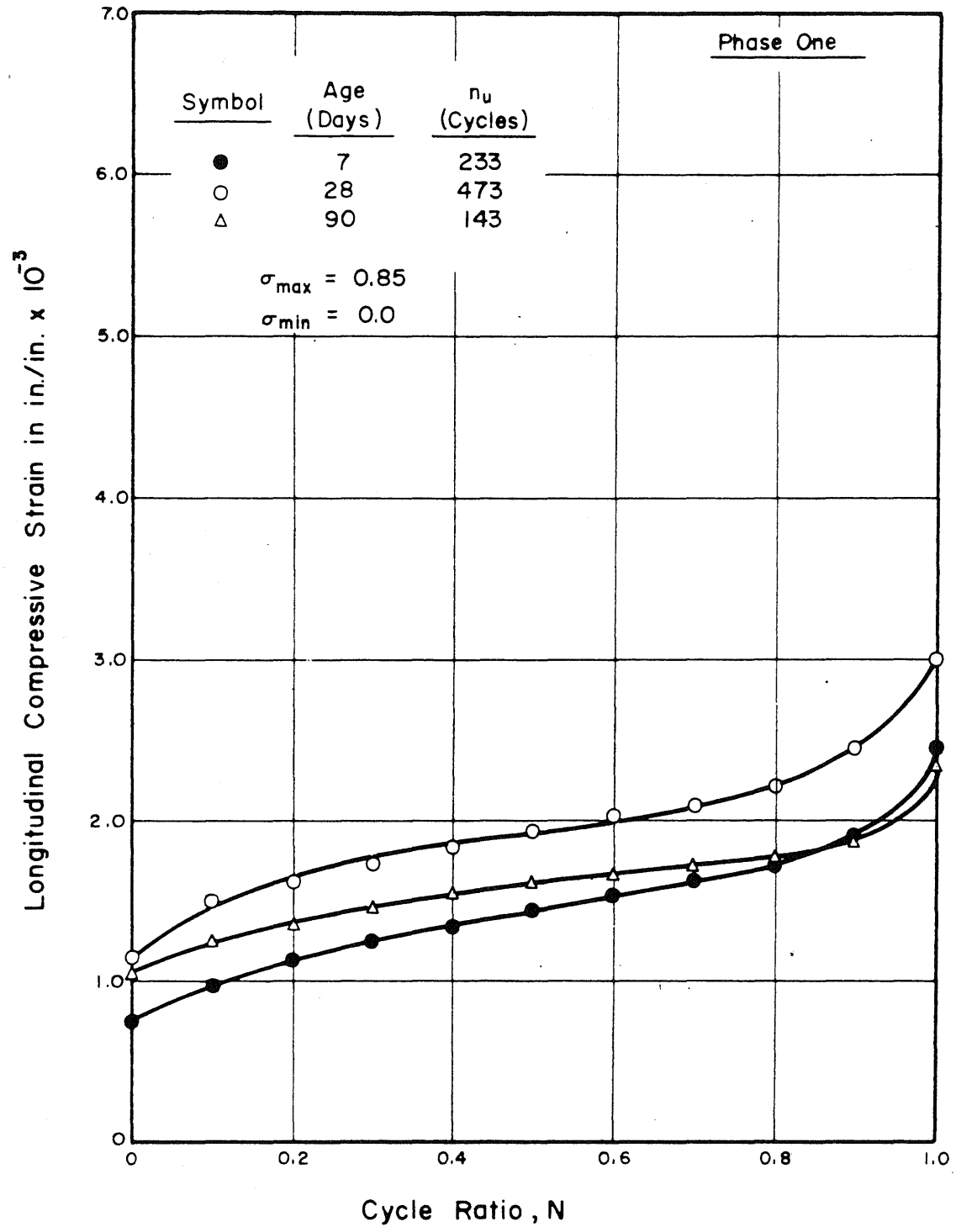

FIG. 4.40 EFFECT OF AGE AT LOADING ON LONGITUDINAL STRAIN-CYCLE RATIO RELATIONSHIP FOR CONCRETE SUBJECTED TO A MAXIMUM STRESS LEVEL OF 0.85 AND A STRESS RANGE OF 0.85

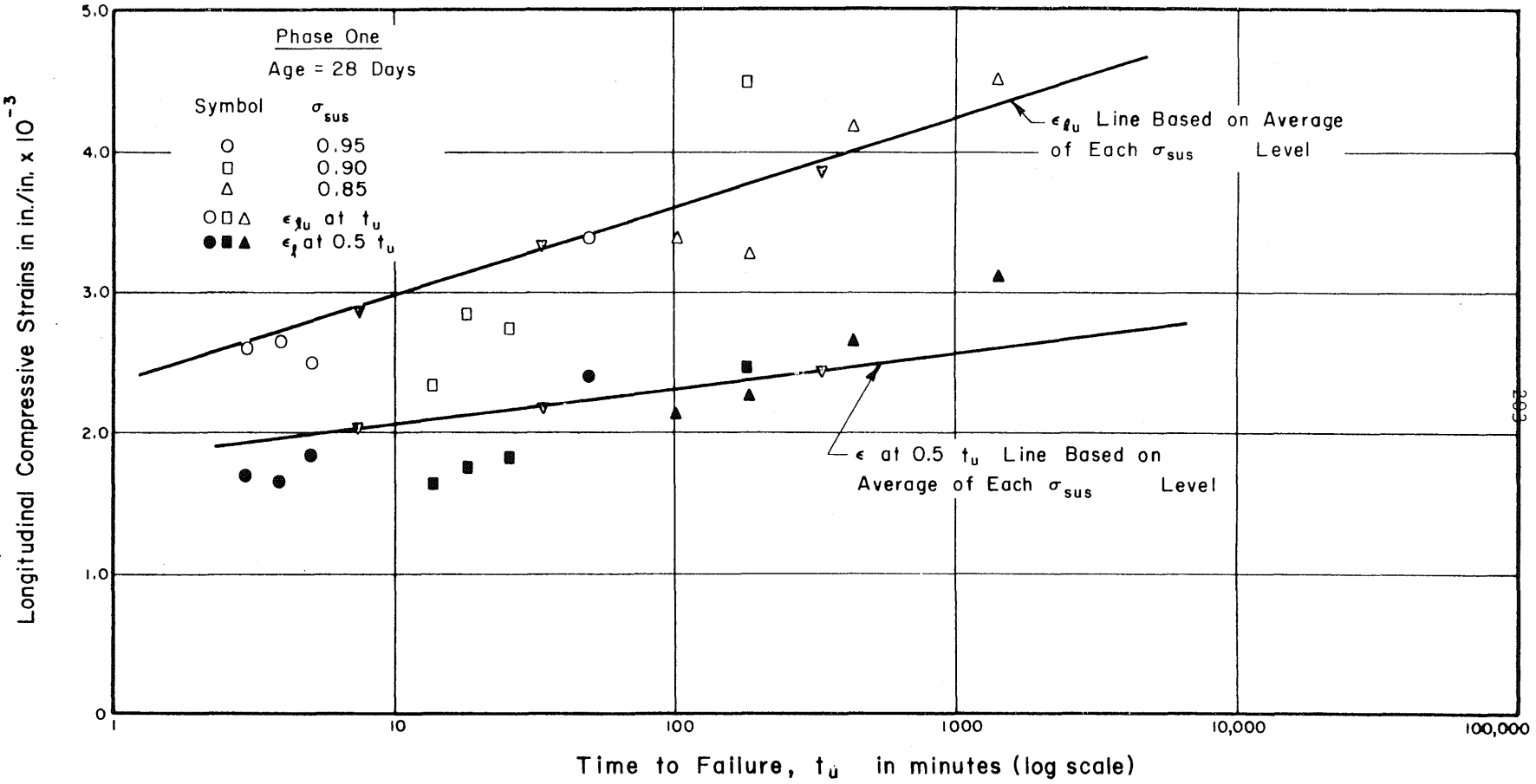

FIG. 4.41 VARIATION OF LONGITUDINAL STRAIN AT HALF LIFE AND AT FAILURE AS FUNCTION OF TIME FOR CONCRETE SUBJECTED TO DIFFERENT SUSTAINED STRESS LEVELS AT AN AGE OF 28 DAYS

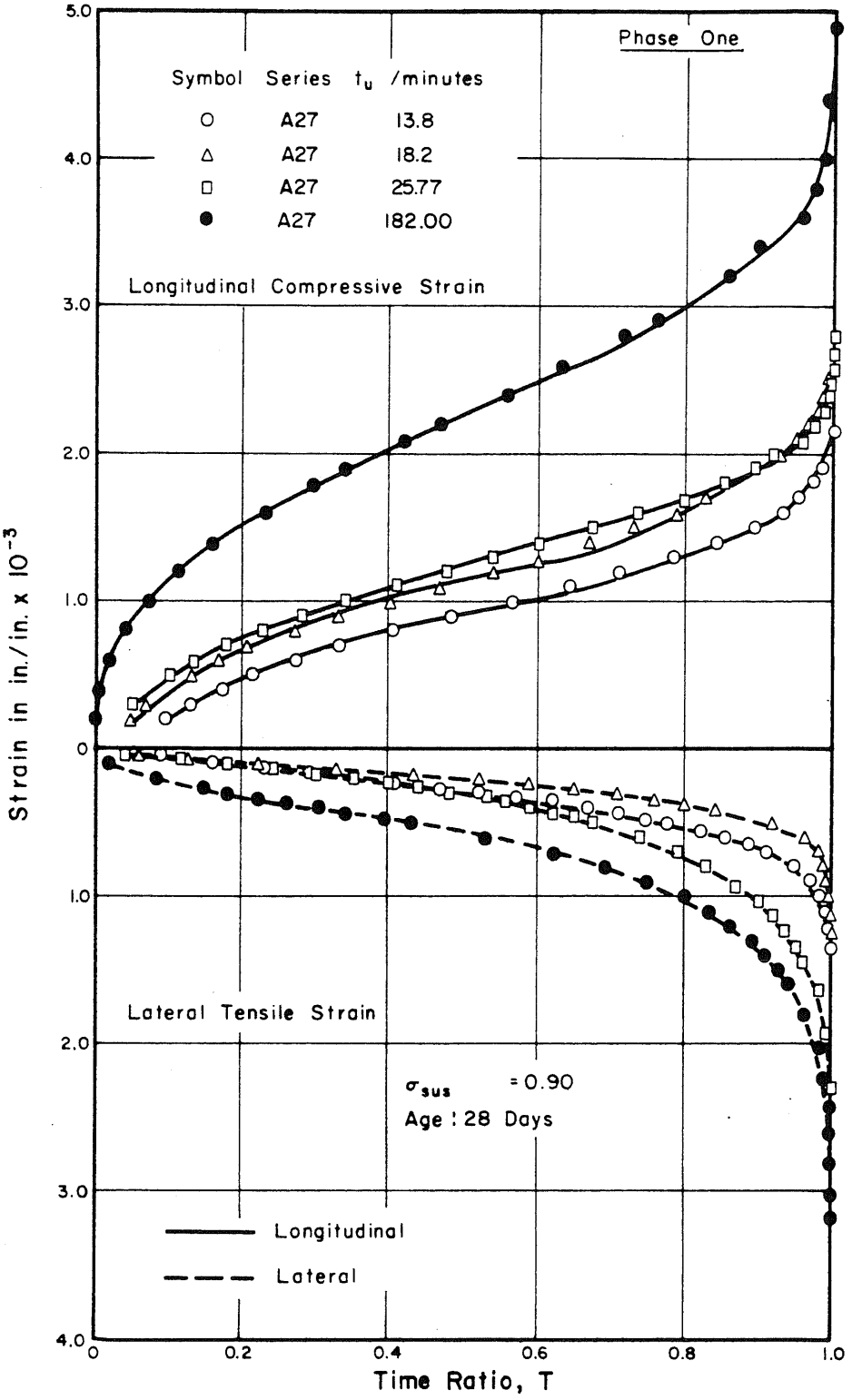

FIG. 4.42 EFFECT OF FAILURE TIME ON LONGITUDINAL AND LATERAL STRAINS — TIME RATIO RELATIONSHIPS OF CONCRETE SUBJECTED TO A CONSTANT SUSTAINED STRESS LEVEL OF 0.90 AT AN AGE OF 28 DAYS

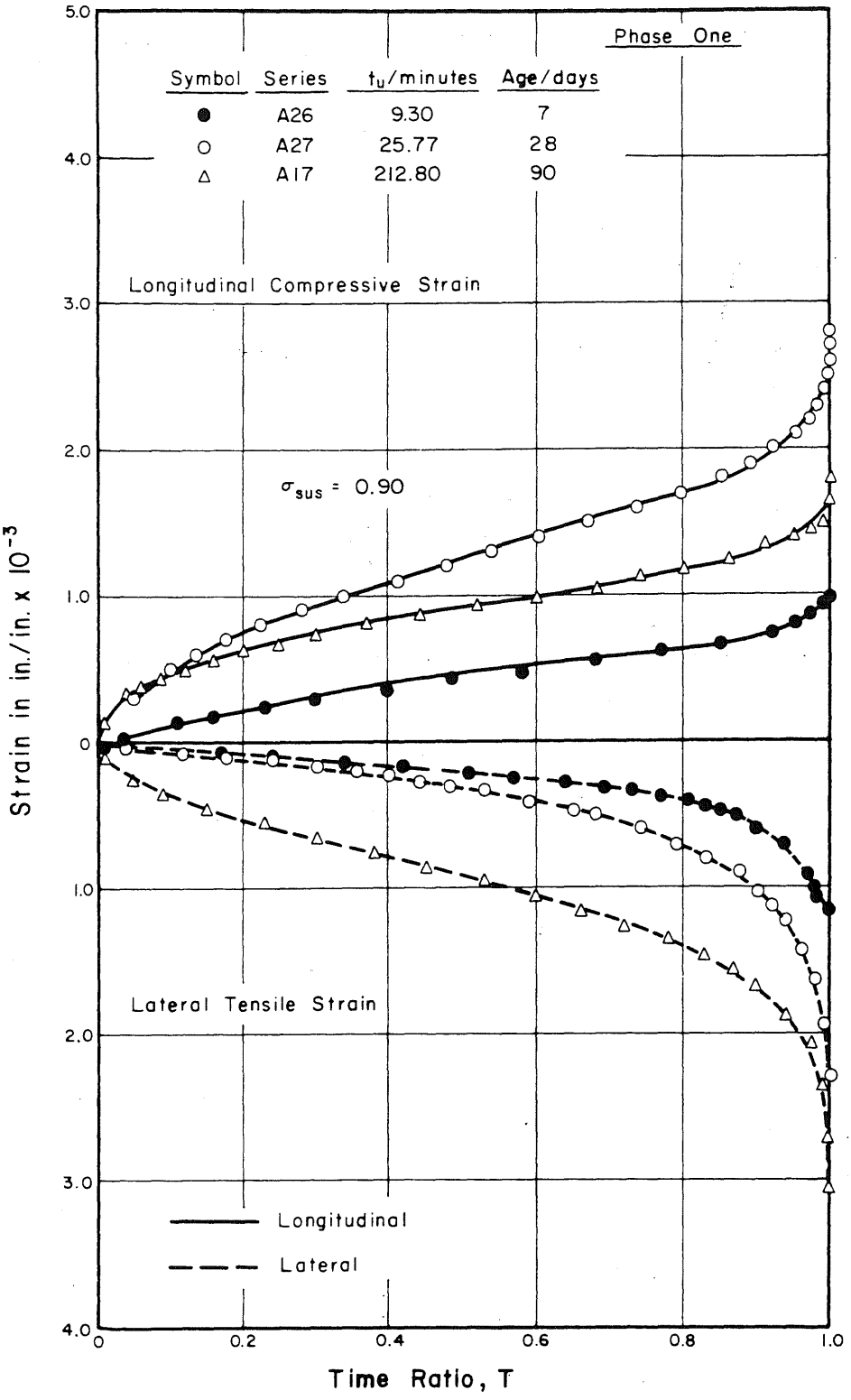

FIG. 4.43 EFFECT OF AGE AT LOADING ON LONGITUDINAL AND LATERAL STRAINS – TIME RATIO RELATIONSHIPS FOR CONCRETE SUBJECTED TO A CONSTANT SUSTAINED STRESS LEVEL OF 0.90

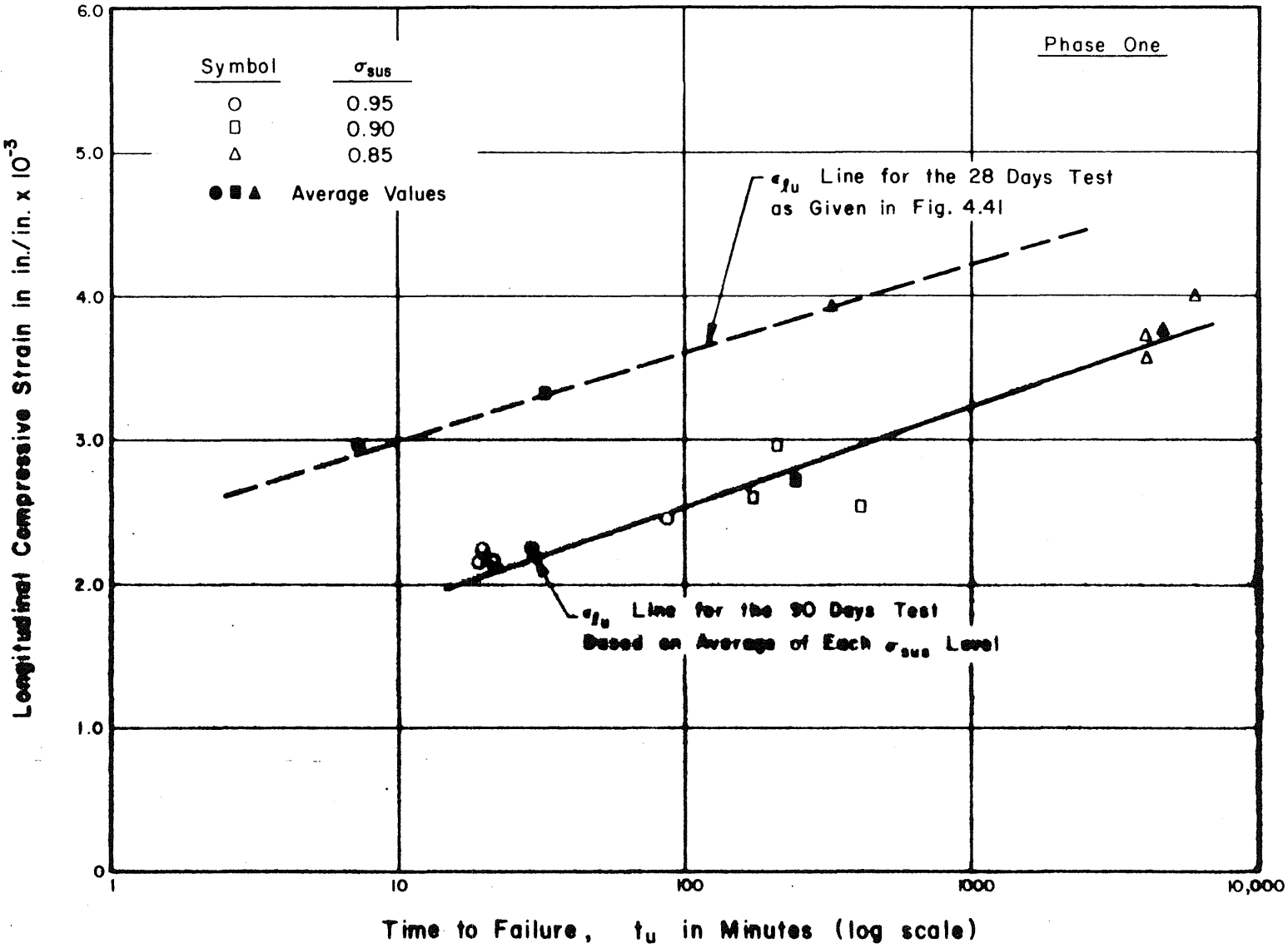

FIG. 4.44 LONGITUDINAL FAILURE STRAIN AS FUNCTION OF TIME TO FAILURE FOR CONCRETE SUBJECTED TO DIFFERENT SUSTAINED STRESS LEVELS AT DIFFERENT AGES

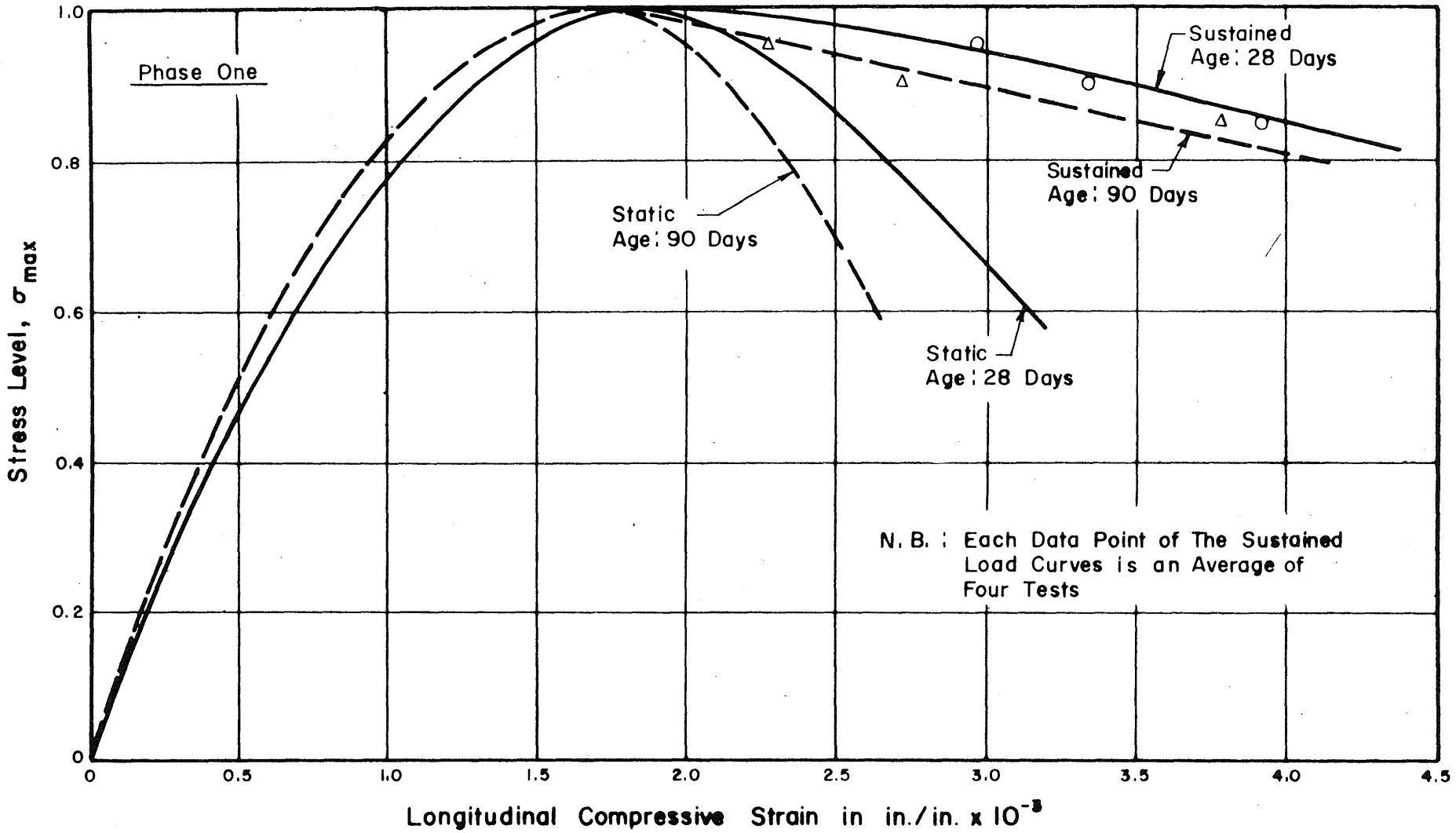

FIG. 4.45 EFFECT OF CONCRETE AGE AT LOADING ON LONGITUDINAL FAILURE STRAIN UNDER SUSTAINED STRESSES AS COMPARED TO THE STATIC STRESS – LONGITUDINAL STRAIN CURVE

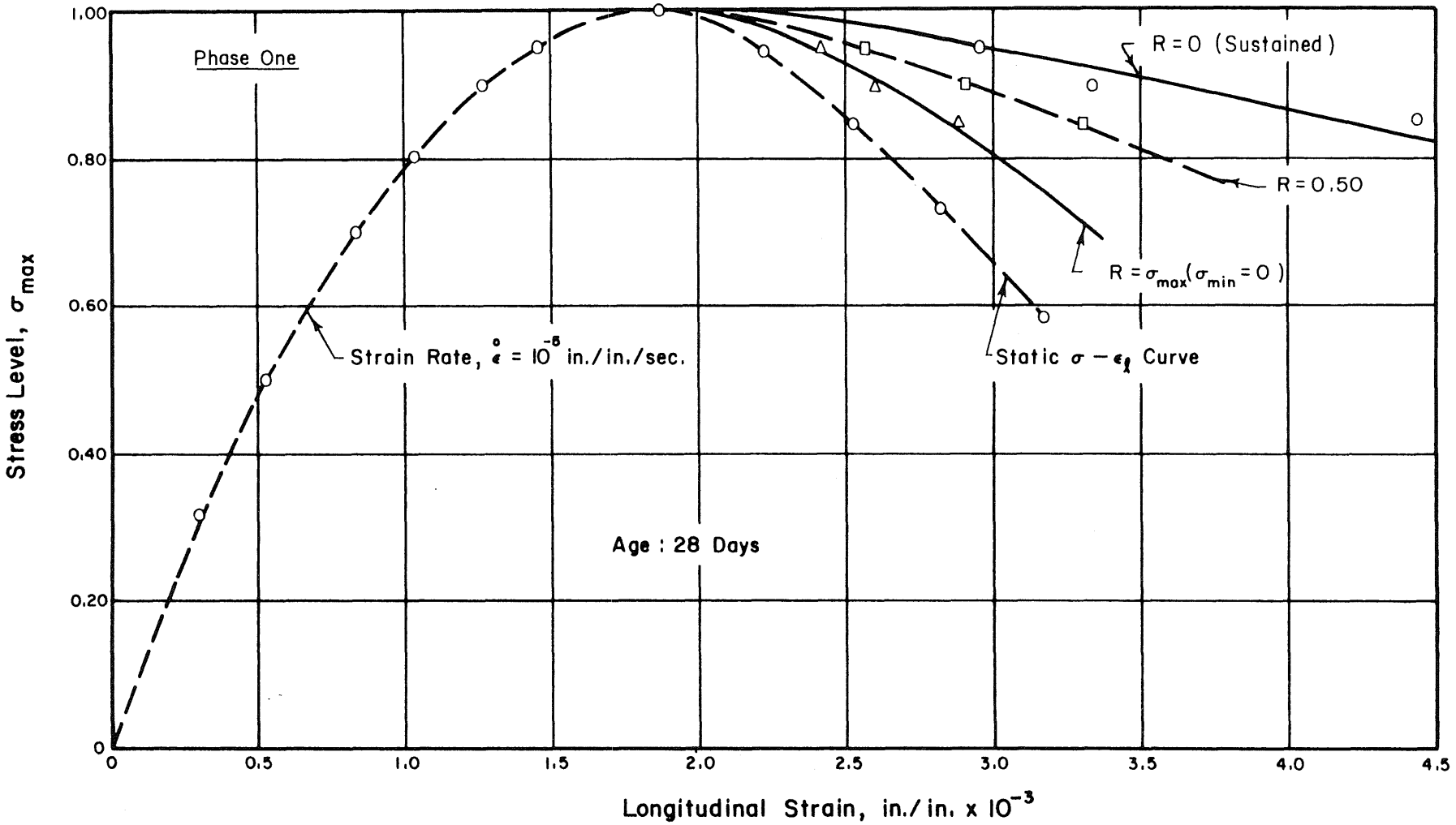

FIG. 4.46 EFFECT OF MAXIMUM STRESS LEVEL ON LONGITUDINAL FAILURE STRAIN AS COMPARED WITH THE STATIC STRESS-STRAIN CURVE—AGE AT LOADING : 28 DAYS

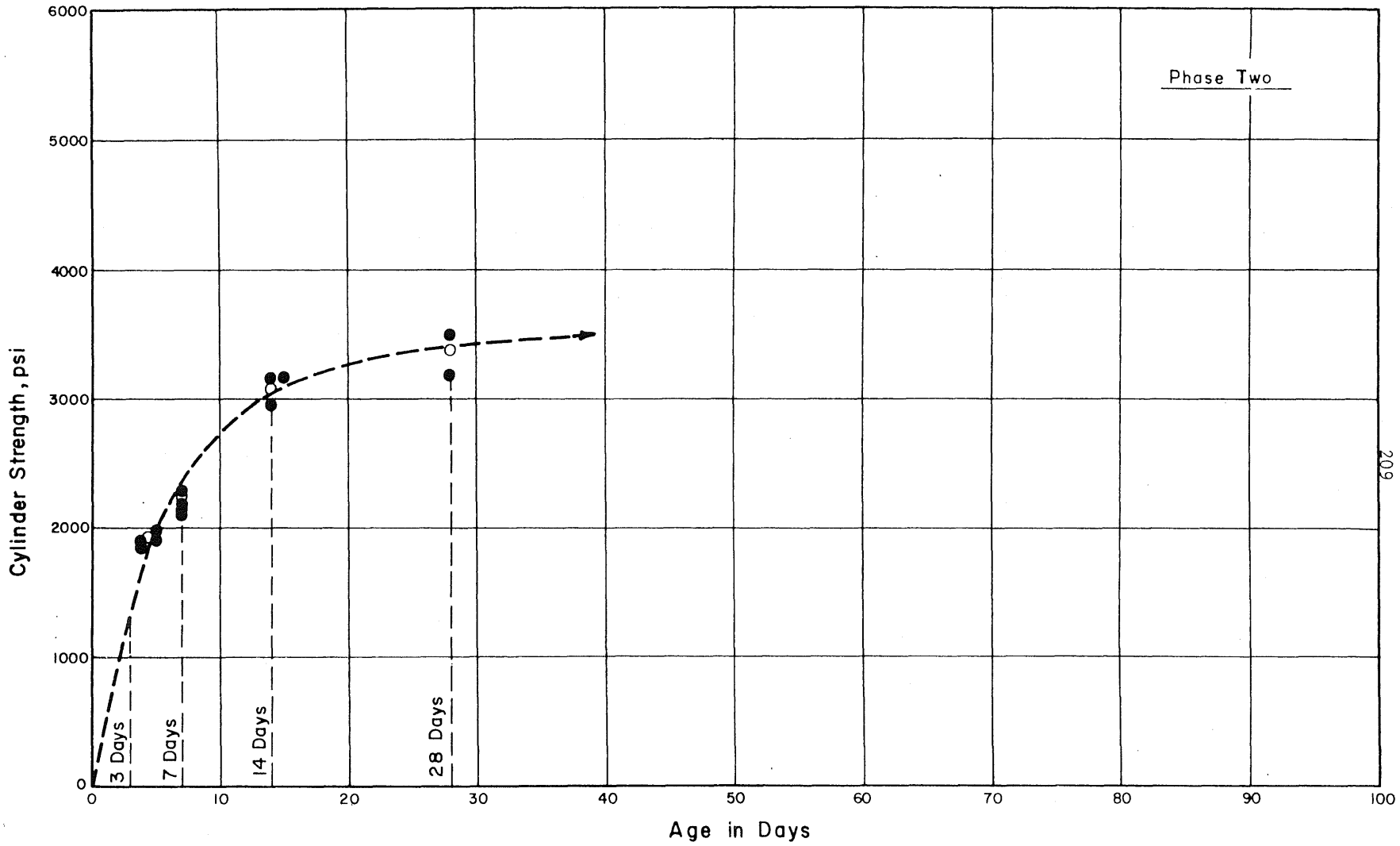

FIG. 5.1 DEVELOPMENT OF CONCRETE CYLINDER STRENGTH WITH AGE : BATCHES C1 TO C5

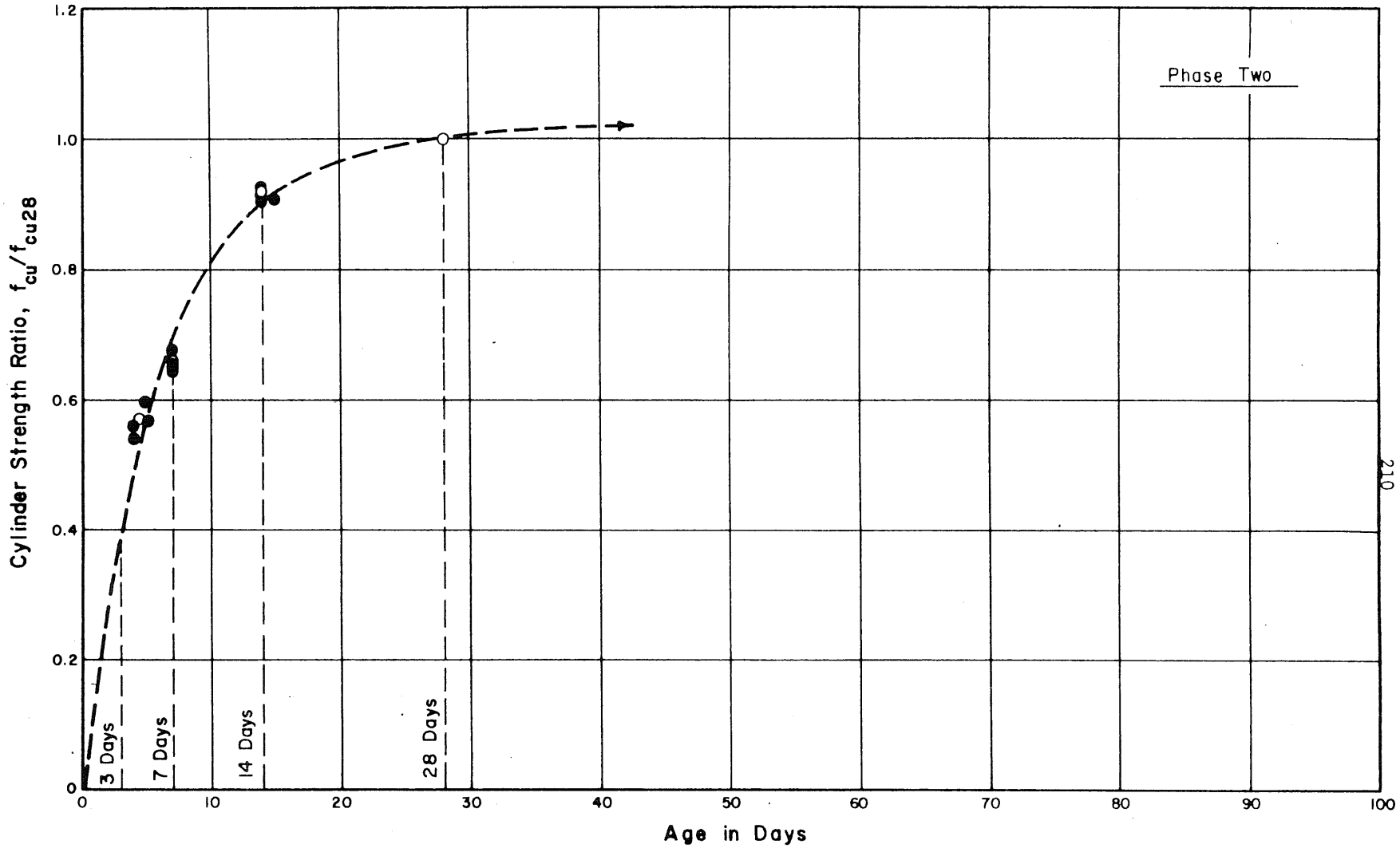

FIG. 5.2 DEVELOPMENT OF CONCRETE CYLINDER STRENGTH RATIO WITH AGE : BATCHES C1 TO C5

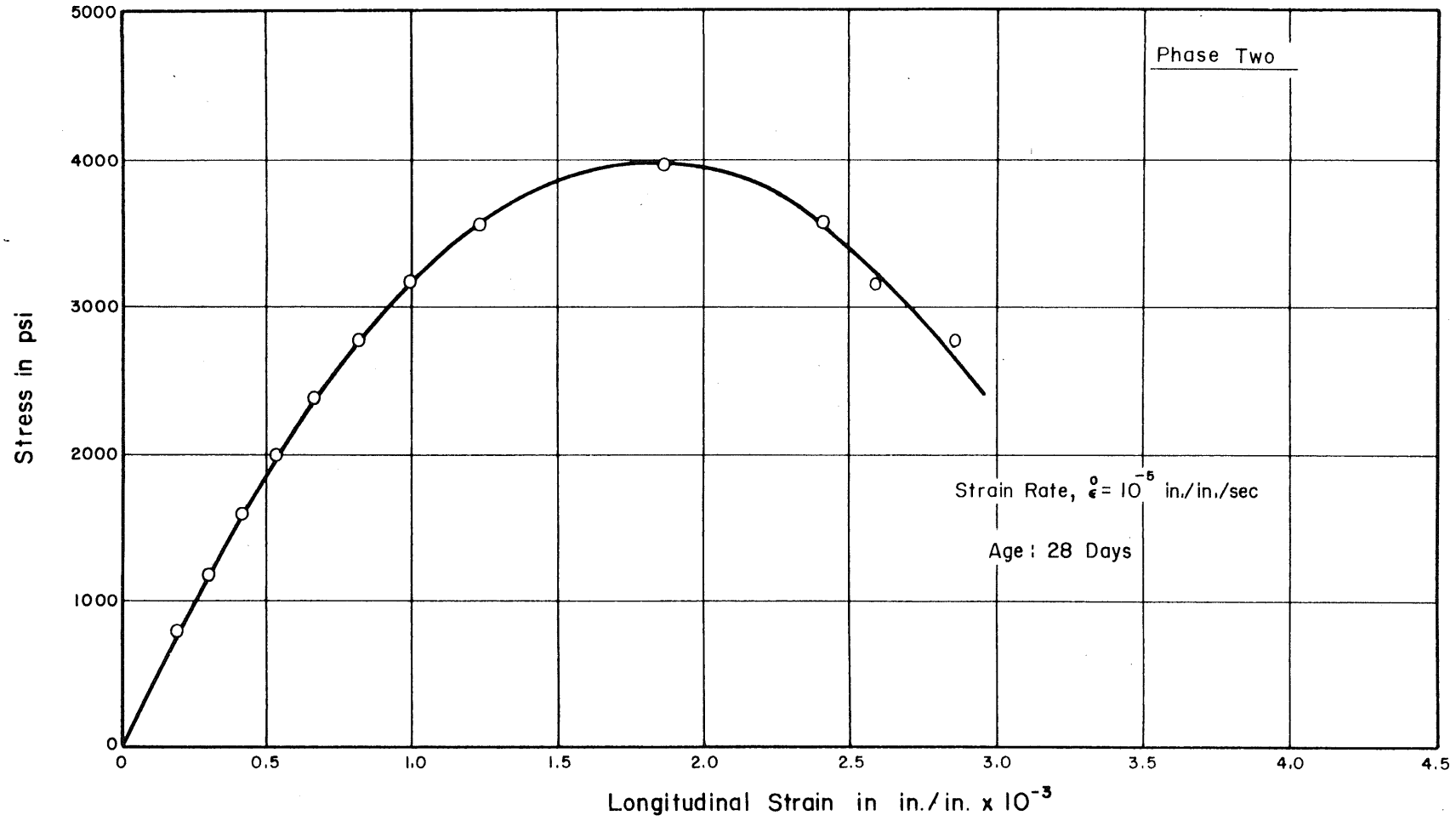

FIG. 5.3 STATIC STRESS–LONGITUDINAL STRAIN CHARACTERISTICS OF CONCRETE PRISMS : $\dot{\epsilon}^{0} = 10^{-5}$ in./in./sec.

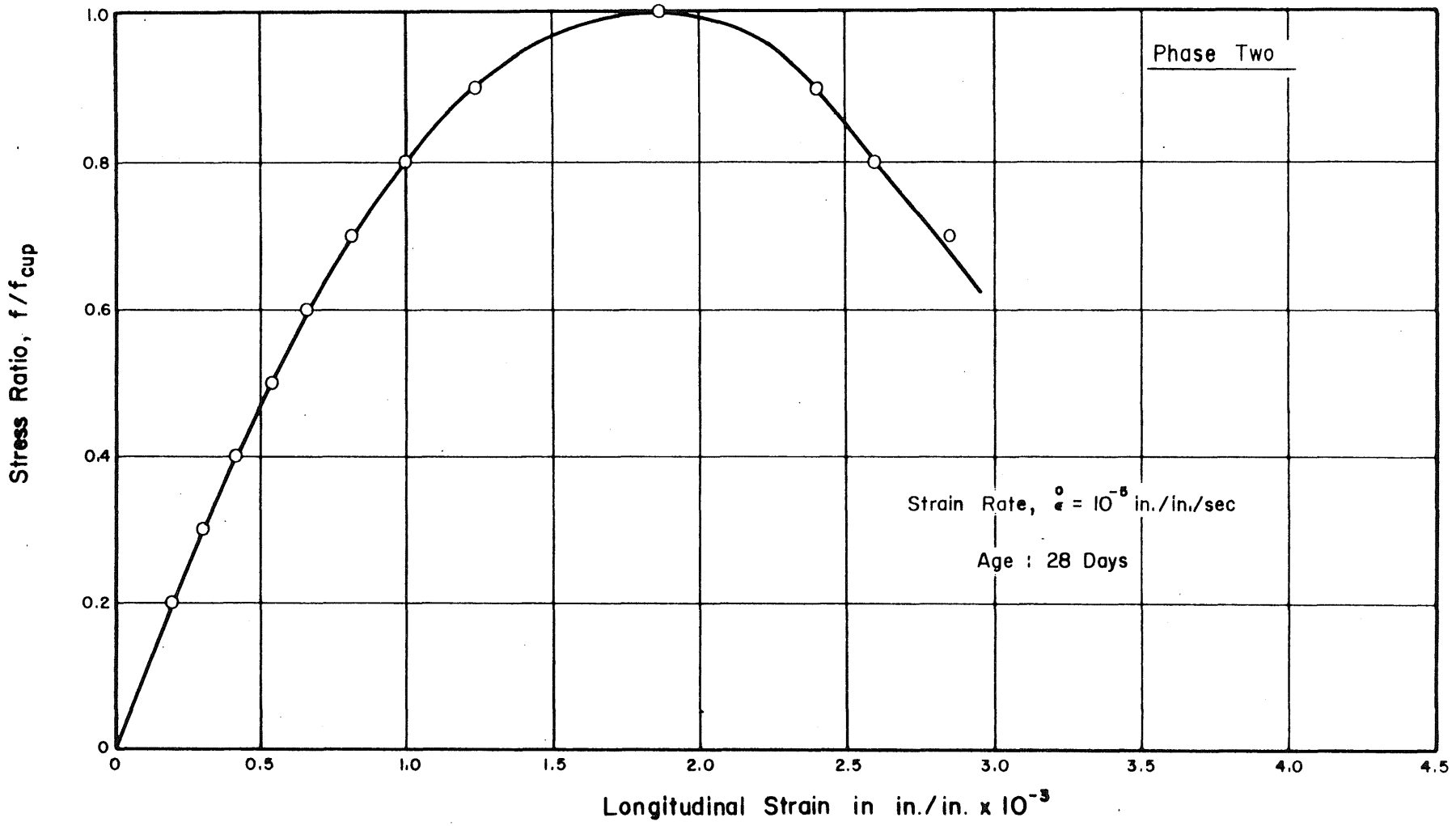

FIG. 5.4 STATIC STRESS RATIO – LONGITUDINAL STRAIN CHARACTERISTICS OF CONCRETE PRISMS : $\dot{\epsilon}^0 = 10^{-5}$ in./in./sec.

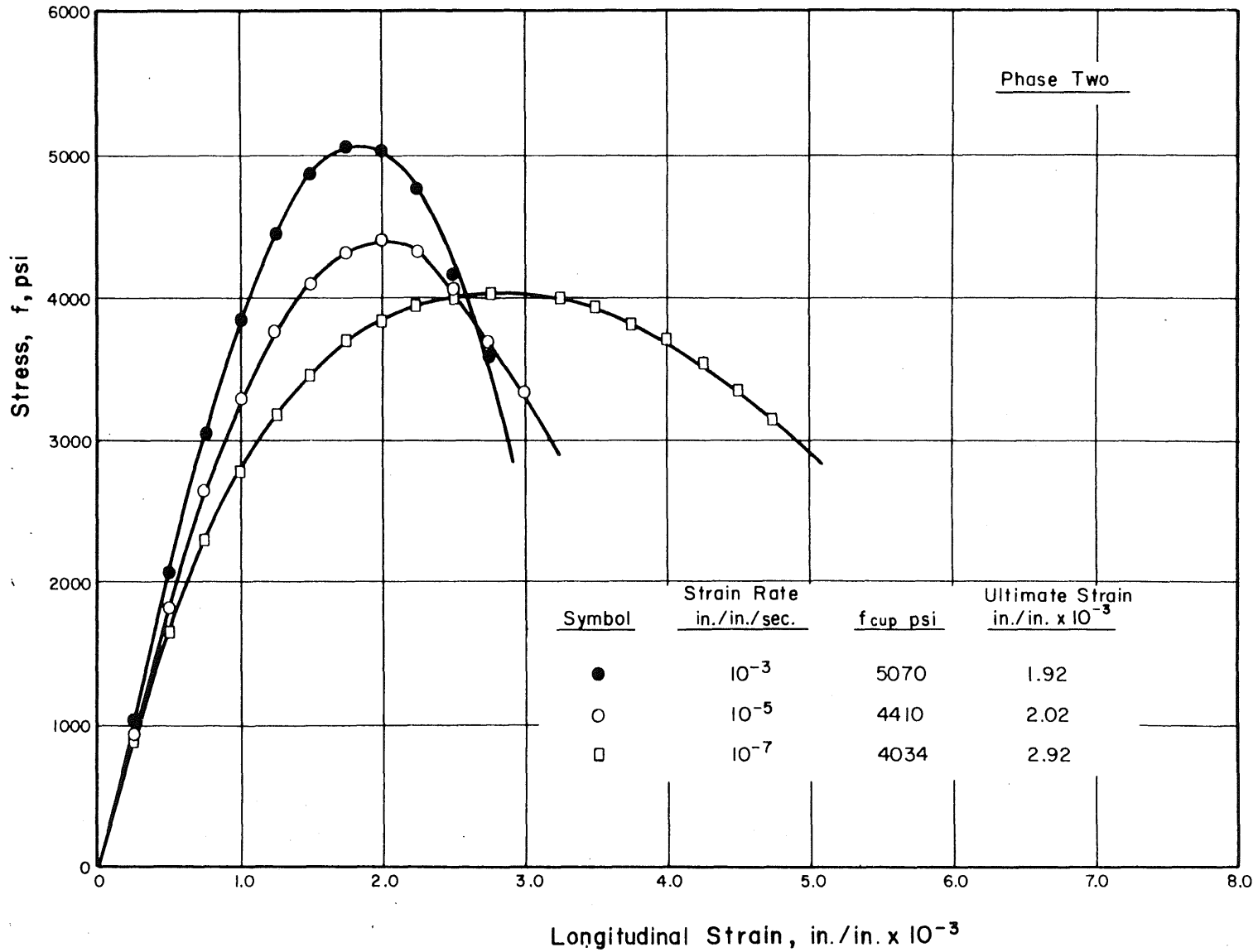

FIG. 5.5 STATIC STRESS — LONGITUDINAL STRAIN CHARACTERISTICS OF CONCRETE PRISMS TESTED AT DIFFERENT STRAIN RATES

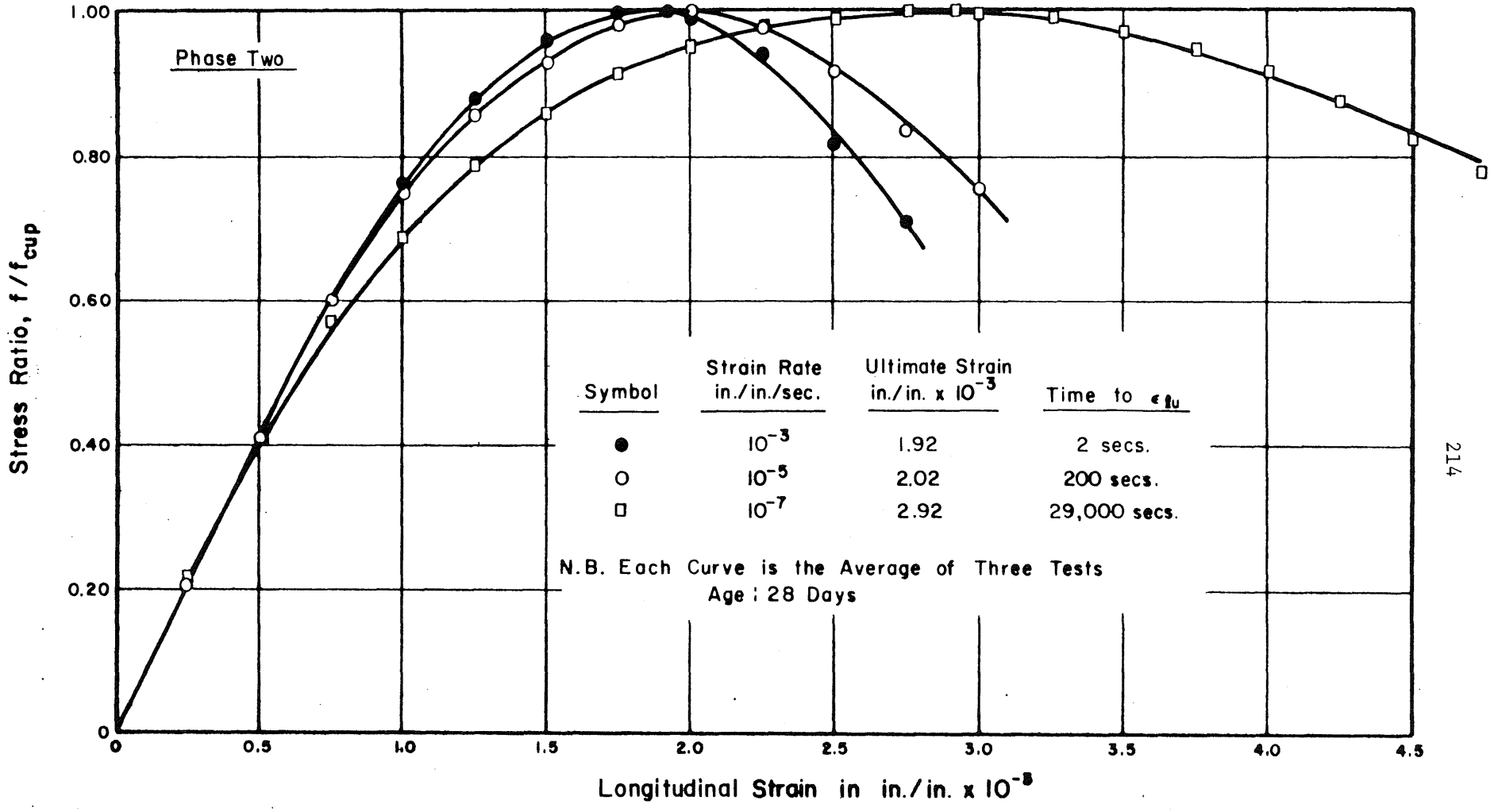

FIG. 5.6 STATIC STRESS RATIO – LONGITUDINAL STRAIN CHARACTERISTICS OF CONCRETE TESTED AT DIFFERENT STRAIN RATES

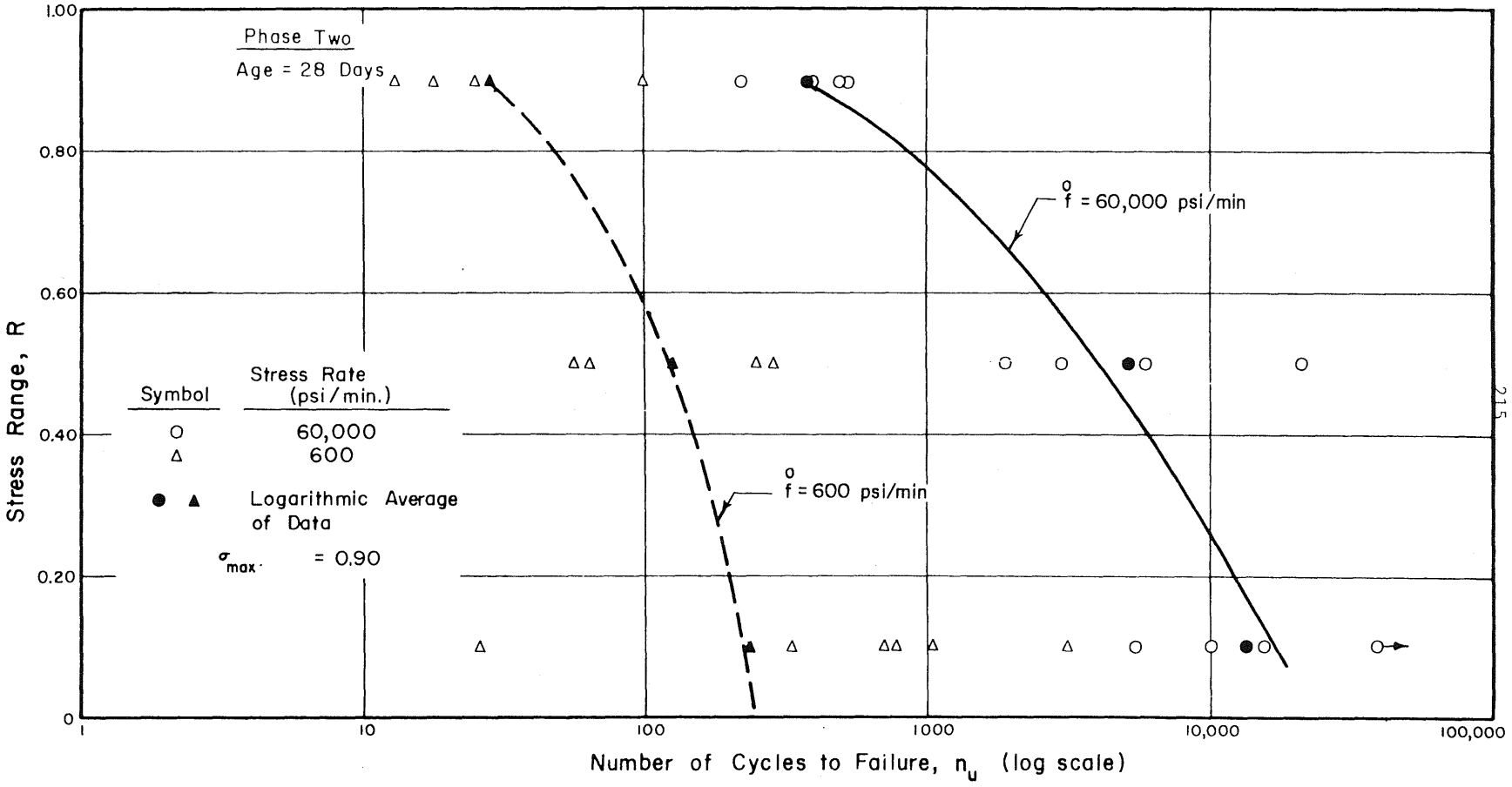

FIG. 5.7 STRESS RANGE – CYCLES TO FAILURE RELATIONSHIP FOR DIFFERENT STRESS RATES : $\sigma_{max} = 0.90$

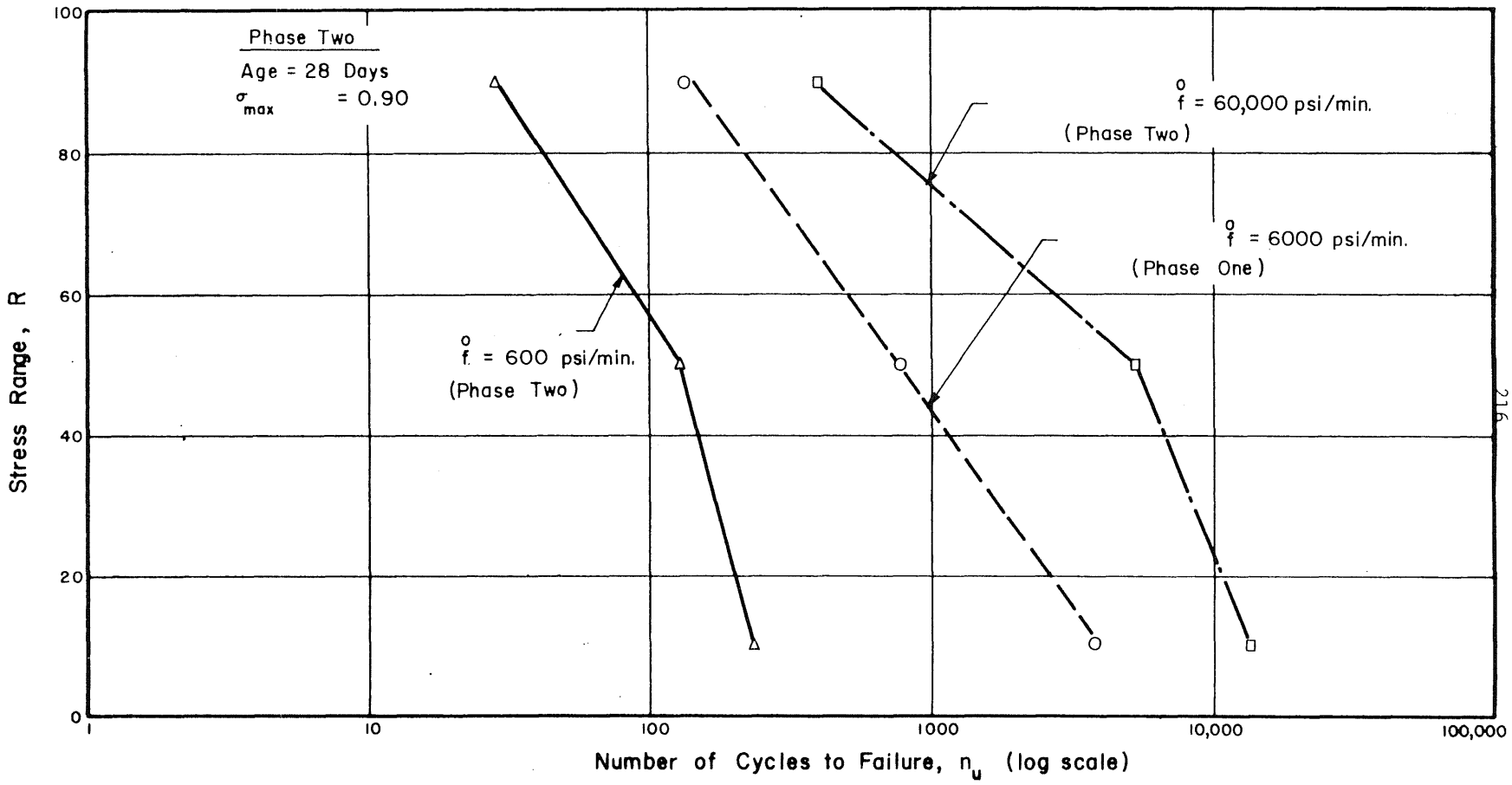

FIG. 5.8 STRESS RANGE – CYCLES TO FAILURE RELATIONSHIP FOR DIFFERENT STRESS RATES: $\sigma_{max} = 0.90$

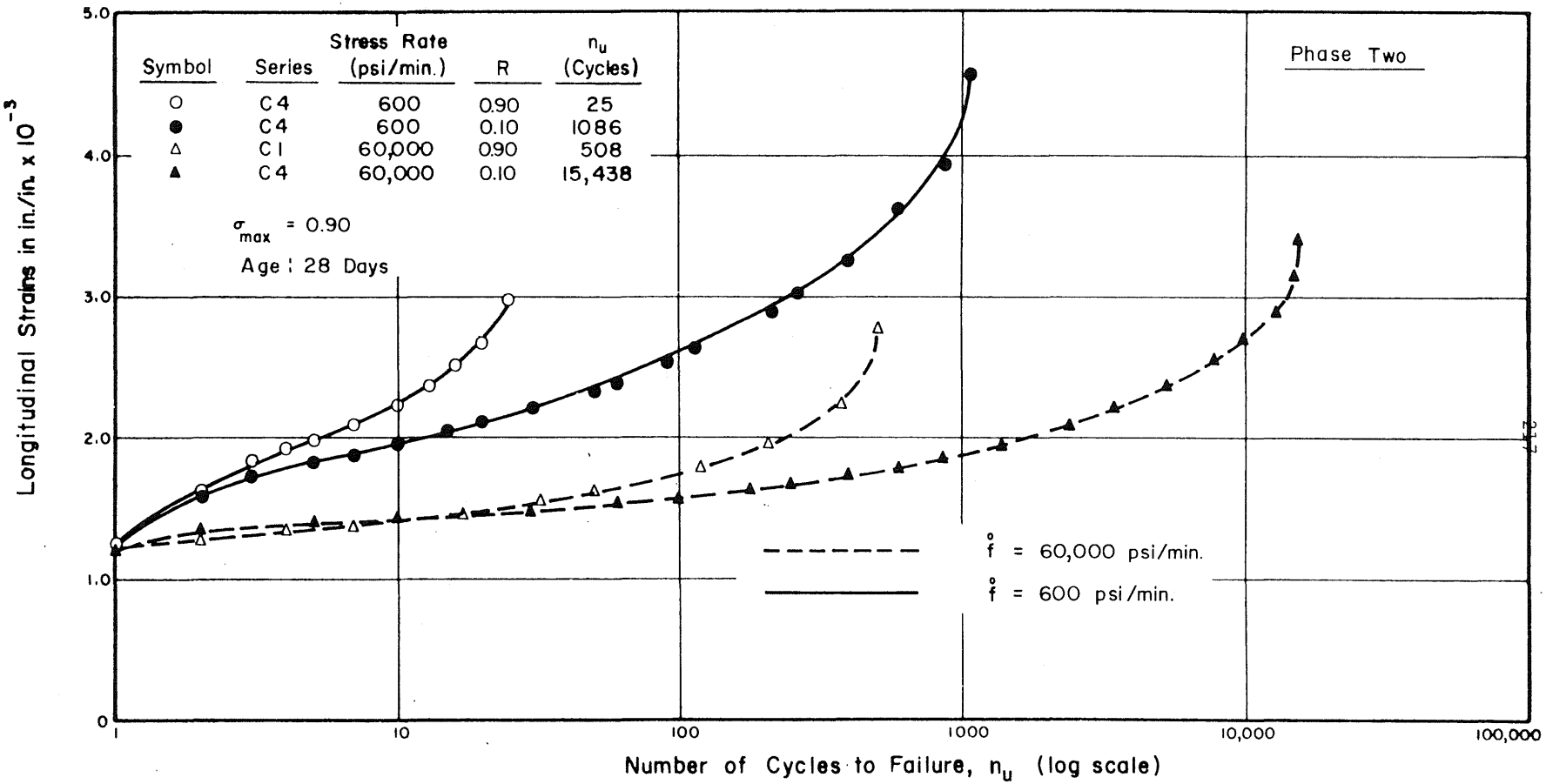

FIG. 5.9 LONGITUDINAL STRAIN AS FUNCTION OF NUMBER OF APPLIED CYCLES FOR DIFFERENT STRESS RATES AND DIFFERENT STRESS RANGES: $\sigma_{max} = 0.90$

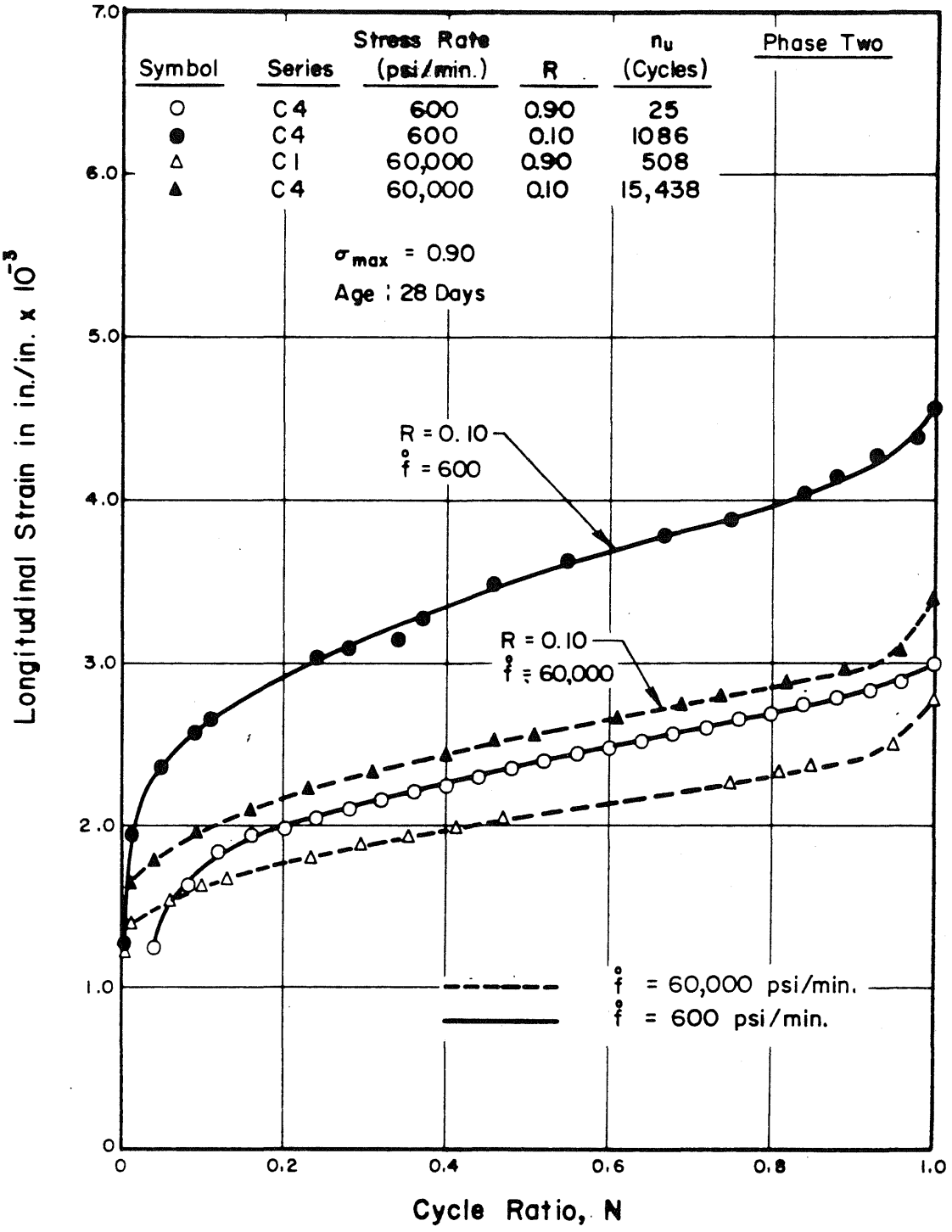

FIG. 5.10 LONGITUDINAL STRAIN AS FUNCTION OF CYCLE RATIO FOR DIFFERENT STRESS RANGES AND DIFFERENT STRESS RATES : $\sigma_{max} = 0.90$

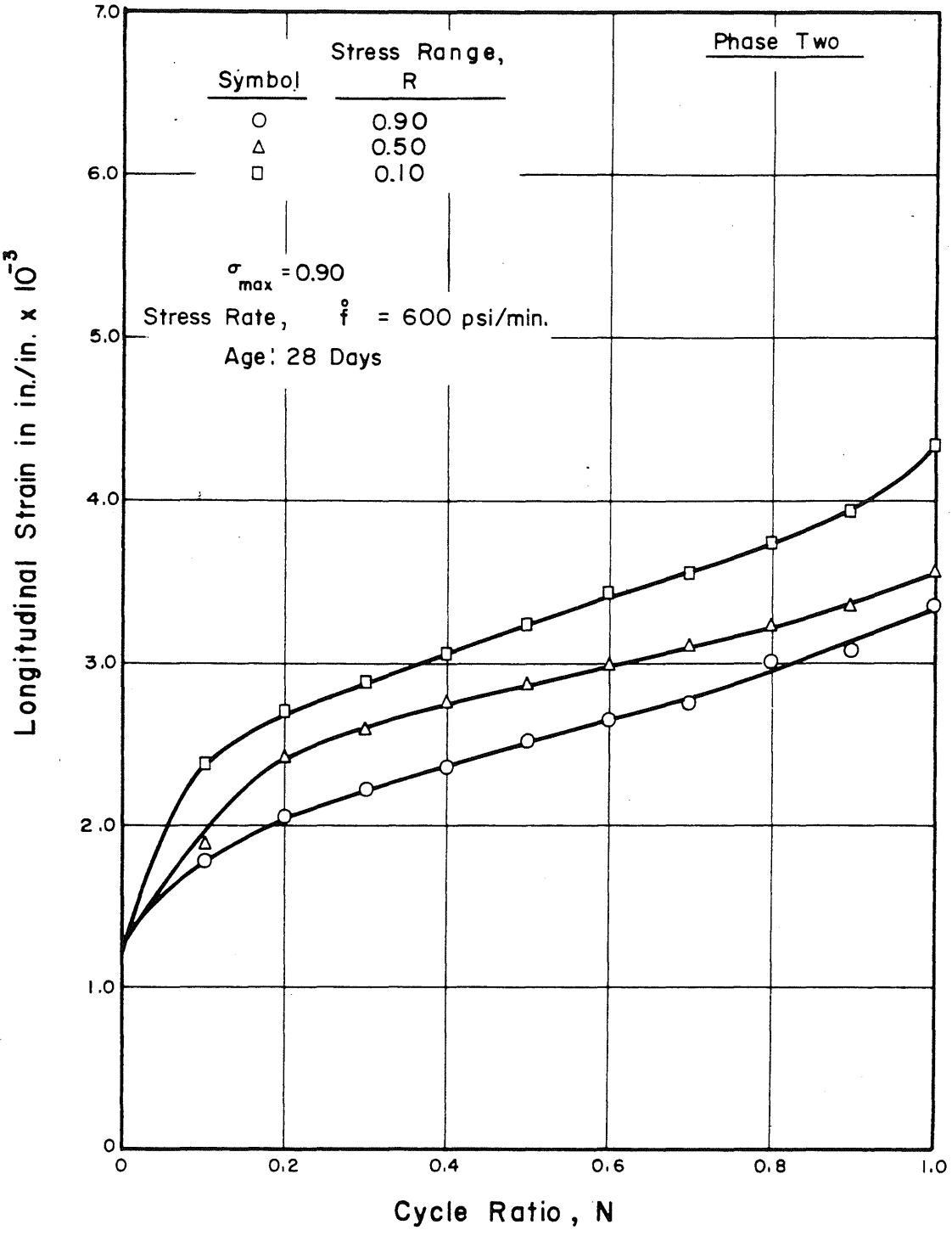

FIG. 5.11 LONGITUDINAL STRAIN AS FUNCTION OF CYCLE RATIO FOR DIFFERENT STRESS RANGES: σ_{max} = 0.90 AND $\dot{f}$ = 600 psi/min.

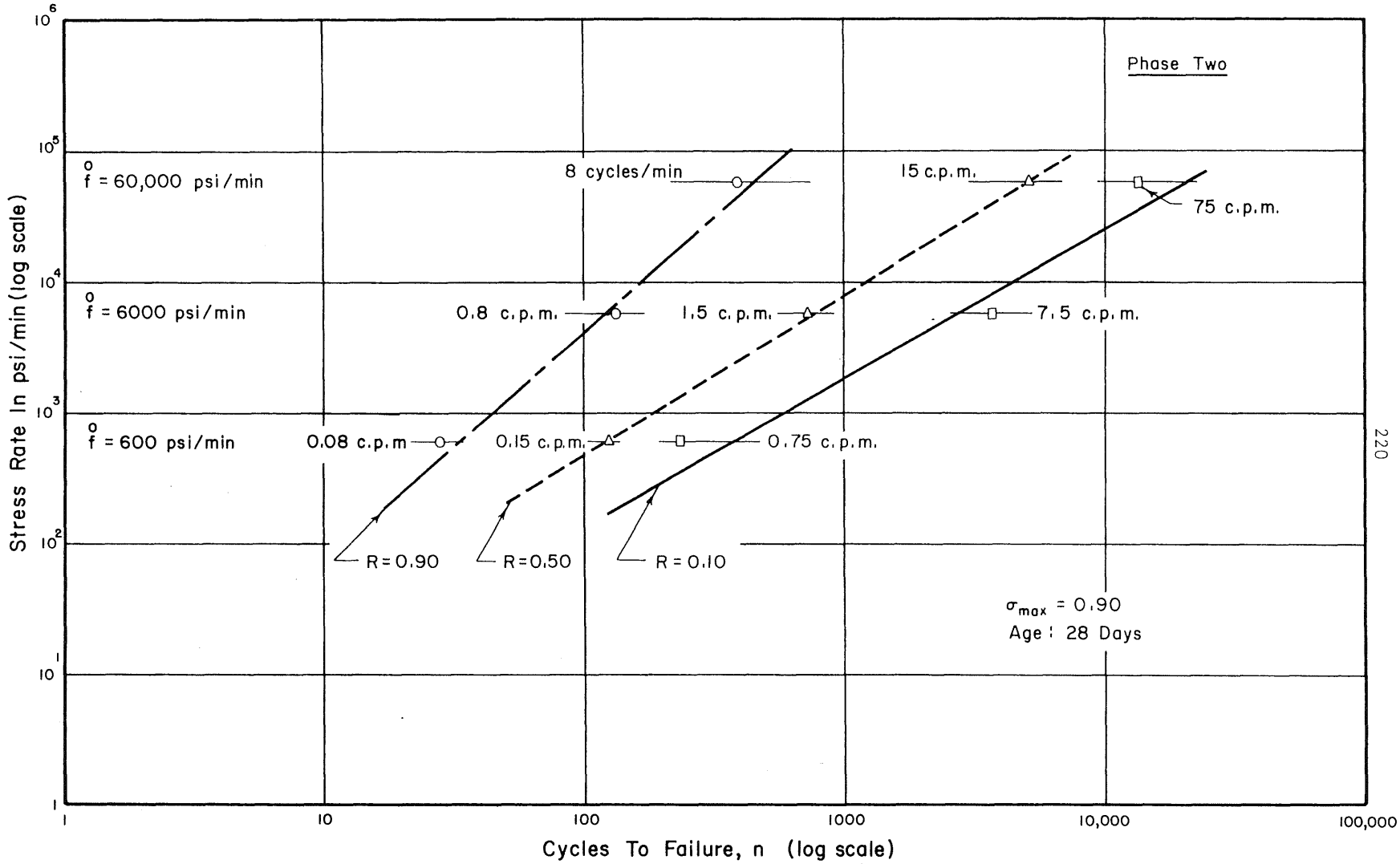

FIG. 5.12 STRESS RATE - CYCLES TO FAILURE RELATIONSHIP FOR DIFFERENT STRESS RANGES: σ_{max} = 0.90

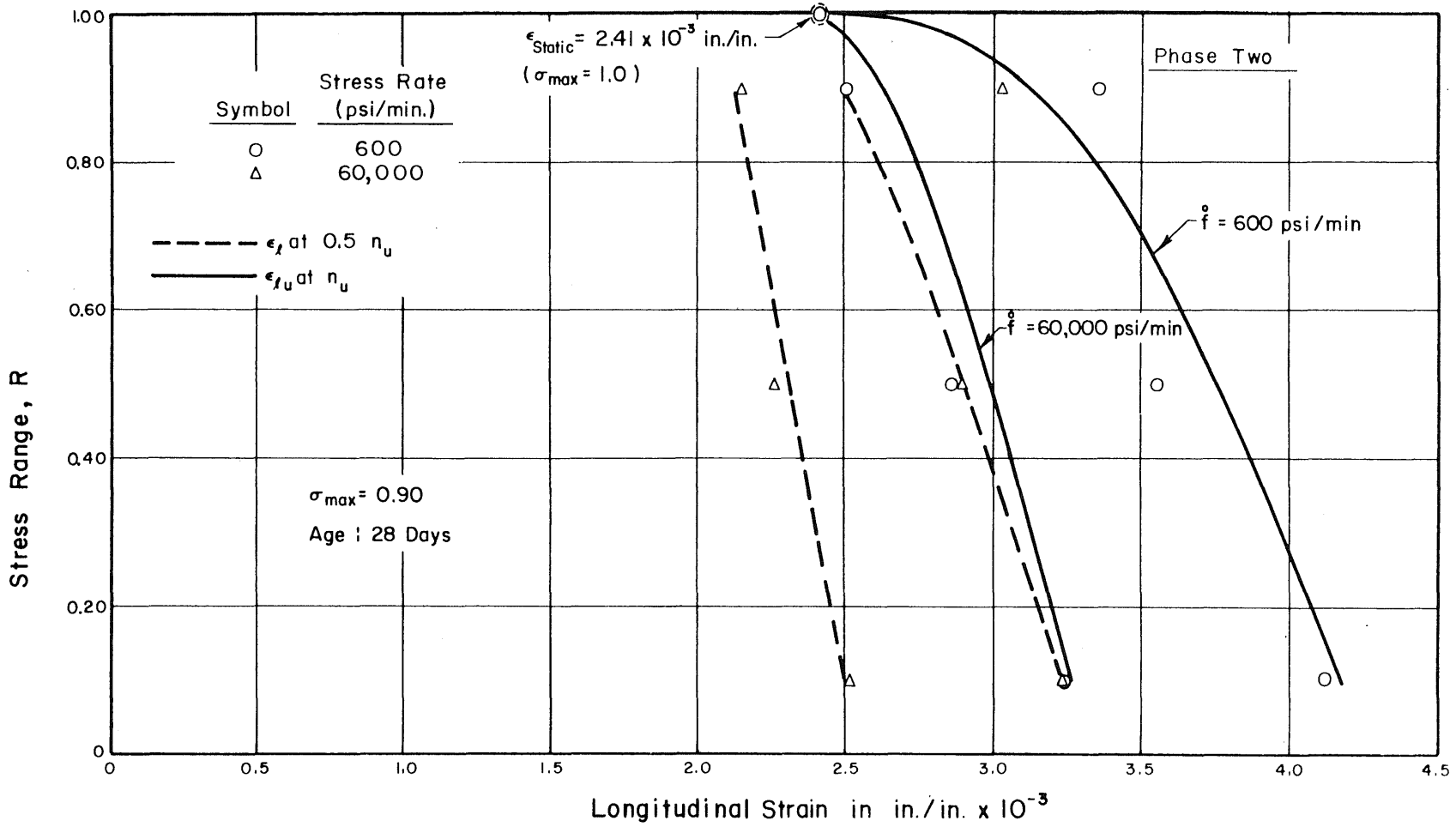

FIG. 5.13 STRESS RANGE – LONGITUDINAL STRAIN RELATIONSHIP AT HALF LIFE AND AT FAILURE FOR DIFFERENT STRESS RATES : σ_{max} = 0.90

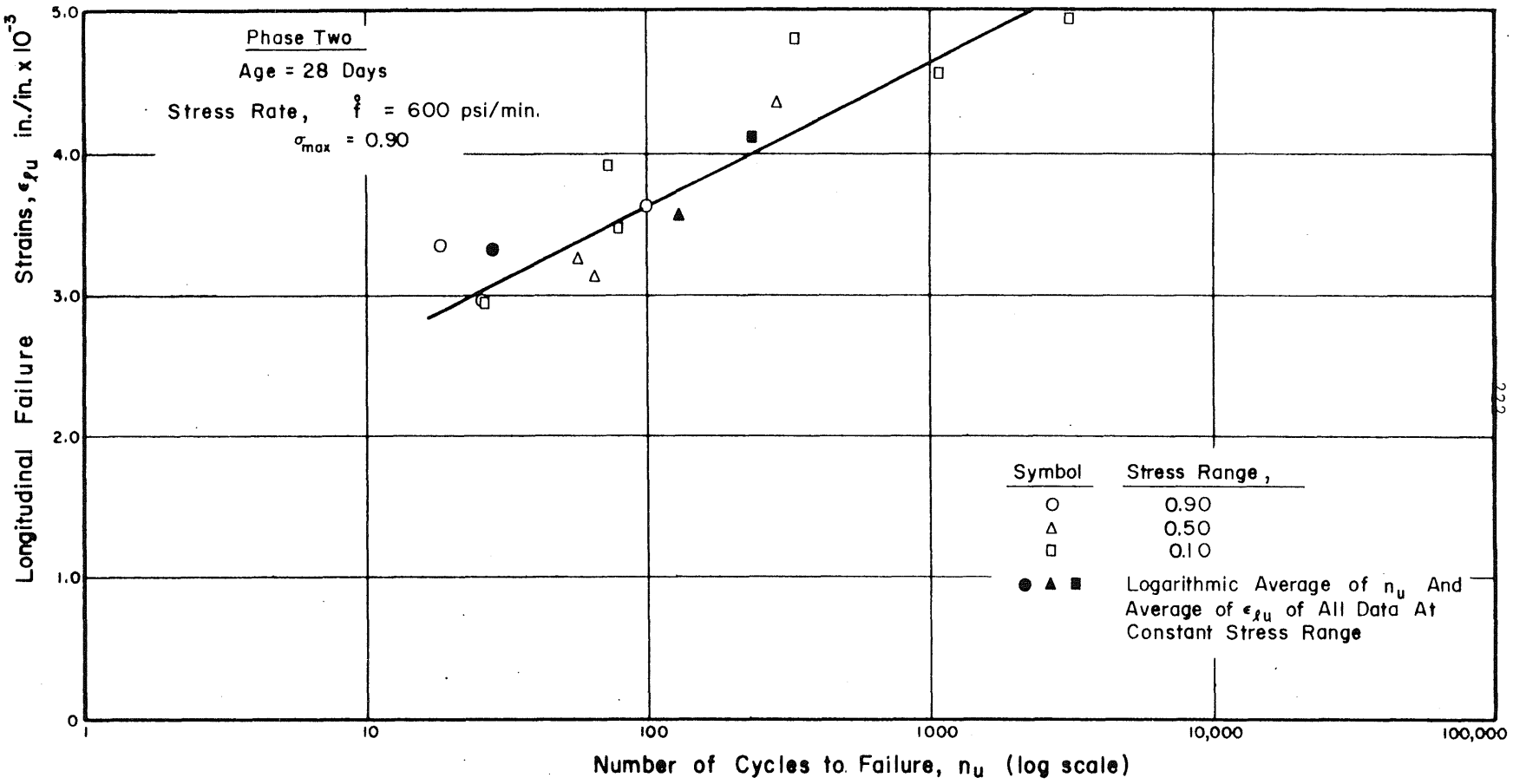

FIG. 5.14 LONGITUDINAL STRAIN AT FAILURE AS FUNCTION OF NUMBER OF CYCLES TO FAILURE: σ_{max} = 0.90, $\dot{f}$ = 600 psi/min.

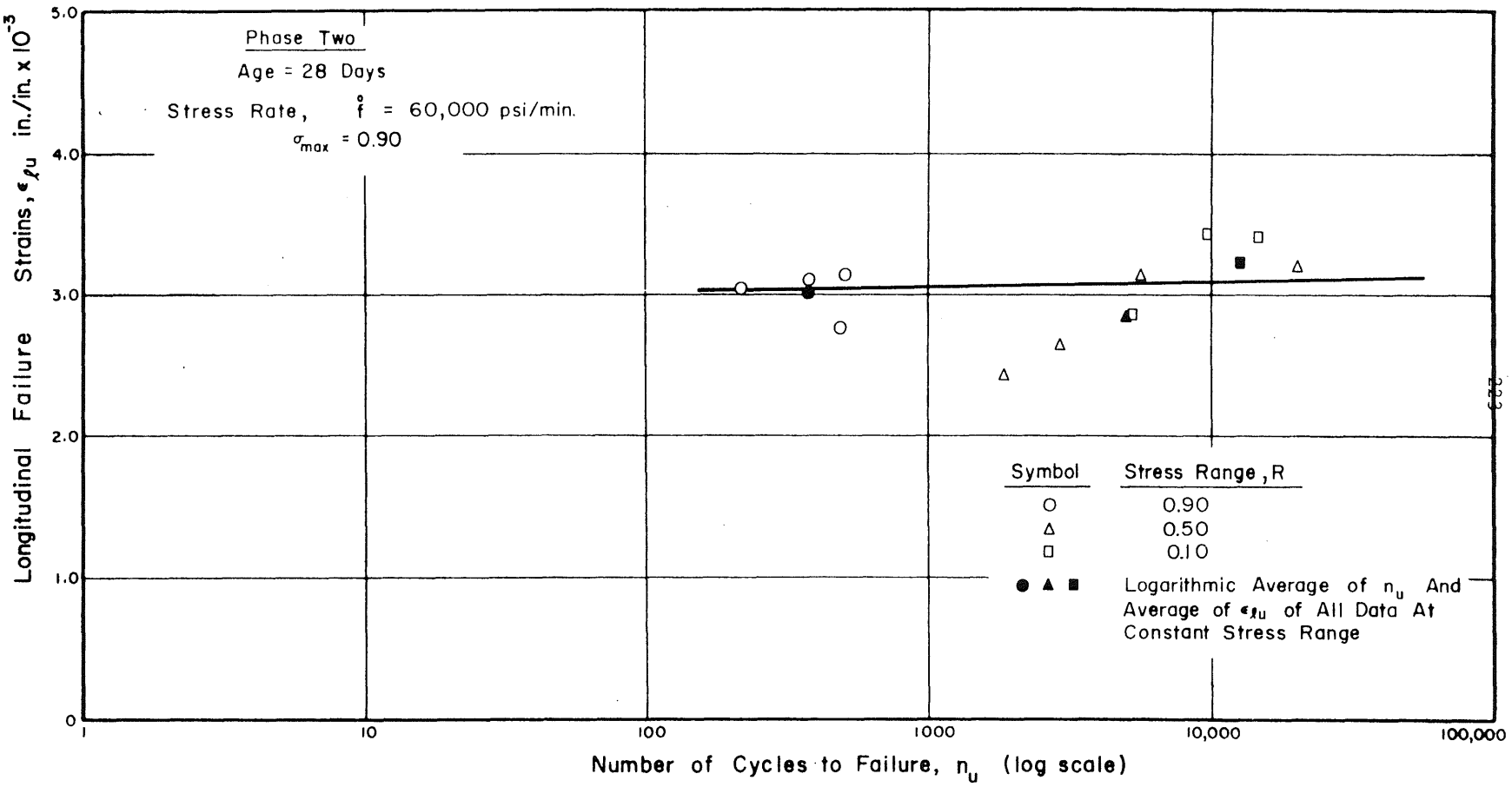

FIG. 5.15 LONGITUDINAL STRAIN AT FAILURE AS FUNCTION OF NUMBER OF CYCLES TO FAILURE: σ_{max} = 0.90 AND $\dot{f}$ = 60,000 psi/min.

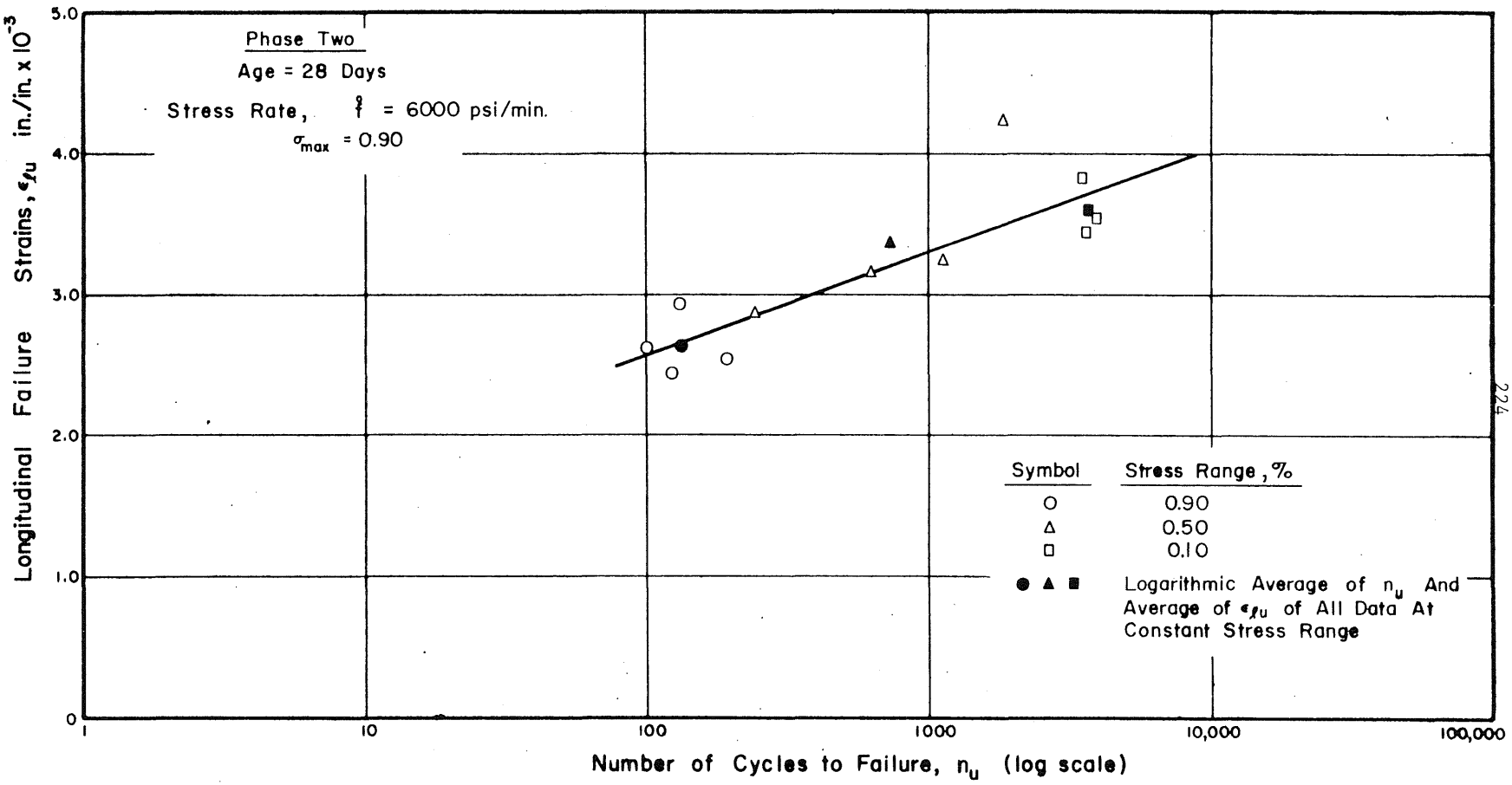

FIG. 5.16 LONGITUDINAL STRAIN AT FAILURE AS FUNCTION OF NUMBER OF CYCLES TO FAILURE : σ_{max} = 0.90 AND $\dot{f}$ = 6,000 psi/min

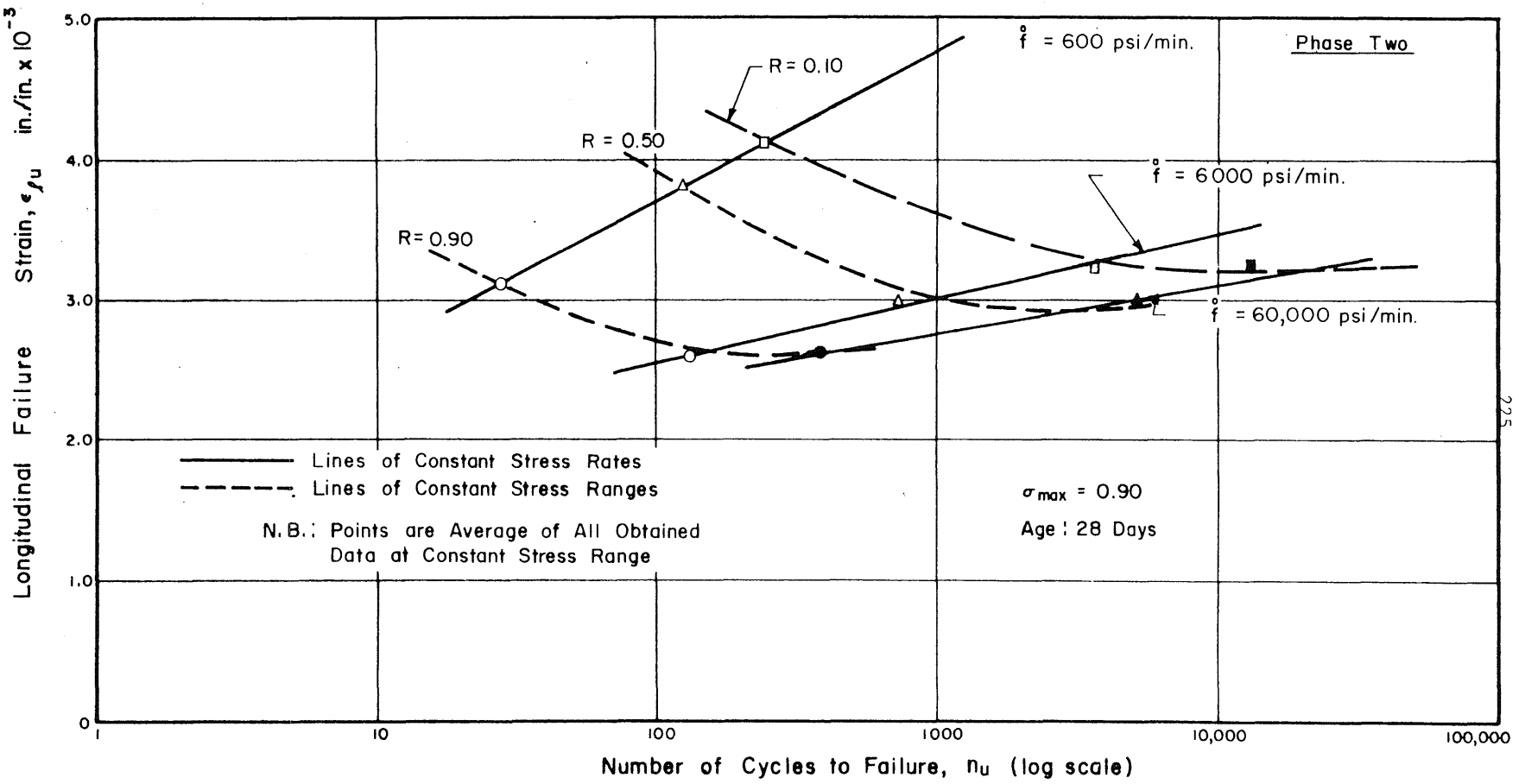

FIG. 5.17 LONGITUDINAL STRAIN AT FAILURE AS FUNCTION OF NUMBER OF CYCLES TO FAILURE FOR DIFFERENT STRESS RATES AND DIFFERENT STRESS RANGES : $\sigma_{max} = 0.90$

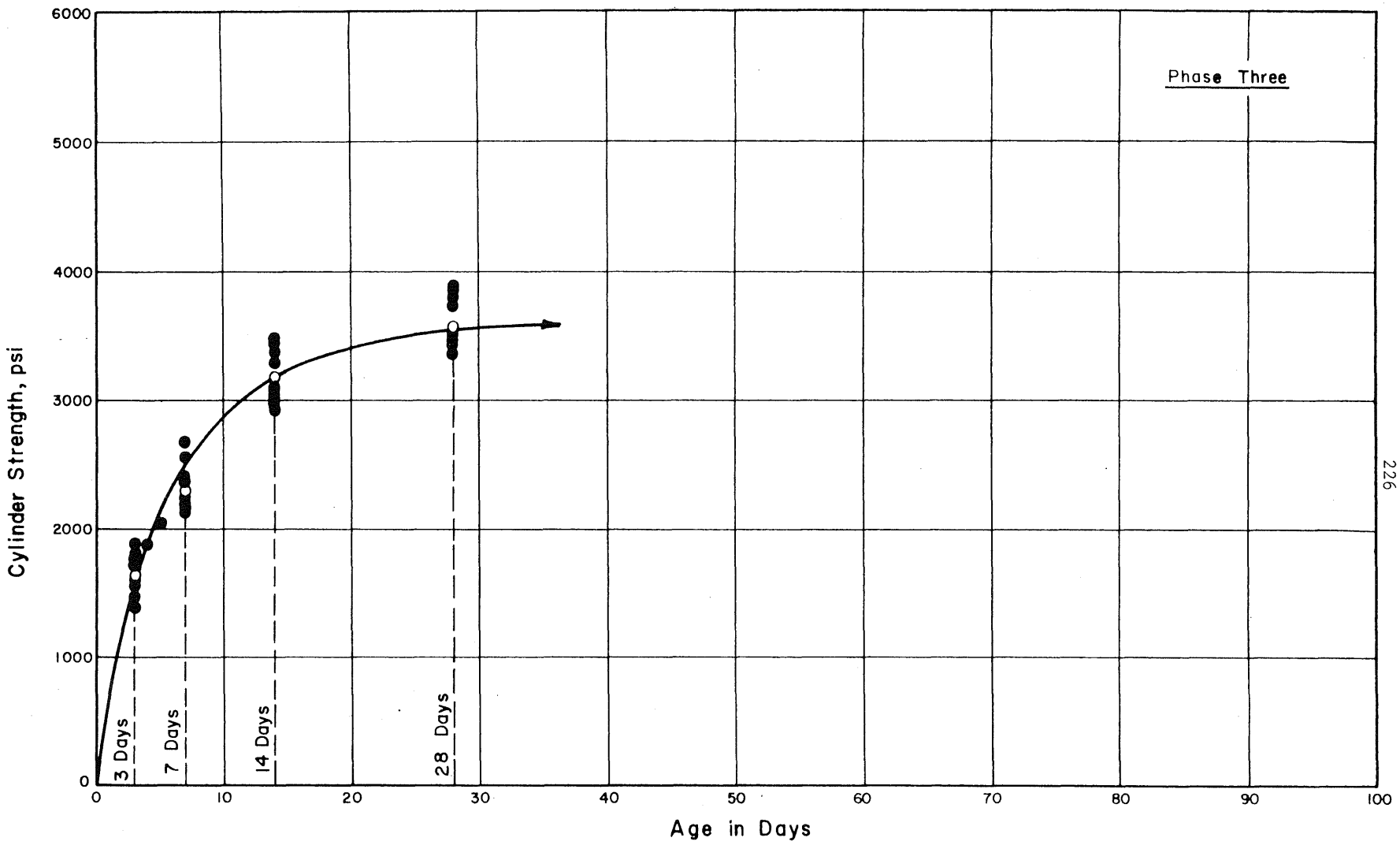

FIG. 6.1 DEVELOPMENT OF CONCRETE CYLINDER STRENGTH WITH AGE : BATCHES B1 TO B12

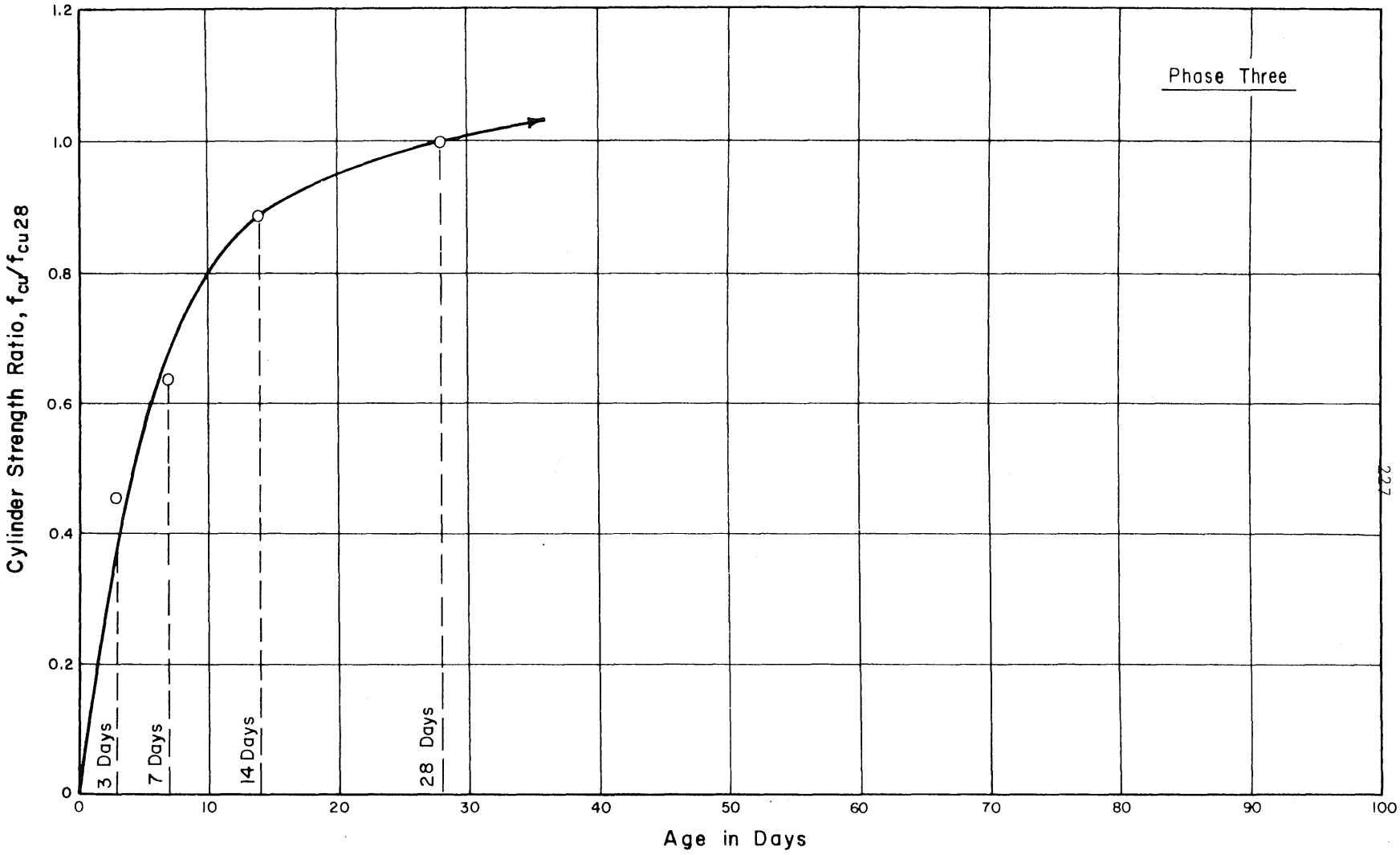

FIG.6.2 DEVELOPMENT OF CONCRETE CYLINDER STRENGTH RATIO WITH AGE : BATCHES B1 TO B12

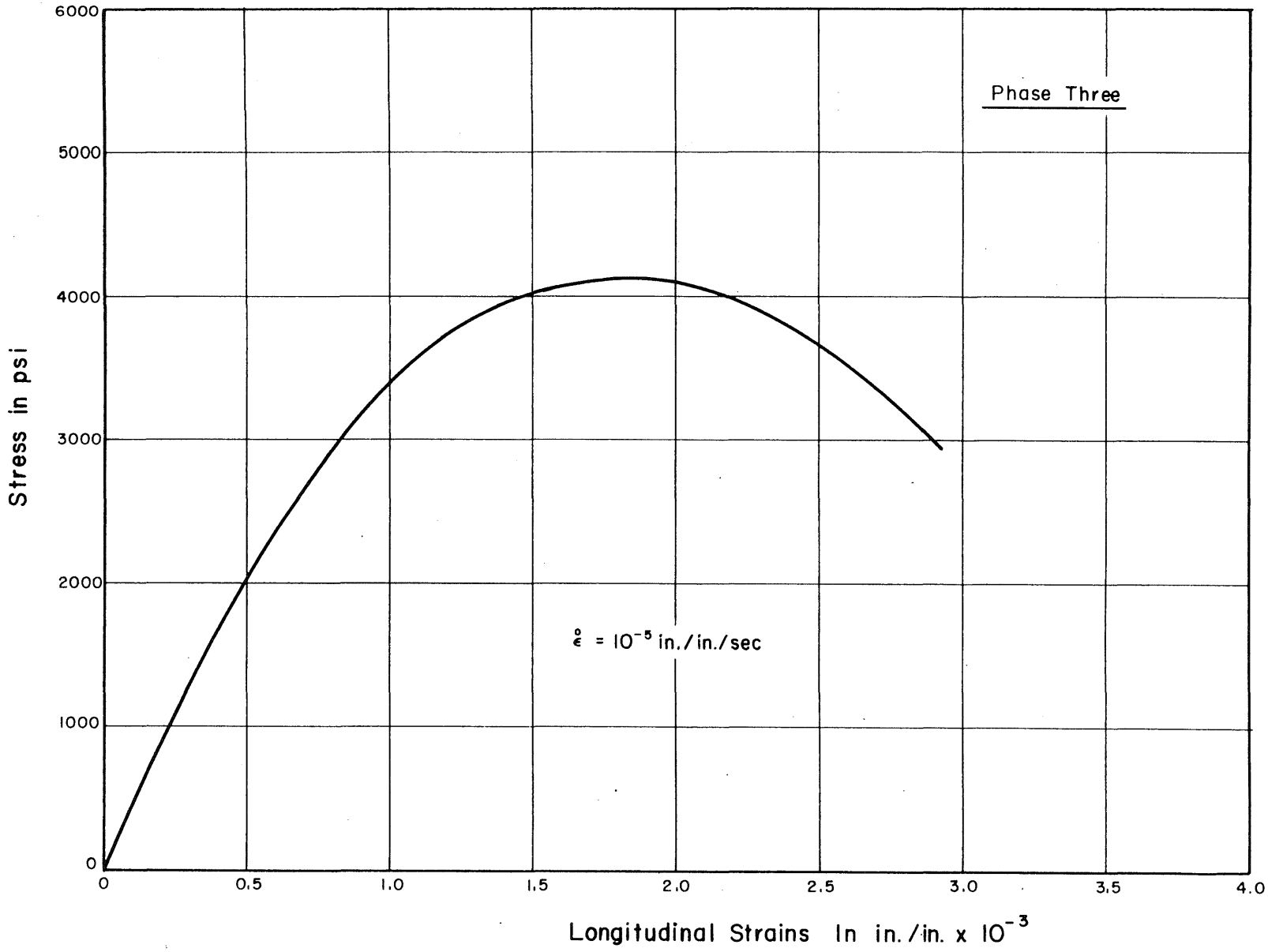

FIG. 6.3 STATIC STRESS – LONGITUDINAL STRAIN CHARACTERISTICS OF CONCRETE PRISMS

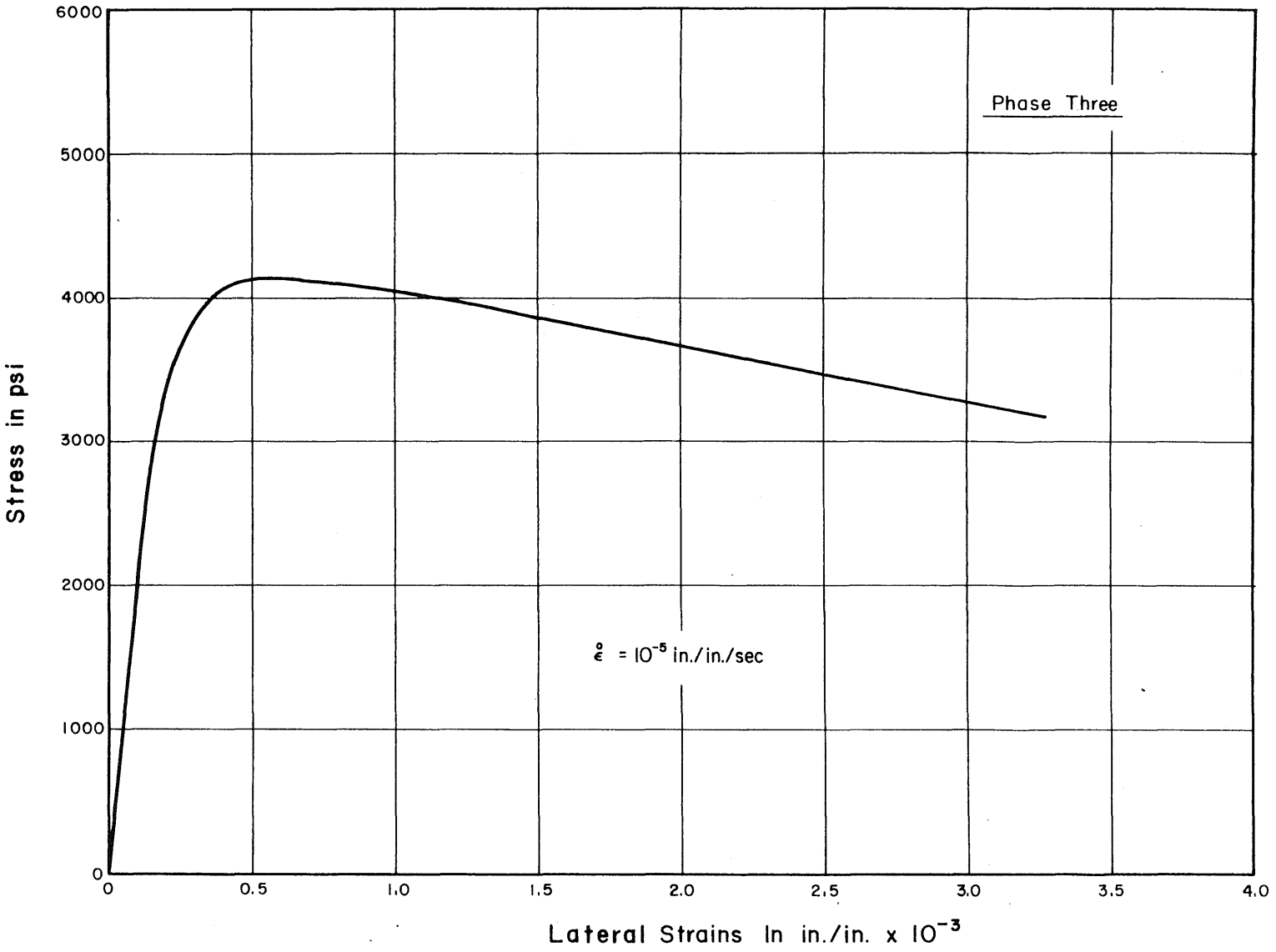

FIG. 6.4 STATIC STRESS – LATERAL STRAIN CHARACTERISTICS OF CONCRETE PRISMS

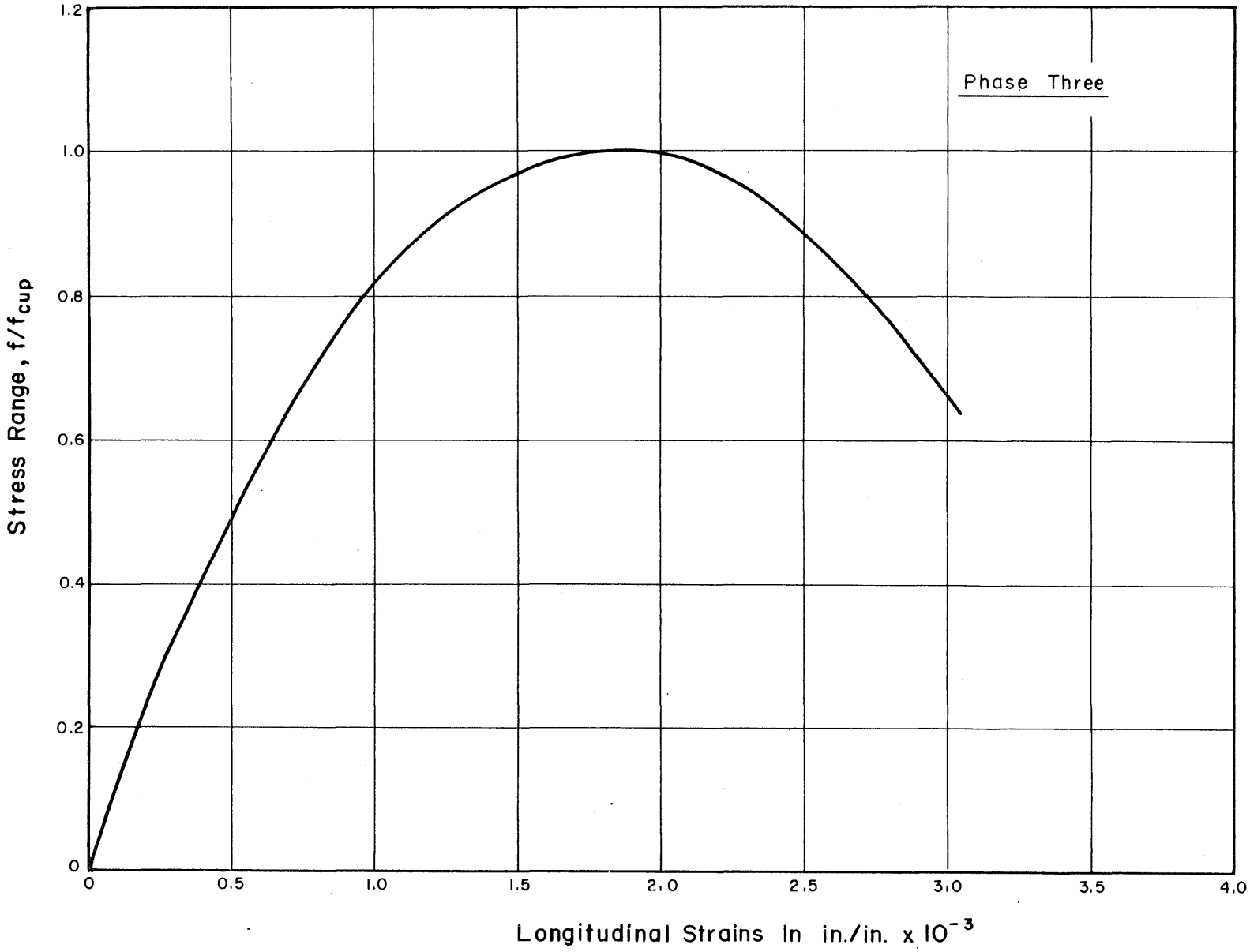

FIG. 6.5 STATIC STRESS RATIO – LONGITUDINAL STRAIN CHARACTERISTICS OF CONCRETE PRISMS

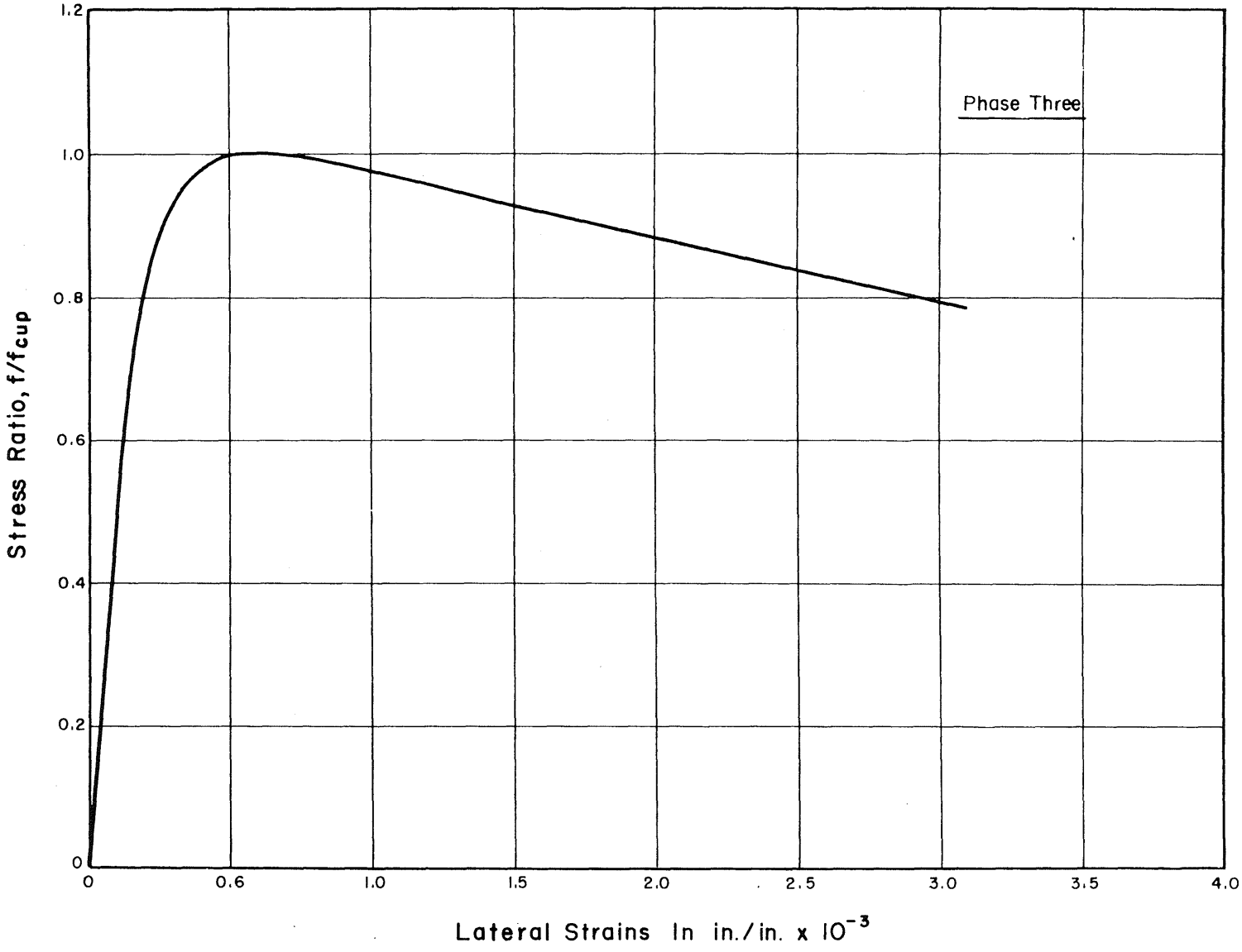

FIG.6.6 STATIC STRESS RATIO – LATERAL STRAIN CHARACTERISTICS OF CONCRETE PRISMS

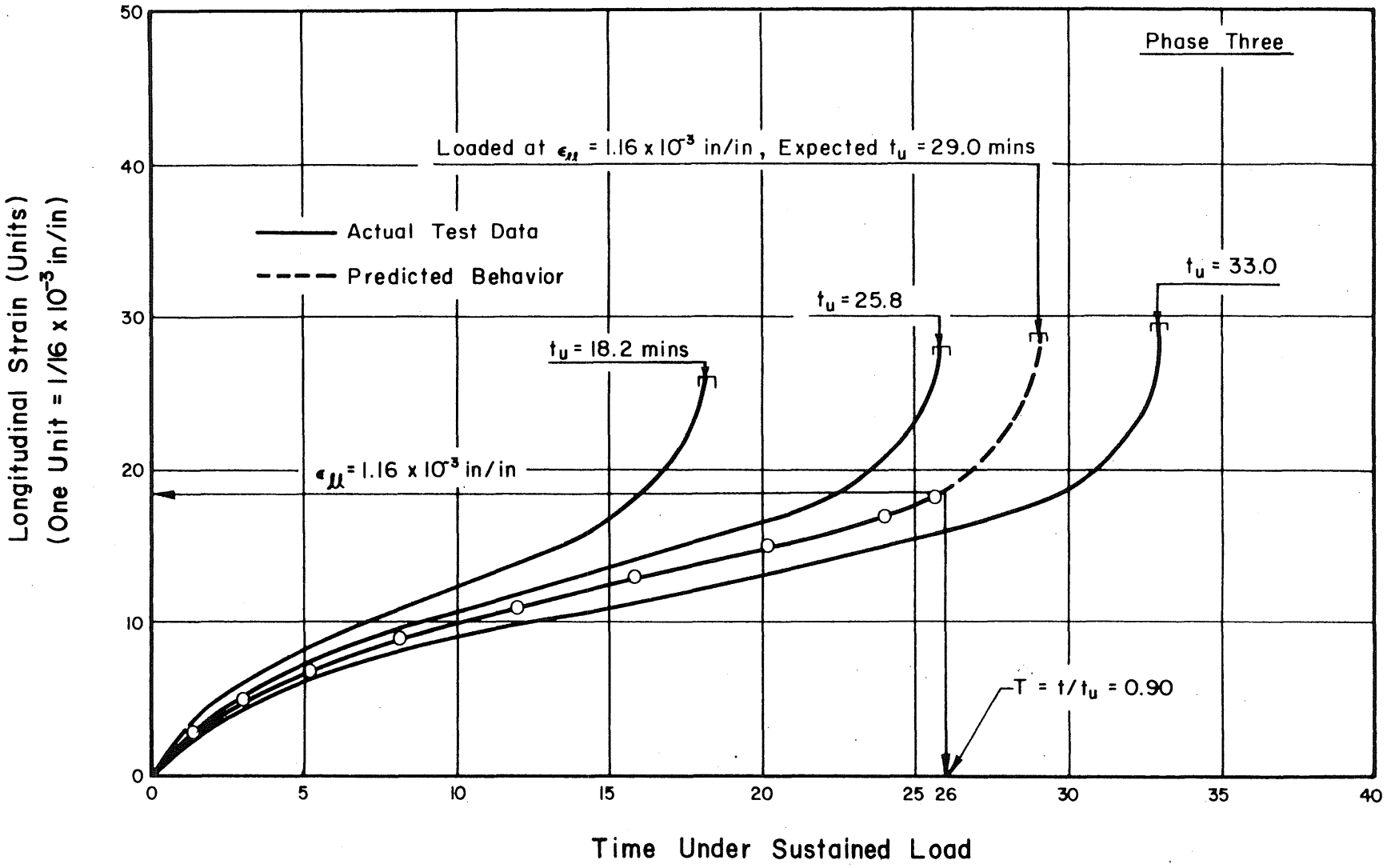

FIG. 6.7 DETERMINATION OF LIFE RATIO OF CONCRETE PRISM FROM THE RELATIONSHIP BETWEEN LONGITUDINAL STRAIN AND DURATION OF LOADING ; σ_{sus} = 0.90

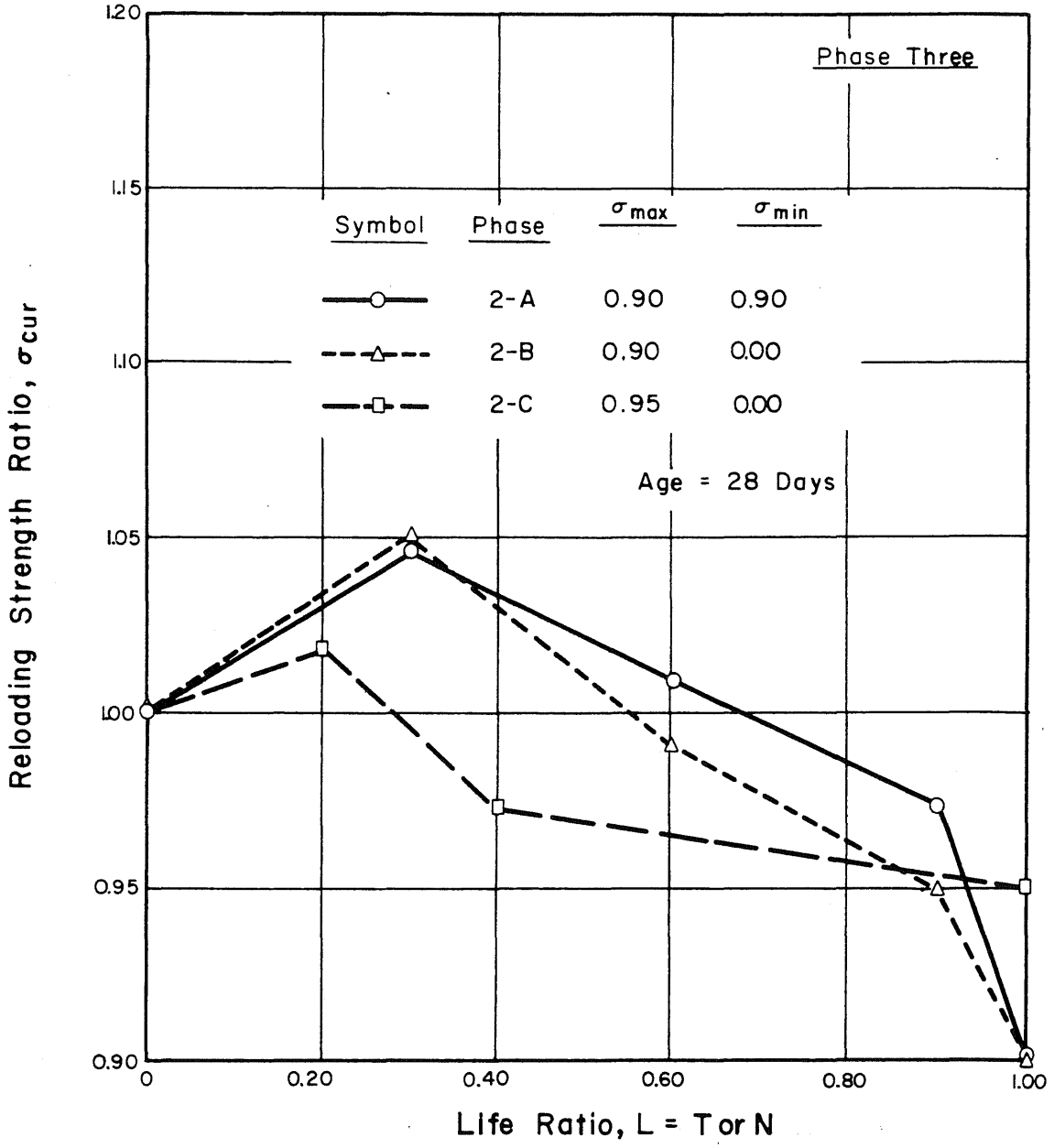

FIG. 6.8 RELOADING STRENGTH RATIO AS FUNCTION OF LIFE RATIO FOR HIGH REPEATED AND SUSTAINED STRESSES

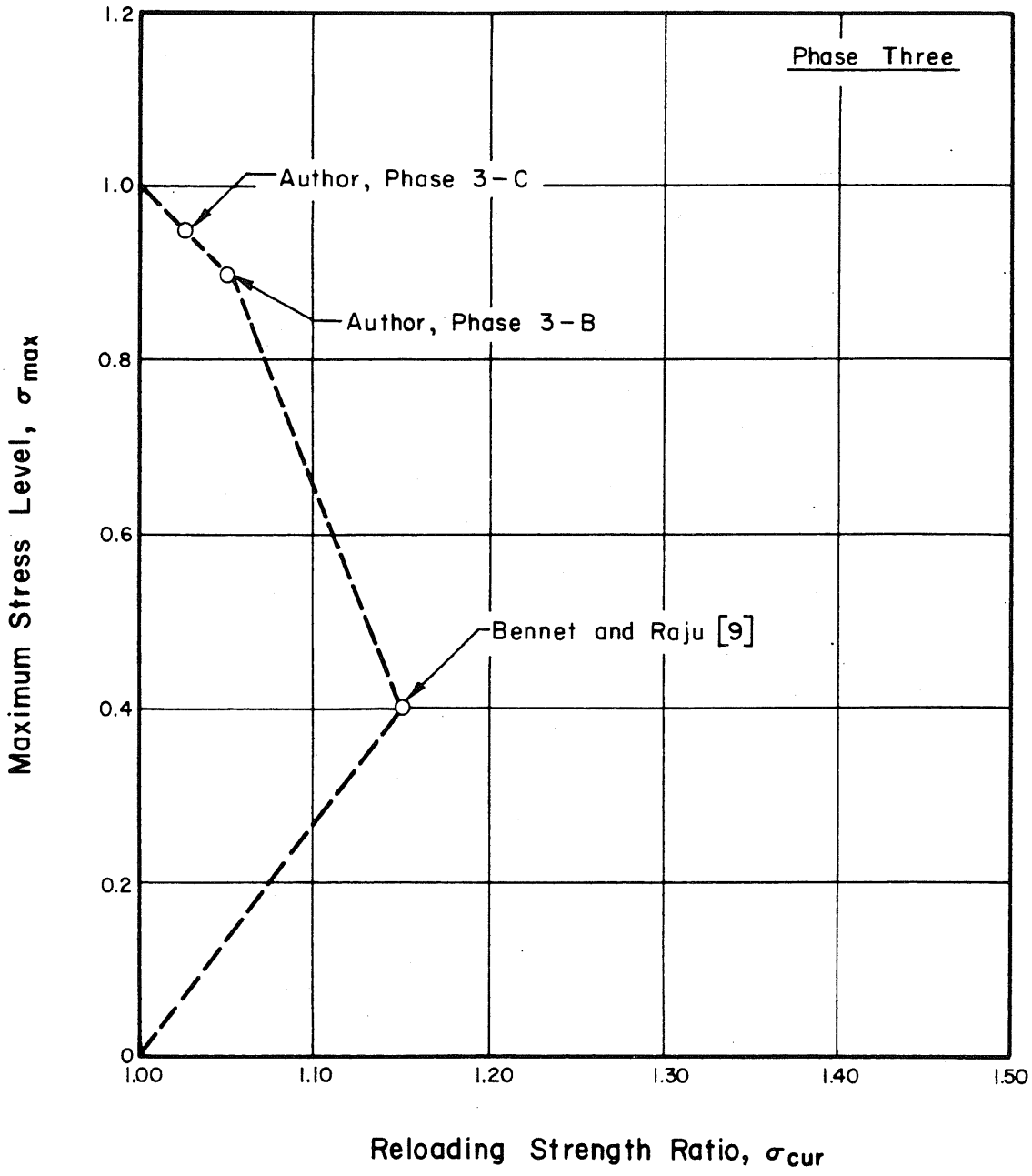

FIG. 6.9 DIAGRAMATIC SKETCH DESCRIBING THE VARIATION OF RELOADING STRENGTH RATIO WITH THE MAXIMUM STRESS LEVEL

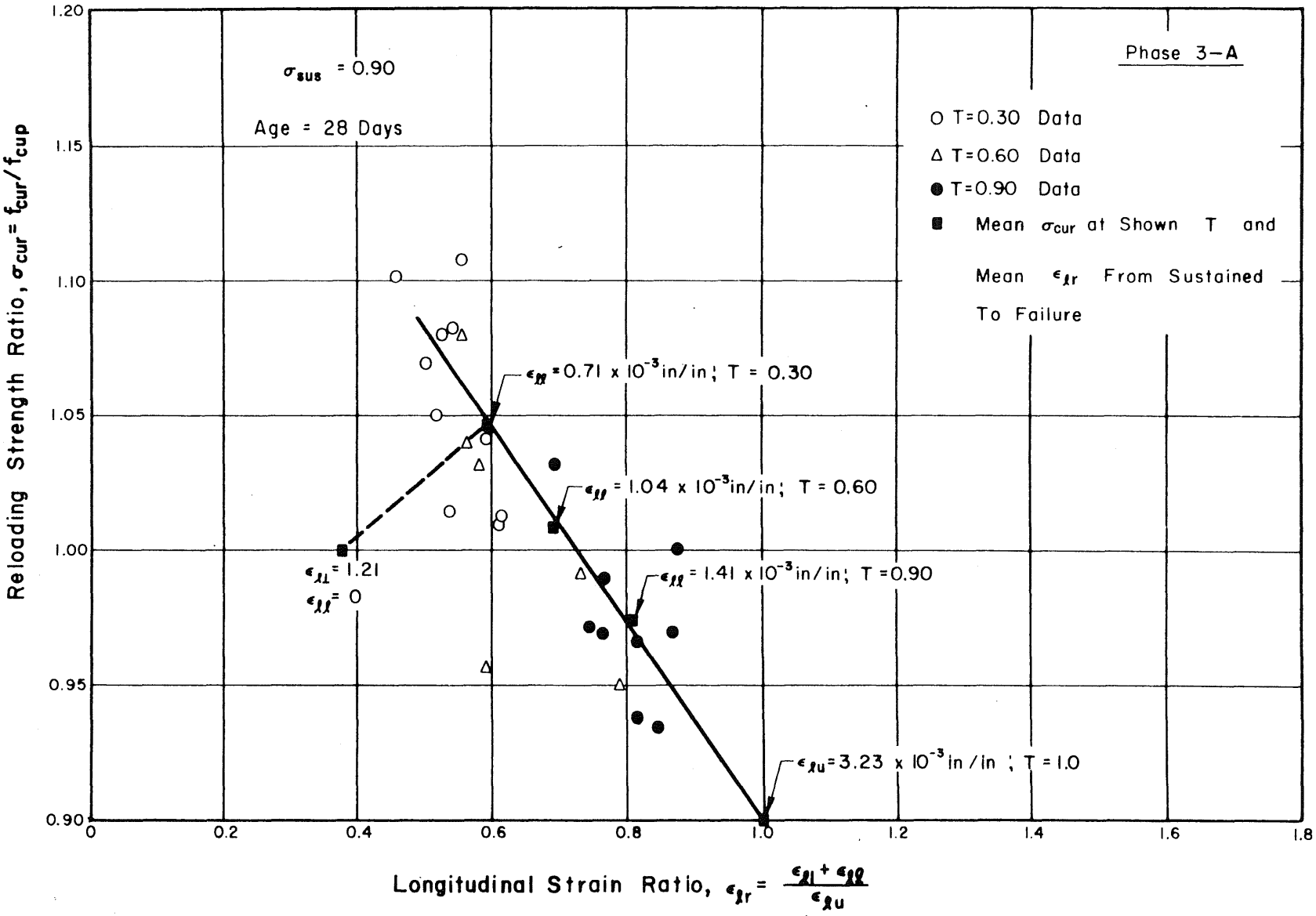

FIG.6.10 RELOADING STRENGTH RATIO AS FUNCTION OF STRAIN RATIO DURING SUSTAINED LOAD TEST ; σ_{sus} = 0.90

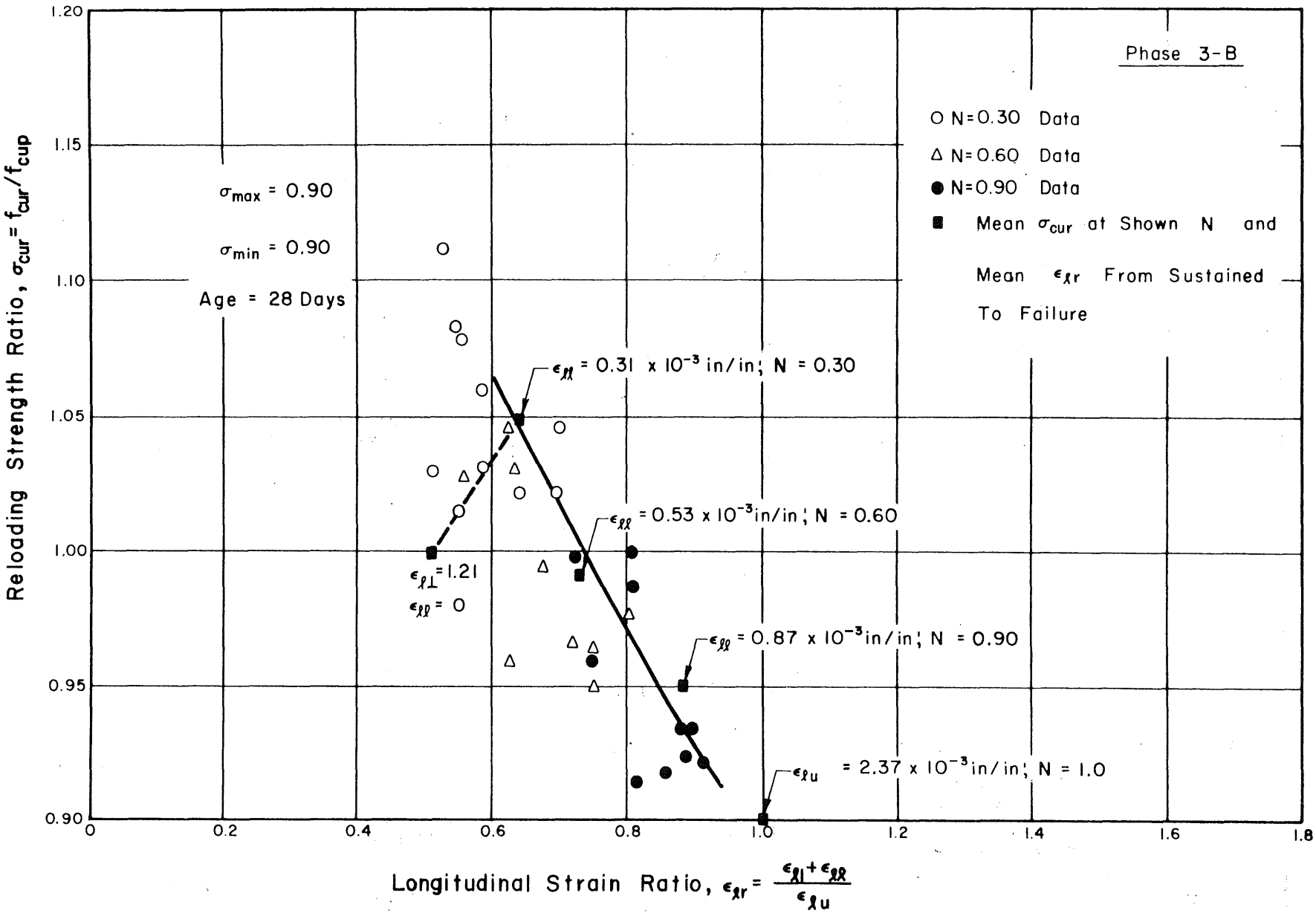

FIG.6.11 RELOADING STRENGTH RATIO AS FUNCTION OF STRAIN RATIO DURING REPEATED LOAD TEST ; σ_{max}= 0.90, R = 0.90

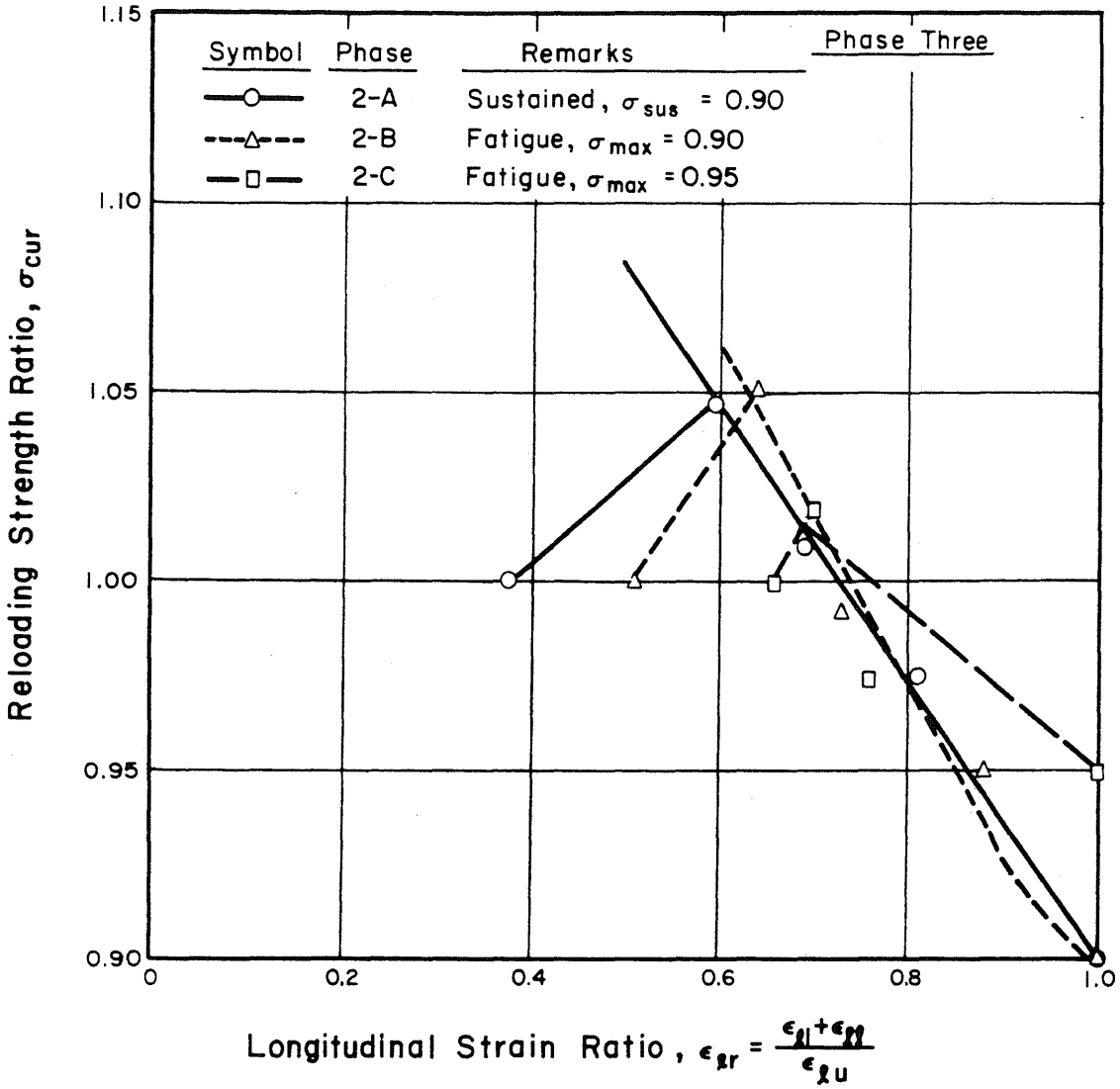

N.B. Given Values are the Means of the Reloading Strength as Obtained from Data at Each Life Ratio Against the Strain Ratio from Specimens Loaded To Failure

FIG.6.12 EFFECT OF TYPE AND MAGNITUDE OF APPLIED LOADS ON RELATIONSHIP BETWEEN RELOADING STRENGTH RATIO AND STRAIN RATIO

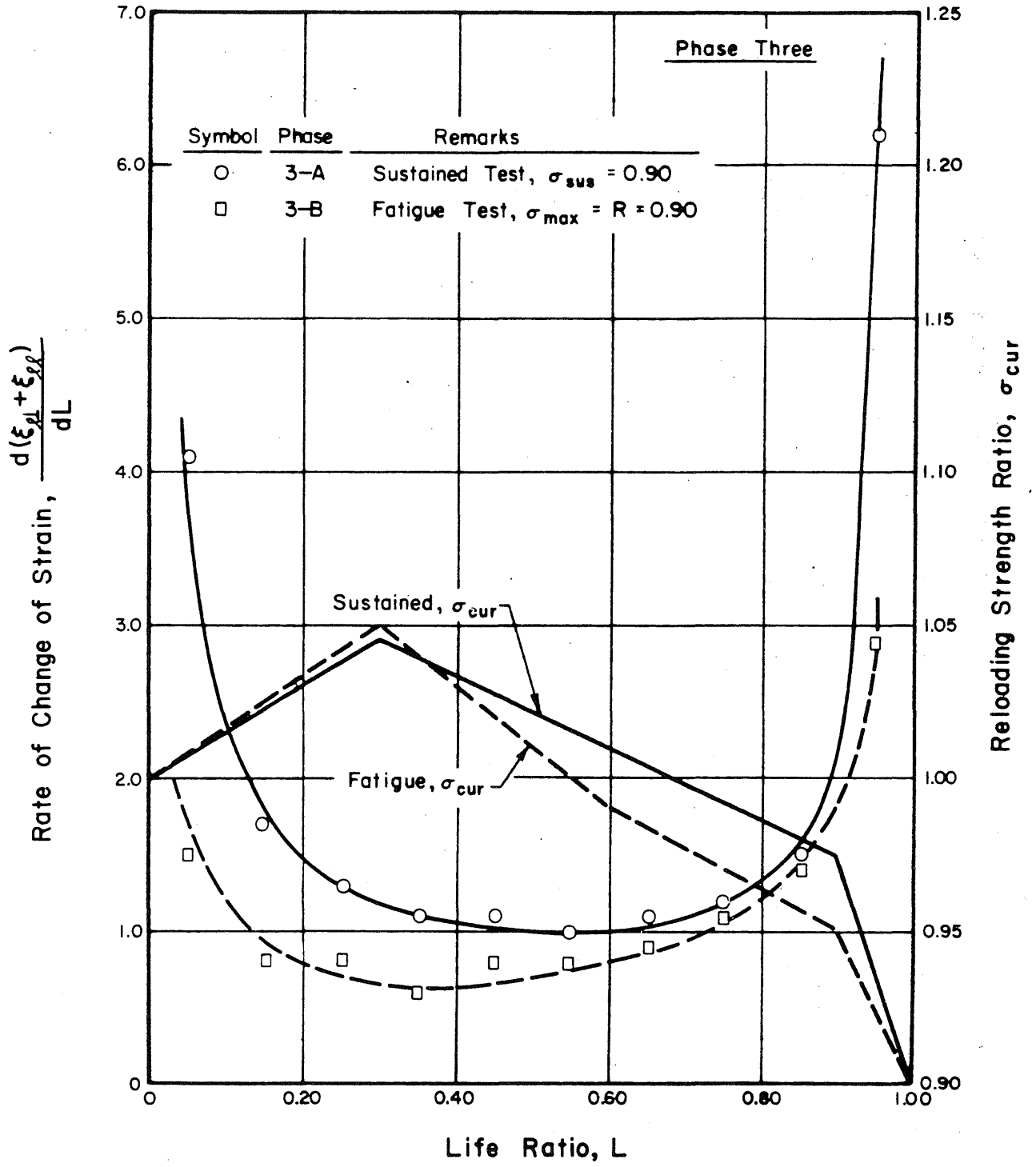

FIG. 6.13 RATE OF CHANGE OF LONGITUDINAL STRAIN AND RELOADING STRENGTH RATIO AS FUNCTIONS OF LIFE RATIO FOR SUSTAINED AND REPEATED LOAD TESTS

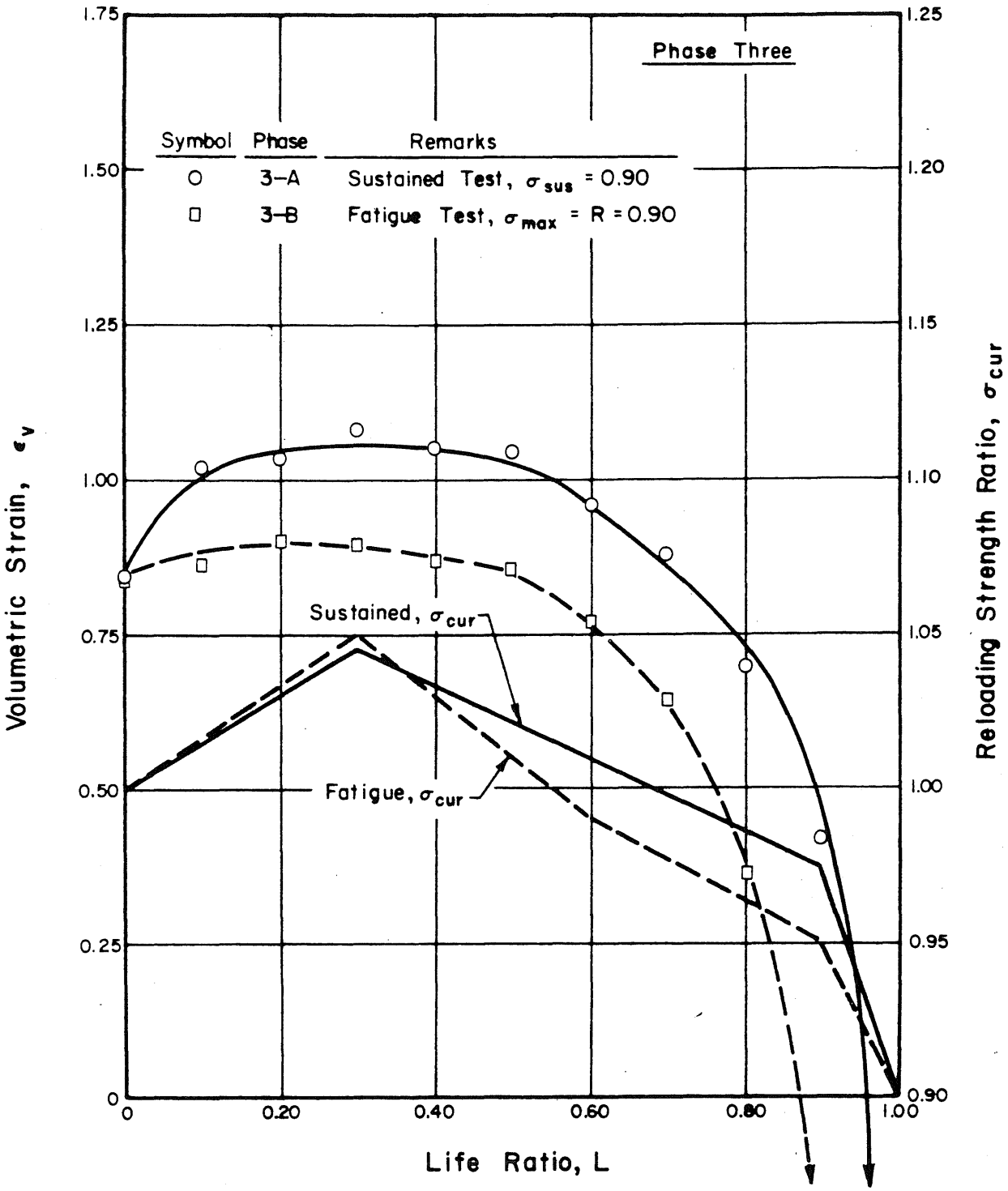

FIG. 6.14 VOLUMETRIC STRAIN AND RELOADING STRENGTH RATIO AS FUNCTIONS OF LIFE RATIO FOR SUSTAINED AND REPEATED LOAD TESTS

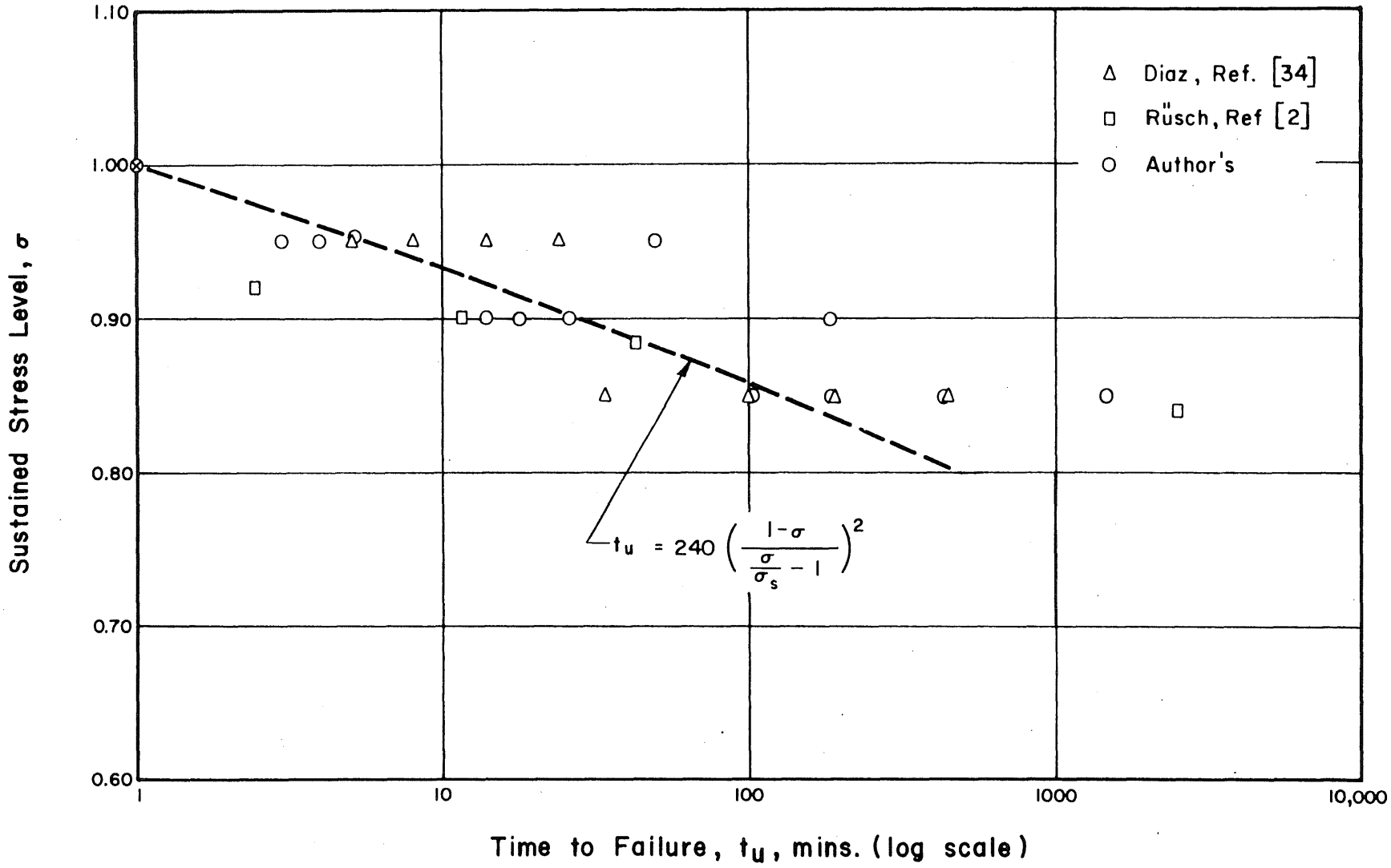

FIG. 7.1 RELATIONSHIP BETWEEN SUSTAINED STRESS LEVEL AND TIME TO FAILURE

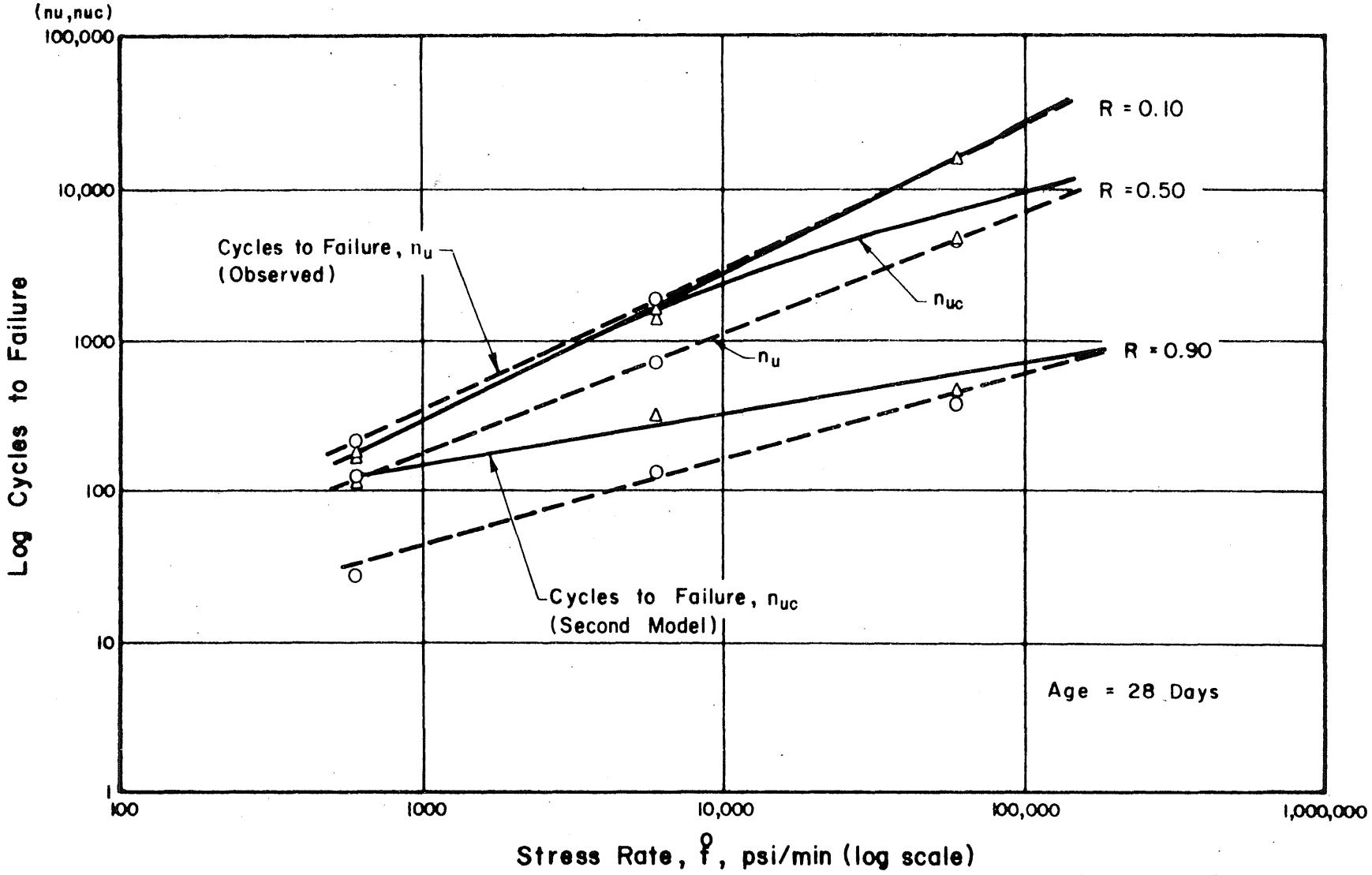

FIG. 7.2 COMPARISON BETWEEN CALCULATED AND OBSERVED FAILURE CYCLES — (SECOND MODEL) $\sigma_{max} = 0.90$; R=0.10,0.50,0.90

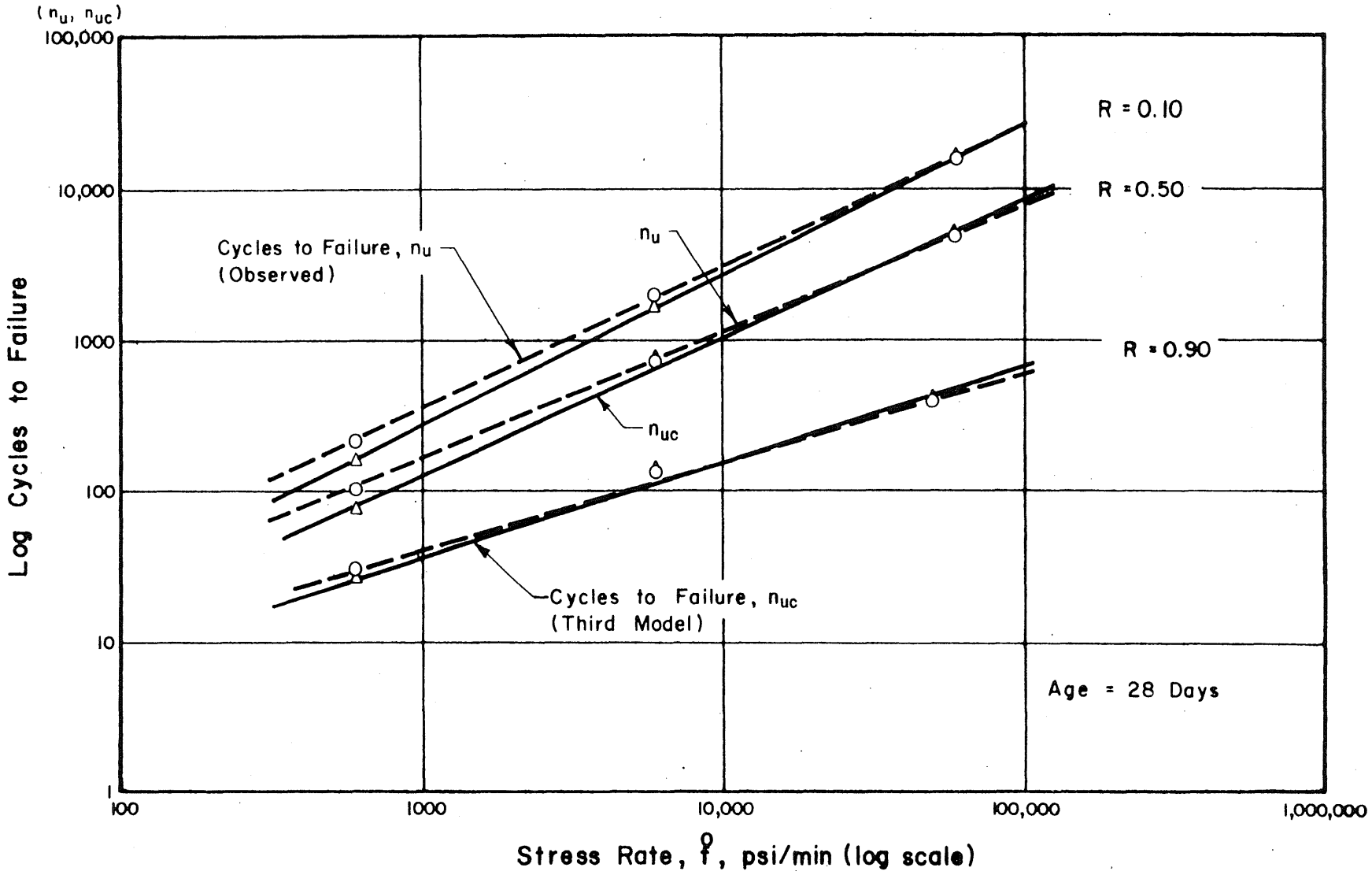

FIG. 7.3 COMPARISON BETWEEN CALCULATED AND OBSERVED FAILURE CYCLES — (THIRD MODEL) $\sigma_{max} = 0.90$; R=0.10,0.50,0.90

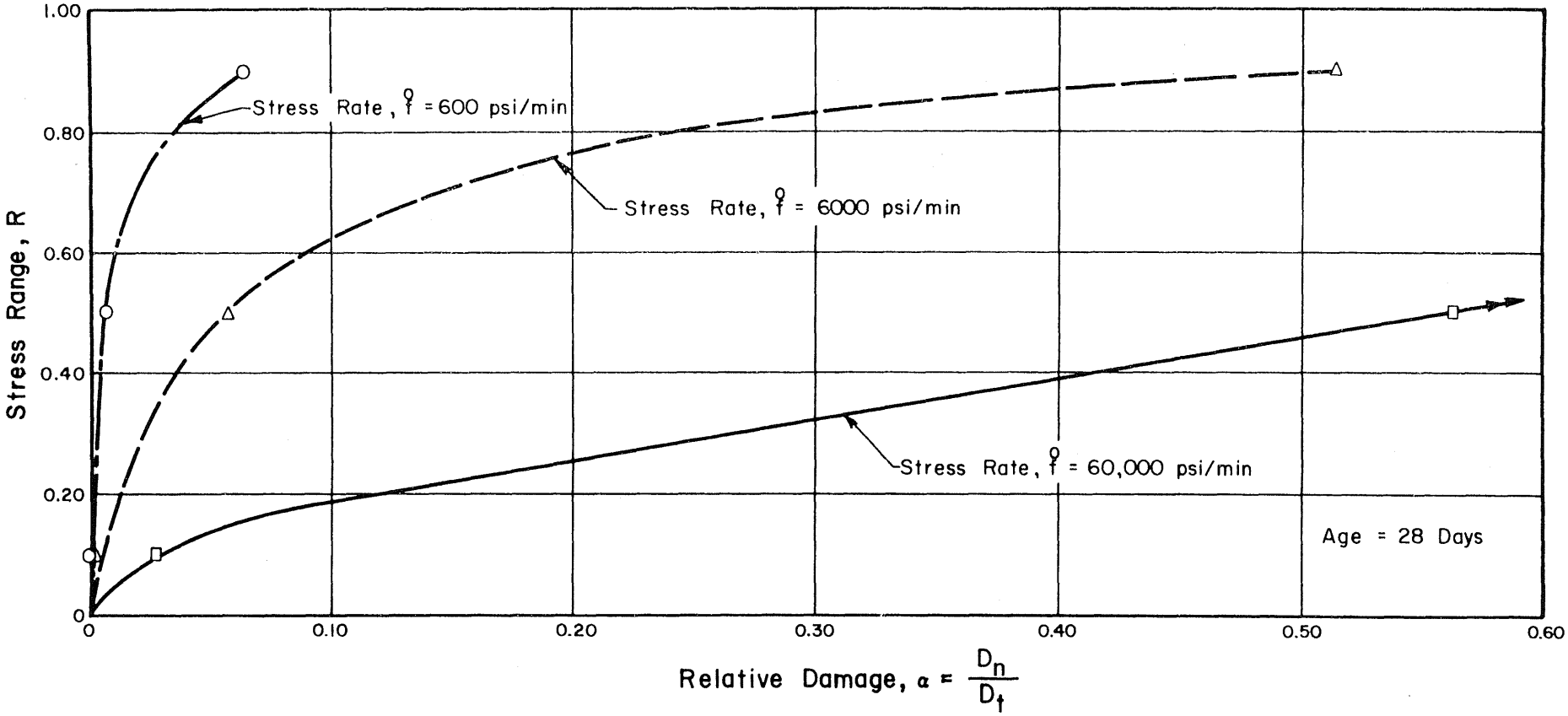

FIG. 7.4 RELATIONSHIP BETWEEN RELATIVE DAMAGE AND STRESS RANGE FOR DIFFERENT STRESS RATES ; σ_{max} = 0.90

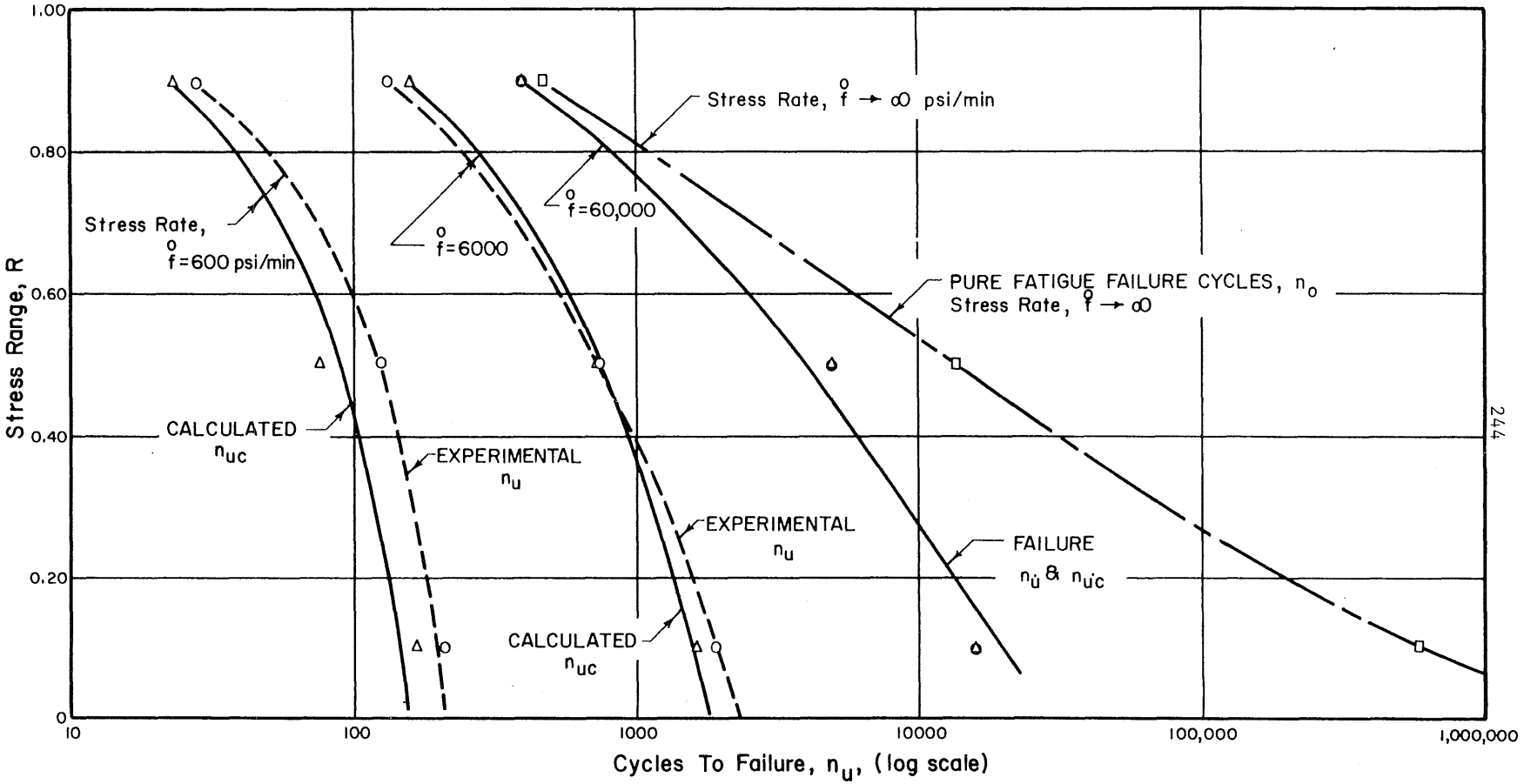

FIG. 7.5 VARIATION OF CYCLES TO FAILURE WITH STRESS RANGE AT DIFFERENT STRESS RATES: CALCULATED AND OBSERVED VALUES AS COMPARED TO "PURE FATIGUE" FAILURE CYCLES

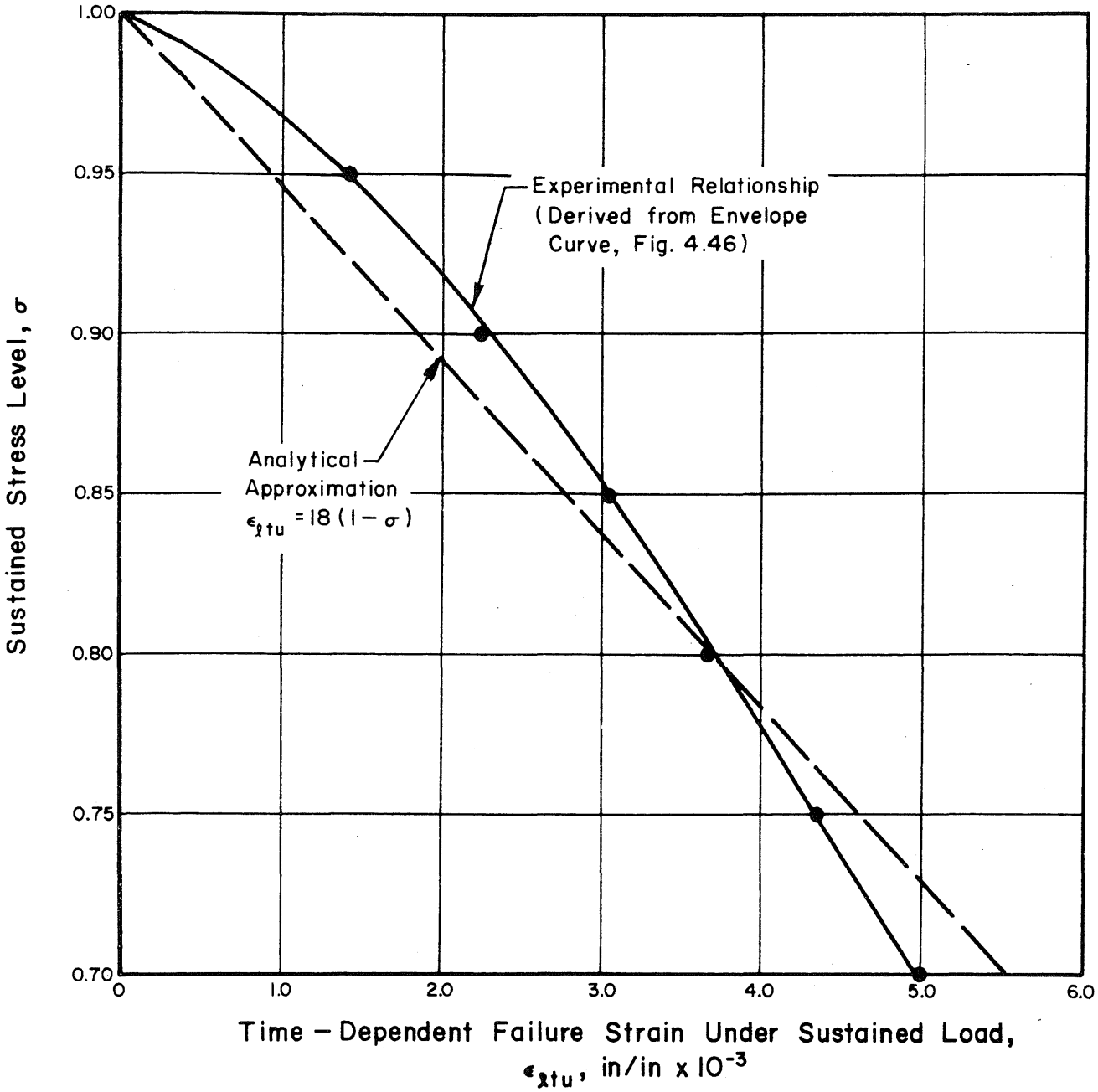

FIG. 7.6 ANALYTICAL APPROXIMATION OF EXPERIMENTAL SUSTAINED STRESS – FAILURE STRAIN RELATIONSHIP

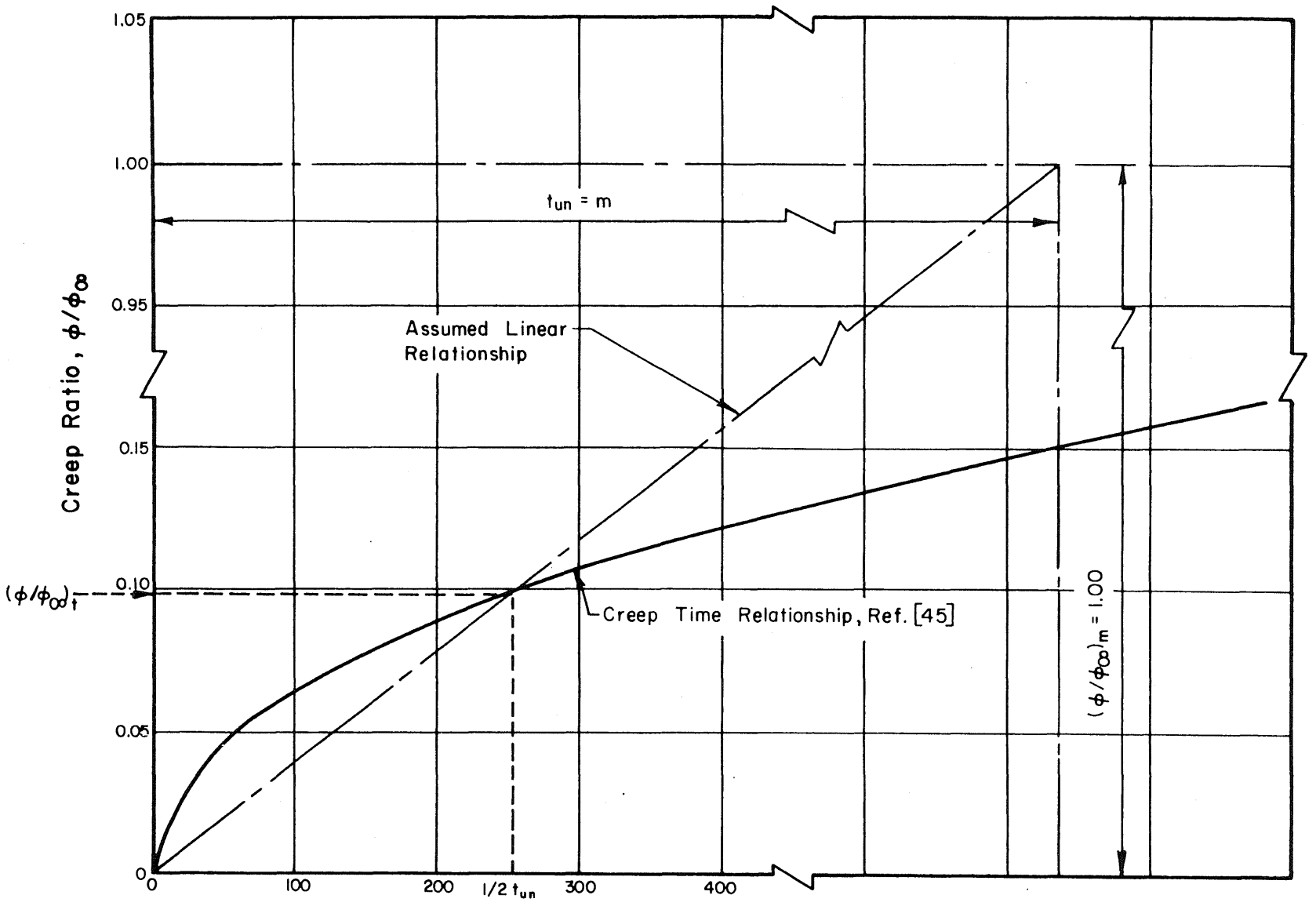

FIG. 7.7 EXPERIMENTAL CREEP – TIME RELATIONSHIP {EXTRAPOLATED FROM [45]}

APPENDIX A

STATISTICAL ANALYSIS

The statistical analysis performed on the experimental data and reported in Tables (5.7, 5.8, 5.9, 6.3, 6.5, 6.7) had the following objectives:

a. To establish the probability level associated with the range of a data set of individual parameters. Examples are the different values of the reloading strength obtained at the same life ratio (Phase Three and the unequal cycles to failure for a constant stress rate (Phase Two).

b. To study the variation of the mean values as a function of selected parameters. Examples are the mean values of the reloading strength at the various life ratios (Phase Three) and the mean value of the cycles to failure at various stress rates (Phase Two). If the mean values are affected by the specific values of the parameters, then the data sets clearly describe different physical phenomena.

A.1 Probability of the Range of a Data Set

It is assumed that the data points follow a normal distribution.

A.1.1 The mean value is defined as:

$$\bar{x} = \frac{1}{n} \sum_{k=1}^{n} x_k$$

where n = number of observations for one parameter

x_k = obtained data points

A.1.2 Sample variance and standard deviations are:

$$s = \left[\frac{1}{n} \sum_{k=1}^{n} (x_k - \bar{x})^2 \right]^{1/2}$$

and

$$s^2 = \frac{1}{n} \sum_{k=1}^{n} (x_k - \bar{x})^2$$

Thus, the probability level of the range of data set is determined as follows:

let $$Z_1 = \frac{\bar{x} - x_{min}}{s}$$

and $$Z_2 = \frac{x_{max} - \bar{x}}{s}$$

where x_{max} and x_{min} are maximum and minimum values of the observations.

The corresponding probability level was determined by entering the Z-values into a normal distribution function table [Ref. 8, pp. 461].

A.2 Comparison of Mean Values

If $\bar{x}_i$ and $\bar{x}_j$ are the mean values of two data sets determined at different values of a parameter it is required to determine the probability that

$$\bar{x}_i > \bar{x}_j$$

Define:

$E(\bar{x}_i)$ the expected sample mean of $\bar{x}_i$

$E(\bar{x}_j)$ the expected sample mean of $\bar{x}_j$

$$S(\bar{x}_i) \qquad \frac{\text{sample standard deviation}}{n_i}$$

$$S(\bar{x}_j) \qquad \frac{\text{sample standard deviation}}{n_j}$$

and

$$Z = \bar{x}_i - \bar{x}_j$$

Assuming that $\bar{x}_i$ and $\bar{x}_j$ are both normally distributed, then Z is also normally distributed with the following characteristics.

$$\text{Expected Mean } E(Z) = E(\bar{x}_i) - E(\bar{x}_j)$$

and

$$\text{Standard deviation } S(Z) = S^2(\bar{x}_i) + S^2(\bar{x}_j)$$

Hence, the probability that $\bar{x}_i > \bar{x}_j$ can be stated as follows:

$$P(\bar{x}_i > \bar{x}_j) = P[Z > 0)$$

and is determined by entering the value of $\frac{E(Z)}{S(Z)}$ in a normal distribution table.

APPENDIX B

TYPICAL TEST DATA

The appendix contains samples of typical data as obtained by tests. The following illustrations are included:

a. Load-strain diagrams in both longitudinal and lateral directions as obtained in a typical static test, Fig. (B.1).

b. Phase One: Test data of batch A20 are given. Data are for σ_{max} = 0.95 and different stress ranges. Examples of load-strain diagrams are given for longitudinal and lateral directions, Figs. (B1 to B5).

c. Phase Two: Typical testing speed test data for σ_{max} = 0.90 and R = 0.50; also included is the variation of load and strain with time as given by the closed loop hydraulic testing machine and the incorporated 8-channel recorder, Figs. (B6 and B7).

d. Phase Three: Reloading strength tests, examples are given for specimens loaded at a life ratio of 0.30, 0.60 and 0.90. These specimens were subjected to σ_{max} = 0.90 and R = 0.90 before loaded statically to failure, Figs. (B8 to B10).

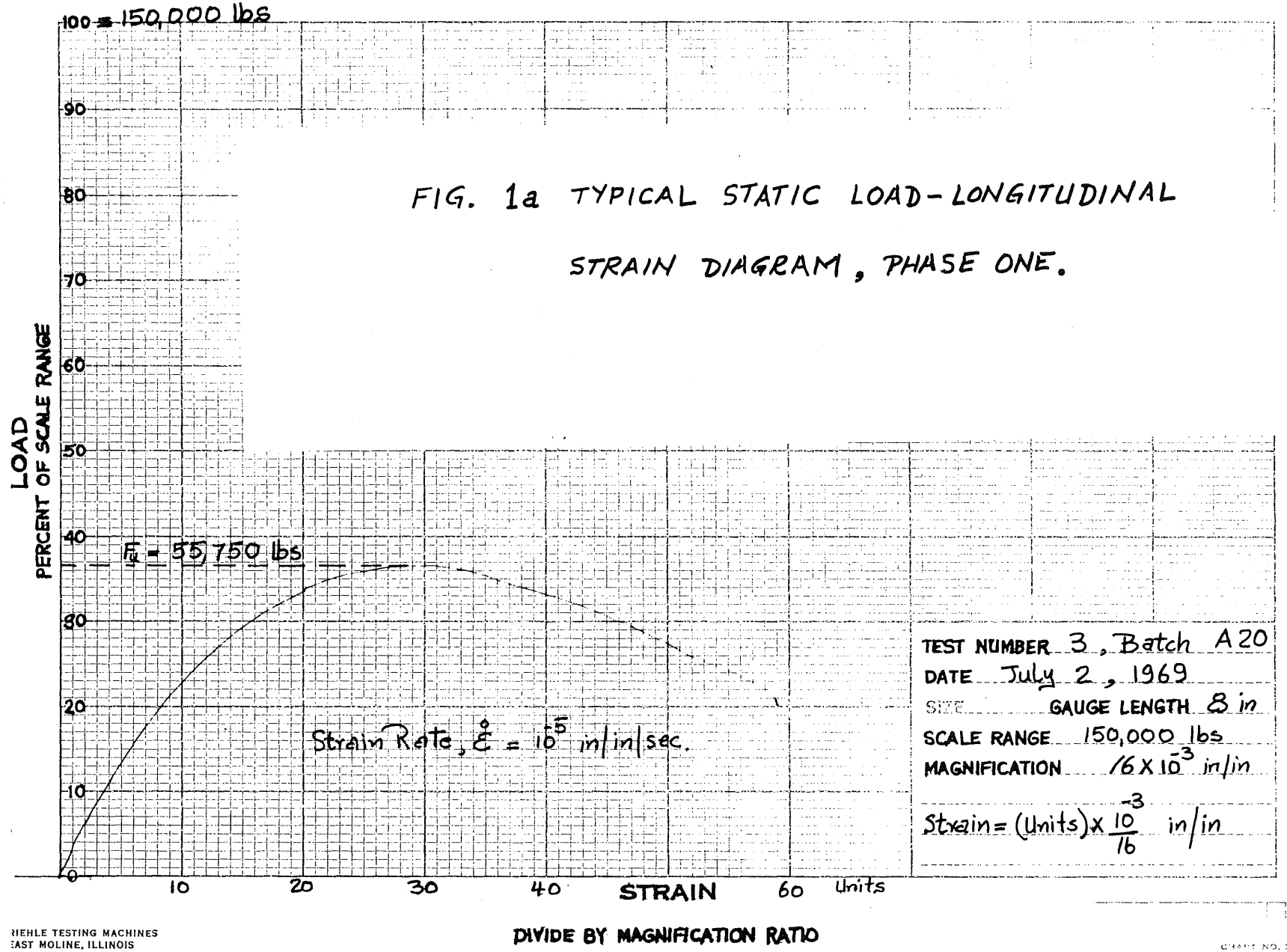

FIG. 1a TYPICAL STATIC LOAD-LONGITUDINAL STRAIN DIAGRAM, PHASE ONE.

DIVIDE BY MAGNIFICATION RATIO

RIEHLE TESTING MACHINES
EAST MOLINE, ILLINOIS

CHART NO. 56-135

FIG. B.1b TYPICAL STATIC LOAD- LATERAL STRAIN DIAGRAM, PHASE ONE

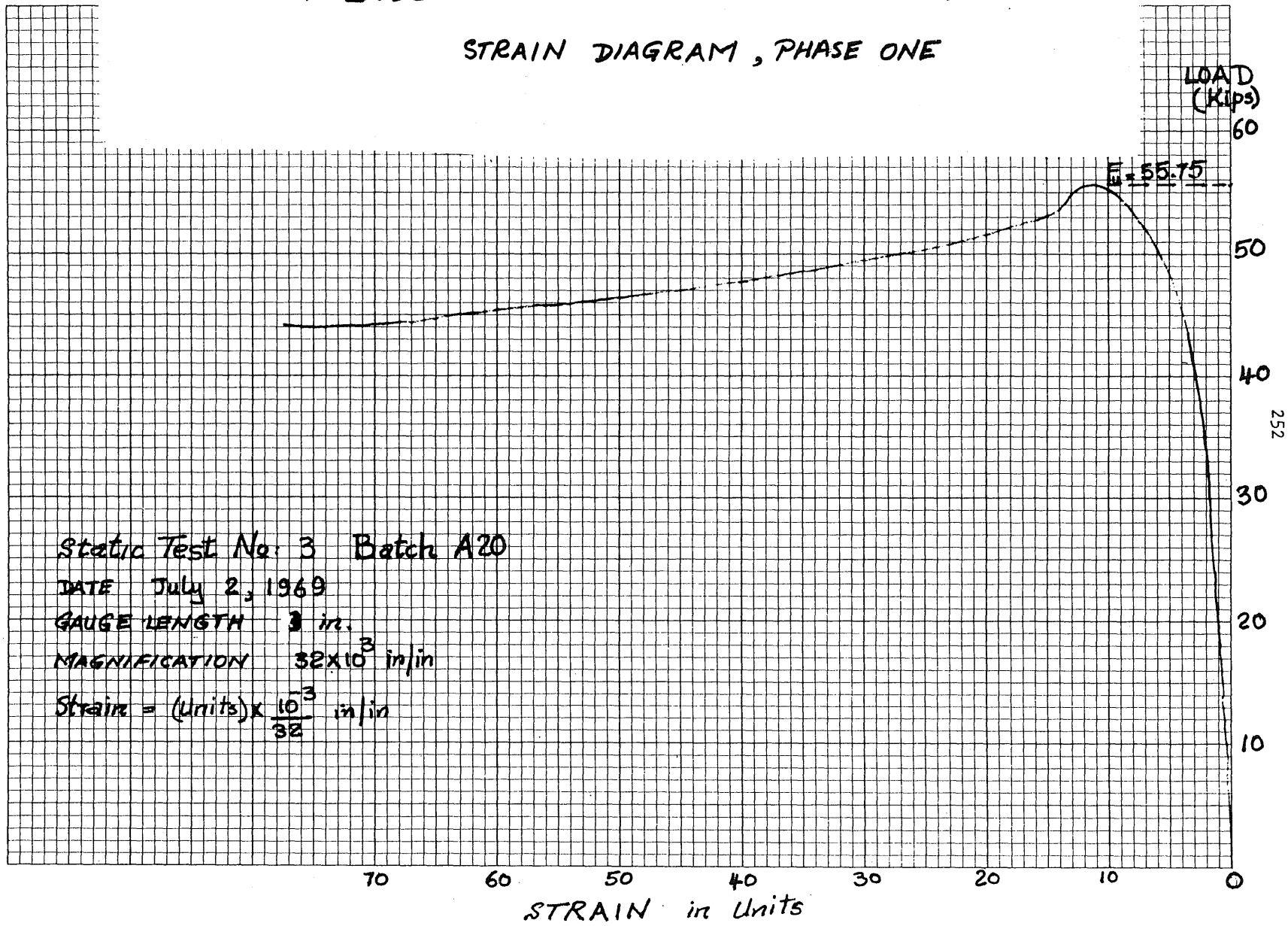

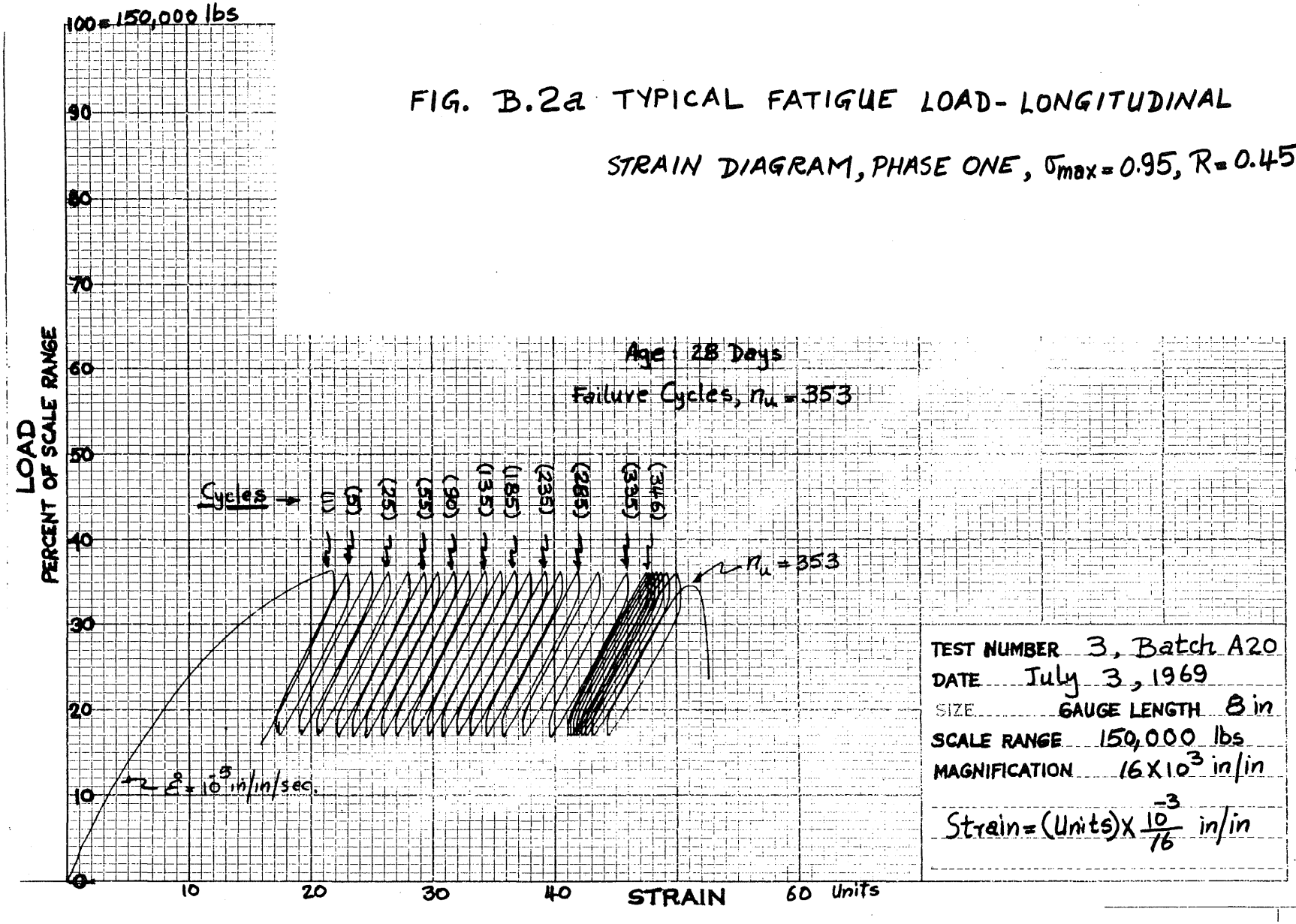

FIG. B.2a TYPICAL FATIGUE LOAD-LONGITUDINAL STRAIN DIAGRAM, PHASE ONE, $\sigma_{max} = 0.95$, $R = 0.45$

RIEHLE TESTING MACHINES
EAST MOLINE, ILLINOIS

DIVIDE BY MAGNIFICATION RATIO

CHART NO. 35-155

FIG. B.2b TYPICAL FATIGUE LOAD-LATERAL STRAIN DIAGRAM, PHASE ONE, $\sigma_{max} = 0.95, R = 0.45$

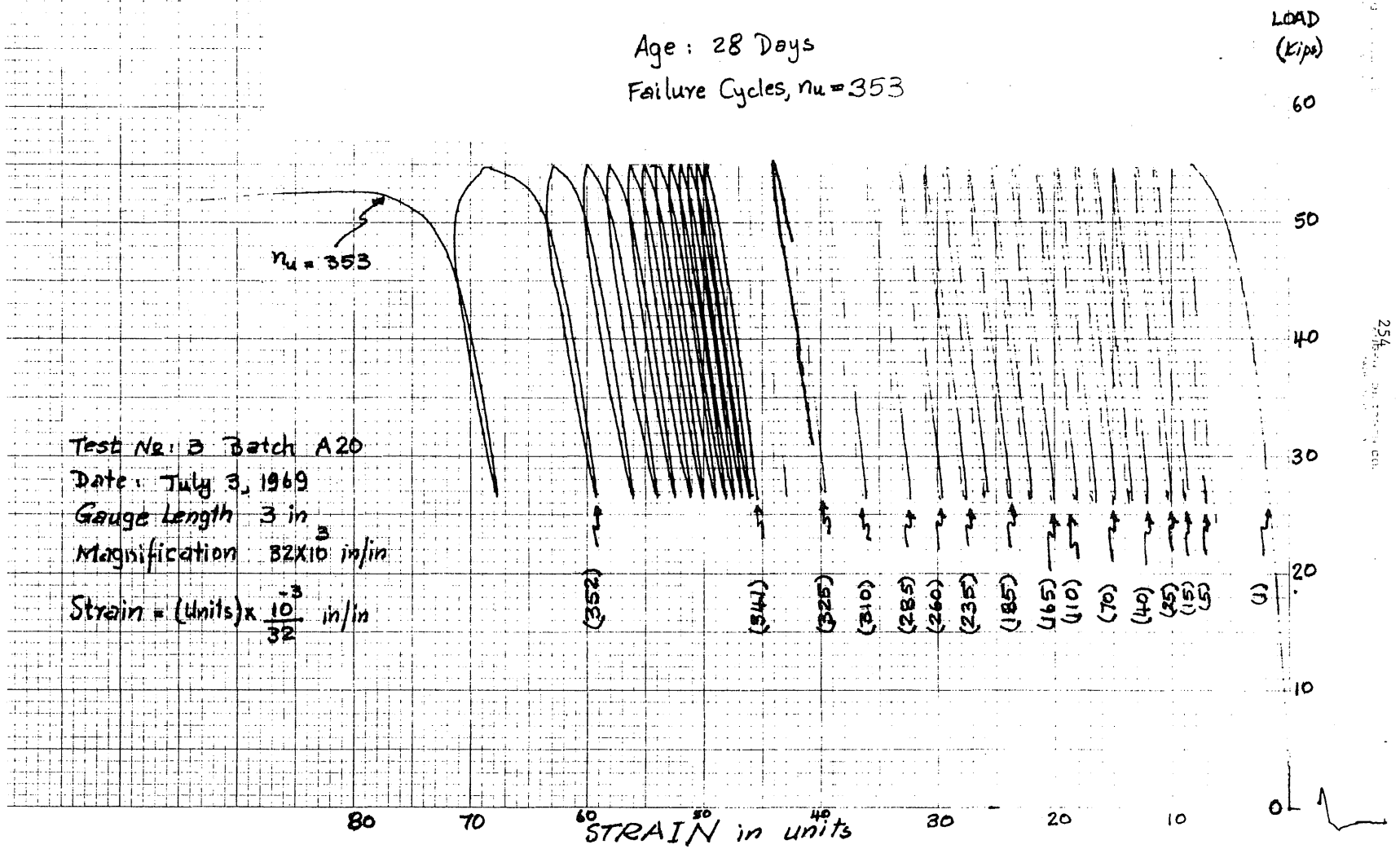

FIG B.3a TYPICAL FATIGUE LOAD-LONGITUDINAL STRAIN DIAGRAM, PHASE ONE, $\sigma_{max} = 0.95$, $R = 0.30$

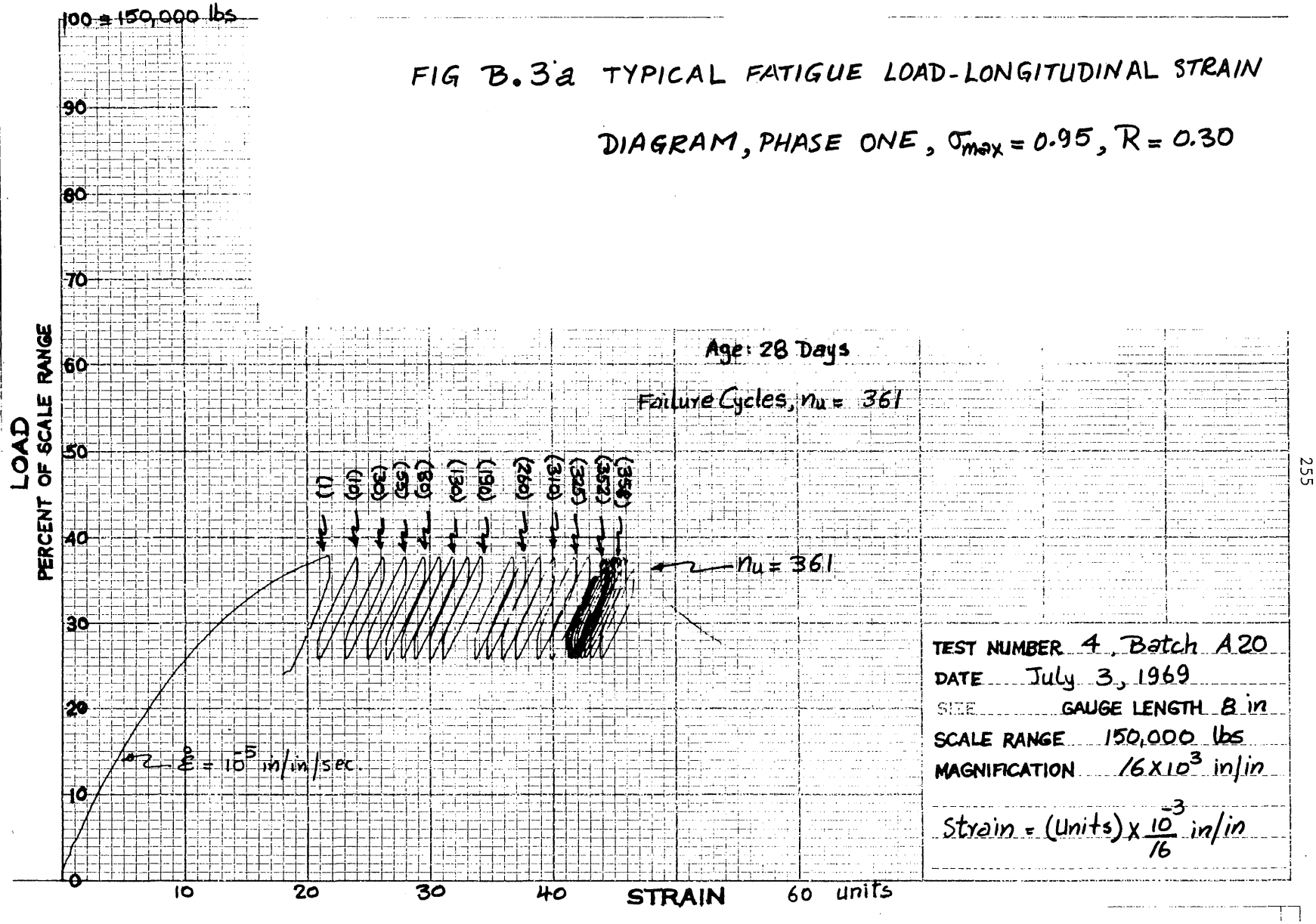

255

RIEHLE TESTING MACHINES
EAST MOLINE, ILLINOIS

DIVIDE BY MAGNIFICATION RATIO

CHART NO. 35-155

FIG. B.3b TYPICAL FATIGUE LOAD - LATERAL STRAIN DIAGRAM, PHASE ONE, $\sigma_{max} = 0.95$, $R = 0.30$

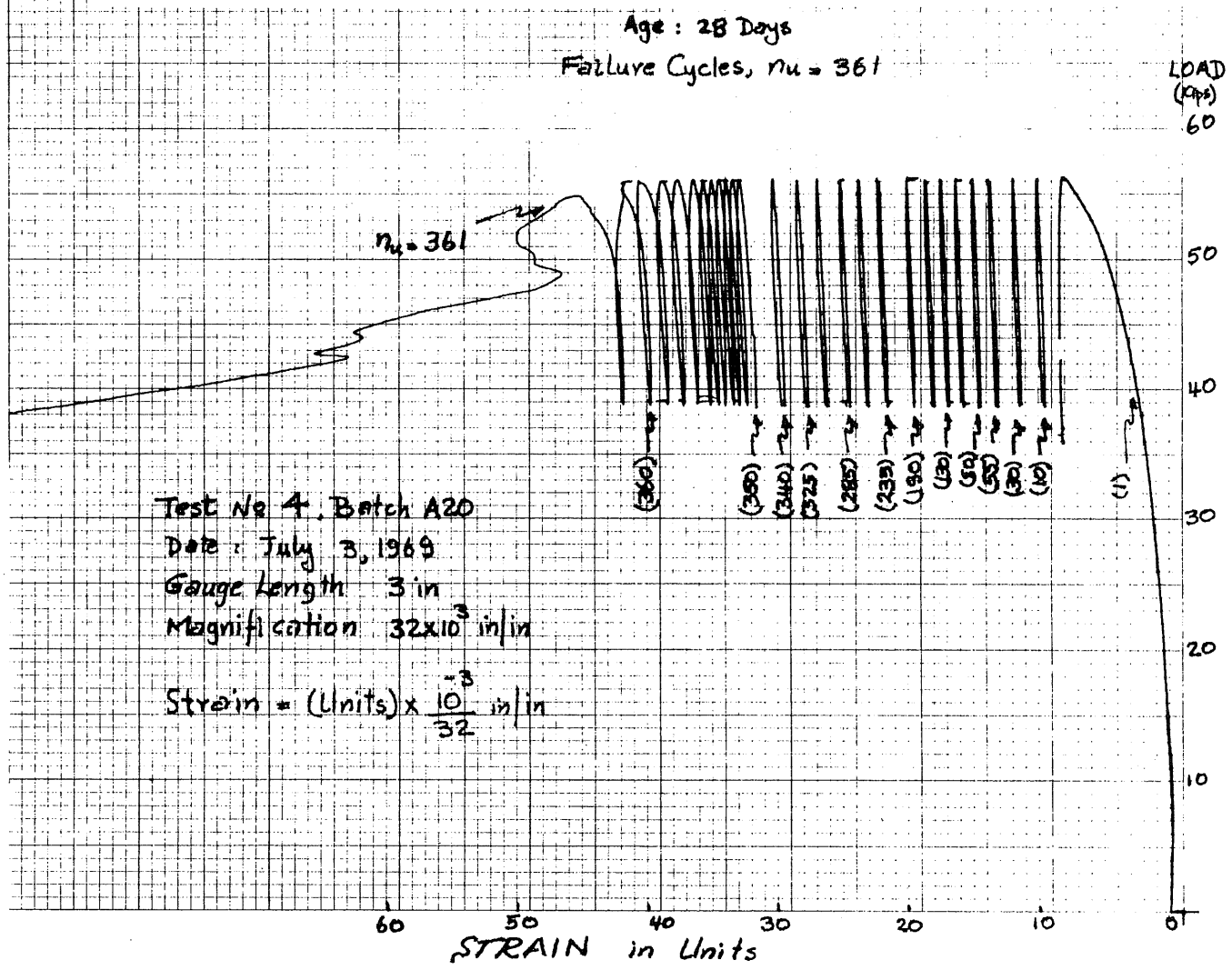

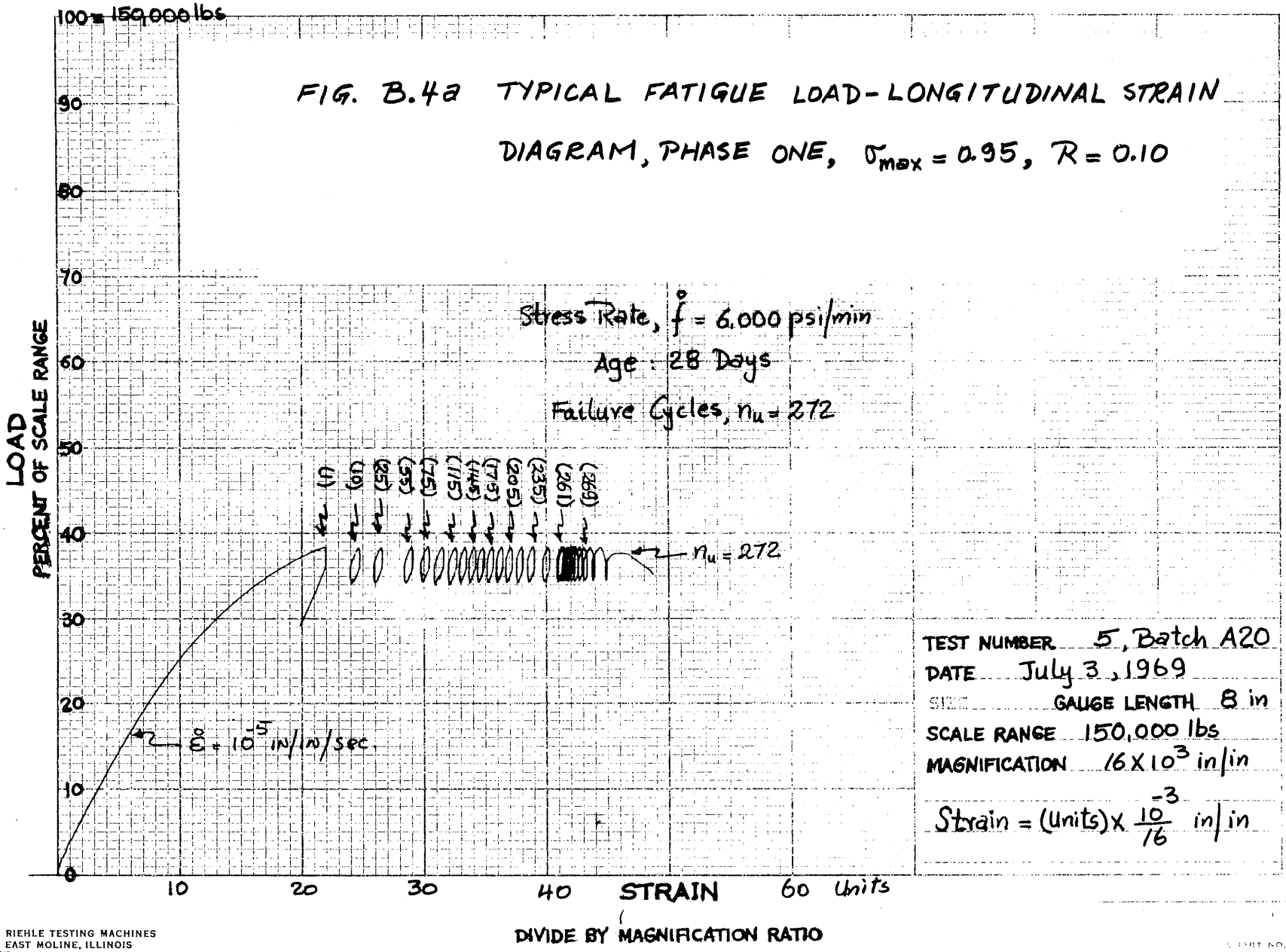

RIEHLE TESTING MACHINES
EAST MOLINE, ILLINOIS

PART NO. 35-195

FIG. B.4b TYPICAL FATIGUE LOAD-LATERAL STRAIN DIAGRAM, PHASE ONE, $\sigma_{max} = 0.95, R = 0.10$

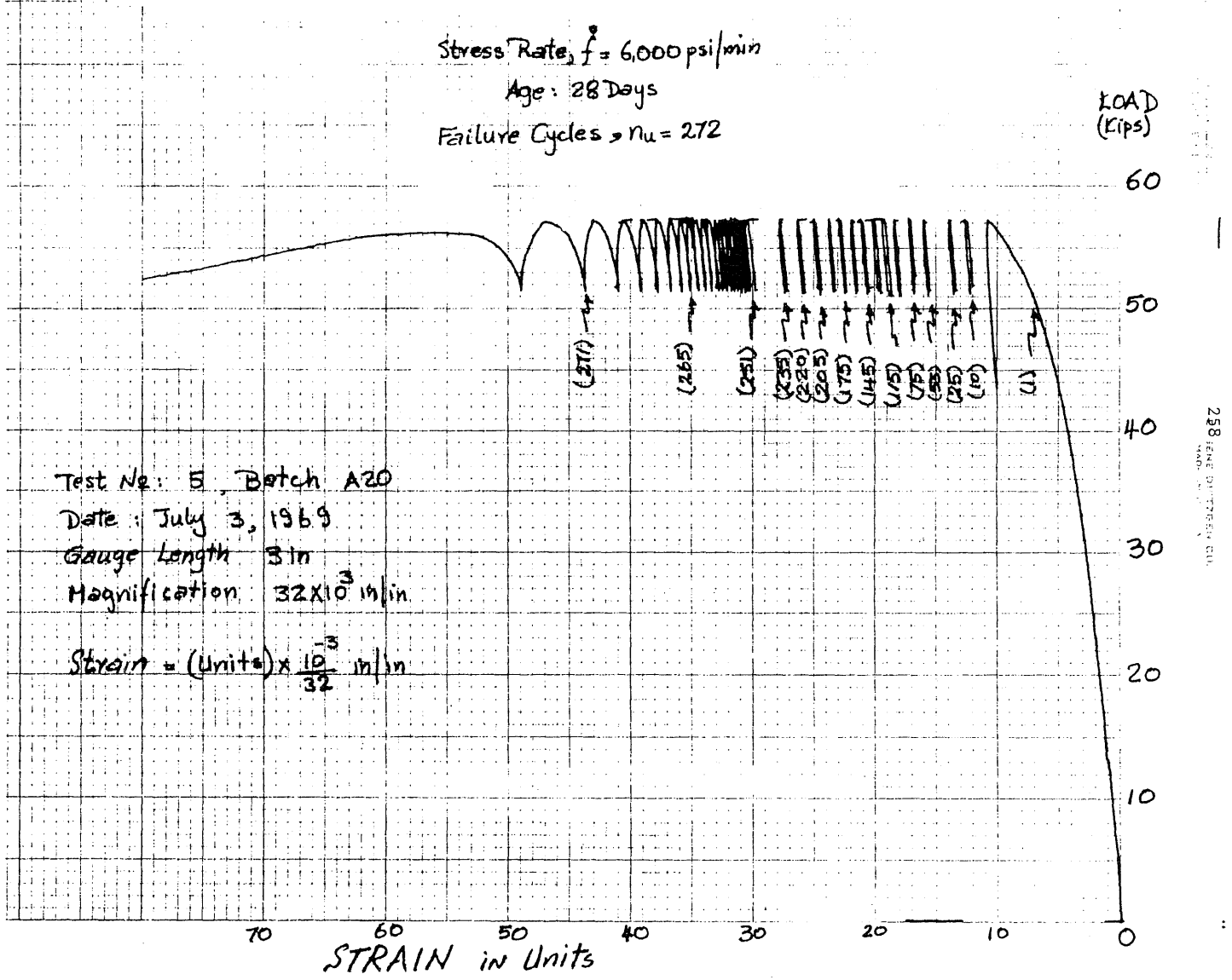

FIG. B.5a TYPICAL SUSTAINED LOAD-LONGITUDINAL STRAIN DIAGRAM, PHASE ONE, $\sigma_{SUS} = 0.95$

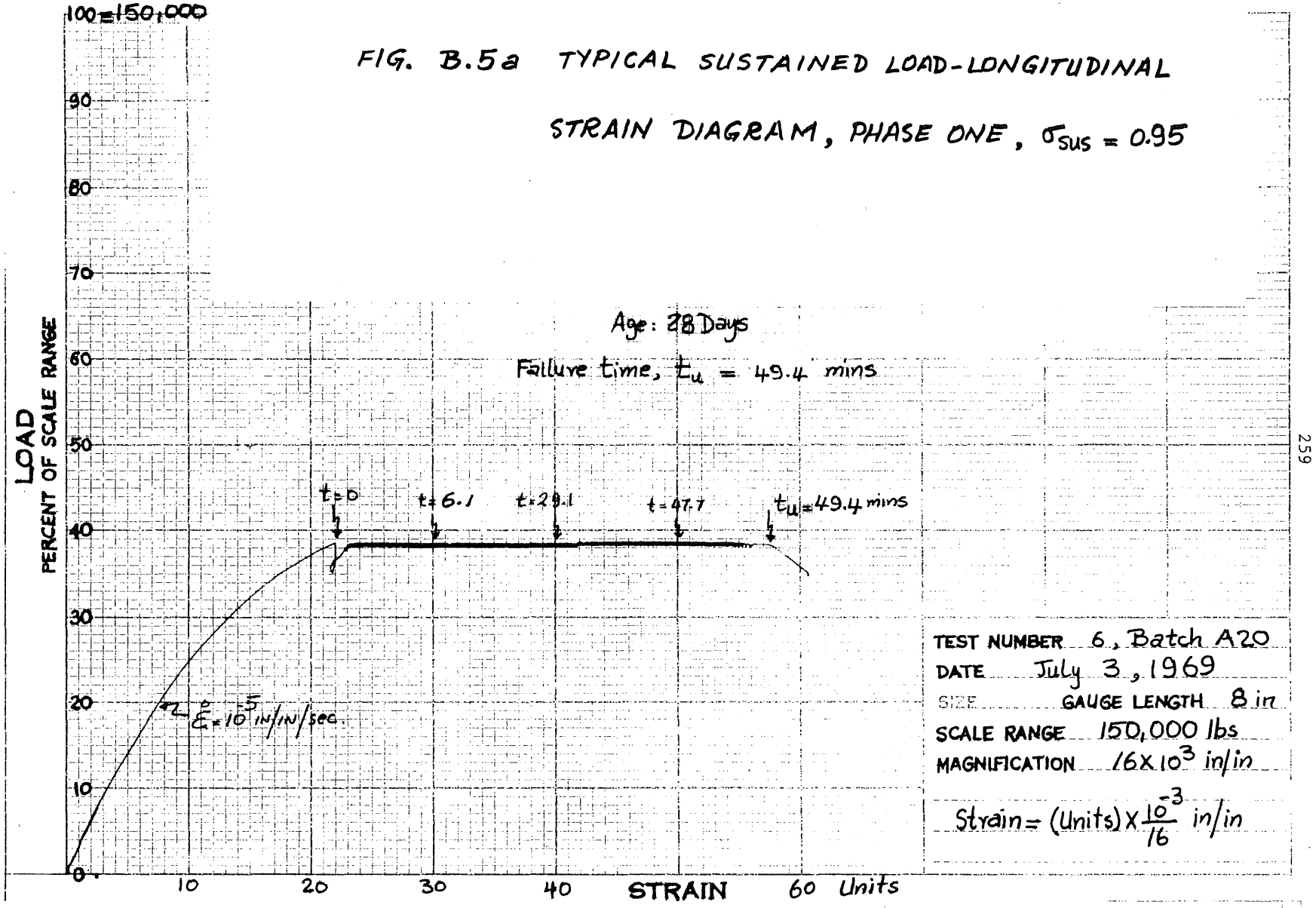

RIEHLE TESTING MACHINES
EAST MOLINE, ILLINOIS

CHART NO. 29-155

FIG. B.5b TYPICAL SUSTAINED LOAD - LATERAL STRAIN DIAGRAM, PHASE ONE, $\sigma_{sus} = 0.95$

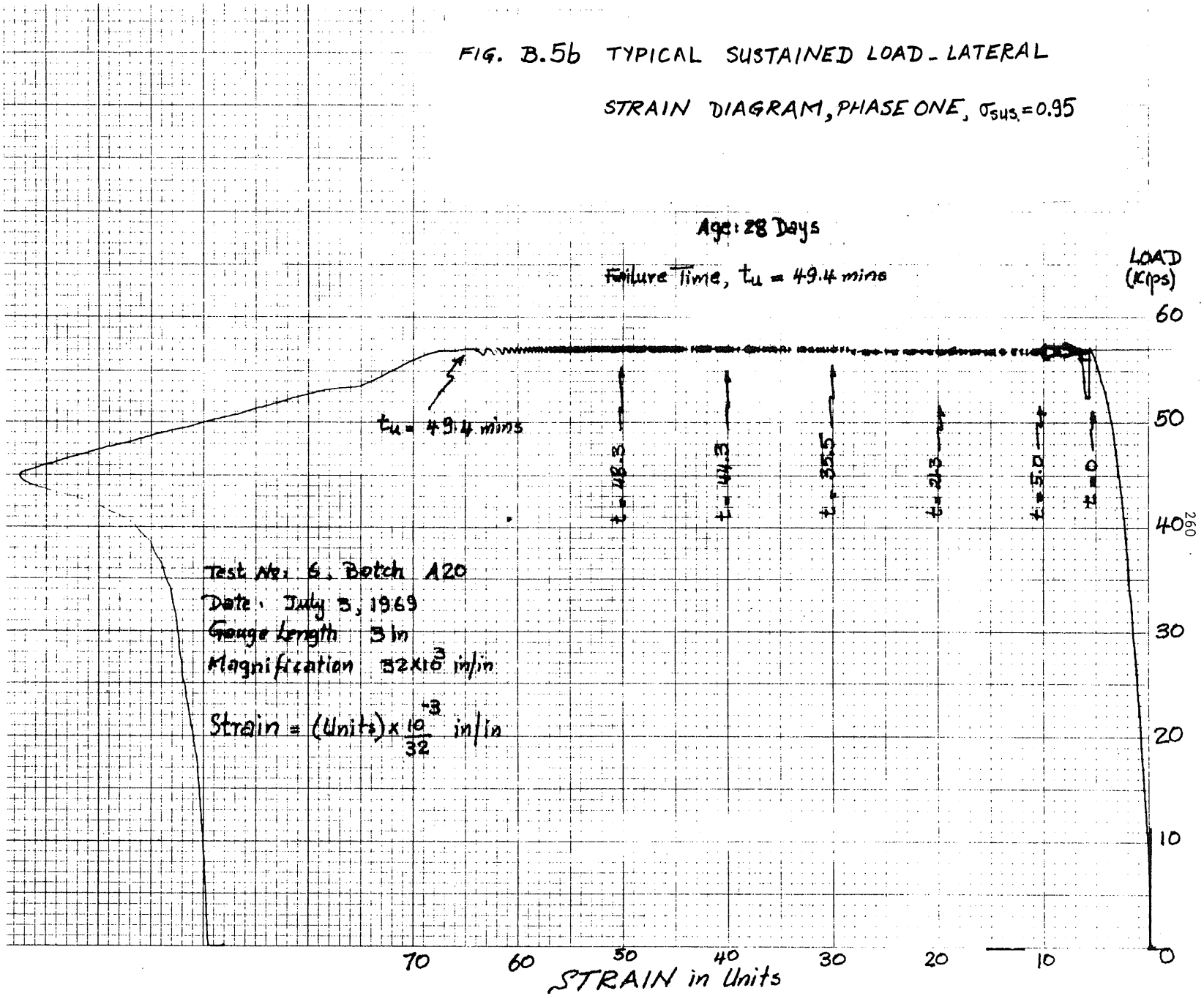

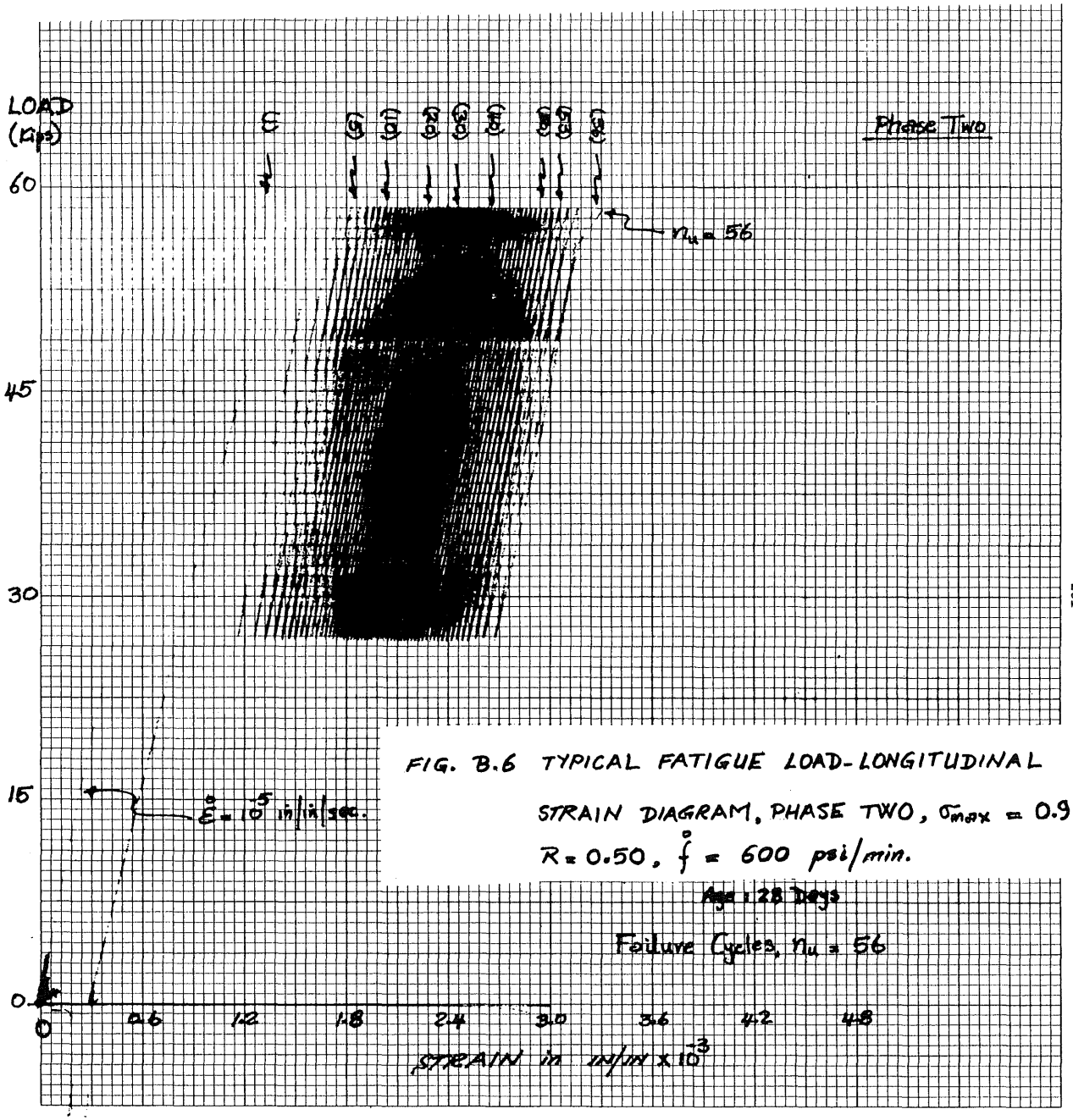

FIG. B.6 TYPICAL FATIGUE LOAD-LONGITUDINAL STRAIN DIAGRAM, PHASE TWO, $\sigma_{max} = 0.90$ $R = 0.50$, $\dot{f} = 600$ psi/min.

Age: 28 Days

Failure Cycles, $n_u = 56$

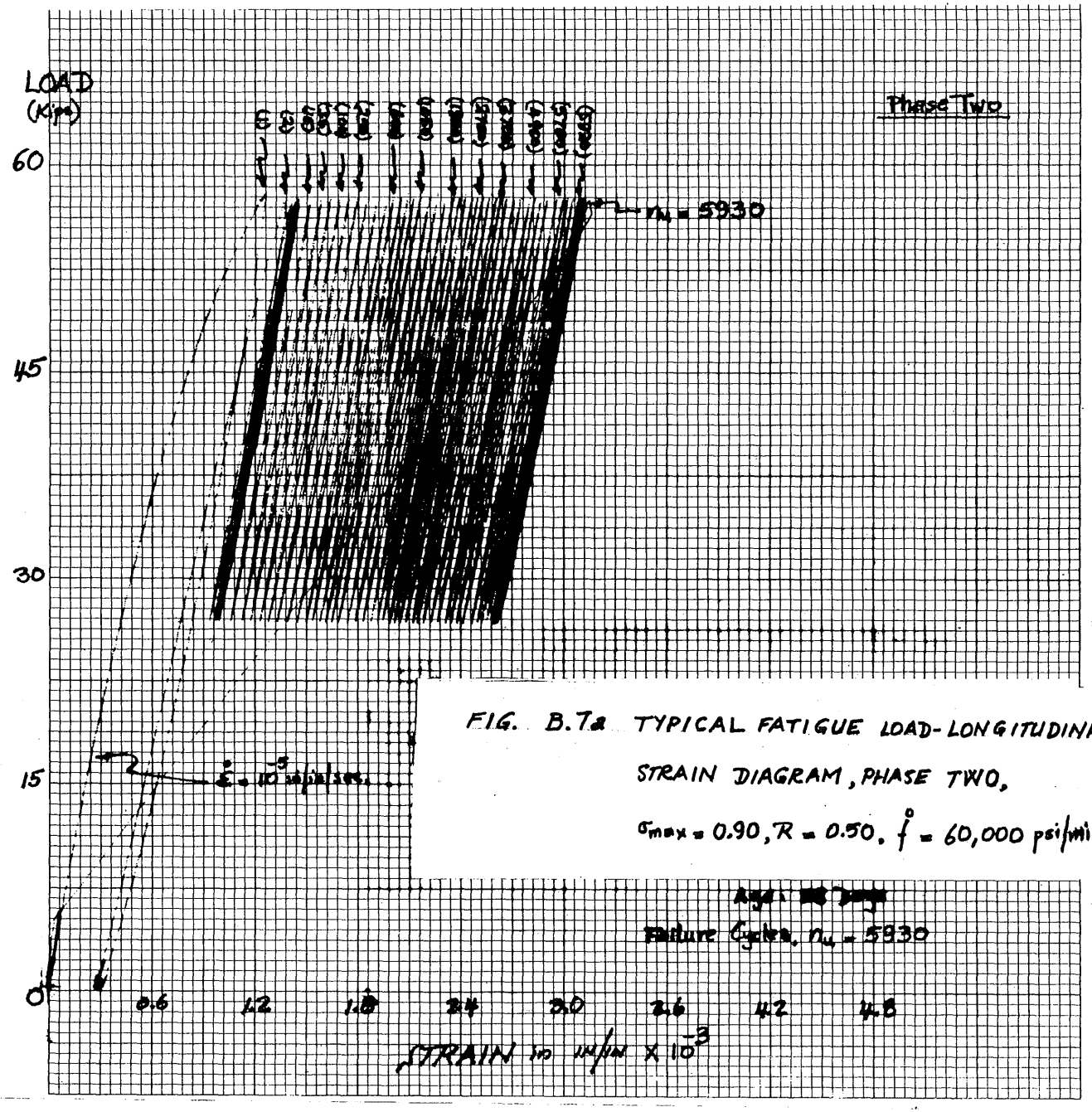

FIG. B.7a TYPICAL FATIGUE LOAD-LONGITUDINAL STRAIN DIAGRAM, PHASE TWO,
$\sigma_{max} = 0.90, R = 0.50, \dot{f} = 60{,}000$ psi/min

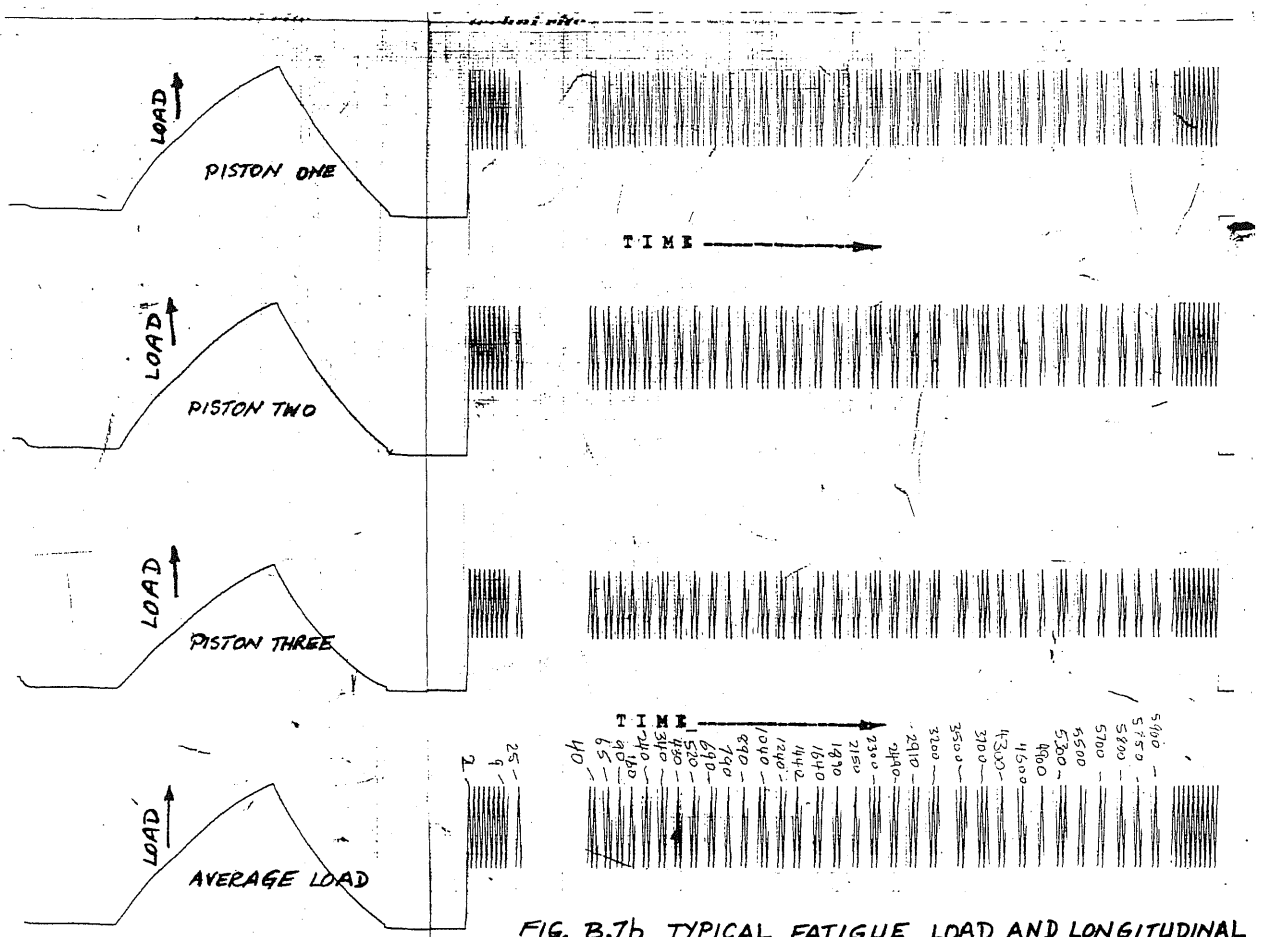

FIG. B.7b TYPICAL FATIGUE LOAD AND LONGITUDINAL STRAIN-TIME DIAGRAM, $\sigma_{max} = 0.90$, $R = 0.50$, $\dot{f} = 60{,}000$ psi/min.

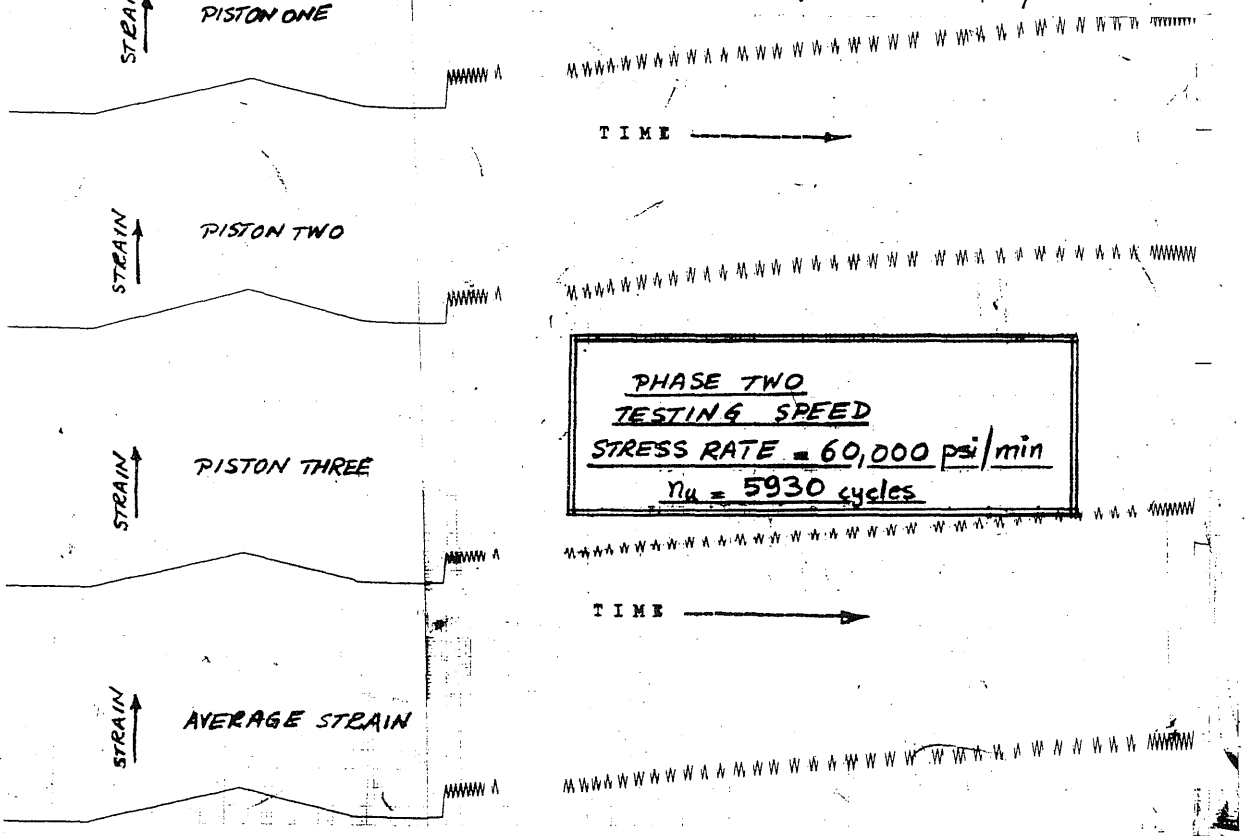

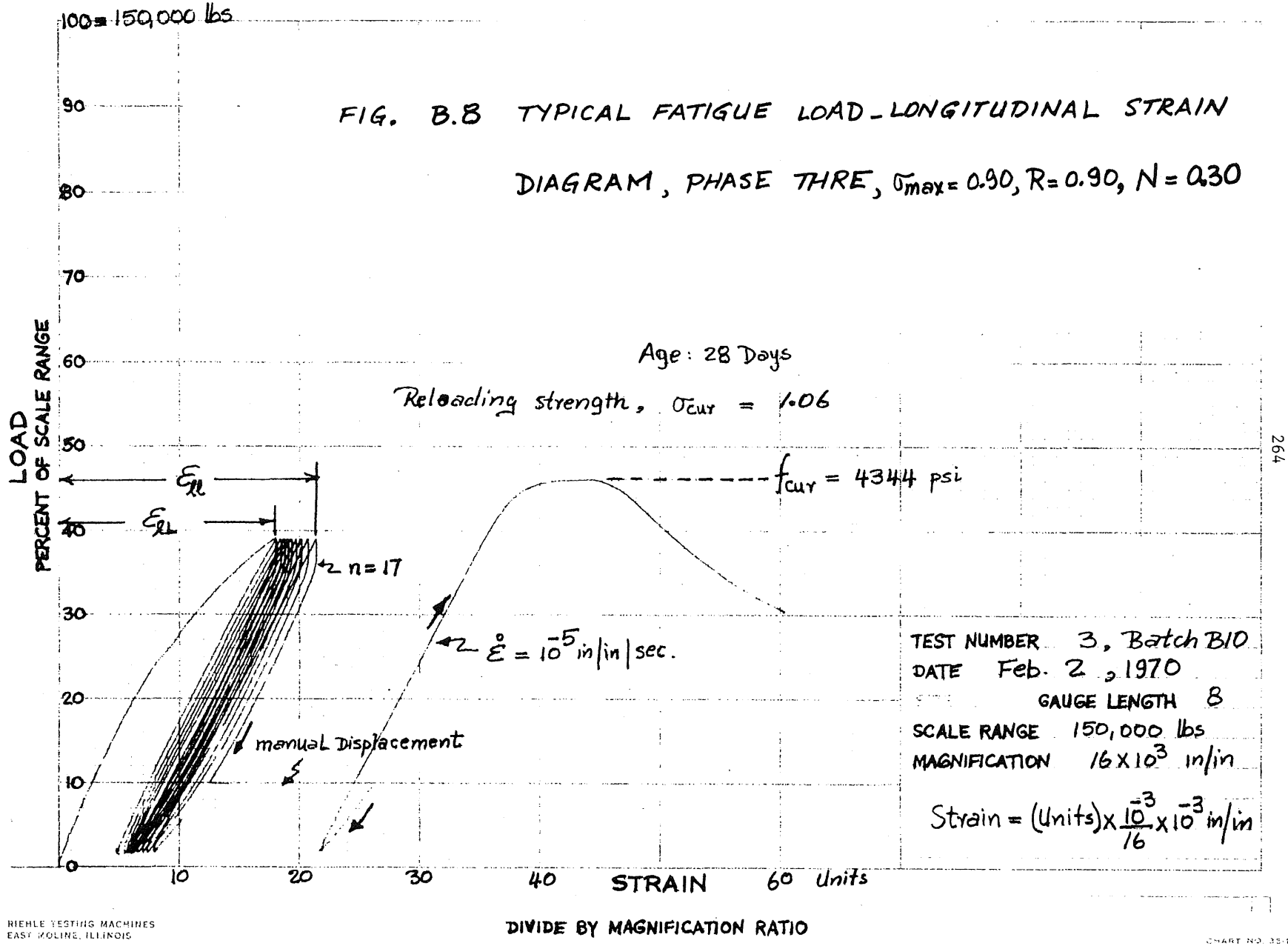

FIG. B.8 TYPICAL FATIGUE LOAD-LONGITUDINAL STRAIN DIAGRAM, PHASE THRE, $\sigma_{max} = 0.90$, $R = 0.90$, $N = 0.30$

DIVIDE BY MAGNIFICATION RATIO

RIEHLE TESTING MACHINES
EAST MOLINE, ILLINOIS

CHART NO. 35-155

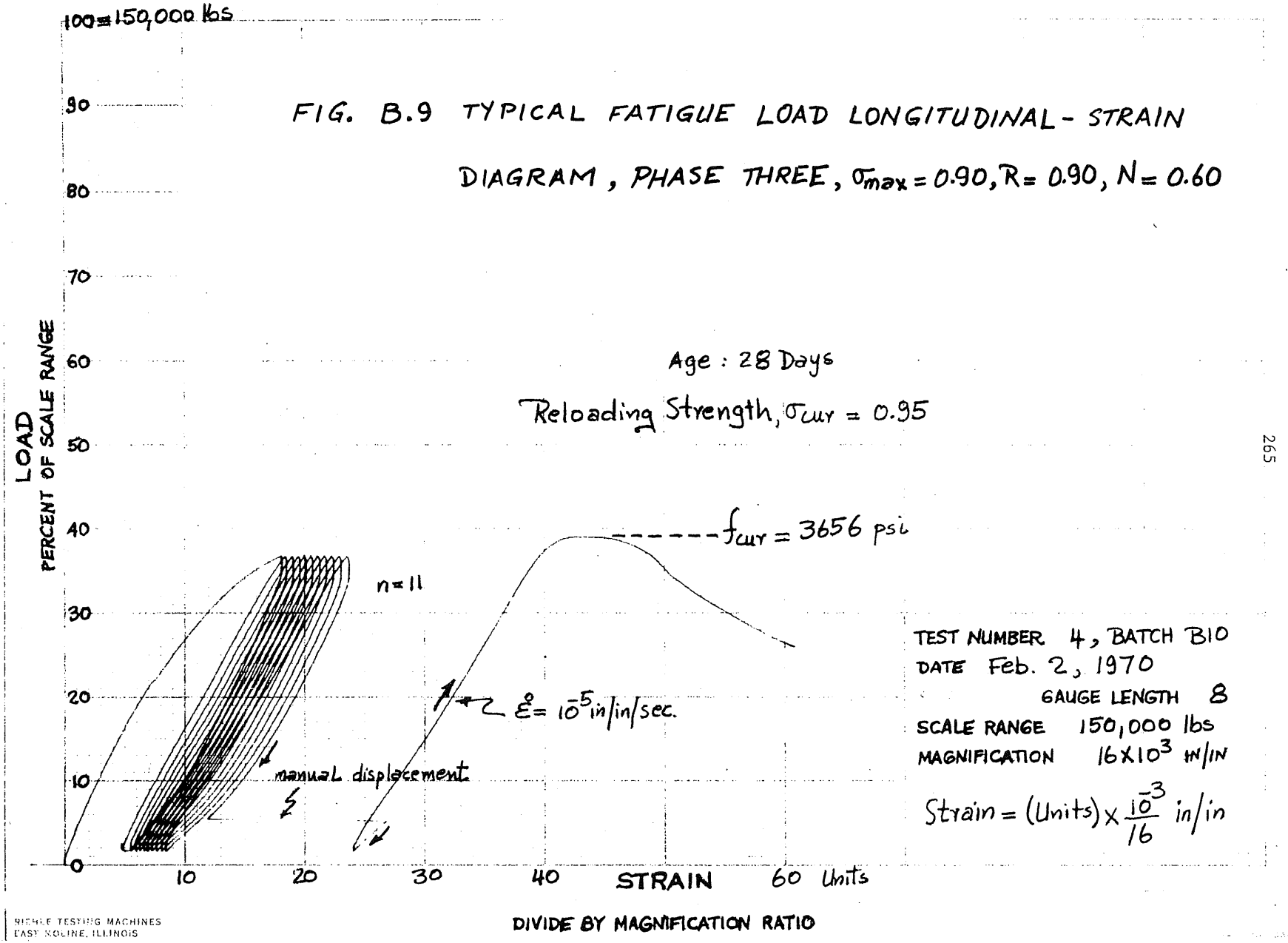

FIG. B.9 TYPICAL FATIGUE LOAD LONGITUDINAL-STRAIN DIAGRAM, PHASE THREE, $\sigma_{max} = 0.90, R = 0.90, N = 0.60$

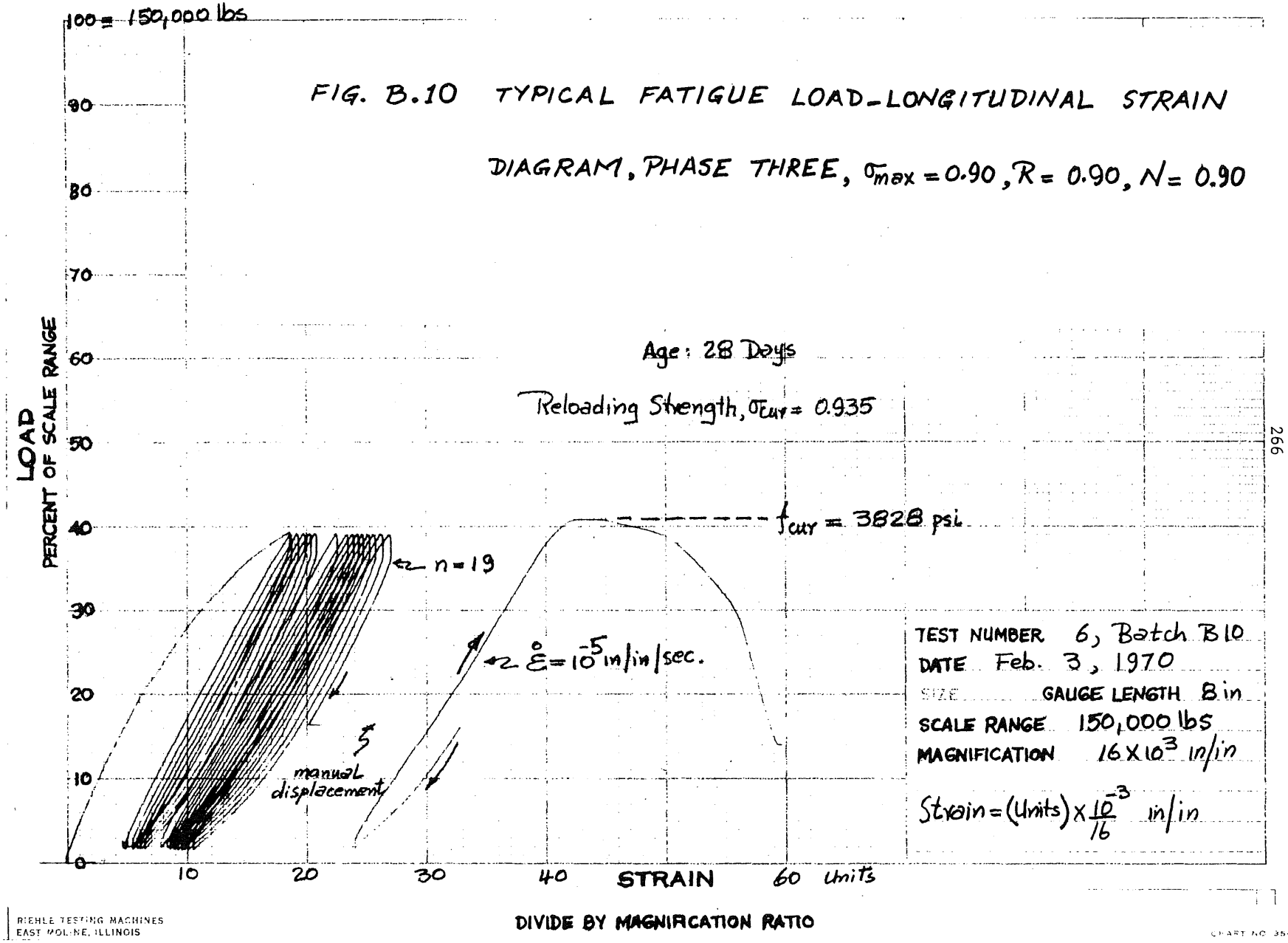
100 = 150,000 lbs
90
80
70
60
50
40
30
20
10
0
LOAD
PERCENT OF SCALE RANGE
10
20
30
40
STRAIN
60 units
DIVIDE BY MAGNIFICATION RATIO
FIG. B.10 TYPICAL FATIGUE LOAD-LONGITUDINAL STRAIN
DIAGRAM, PHASE THREE, $\sigma_{max} = 0.90$, $R = 0.90$, $N = 0.90$
Age: 28 Days
Reloading Strength, $\sigma_{cur} = 0.935$
$f_{cur} = 3828$ psi
n = 19
$\dot{\varepsilon} = 10^{-5}$ in/in/sec.
5
manual displacement
TEST NUMBER 6, Batch B10
DATE Feb. 3, 1970
SIZE GAUGE LENGTH 8 in
SCALE RANGE 150,000 lbs
MAGNIFICATION 16×10^{3} in/in
Strain = (Units) $\times \frac{10^{-3}}{16}$ in/in
RIEHLE TESTING MACHINES
EAST MOLINE, ILLINOIS
CHART NO 35-155